Uptake of manganese into the exoskeleton of the swimming crab *Liocarcinus depurator* (L.) in relation to biomonitoring and biosorption

_____

Faridah Mohamad

Thesis submitted for the degree of
Doctor of Philosophy

Division of Environmental and Evolutionary Biology
Faculty of Biomedical and Life Sciences
University of Glasgow
Glasgow
G12 8QQ

February 2008

Abstract

The swimming crab *Liocarcinus depurator* (L.) is a common member of the benthic fauna in Scottish waters, and is often caught as bycatch from the common lobster fishery grounds. This study aims to employ the species in relation to the biomonitoring potential for Mn in the Scottish inshore waters and in UK monitoring programmes by choosing Loch Fyne in the west coast of Scotland as a naturally high Mn area and the Clyde Sea area as the reference area. The ability of the crushed carapace to remove Mn from aqueous solution in a biosorption column system in the remediation of contaminated waters was also investigated as an attempt to turn this un-commercial species into beneficial use.

Measured using standard atomic absorption spectroscopy (AAS), the concentrations of Mn in the tissues of the swimming crab *L. depurator* from Loch Fyne were consistently higher than in the tissues in crabs from the Clyde Sea area. The metal concentration differed according to sexes, and to the tissues in the order of the exoskeleton (carapace, gills) > hepatopancreas > crusher claw muscle and gonads. The trend observed in *L. depurator* was comparable to the shore crab, *Carcinus maenas* which is an established biomonitor for metals collected within the vicinity of both study areas.

A series of different exposures of *L. depurator* to Mn in sea water (10ppm and 20ppm) for up to 21d, followed by a depuration period of 47d were performed under controlled laboratory conditions. Temporal changes in Mn concentrations in the exoskeleton of individual crabs were monitored by autotomizing a walking leg at weekly intervals. Mn concentrations in other tissues at given sampling points were obtained by sacrificing a batch of crabs at each sampling time. The hard tissues (dorsal carapace and leg exoskeleton) irreversibly accumulated Mn from the water whereas the soft tissues both accumulated Mn when exposed, and eliminated Mn after a period of depuration in clean sea water. As a result, the use of the exoskeleton of autotomized legs to represent Mn accumulation in the whole exoskeleton of a crab was established, and the accumulation of Mn from the water into the crabs tissues particularly the exoskeleton was confirmed.

The ability of dried and crushed carapace particles from the swimming crab *L. depurator* to remove Mn from aqueous solutions was studied using a packed bed up-flow biosorption column system. From a batch experiment carried out at room temperature on fine carapace particles with a diameter of less than 300µm and 100ml of 80ppm Mn in distilled water, the data fitted the Freundlich adsorption isotherm with an adsorption capacity K_F=22.82 mg.g^{-1}. The breakthrough curves generated from a series of up-flow biosorption experiments (constant flow rate of 100ml.h^{-1}, 72h sorption) indicates the great potential of the crab carapace particles to remove Mn from a solution. The removal depended greatly on the initial concentrations of the solution and the amount of carapace particles used which can be expressed as mass or the height of the column beds. Greater column bed heights increase Mn removal capacity which in the columns could be observed visually through progressive colour change of the beds. Experiments repeated using the carapace particles of the Norway lobster, *Nephrops norvegicus* (L.) generated similar trends and comparable data with the ones observed for *L. depurator*.

Scanning electron microscopy (SEM) and SEM combined with electron dispersive analysis of x-ray (SEM-EDX) were applied to examine the morphology of the dorsal carapace and gills of *L. depurator*, and also the form and site of Mn deposition onto both the intact carapace of *L. depurator* and onto Mn-biosorbed carapace particles. The dorsal carapace of *L. depurator* resembles the typical crustacean cuticle with three main layers, the epi-, exo- and endocuticles made up primarily by $CaCO_3$. Mn deposited onto the carapace especially on exposed inner layers and broken edges of the carapace particles in the form of Mn-rich nodules, which in 72h could create a layer visually observed as blackening of the particles. Deposition onto the gill surface took the form of fine particles scattered on the lamellae. Exposure of an isolated carapace to 80ppm Mn solution indicated the barrier-effect played by the epicuticle to Mn deposition onto the external surface. This barrier was lost when the surface is abraded. The membranous layer on the internal side did not act as a barrier, and penetration of Mn up to approximately 50µm into the endocuticular layers was detected. These results correlated with AAS measurements which indicated that internal exposure of the carapace resulted in a three times higher concentrations of Mn compared with external exposure.

Based on the wide distribution of *L. depurator* around the UK coast and its habit of resting on the bottom sediment, the results of this study propose *L. depurator* as a biomonitor species for Mn in the bottom water, particularly in the Scottish waters. Given the abundance of the species in common lobster fishery grounds in Scotland and often caught as bycatch in the trawls, *L. depurator* could provide a continued source of materials if the carapace is to be converted into a good Mn-removing agent in Mn contaminated waters.

Author's Declaration

I hereby declare that I am the sole author of this thesis and performed all of the works presented, except the preparations of specimens for SEM viewing in Chapters 5 and 6. The specimens were prepared by the following:

- Margaret Mullin – IBLS Electron Microscopy Unit, University of Glasgow
- Peter Chung and John Gillespie – Geology and Earth Science Microscopy Unit, University of Glasgow

_____

Faridah Mohamad

Date: 27 February 2008

Acknowledgements

My greatest gratitude goes to the following:

My supervisor, **Professor Douglas Neil** - for EVERYTHING: the time, the patience, the guidance, and especially, the kindness.

My co-supervisor, **Professor Alan C. Taylor** – for wasting no time at all on anything I gave him to comment, anytime, anywhere despite his 'busi'ness.

Dr. Ian Pulford from the Chemistry Department for reviewing the Biosorption chapter.

To the people in the lab, especially **Pat** (my AAS guru) and **John** (the sole provider of the famous John's Sea Water).

And people in the office: **Leandro**, **Rosanna** and **Nick**. And especially to **Sebastian**, thanks a million, couldn't have done this without you. And also especially to **Amaya**, thanks for having Maria – it means a lot to me - she reminds me of the time that passed... Ostias!!!!

To **Intan Rohani**, **Zayyana Shehu** and **Cynthia Lee** in Glasgow Caledonian University – it was because of you lot that I managed to finish my writing up. I love your library, and will surely miss it a lot. Thanks a million people!

To my dear friends in UMT and in Glasgow (and also ex-Glaswegian Malaysians) for the prayers we make (and keep on making) for each other.

And to my dearest brothers and sisters, nieces and nephews back home… I will return soon and this time it's for real!!!

Faridah
Room 512
Graham Kerr Building

Table of Contents

List of Tables

List of Figures

1 General Introduction

1.1 Accumulation of heavy metals in decapod crustaceans

Heavy metals have been defined as metals with a relative density to water of greater than five (Walker *et al.*, 2001). However the term 'heavy metals' has been replaced in recent years by a classification scheme that considers their chemistry rather than their relative density (Nieboer and Richardson, 1980). The metals are classified into Class A (oxygen seeking), Class B (sulphur or nitrogen seeking) or Borderline elements.

Heavy metals are natural components of all the compartments of the environment and may be released into the environment from natural or geological sources. Erosion and alteration of rocks release the metallic elements into soil and water, making them available for plants and animals (bioavailable). For example, Loch Fyne in the west of Scotland, being quite isolated from the open sea, experiences naturally elevated concentrations of manganese (Mn), a metal belonging to the Borderline elements that exhibit aspects of both Classes A and B. The sediments and pore waters in this area were reported to contain a significantly higher amount of Mn compared to other Mn-rich sites elsewhere (Bartlett *et al.*, 2007). Apart from such natural sources, an increase in human activities, particularly industrial, has generally intensified environmental pollution and accelerated the deterioration of some ecosystems (Veglio and Beolchini, 1997) thus threatening numerous coastal ecosystems with heavy metals pollution (UNEP, 1999).

Aquatic organisms may be exposed to heavy metals dissolved in the ambient water, either from natural sources or as pollutants released as a result of human activities such as mining or industrial processes. They may take up these metals, and have

the potential to accumulate them to high concentrations (Mortimer and Connell, 1993; Mortimer and Miller, 1994).

Human concern about metals has mainly focused on the highly toxic, rare and non-essential heavy metals like Pb, Hg and Cd. In nature, Mn is one of the most abundant elements, particularly in the soft bottom sediments of oceans (Hernroth *et al.*, 2004) and one of the important micronutrients in the aquatic environment (Cover and Wilhm, 1982). Due to its high prevalence and possibly due to its status as an essential metal, the potential danger of Mn has been mostly neglected. It is an unforeseen toxic metal in the marine environment since it may occur in toxic concentrations in the bottom water after hypoxic conditions (Baden and Eriksson, 2006). At these high levels, it can pose a threat to aquatic organisms (Forstner and Prosi, 1979 in Sanders *et al.*, 1998). In sea water, 58% of total Mn occurs as free hydrated ions (Simkiss and Taylor, 1989) which is believed to be readily available for uptake by exposed organisms.

Environmental research efforts that commenced in the 1960s have revealed that many marine invertebrates accumulate metals in their tissues from the environment (Lam and Wu, 2003). The metals might be taken up directly from the surrounding aquatic medium or they may be ingested via food particles or contaminated prey items. Therefore the relative proportion from each route varies with the invertebrate type and the relative bioavailabilities of the metal in the water and diet (Rainbow and Wang, 2001). Decapod crustaceans absorb trace metals from their food sources, and additionally in the case of aquatic species, via their permeable body surfaces such as the gills, without resort to active transport mechanisms (Rainbow, 1988). The trace metal content of a decapod crustacean can be divided into three components – metal passively adsorbed onto the cuticle, metal in the gut not assimilated into the body, and absorbed metal accessible to physiological processes. Passively adsorbed metal does not usually represent the major component, even of the cuticle component itself, since more cuticular metal is derived from internal sources and is in turn only a small fraction of the absorbed metal content incorporated via internal physiological processes (Rainbow,1988).

A vast number of invertebrates have been proposed as biomonitors of environmental pollutants. Mussels are the most popular ones, being globally used to monitor a range of metals in countries worldwide, through a project called Mussel Watch Programme. The mussel watch exercise was performed round the coast of Scotland as early as in 1977 (Davies and Pirie, 1980). The biomonitoring concept arose from the realization that many contaminants could cause significant biological effects at low environmental concentrations (sometimes below detection levels). Research attention turned to effects monitoring (i.e. biologically-based) rather than contaminant monitoring (i.e. chemically-based) (Lam and Gray, 2003). The effects of contaminants on aquatic communities i.e. temporal and spatial changes in selected biological systems/parameters, are used to indicate changes in environmental quality and conditions (Lam and Wu, 2003). These responses might be behavioural, physiological, histopathological, biochemical or immunological (Schuwerack *et al.*, 2001) or may affect other aspects of the biology of the organisms of choice.

To date, numerous publications have reported the bioaccumulation of manganese in decapod crustaceans (the amount taken from water as well as ingestion via diet), and emphasis of these studies has been on the suitability of decapod crustaceans as bioindicator organisms for the marine ecosystem. Crabs in particular act as appropriate indicator organisms due to certain factors, including abundance in numbers and biomass, as well as relatively low mobility compared to other marine organisms such as fish (Mortimer, 2000; Monserrat *et al.*, 2007). Heavy metal content differs significantly among different organs in a freshwater crab, *Potamonautes perlatus* (Reinicki *et al.*, 1988) and also in the marine Norway lobster, *Nephrops norvegicus*. Lobsters from an area with relatively high concentrations of manganese were found to accumulate a significantly higher concentration of the metal in the body, especially in the carapace, while muscle tissues showed the lowest concentration (McColl, 2004). The exoskeleton has been found to account for the major proportion of body burden of manganese (95%) in the shore crab, *Carcinus maenas* (Bjerregaard and Depledge, 2002), which suggests that the carapace might act as a sink for deposition of the metal (Steenkamp *et al.*, 1994).

1.1.1 Some factors affecting metal accumulation

Different metals show different behaviours in bioaccumulation; for example they may be accumulated at different concentrations in different tissues. In the shore crab *Carcinus maenas* exposed to metals for 32 days, cadmium bioaccumulates primarily in midgut gland tissues, copper in gill tissues and zinc in muscle tissues (Martin-Diaz *et al.*, 2005). In the same experimental study, concentrations of cadmium in different tissues seemed to reflect the exposure of the crabs to this metal, whereas concentrations of copper and zinc did not reflect the exposures. When the mangrove crab *Ucides cordatus* was exposed to Mn in sea water, the metal accumulated in different tissues in proportion to the exposure concentration, but to different absolute levels: highest in the gills, followed by the hepatopancreas, and least in the muscle tissue (Correa Jr. *et al.*, 2005).

Different species accumulate metals at different rates, depending on how they handle the metals (Rainbow, 2006). For marine crustaceans, metal accumulation processes vary not only between genera, but also between closely related species, some being net accumulators, while others are regulators (Rainbow, 2002). Net accumulation occurs when the rate of uptake into an organism exceeds the rate of excretion.

Metal bioaccumulation can also be affected by the individual size of the organism. Smaller animals accumulate more metals in both freshwater crabs (Reinicki *et al.*, 1988; Steenkamp *et al.*, 1994) and marine crabs (Bjerregaard and Depledge, 2002). However the statement does not apply to all taxa. No significant relationship was found between the size of crustaceans, *Acanthephyra eximia*, *Aristeus antennatus* and *Polycheles typhlops* and total body manganese concentrations (Kress *et al.*, 1998). Samples of a wide range of sizes are therefore essential to avoid over- or underestimation of the metal levels in a population under study.

A sex-difference in metal accumulation is not a general rule in decapods, but it has been reported in some species. Mouneyrac *et al.* (2001), Turoczy *et al.* (2001) and Al-Mohanna and Subrahmanyam (2001) found no difference in metal accumulation (of Cd, Pb and Zn, and also Mn in the last study) between sexes in three different

crab species. However, other studies reported that the accumulation does vary significantly between male and female animals (lobster *Nephrops norvegicus* - Canli and Furness (1993), Canli *et al.* (1997); crab *Potamonautes warreni* – Sanders *et al.* (1998); shrimp *Pleoticus muelleri* – Jeckel *et al.* (1996)). The inconsistent relationship between sex and metal accumulation in biomonitor species suggests the importance of treating the data separately according to sexes for analyses in order to obtain more reliable outcomes of the impact of exposure.

1.2 Manganese in the marine environment

Mn, a metal classified as a borderline element by Nieboer and Richardson (1980), is one of the common contaminants in aquatic systems (Phillips, 1995). Mn in marine sediments could be released into the bottom water and become bioavailable, especially during hypoxic events (Eriksson and Baden, 1998). Mn is essential for many metabolic functions in marine animals, and for this reason has perhaps attracted less interest from scientists concerned with the accumulation of xenobiotic metals. Many publications have focussed on more 'dangerous' contaminating metals including zinc, cadmium, lead and mercury.

However, in excess, Mn is toxic especially as a neurotoxin (Baden *et al.*, 1995; Baden and Eriksson, 2006), and can bring about various impacts on the exposed animals. A high Mn content was found in a blue crab *Callinectes sapidus* with shell disease or lesions (Weinstein *et al.*, 1992) whereas deposition of manganese dioxide gives rise to blackening or browning of the gills and carapace of the Norway lobster *Nephrops norvegicus* (Baden *et al.*, 1990). Among the latest findings are that Mn can be strongly accumulated in the lateral antennule of *N. norvegicus* (Baden and Neil, 2003). This impairs chemosensory function controlling food searching behaviour of the animal, so that there is a doubling of the time to detect the odour of food stimuli (Krang and Rosenqvist, 2006). All these findings highlight the importance of treating Mn, even though essential in small amounts, as one of the metals that should be frequently monitored especially in areas prone to frequent

hypoxic events. One of the ways to do this is by measuring the concentrations in biomonitor species. The quest for more suitable biomonitors of Mn is therefore justified.

The Mn concentrations in ocean sediments can reach as high as 80 mg.g^{-1} dry weight, as in certain Atlantic deep-sea clays (Chester *et al.*, 1973 in Baden and Eriksson, 2006). The sediment pore water may contain 0.16-24.0mg.l^{-1} (ppm) Mn (Magnusson *et* al., 1996) whereas bottom water concentrations are about a thousand times lower, at between 0.18-16.5μg.l^{-1} (Hall *et al.*, 1996). Mn becomes bioavailable in water when reduced during hypoxic or anoxic conditions in the sediment, during which time the concentrations in the bottom water can rise by several orders of magnitude to 1.5 mg.l^{-1}, as in the Kiel Bight (Balzer, 1982), and even to 22 mg.l^{-1} in the Orca Basin in the Mexican Gulf (Trefry *et al.*, 1984). Mn solubility and thus bioavailability increases with decreasing oxygen tension and pH (Wollast *et al.*, 1979 in Baden and Eriksson, 2006).

During periods of hypoxia, the release of Mn^{2+} from the sediments increases manganese concentrations in the bottom water (Baden *et al.*, 1995) that is readily available for uptake by organisms. As a consequence of eutrophication in the marine coastal waters, the oxygen demand from the sediments increases, followed by an enhanced flux of manganese from the sediment to the overlying waters (Baden *et al.*, 1995; Hernroth *et al.*, 2004).

1.3 Biomonitoring of metals

A biomonitor refers to an animal species that can accumulate heavy metal in its tissues and may therefore be monitored as a measure of the bioavailability of the metals in the ambient habitat (Rainbow, 1995). Biomonitor species are widely used for monitoring coastal and estuarine environments for the bioavailability of metals (Bryan and Langston, 1992; Rainbow, 1993). An ideal biomonitor species must fulfil several criteria: they must be easily identified, relatively sessile, abundant,

cosmopolitan in geographical distribution, hardy enough to survive high concentrations of metals, long-lived and available for sampling throughout the year, of sufficient size to allow the collection of enough samples for analysis and be net accumulators of the metal of interest (Rainbow, 1995). As will be demonstrated, most of these criteria are met by the swimming crab *Liocarcinus depurator*.

Metal contamination in the marine environment is normally measured in both the water and in the sediment. The measurement of dissolved metal concentrations presents analytical problems due to a number of reasons. These concentrations are typically low (and often below detection limits) and vary greatly over time (Rainbow, 1995). However, some contaminants at very low concentrations in water and sediments can sometimes be accumulated and measured in the organisms. Moreover, the concentration measured in biomonitor species reflects not only the total metal concentration occurring in the medium, but it also provides the value of the fraction of the metal readily available for uptake by organisms (i.e. bioavailable). Therefore, the measure of metal concentrations in the biomonitor species is considered of more ecological significance.

Heavy metals accumulated in marine organisms are easily measured, not liable to contamination and provide a time-integrated measure of metal supply (according to species) of bioavailable metal. Thus the fraction of metal of direct ecotoxicological relevance is measured unambiguously (Rainbow, 1995). Biomonitors are now used widely to establish temporal variations in the bioavailable concentrations of heavy metals in coastal and estuarine waters (Phillips and Rainbow, 1993; Eriksson, 2000). The choice of a biomonitor generally follows the understanding of metal kinetics, including rates of uptake into and loss from the body. These data are normally obtained via series of laboratory experiments (Rainbow *et al.*, 1990), but should be complemented by field data (Rainbow, 1995).

The biology of an organism is a key feature in the choice of biomonitors. That includes its mode of feeding, life history and breeding season, length of life and most importantly the kinetics of metal accumulation. An understanding of such aspects of the biology of biomonitor species allows identification of a source of metal contamination (Rainbow, 1995). To date, several genera of sedentary marine

invertebrates of cosmopolitan distribution have been widely used as biomonitors. They include the mussels *Mytilus spp.* and *Perna spp.*, oysters from the genera *Ostrea* and *Crassostrea* and barnacles of the genus *Balanus* (Rainbow, 1995). A list of marine invertebrates of potential biomonitoring application is given by Galloway *et al.* (2004). A common problem encountered in the deployment of organisms in a biomonitoring programme is the precision of their identification to the species level. Confusion arises for example when identifying the mussels *Mytilus edulis, M. galloprovincialis* and *M. trossulus* (Seed, 1992 in Rainbow, 1995), and when identifying species of the genus *Saccostrea*. Since the accumulation of metals might differ significantly between species, the correct identification of the biomonitor species is crucial. In this feature, the swimming crab *L. depurator* chosen for the present study has a diagnostic character that makes it easily differentiated from closely related species.

In marine ecosystems, crustaceans play key ecological roles as planktivorous grazers, epibenthic scavengers or prey species, making them suitable as biological indicators of environmental perturbation (Lorenzon *et al.*, 2001). Crabs are appropriate indicator organisms as they are the most abundant group of aquatic sediment macrofauna, both in terms of numbers and biomass. They are also relatively immobile (Smith *et al.,* 1991; Monserrat, 2007), and therefore could well reflect the environmental conditions of the specific area of study. Brachyuran crabs are good accumulators of metals and have been used as model organisms in a number of studies on trace metal accumulation and internal metal handling, with *Carcinus maenas*, *C. mediterraneus* and the blue crab *Callinectes sapidus* as the most intensely investigated species (Bjerregaard and Depledge, 2002).

Thus *C. maenas* has been used as a biotest for a series of metals including chromium, nickel, copper, zinc and lead (Martin-Diaz *et al.*, 2007) and also for cadmium and mercury (Elumalai *et al.*, 2007), cadmium and zinc (Martin and Rainbow, 1998), and copper and zinc (Pedersen *et al.*, 1997). The blue crab *Callinectes sapidus* has also been reported to show a similar trend (Karouna-Renier *et al.*, 2007; Brouwer *et al.*, 1984; Engel and Brouwer, 1984). Crabs can also accumulate Mn in various environmental settings e.g. *Ucides cordatus* in the mangrove (Correa Jr. *et al.*, 2005), the blue crab *Portunus pelagicus* (Al-Mohanna

and Subrahmanyam, 2001) and the soldier crab *Mictyris longicarpus* (Weimin *et al.*, 1994) in the marine environment, and *Potamonautes warreni* in freshwater lakes and streams (Steenkamp *et al.*, 1994; Sanders *et al.*, 1998). All these reports suggest the great potential held by the crabs as biomonitors for metals in various environments.

Despite bearing similar characteristics and behaviour, the abundant swimming crab *Liocarcinus depurator* has so far attracted less attention as an indicator species. This offers another potential bioindicator species that is easily sampled and could be obtained cheaply from the fisheries-related industries (see Section 1.5 below).

For Mn, both stomatopods (*Squilla mantis:* Blasco *et al.*, 2002) and lobsters are established biomonitors. Thus, the Norway lobster *Nephrops norvegicus* accumulates Mn in the exoskeleton (Baden *et al.*, 1999; Baden and Neil, 2003), and its haemocyanin concentration is reduced significantly (by up to 15%) on exposure to hypoxia coupled with dissolved Mn for periods up to 3 weeks (Baden *et al.,* 2003). As a consequence, the Mn concentrations in *N. norvegicus* haemolymph are negatively correlated with the oxygen saturation under ecosystem hypoxia (Eriksson, 2000). This observation was later confirmed and extended in another lobster species *Homarus americanus,* in which the Mn concentration measured in the gills was used as an index of exposure to reducing conditions (Draxler *et al.*, 2005).

The toxicity of Mn in the Norway lobster was demonstrated by Hernroth *et al.* (2004) who report a significant effect on *N. norvegicus* blood. After being exposed to 20µg.ml^{-1} of the metal for 10 days, the lobster accumulated 24.1µg.ml^{-1} Mn in the haemolymph, with 60% reduction in total haemocyte count. The metal was also found to lower degranulation of haemocytes, thus reducing the release of prophenoloxidase system into the haemolymph necessary for the immune defense against infection. Their observations highlight the importance of treating Mn as one of the metals with a potential deleterious effect on crustacean physiological systems, despite being regarded as a non-dangerous pollutant compared with others.

1.4 The swimming crab *Liocarcinus depurator* Linn. (1758)

Liocarcinus depurator (L.) (Fig. 1-1), commonly known as the harbour swimming crab, is one of the commonest portunid crabs in the inshore waters around European coasts. Due to its abundance and wide distribution, *L. depurator* is one of the most important bycatches of the Mediterranean demersal fishery (Abello, 1989) and is also present in 90% of lobster trawls in the Clyde Sea Area (Wieczorek *et al*., 1999 in Bergmann and Moore, 2001). In the Clyde Sea area of Scotland, it is commonly caught as a bycatch in lobster trawls at depths of 40-50m as it is sympatric with and possibly in limited competition with the lobster *Nephrops norvegicus* (Glass, 1985). In contrast to its close relative, the velvet swimming crab *L. puber*, for which there is a large export fishery, *L. depurator* is not a commercial species (Glass, 1985). This may be due to its relatively smaller size, that seldom exceeds 55mm carapace width. They are normally discarded back to the sea, although it is known that 25% do not survive due to physical injuries or physiological stresses of capture (Bergmann and Moore, 2001).

L. depurator crabs inhabit the lower shore and sublittoral zone on fine, muddy sand and gravel with full salinity (30-40 psu) at a depth of between 5-300m in all UK and Irish coasts, and is globally distributed from Norway to West Africa including the Mediterranean. They can be identified by the following anatomical features that are characteristic of the species: carapace broader than long, relatively flat, with numerous transverse, hairy crenulations; antero-lateral margins of the carapace with five pointed teeth; wide orbits and three similar-sized rounded lobes between eyes; front of carapace with a median lobe slightly more prominent than two similar flanking lobes; and pereiopods 2-4 of slight build while pereiopod 5 with violet-tinted, strongly paddled dactylus (Hill, 2003).
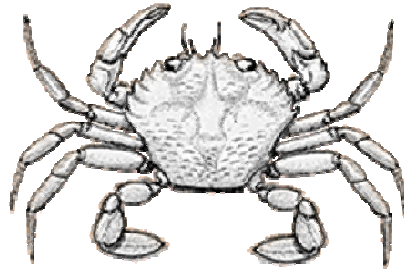
Fig. 1-1. *Liocarcinus depurator* (L.). (Illustration by Hayward and Ryland, 1990)

The males generally reach maturity at about 30mm carapace width (CW) at the age of about a year, and will grow up to 56mm CW. The females are slightly smaller, reaching 24mm CW at maturity and a maximum CW of 51mm (Muino *et al.*, 1999). To date, information on the life span is still lacking. In terms of feeding, they are solitary and considered to be active carnivores and scavengers (Freire, 1996) which feed upon sessile or slow moving benthic macroinvertebrates and small invertebrates like polychaetes, molluscs, ophiuroids and fish (Glass, 1985).

L. depurator is generally very quiescent, with the most common attitude it adopts being to remain immobile on the surface of the sediment. Despite being called the swimming crab, in fact it swims only intermittently in bursts of 4-5 seconds duration, and then only if provoked (Gale, 1986). It is available throughout the year, but was reported by Glass (1985) to show a peak in abundance in September and October with the males being twice as abundant compared to females.

1.5 Biosorption of metals

Much evidence has been put forward regarding the ability of marine organisms to accumulate metals from the environment. The usage of these organisms to monitor the level of contaminants in the environment has also been explored. However,

attempts to exploit their ability to accumulate metals, and in turn to use them to remediate waters contaminated by those metals, have rarely been made.

Biosorption is a process that utilizes inactive biological materials to sequester toxic heavy metal ions (Kim, 2004) from aqueous solutions by physicochemical mechanisms (Vijayaraghavan *et al.*, 2004). Some have defined it simply as a passive immobilization of metals by biomass (Kadukova and Vircikova, 2005). This process involves several metal-binding mechanisms, including ion exchange, complexation, coordination, chelation, microprecipitation or adsorption (Volesky, 2001). As heavy metal discharges continue to increase, removing them from aqueous solutions has become a challenge for this century (Volesky, 2001).

Biosorption began to be investigated in the 1980s (Volesky, 2001) and is becoming a popular technique in the search for ways to remove or recover metals from waste streams (Vijayaraghavan *et al.*, 2004). It has become an important component of the integrated approach to the treatment of aqueous effluents (Veglio and Beolchini, 1997; Aksu, 2005). Biosorption is preferred to conventional metal removal techniques as it offers several advantages, i) it normally uses biomass raw materials that are either found in abundance, or ii) it is very cost-effective since it uses wastes or byproducts from other industrial operations (Volesky, 2001), and therefore can be obtained cheaply from the industries.

Biosorption, by a prokaryotic and/or eukaryotic biosorbent, drew scientific attention only as recently as the 1990s. In the early 1980s, microbiologists had already observed that microbial cells had the ability to concentrate, in their cellular mass, metals that existed in dilute concentrations in their aqueous environment. In an indirect way, biosorption of metals was being used by microbiologists in the process of staining microbial cells in order to increase their electron density, so they could be better studied under the electron microscope (Tsezos, 2001). The increasing awareness and concern about the environment in the 1970s stimulated research for new technologies to treat waste waters polluted by metals. The demand for inexpensive remedial technology led researchers to utilize the accumulating ability of microbial biomass to biosorb metals from aqueous solutions. This formed the

background for the design of novel waste water treatment processes using biomass (Tsezos, 2001).

As a result of these microbiological observations, biosorption began to be applied, and developed with the application of mostly microbes like bacteria, yeast and moulds as biomass for metal biosorption (Vieira and Volesky, 2000). Despite being long recognized as a good accumulator of metals, crab shell has only been recently been discovered to perform well as a biosorbent material (Lee *et al.*, 1997; An *et al.*, 2001) for a broad range of metals.

The quantitative foundation for comparing any sorption process is the relatively simple batch equilibrium contact experiment (Vieira and Volesky, 2000). Batch studies provide a measure of the biosorbent (biomass) metal uptake at equilibrium. The equilibrium metal uptake and concentration relationship is normally expressed by the conventional sorption isotherm curve. Among the common adsorption isotherms applied to many biosorption data are the Langmuir and Freundlich adsorption isotherm model (explained in Section 4.1.1). The feasibility of using particular biosorbent materials to remediate waste water is assessed via a flow-through column study, from which a breakthrough curve is normally plotted as a means of expressing the results.

Among various biomasses tested, crustacean carapaces appear to represent economically attractive materials for the removal of heavy metals (cadmium, zinc, copper and lead) from industrial effluent (Boukhlifi and Bencheikh, 2000). Chitin, a natural biopolymer found in crustacean shells, is able to bind and therefore remove metals from a solution (Boukhlifi and Bencheikh, 2000; Vijayaraghavan *et al.*, 2004). Apart from a very fast adsorption, the use of crustacean shells has become especially advantageous due to its rigid nature, because the metals can then be recovered from the shells during a desorption process. The rigidity of the shell also confers another advantage, as it allows the recovery of precious metals particularly from the effluent of specialized industries (Boukhlifi and Bencheikh, 2000).

It has been recently discovered that crab shell also has the potential for removing heavy metal ions (Lee *et al.*, 1997; An *et al.*, 2001). Vijayaraghavan *et al.* (2004)

identified crab shell as a suitable biosorbent for the continuous removal of nickel(II) ions from aqueous solution. Chitin and $CaCO_3$ components of the shell were postulated to be playing the key roles in the removal process. $CaCO_3$, the major component of a crab shell, forms a strong metal- CO_3 precipitate and complexes with chelating agents, e.g. the chitin (Patterson *et al.*, 1977 in Lee *et al.*, 1997). Lead from aqueous solutions was taken up by the crab shells by dissolution of $CaCO_3$, followed by adsorption of the microprecipitates onto chitin on the shell surface (Lee *et al.*, 1997). The adsorption occurred rapidly and was normally complete within 2h. The crab shell also showed preference for certain metals compared to the others. For instance, the affinity for cadmium was lower than for chromium and lead (Kim, 2003). In contrast to these findings, knowledge about the biosorption of manganese is almost non-existent. For this reason, a study has been carried out to determine the ability of carapace particles from *Liocarcinus depurator* to remove Mn from aqueous solutions using a packed-bed up-flow column (see Section 4.1 – aims).

1.5.1 Some factors affecting biosorption

Biosorption performance of any biosorbent is generally influenced by several factors. The pH is an important determinant in the biosorptive process since it affects the chemistry of the metals, the activity of the functional groups in the biosorbent and the competition of metallic ions (Galun *et al.*, 1987). Temperature also affects biosorption to a certain degree whereas a temperature between 20-35°C does not influence biosorption performance (Aksu, 1992). Biosorption in some cases can be selective (even though biomass are broad-ranged) and the removal of one metal may be influenced by the presence of other metals (Veglio and Beolchini, 1997).

The biomass concentration in solution seems to influence the specific uptake. The uptake might be explained by the number of sites existing in the biosorbent material, the accessibility of the sites, their chemical state (i.e. availability) and the affinity between site and metal (i.e. binding strength) (Vieira and Volesky, 2000). In both batch and column biosorption processes other factors, including metal

concentration, competing ions and particle size of the biosorbent, also play an important role in determining biosorption performance (Bailey *et al.*, 1999).

1.6 Aims of the study

Based on the considerations above, the aims of this study relate both to the biomonitoring potential of *L. depurator* for Mn in the Scottish inshore waters and in UK monitoring programmes, and to the ability of crushed carapace to remove Mn from aqueous solution in a biosorption column system.

As this crab is a common member of the benthic fauna both in the Clyde Sea area, and in adjacent sea lochs, such as Loch Fyne, where there is natural enrichment of Mn in the sediments, an opportunity is provided to field-test the suitability of *L. depurator* as a biomonitoring species for Mn. The Mn concentration in the crabs might be expected to reflect the spatial ambient Mn concentrations, and thus the macroscale natural exposure of their environments. Since the crabs spend most of their time resting on the sediment, and seldom burrow themselves, it is also likely that their accumulations will reflect the availability of Mn in the bottom water.

As this crab is also found in abundance as a bycatch in the fisheries in these areas, and is normally discarded to the sea, the potential of using the shell material from this bycatch species for beneficial purposes, to remediate polluted water, has been explored. These aims have been achieved by addressing the following specific objectives, which will be described in the five following chapters.

In Chapter 2 the concentrations of Mn in the tissues of the harbour swimming crab *Liocarcinus depurator* (L.) from two localities (Loch Fyne and the Clyde Sea area, Scotland) are compared, and the potential of this species as a biomonitor for Mn is evaluated. The results are compared to the observations of the established biomonitoring species *Carcinus maenas*.

In Chapter 3 the accumulation and retention of Mn by *L. depurator* is determined for various body tissues and under different controlled exposure and depuration conditions. In particular, the use of the exoskeleton of autotomized legs to represent Mn accumulation in the whole exoskeleton of a crab is established.

In Chapter 4 the ability of carapace particles from the swimming crab *L. depurator* to remove Mn from aqueous solutions in a biosorption column system has been studied. The breakthrough curves generated from this series of experiments provide an indication of the sorption capacity of the crab carapace particles. These properties are compared with those of the Norway lobster, *Nephrops norvegicus.*

Chapter 5 describes the basic morphology of the dorsal carapace and gills of *L. depurator*, and in Chapter 6 the form and site of Mn deposition onto both the intact carapace of *L. depurator* and onto Mn-biosorbed carapace particles are analysed using the technique of scanning electron microscopy combined with energy dispersive x-ray analyses (SEM-EDX).

In a final discussion chapter (Chapter 7) the relationships between the observations in live *L. depurator* and the results of the experiments on isolated exoskeletal materials carried out in individual chapter is established. The results were also compared to some major works on the related topics, both supportive and contradictory. The potential application of *L. depurator* in biomonitoring and biosorption aspects and its comparability with established ones is also addressed.

2 Manganese in the swimming crab *Liocarcinus depurator* (L.) and the shore crab *Carcinus maenas* (L.) from Loch Fyne and the Clyde Sea area, Scotland

2.1 Introduction

Loch Fyne is one of more than a hundred sea lochs on the west of Scotland. It is separated from the sea by a very shallow sill that limits water exchange, leaving the bottom water in particular with an increased metal burden. The metal is initially supplied to the loch through sedimentation of riverine oxidized material (Overnell *et al.*, 2002). As a result of the geology of this area, it experiences natural elevation of manganese concentration. The sediment contains ~1 to 4.5 wt% manganese, whereas the pore-waters contain an elevated concentration of ~250 to 600µM (13.7-33.0 ppm). These two values are well above the levels measured in other manganese-rich sites elsewhere (Bartlett *et al.*, 2007). Due to biogeochemical processes, these Mn-rich sediments release solubilised Mn into the bottom water in the form of Mn^{2+} (Oweson *et al.*, 2006). In a fjiordic loch such as Loch Fyne, this could be potentially exarcebated by eutrophication, which increases the oxygen demand from sediments and leads to an increase in the soluble forms of Mn in the bottom water (see Sect. 1.2) although there are no reports of this occurring.

In comparison, the Clyde Sea area has a lower manganese concentration due both to its geology and its location closer to open sea. Moreover, a greater renewal of water in the area also prevents eutrophication and thus minimizes the incidence of high Mn concentrations in the bottom water.

It has been extensively reported that decapod crustaceans accumulate metals including manganese, particularly those living in contaminated areas. Crabs, being

abundant and relatively immobile have been used as biomonitors for a range of metals in aquatic environments. (Sect. 1.3: Biomonitoring of metals). One of the crab species found in abundance in both Loch Fyne and the Clyde Sea area is the swimming crab *Liocarcinus depurator* (L.). It inhabits the sublittoral zone on fine, muddy sand and gravel with full salinity at a depth between 5-300m (Hill, 2003). It is present in 90% of lobster trawls in the Clyde Sea area (Wieczorek *et al.* (1999) in Bergmann *et al.*, 2002) which agrees with a report that it is one of the most important bycatches of the Mediterranean demersal fishery (Abello, 1989). Despite bearing similar characteristics and behaviour to other biomonitor crabs, *L. depurator* has so far attracted less attention as an indicator species. Owing to the fact that it appears in most commercial fish and lobster catches, *L. depurator* has the potential to be a useful biomonitor for manganese in the related fishing grounds.

Another crab species that inhabits both Loch Fyne and the Clyde Sea area is the shore crab *Carcinus maenas* (L.), which is one of the most extensively studied decapod species in relation to metal monitoring. It can be found on all types of shore from high water to depths of 60m in the sublittoral and tolerates a wide range of salinities. In contrast to *L. depurator*, *C. maenas* is predominantly a shore and shallow water species (Neal and Pizzolla, 2006). However it may also venture into deeper water, as it is sometimes caught in lobster trawls within these areas.

This study was carried out with two objectives: i) to compare the concentrations of manganese in the tissues of the swimming crab *Liocarcinus depurator* (L.) and the shore crab *Carcinus maenas* in two adjacent areas, Loch Fyne and in the Clyde Sea area which differ in their Mn levels due to geochemical factors (rather than to eutrophication), and ii) to investigate the potential of *L. depurator* as a biomonitor for the metal in Scottish waters. *L. depurator* was chosen due to its abundance in the area, and also because, as benthic organisms, they spend most of their time within the bottom water where manganese is directly released from the sediments. *C. maenas* was chosen as a reference species as it is an established biomonitor for metals.

2.2 Materials and Methods

A total of 247 swimming crabs, *L. depurator* (100 females, 147 males) with carapace widths ranging between 43-52mm were obtained from Loch Fyne (around $55^o55'N$ $5^o22'W$, depth 50-150m) and from the Clyde Sea area (around $55^o40'N$ $4^o56'W$, depth 50-150m). The locations are shown in Figure 2-1. A total of 38 shore crabs *C. maenas* (57-82mm) were creeled closer to the shore in both areas. The crabs were collected between November 2004 and May 2005.

2.2.1 Tissue preparation

The crabs were sacrificed by placing them in a freezer (-20^oC) for 3h. Five tissue samples were removed from each individual: dorsal carapace, gills, hepatopancreas, crusher claw muscle, and gonads. The dorsal carapace was wiped clean of any dirt on the outer surface, and any residual material on the internal surface was removed. The samples were collected in pre-weighed glass vials and the wet weight of each tissue was recorded. The tissue samples were then freeze-dried (Edwards Modulyo) for 24h and the tissue reweighed to obtain the dry weight.

Manganese determination was carried out on the dried samples from each individual. The data were compared between locations, sexes and among different tissues.

2.2.2 Manganese measurement

Samples of 100-300mg of the dried tissues were transferred to acid-washed 50ml conical flasks and were digested following a standard method. A volume of 10ml of Analar concentrated nitric acid (70%, trace analysis grade, Fisher) was added to the flasks and they were heated at 200^oC on a hotplate for several hours until the

tissues had completely dissolved. The remaining solution was then made up to 10ml by adding distilled water. The 10ml final solution was used to determine the manganese concentration using flame atomic absorption spectrophotometer (Philips PU9200). A calibration curve was constructed by analyzing standard solutions of 1.25, 2.50 and 5.00ppm manganese (Mn AAS standard solution, Aldrich). The samples were checked against TORT-2 (lobster hepatopancreas reference material for trace metal, National Research Council Canada). The concentration of the metal in the digested sample was then expressed as μg Mn.g^{-1} dry tissue.

2.2.3 Statistical analysis

Using the statistical package Minitab 13, the differences between the different tissues and the different samples were determined using one-way ANOVA. The differences between the two locations and between sexes were determined using t-tests. Significance was accepted at $p < 0.05$.

2.2.4 Validation of sample processing and measurement protocols

Manganese measurement using an atomic absorption spectrophotometer (Philips PU9200) in tissues of a crab is the major protocol used throughout this project. Therefore, a few standard methods including acid digestion with nitric acid, calibration of the AAS machine and the use of standard solutions were validated prior to making the measurements on real samples in order to ensure a valid data set. The impact of different sample handling procedures such as scrubbing and grinding on Mn concentrations especially of the carapace was also investigated.

2.2.4.1 Validation of digestion protocol

Four female crabs were sacrificed by freezing (-20°C, 3h). The gonads and hepatopancreas were retrieved and placed in separate glass vials. These tissues were used as they provide large amounts for each animal and thus could be divided into 3-4 similar portions for parallel digestion. These tissues were freeze dried for 24h. Each freeze dried sample was then divided into similar portions weighing between 100-300mg each. Each portion was digested following a standard method in separate acid-washed 50ml conical flasks as described in Section 2.2.2.

2.2.4.2 Validation of AAS protocols (the need for frequent calibration of the machine)

Calibration of the AAS was carried out using Mn standard solutions. Three standards (1.25, 2.50 and 5.00ppm) were prepared by pipetting 125, 250 and 500µl of Mn standard solution for AAS (Fluka) into 100ml volumetric flasks. Distilled water was then added to make up to volume.

Twelve dorsal carapaces were rinsed in distilled water and were freeze dried. Approximately 200mg of each sample was then acid digested following a standard protocol as in Section 2.2.2. The final 10ml solutions of the digested samples were then measured for manganese using AAS. In the first trial, the AAS machine was calibrated using Mn standards prior to the measurements. No other calibration was done thereafter until the end of the measurements. Mn concentrations were repeatedly measured (5 times) in all the samples. The measurements were done on sample 1, followed by sample 2, 3 until 12. This was repeated until 5 measurements were obtained giving readings 1-5 for samples 1-12.

In the second trial, the AAS machine was calibrated, then Mn concentrations in samples 1-12 were measured. Then the machine was calibrated again, and the measurements were repeated in the same manner. These steps were repeated until 5 Mn readings were obtained (reading 1-5) for every sample.

The results are expressed as the percentage each measurement differed from the first measurement (% deviation), calculated follows:

$$\% \text{ deviation} = \frac{(\text{Reading X} - \text{Reading 1})}{\text{Reading 1}} \times 100$$

2.2.4.3 Manganese measurements using old and new standards (the life of Mn standards)

As a routine procedure, 100ml of Mn standard solutions of 1.25, 2.50 and 5.00ppm were prepared prior to measurements on AAS machine. Normally, these standards would also be used for later measurements. In this section, Mn concentrations in 103 samples of various crab tissues were measured by calibrating the AAS machine using both old (more than a month old) and new standards (less than a week). The measurements were carried out by repeating the calibration after 12-15 samples, first using the old Mn solutions followed by newly prepared ones. The readings were plotted against each other and a regression line was generated.

2.2.4.4 Effect of scrubbing and grinding the samples on Mn concentrations

Measuring Mn in the carapace was one of the main procedures used in this project. Therefore, in this section, the effect of scrubbing the outer surface and grinding the dried materials on the concentrations of Mn measured was investigated.

In order to investigate the need to scrub the sample during preparation, 17 dorsal carapaces were divided into halves. The right sides were thoroughly brushed and rinsed twice with distilled water, while the left sides were wiped with a piece of clean paper towel to wash away all debris or sediment that might have deposited onto them. Both sides were then freeze dried, digested and measured for Mn concentration.

In most cases, only a fraction of the dorsal carapace was used for Mn measurements, while the remaining was kept for other purposes including electron microscopy, biosorption experiments etc. Due to the rugged surface of the carapace, there was concern that Mn concentrations measured might depend

largely on the part selected for measurement. The ridges on the surface might also collect more Mn compared to smoother areas. To investigate the importance of grinding the dorsal carapace in order to generate homogeneous samples, 10 dorsal carapaces were freeze dried. For crabs 1-7, the carapace was divided into 4 pieces of about the same size (samples 1-4). The pieces were acid digested in separate conical flasks and the Mn concentration was determined. For crabs 8-10, the dried carapace was first ground into powder using a mortar and pestle. The powder was then divided into similar portions (samples 1-4), acid digested and measured for Mn separately. The data were expressed as the percentage of the deviation from the concentration in sample 1 for each crab carapace.

2.3 Results

2.3.1 Validation of AAS protocol

Digestion: Parallel digestions of portions of the same tissues yielded similar concentrations (Table 2-1). Hepatopancreas 2 and 3 showed a substantial variation ($3.87\pm0.755\,\mu gMn.g^{-1}$, range $2.47\text{-}5.98\,\mu gMn.g^{-1}$; and $6.26\pm0.743\,\mu gMn.g^{-1}$, range $4.20\text{-}7.48\,\mu gMn.g^{-1}$, respectively). However, the concentrations in the other tissue samples showed only minute fluctuation of less than $1\mu gMn.g^{-1}$. The variation seen in hepatopancreas 3 and 4 might be due to the small amount used to make up each portion which was less than 150mg. These results confirm that complete digestion was achieved, and that Mn concentration measured in one part of the soft tissues could be used to represent the concentration in the whole organ. This is especially true if the amount used could be maintained at ≥200mg for any digestion.

Calibration: Figure 2-2 shows how much the Mn concentrations measured on the second to the fifth time differed from the first measurements for each sample. The difference is expressed as percentage deviation from Reading1. The measurements were observed to decrease and by the fifth measurements, the Mn concentration was measured approximately 5-17% lower than the first measurements. However,

when calibration was repeated every 12 samples, the Mn concentrations measured in the same samples were more stable and remained well within ±5% of Reading1 (Figure 2-3). Therefore, repeated calibration is crucial in order to obtain a more reliable data set for Mn measurements particularly when dealing with large number of samples.

Standard solutions: Mn concentrations in the samples measured using old standard solutions proved to be proportionately lower (linear regression, R^2=0.9923) compared to the newly prepared ones (Fig. 2-4). Data obtained using old standard solutions could safely be corrected by multiplying it by a factor of about 1.4 as shown in Figure 2-4.

Scrubbing: Figure 2-5 shows the Mn concentrations in scrubbed and unscrubbed carapace. There was no significant difference between scrubbed (43.90±5.97 μgMn.g^{-1}, range: 12.04-174.16 μgMn.g^{-1}) and unscrubbed samples (48.02±7.98 μgMn.g^{-1}, range: 8.33-131.03 μgMn.g^{-1}) (t-test, p=0.682). Therefore, wiping with clean paper towel is sufficient to remove deposited materials on the carapace. In this section, an assumption was made that both sides of the crab (left and right) contain similar amount of Mn within the dorsal carapace as the structures are purely mirror image of one another.

Grinding: Figure 2-6 shows that ground samples of the same crab carapace (7-10) gave similar Mn concentrations; in this case the difference between the values remain lower than 5%. Carapace samples 1-6 showed a greater variability between the readings which was generally between 10% to as high as 60%. This observation indicates the uneven distribution of Mn within the dorsal carapace. Therefore, simply taking a small piece to measure the concentration of the metal could not represent the real concentration of the whole tissue. Grinding provided a more homogenous sample.

2.3.2 Manganese concentrations in different batches of Liocarcinus depurator

The manganese concentrations in tissues collected on the different sampling occasions were compared. The data were analysed separately according to the sexes and locations (Tables 2-2 and 2-3). For four of the tissues, there was no significant difference between the batches obtained on the different sampling occasions (ANOVA, p>0.05) and so the data for each of these were pooled as a single mean to represent each location. For the crusher claw muscle, manganese was found to differ significantly between the different batches for both locations and for both sexes (Loch Fyne; t- test, p-values=0.003 and 0.027; and the Clyde sea area; ANOVA, p-values=0.031 and 0.023 for the male and female respectively). The data also indicate that the crabs for each batch in both locations were homogenous in size (ANOVA, p-values=0.127 – 0.950), this suggests that the impact of size on the manganese concentrations in these individuals could be neglected.

Due to these findings, the data for manganese concentrations from different sampling occasions were pooled for further comparisons between locations.

2.3.3 Manganese concentration in Liocarcinus depurator from the Clyde Sea area and Loch Fyne

Figure 2-7 shows the manganese concentration in the different tissues of male and female *L. depurator* respectively from Loch Fyne and the Clyde Sea area. The female groups from Loch Fyne (carapace width, CW=43.72±0.60mm) and the Clyde Sea area (CW=43.85±0.45mm) were homogenous in terms of size (t-test, p-value=0.872), whereas the males from Loch Fyne (CW=47.82±0.40mm) were slightly larger than those from the Clyde Sea area (CW=44.79±0.80mm) (t-test, p-value <0.05). However, the difference could be ignored as the calculated R^2 was only 8.7%.

There were significant differences in the manganese concentrations between the tissues in animals from each site (ANOVA, p-value <0.001 for all groups). The two exoskeletal tissues (carapace and gill) were found to have the highest concentration of manganese (>100µg Mn.g^{-1} dry tissue) compared to the other tissues. Of the other tissues measured, the highest Mn concentration was found in the hepatopancreas, and the lowest concentrations were found in the crusher claw and the gonads (< 25µg Mn.g^{-1} dry tissue). The same trend was observed in both males and females, although the manganese concentrations within the individual tissues of females tended to show greater variability than in males (as demonstrated by the high SE values).

The manganese concentrations in all tissues were found to be significantly higher in crabs from Loch Fyne than in those from the Clyde Sea (ANOVA, p-values= <0.001–0.008 for males, <0.001–0.009 for the females). The difference is especially apparent in the two exoskeletal tissues i.e. the carapace and the gills. However, the R^2 values for the carapace are the largest of 43.58% and 47.87% for both the male and female groups, respectively, with manganese measuring around 3.6 and 4.5 fold higher in crabs from Loch Fyne than in crabs from the Clyde Sea area.

2.3.4 Manganese concentrations in Carcinus maenas *from Loch Fyne and the Clyde Sea area*

The manganese concentrations in five tissues of *C. maenas* from both areas are shown in Figure 2-8. A similar pattern of concentration differences between the tissues and locations to that seen in *L. depurator* was observed, although at a lower magnitude. The concentration of manganese was significantly higher in all tissues in male crabs from Loch Fyne compared to the Clyde Sea area, except for the hepatopancreas (t-test, p-values= <0.001-0.023). The highest concentration was in the exoskeletal samples (carapace and gills), followed by the hepatopancreas, while the lowest occurred in the crusher claw muscles and the gonads. A similar pattern

occurred in the female groups, although they were not statistically significant (t-test, p-values= 0.151-0.892).

2.4 Discussion

The objective of this study was to determine the manganese concentrations in the tissues of the swimming crab *Liocarcinus depurator* from Loch Fyne, a site with manganese concentrations as high as 10ppm (Calvert and Price, 1970) and the Clyde Sea area which has a much lower manganese concentration. *L. depurator* was found in abundance at both locations, and could be easily sampled all year in the bycatches of lobster trawl fisheries in the two areas. Despite its name, this crab is relatively sedentary, spending most of its time resting on the bottom sediment surface. As it bears the characteristics required for an indicator organism, its potential as a biomonitor of environmental manganese in the Scottish inshore waters was investigated. The trend of accumulated manganese in *L. depurator* was compared with an established crab biomonitor, the shore crab *Carcinus maenas* which was also obtained at both study locations.

2.4.1 Manganese concentration in crabs from different locations

Significantly higher manganese concentrations were found in all tissues (dorsal carapace, gills, hepatopancreas, gonads and crusher claw muscles) of crabs from Loch Fyne compared to those collected from the Clyde Sea area. These differences in manganese concentrations, especially in the carapace and the gills, might indicate the different levels of exposure to the metal in their natural environments. This finding is not surprising as several other studies have obtained similar results.

This study confirms that uptake of Mn will take place from sea water with elevated Mn concentrations under normoxic conditions. More pevious studies of environmental uptake (as distinct from laboratory exposures) have examined eutrophic events, where reducing conditions have been causal to the elevated Mn in the bottom water. The choice of Loch Fyne and the Clyde Sea area allowed a comparison to be made of the effects of different ambient Mn concentrations in the absence of the hypoxic conditions.

The Norway lobster *Nephrops norvegicus* has been established as a bioindicator of marine manganese contamination (Baden *et al.*, 1995). Individuals from 'contaminated' sites (Skagerak and Kattegat, Sweden) were found to show higher concentrations in the tissues compared to those collected from sites having much lower manganese concentrations (Faroe Island). Baden and Neil (2003) reported that manganese accumulation in the exoskeleton (carapace and other appendages) increases with the duration of exposure and with exposure concentration. The concentration remained high even after the animals were transferred to undosed water for three weeks. Their observation highlights the contrast between the nature of accumulation of manganese in the exoskeleton and the accumulation in internal tissues. In the latter, manganese is regulated, so that its concentration is limited, and it also has a relatively rapid elimination (Baden *et al.*, 1999). *Liocarcinus depurator* shows a similar trend, as a greater difference could be observed between the exoskeletal tissues (dorsal carapace and gills) in animals from Loch Fyne and the Clyde Sea area compared to other internal tissues.

Metal accumulation processes in crustaceans have been observed to vary not only between families, but also between closely related species (Rainbow, 1990), and therefore extrapolating the results in Norway lobsters to other decapod species should be made very cautiously. In this study, the observations made for *Carcinus maenas* collected from the shore at the two locations also show higher concentration of manganese in Loch Fyne waters compared to the Clyde Sea area. MacFarlane *et al.* (2000) reported higher concentrations of lead in a semaphore crab *Heloecius cordiformis* from contaminated river estuaries in Australia. The ability to indicate environmental metals, particularly manganese, was also shown in the freshwater crab *Potamanautes warreni* in Africa (Steenkamp *et al.*, 1994), in the

rock crab *Cancer irroratus* from Canada (Chou *et al.*, 2002) and also in marine crabs such as *Callinectes sapidus* from North Carolina (Weinstein *et al.*, 1992). These worldwide findings from a variety of habitats suggest that crabs have great potential as biomonitors for environmental metals. The observations in the Scottish waters therefore add another species to this list.

2.4.2 Manganese concentration in different sexes and tissues

From this survey, manganese concentrations were significantly elevated in crabs from Loch Fyne. However the manganese concentrations were also found to vary between the sexes, an observation that led us to treat the data separately according to sex. This finding is in agreement with MacFarlane *et al.* (2000) who reported higher accumulation of metal in the hepatopancreas of female *H. cordiformis* compared to males. In the same study, accumulation of metal was also found to be size-dependant, with smaller males accumulating relatively more lead than larger males. However, no comparison can be made with the present data in terms of size, due to the homogenous size of the crab samples.

Although manganese concentrations in the tissue samples from crabs from Loch Fyne were significantly higher compared to those from the Clyde Sea area, they were found to be in the same decreasing order of: the exoskeletons (carapace, gills) > hepatopancreas > gonads and crusher claw muscle. High concentrations in the exoskeleton have been widely reported by other researchers. In the marine lobsters *Homarus vulgaris* (Bryan and Ward, 1965) and *Nephrops norvegicus* (Baden *et al.*, 1995), the exoskeleton bears 98% of body manganese content. The metal is incorporated in the calcium carbonate of the exoskeleton (Baden *et al.*, 1994) where it is thought to be detoxified (Baden *et al.*, 1995).

Eriksson (2000) reported that the manganese concentration in the hepatopancreas and muscle tissue of Norway lobsters, *Nephrops norvegicus* was constant and less affected by environmental exposure, but the concentrations in the gills increased in response to the increasing manganese exposure concentrations. Baden *et al.*

(1995) reported very high concentrations of manganese in the exoskeleton of *N. norvegicus* after exposure to this metal. The authors of both papers suggested that the high concentrations of manganese in the exoskeleton were partly attributable to surface adsorption. Another factor in this greater uptake is that both the gills and the carapace (that made up the exoskeleton) are directly exposed to the environmental manganese compared to other soft internal tissues.

The differences in the concentrations of manganese in the tissues found in this study might be explained by the different sources of manganese to which the crabs were exposed. Metals taken up by crustaceans from solutions tend to accumulate mainly in the gills and the exoskeleton (Brouwer *et al.*, 1995), whereas metals taken up from diet tend to accumulate in the hepatopancreas and in the muscles (Canli and Furness, 1995). Manganese in particular, if taken up from solution might never enter the muscle tissues, but only remain in the haemolymph as it is being transported for detoxification or excretion (Baden *et al.*, 1994). As the data here show high concentrations in the exoskeleton, it might be safe to assume that the manganese measured in *L. depurator* in Loch Fyne and the Clyde Sea area is indicative of the bioavailable manganese in the surrounding water, which fits precisely the purpose of the investigation.

2.4.3 Manganese concentration in tissues of crabs of different species

The general trend of manganese concentrations in the tissues of *L. depurator* matches well with that seen in *C. maenas* at both of the locations studied although the actual concentrations are lower in *C. maenas*. As *C. maenas* is already established as a bioindicator of certain metals in the water, and the fact that *L. depurator* also shows the same trend suggest that *L. depurator* might also possess the same ability to indicate manganese in the environment. The different concentrations observed in these two crab species might be attributable to the different habitats occupied by the two species: *L. depurator* occupies deeper water

down to a depth of 300m, whereas *C. maenas* inhabits shallower water (down to not more than 60m depth) and the rocky shores. Since manganese release from the sediment normally occurs at the interface between the sediment surface and the bottom water, it would be expected that *L. depurator* might be exposed to higher concentrations of bioavailable manganese than *C. maenas*, and this therefore leads to the higher concentrations measured in the tissues of *L. depurator*. If the observation of MacFarlene *et al.* (2000) on *H. cordiformis* that smaller individuals accumulate more metal than larger ones also applies to these two crabs, the smaller size of *L. depurator* (40-50mm) compared to *C. maenas* (63-77mm) might also contribute to the higher accumulation of manganese from the water in *L. depurator*. These results suggest that both species could indicate manganese levels in their specific habitats; *C. maenas* in the shallower water and *L. depurator* in the deeper inshore water.

2.5 Conclusions

This survey provides evidence that *Liocarcinus depurator* crabs collected from two locations having different manganese concentrations possesses different concentrations of manganese within their bodies. Manganese is significantly higher in all tissues of crabs from Loch Fyne compared to Clyde Sea area in both the female and male groups, suggesting that both sexes of this species do indicate manganese level in their environment. The metal content in the tissues differs significantly in the order of exoskeleton (carapace and gills) > hepatopancreas > crusher claw muscle and gonads, suggesting that exposed surfaces might be the major routes for manganese uptake in this species, and therefore are better indicators compared to soft tissues. The trend observed in *L. depurator* matches well with the established indicator species, *C. maenas* suggesting the great potential it holds as another biomonitor for manganese in the Scottish waters.

Table 2-1 Manganese concentrations in the hepatopancreas and gonads (μg Mn.g^{-1} dry tissue) of 8 crabs following parallel digestions

Tissue	Number of Replicate	Dry weight dissolved (g)	Mn concentration (μg Mn.g^{-1} dry tissue)	Average Mn ± SE (μg Mn.g^{-1} dry tissue)
Hepatopancreas 1	4	0.200-0.263	4.04-5.00	4.64±0.224
Hepatopancreas 2	3	0.163-0.209	3.68-4.78	4.19±0.321
Hepatopancreas 3	4	0.081-0.124	2.47-5.98	3.87±0.755*
Hepatopancreas 4	4	0.107-0.119	4.20-7.48	6.26±0.743*
Gonad 1	4	0.121-0.169	5.70-6.25	5.92±0.121
Gonad 2	3	0.203-0.244	4.43-4.92	4.69±0.141
Gonad 3	4	0.208-0.233	3.86-4.33	4.11±0.125
Gonad 4	4	0.228-0.288	4.51-5.79	5.20±0.262

*SEs indicate high variations in Mn concentrations among the replicates. This might be due to the smaller amounts used compared to other samples

Table 2-2 Manganese concentrations (µg Mn.g^{-1} dry tissue) in a range of tissues of *Liocarcinus depurator* from Clyde Sea area. Data (means ± SE) are presented for batches of crabs collected on different occasions during 2004 and 2005.

Batch	N	Carapace width (mm)	Carapace	Gills	Crusher claw muscle	Gonad	Hepatopancreas
Males							
Nov 04	2	46.00±6.00	33.29±2.92	29.18±2.17	7.93±1.48	-	17.76±0.65
Dec 04	10	45.56±2.14	54.70±9.76	84.90±18.0	5.68±0.87	6.90±4.28	20.62±2.11
Jan 05	26	44.36±1.31	48.88±5.86	77.20±12.3	5.33±0.86	12.17±2.64	23.05±2.+15
Feb 05	21	44.84±1.14	35.04±3.74	51.32±4.82	2.54±0.73	4.98±1.39	21.2±1.84
p-value		0.950	0.152	0.136	0.031	0.111	0.791
Females							
Nov 04	7	47.50±1.80	53.40±10.5	20.76±1.68	7.36±1.34	8.07±1.07	13.60±1.32
Dec 04	14	43.73±0.93	42.10±3.91	38.21±7.14	7.30±0.63	9.52±0.81	21.30±1.90
Jan 05	31	43.29±0.72	63.50±10.5	57.40±14.5	6.59±0.70	8.88±0.65	24.41±1.21
Feb 05	26	43.75±0.77	61.30±6.16	57.77±7.24	4.18±0.72	9.11±0.50	22.66±0.85
p-value		0.127	0.448	0.324	0.023	0.775	0.001

Statistical analysis: One-way ANOVA, significance accepted at p<0.05.

Table 2-3 Manganese concentrations (µg Mn.g^{-1} dry tissue) in a range of tissues of *Liocarcinus depurator* from Loch Fyne. Data are expressed as µg Mn.g-1 dry weight tissues (means ± SE) and are presented for batches of crabs collected in April and May, 2005.

Batch	N	Carapace width (mm)	Carapace	Gills	Crusher claw muscle	Gonad	Hepato-pancreas
Males							
April 05	19	48.17±0.74	135.30±7.72	123.10±14.90	18.87±3.31	18.02±1.61	23.60±2.70
May 05	73	47.73±0.46	168.40±10.30	128.30±11.00	10.71±1.08	13.56±1.25	41.84±5.78
p-value		0.651	0.114	0.821	0.003	0.087	0.113
Females							
April 05	4	44.75±1.67	167.40±18.00	43.19±8.11	38.57±8.86	11.71±1.93	38.45±5.84
May 05	27	43.57±0.65	277.90±34.50	112.5±23.80	17.88±3.65	11.68±1.51	105.80±21.60
p-value		0.518	0.235	0.278	0.027	0.993	0.247

Statistical analysis: t-test, significance accepted at p<0.05.
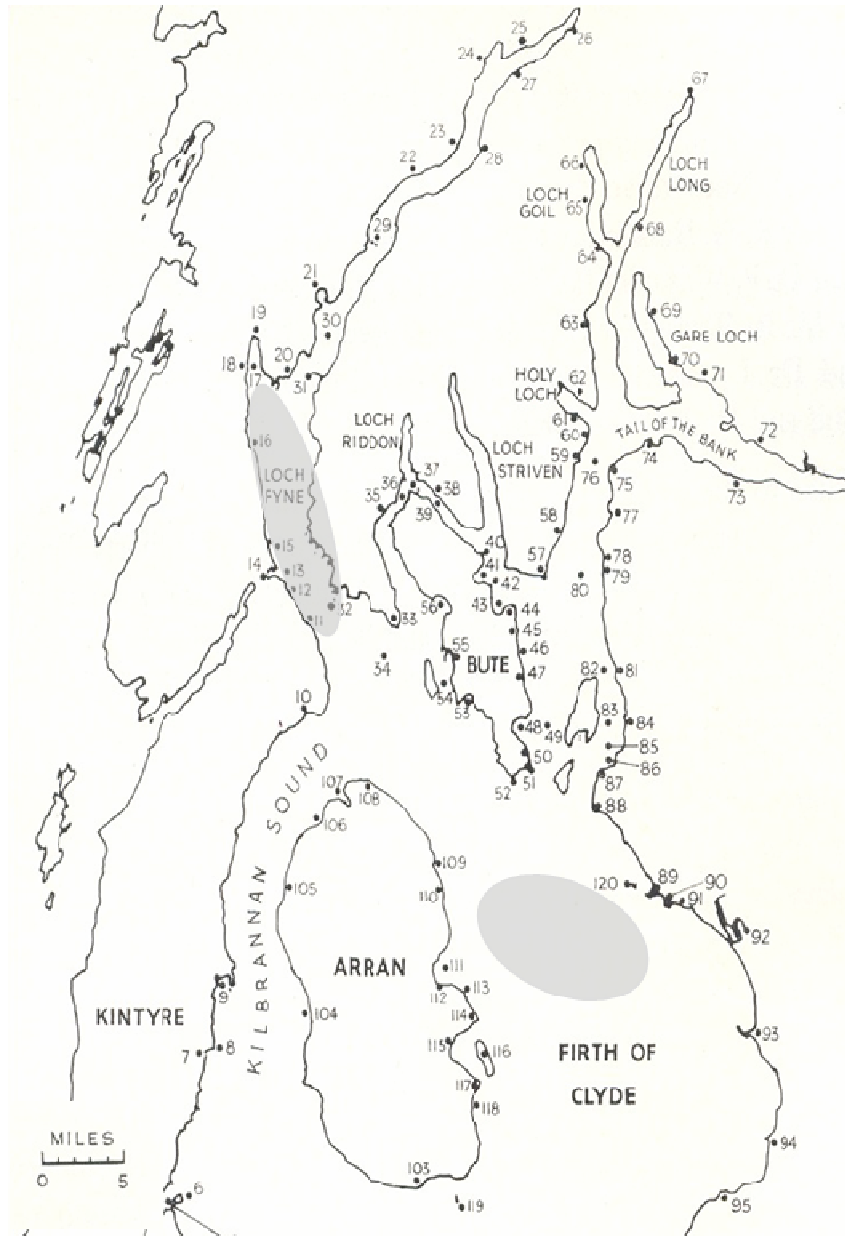
Fig. 2-1. Map showing the study areas Loch Fyne and the Clyde Sea area (shaded) from where the crab samples were collected. The map is from Allen (1967) with the numbers referring to their crustacea survey points.
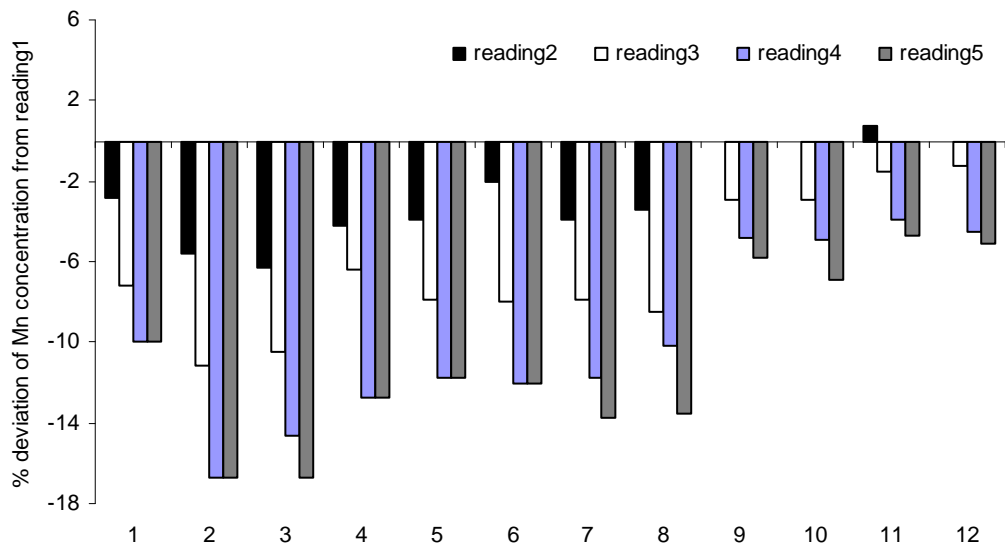
Fig. 2-2. Percentage difference of Mn concentrations of 12 samples measured on a first occasion and on 4 subsequent occasions thereafter. Calibration with Mn standard solutions was done only once at the beginning of the sequence.
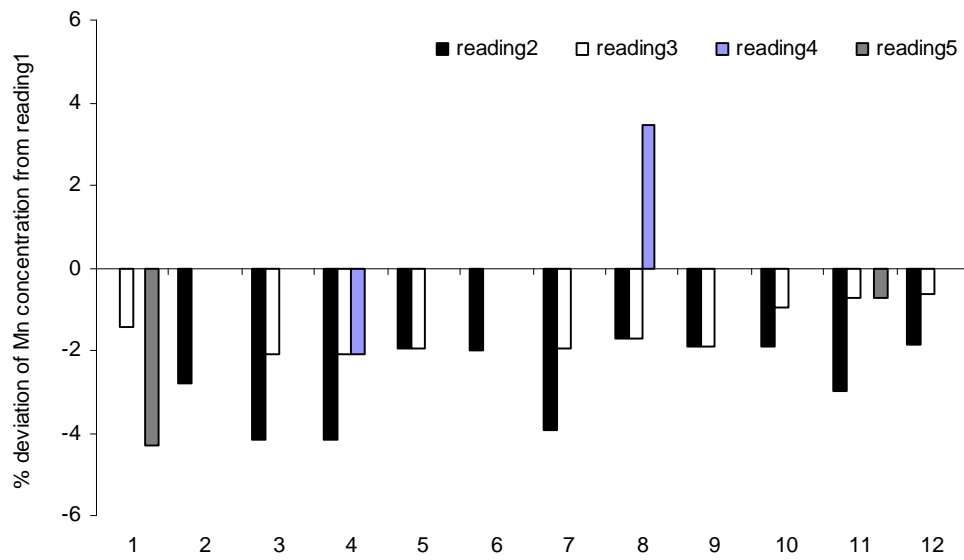
Fig. 2-3. Percentage difference of Mn concentrations of the same 12 samples as in Fig. 2-2 measured on a first occasion and on 4 subsequent occasions thereafter. Calibration with Mn standard solutions was done before taking readings 1, then was repeated before readings 2, 3, 4 and 5. Repeated calibrations brought the difference between reading1 and the subsequent readings down to less than 5%.
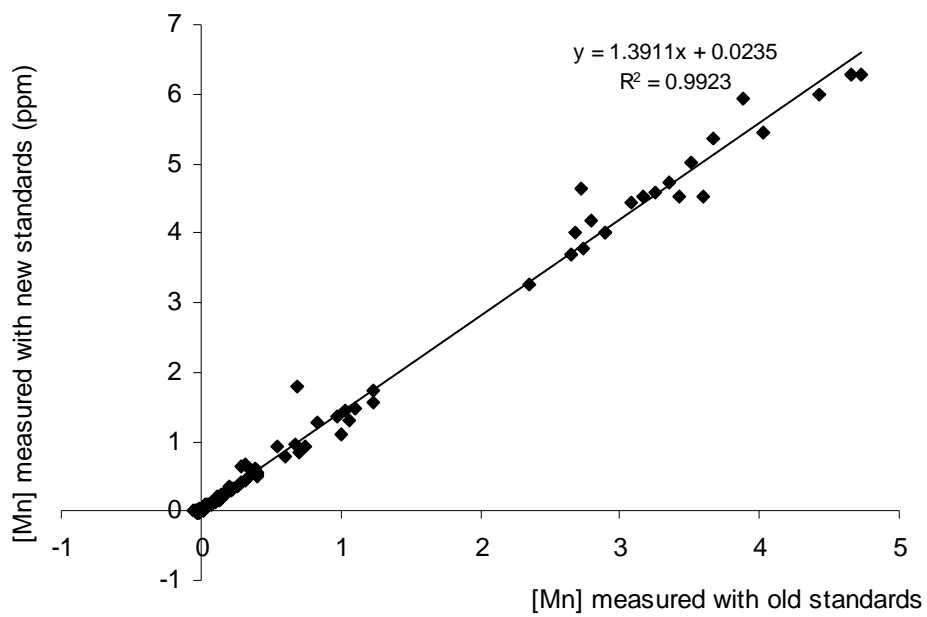
Fig. 2-4. Relationship between Mn measurements in the same samples measured using old (≥ a month) and newly prepared (≤ a week) standard solutions (n=103). The concentrations measured proportionately lower when old standard solutions were used to calibrate the AAS.
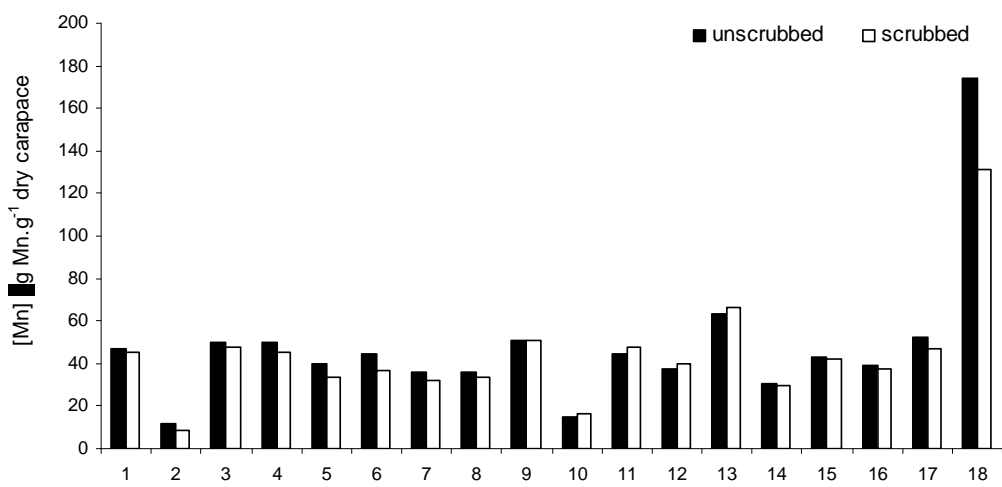
Fig. 2-5. Mn concentrations in the scrubbed and unscrubbed dorsal carapace of 18 crabs. The scrubbing was found not to affect the concentrations of the samples significantly (t-test, p=0.682)
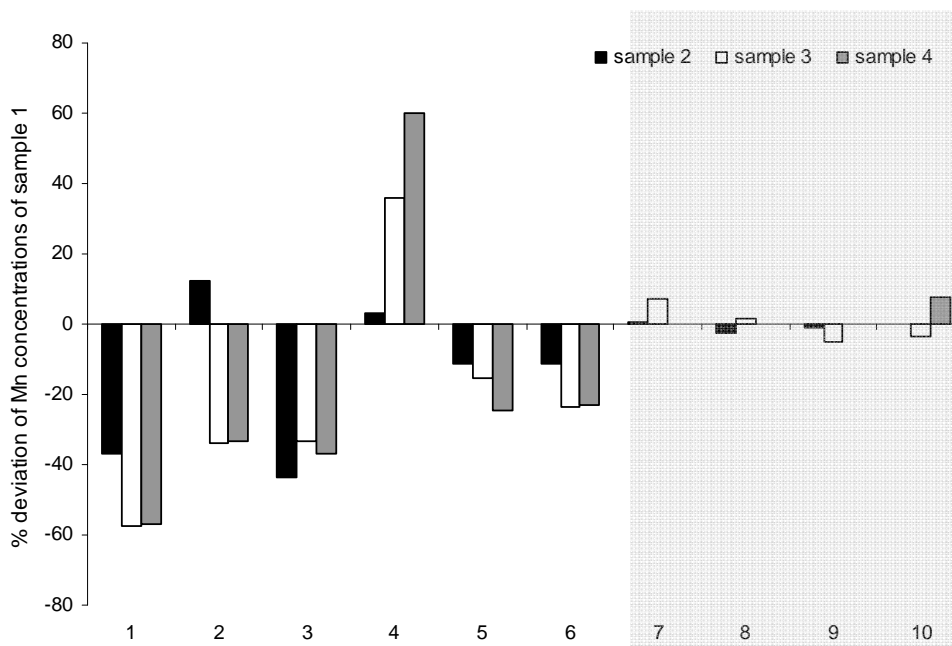
Fig. 2-6. Percentage difference of Mn concentrations in ground and non-ground dorsal carapace from the same individuals compared to sample 1. Samples of crabs 7-10 (shaded area) were ground to powder before being divided into samples 1-4. This made them more homogenous, and reduced the difference between the repeated measures to below 10%.
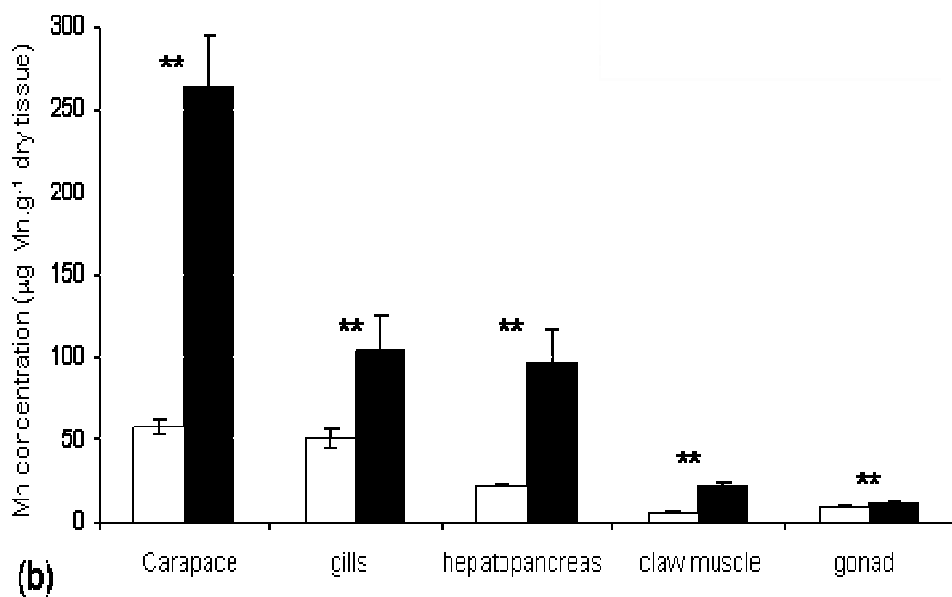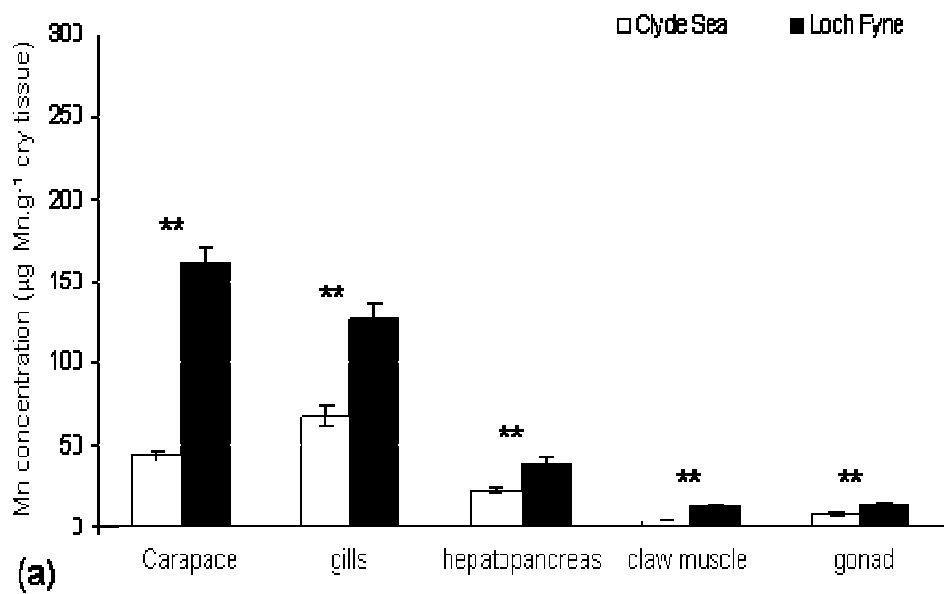
Fig. 2-7. Manganese concentration expressed as µg Mn.g^{-1} dry weight tissues (means ± SE) in various tissues of *L. depurator* from the Clyde Sea area and from Loch Fyne. (a) Males (N=92 and 59, respectively), and (b) Females (N=78 and 31, respectively). t-test, ** *P*<0.01.
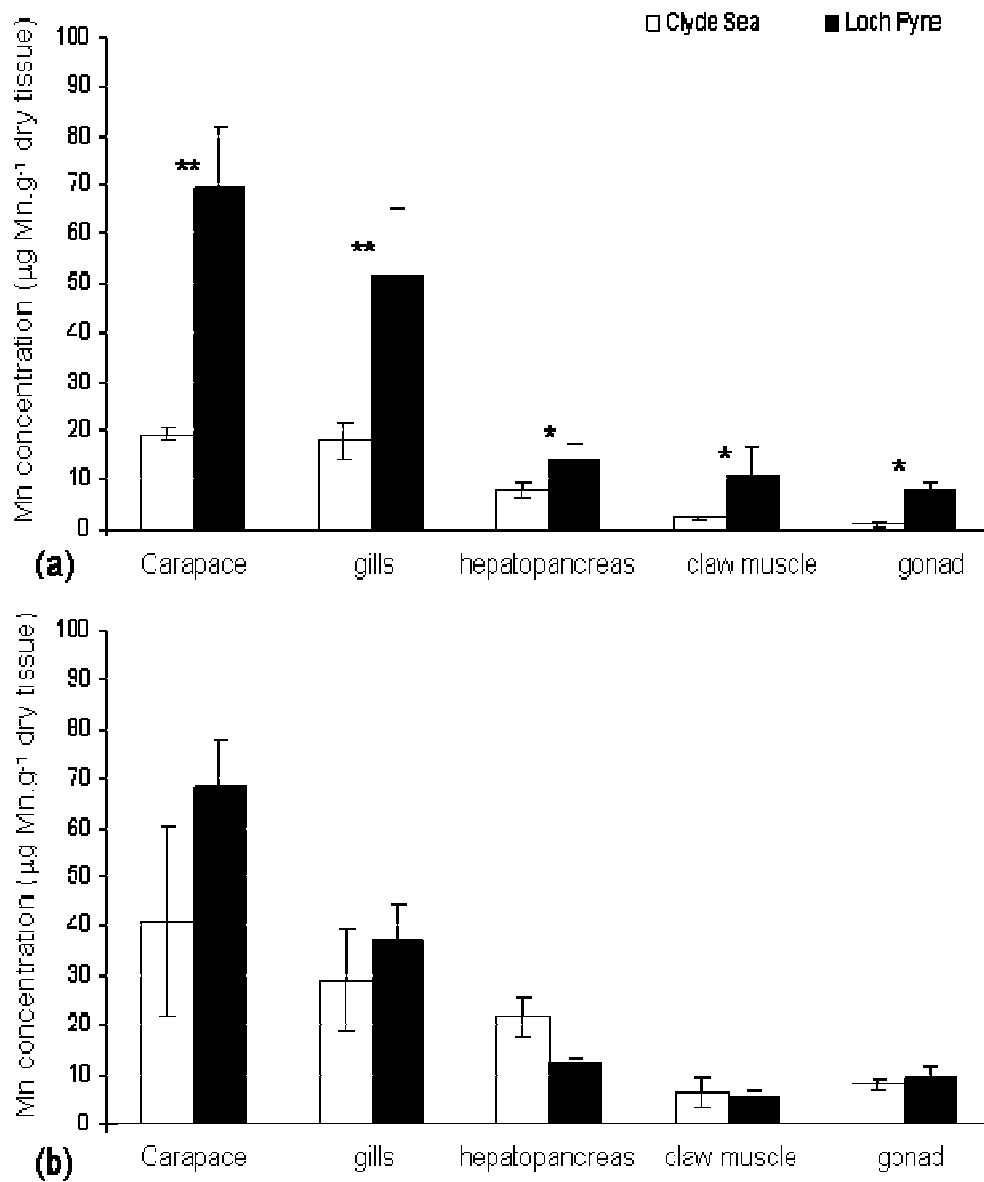
Fig. 2-8. Manganese concentration expressed as µg Mn.g⁻¹ dry weight tissues (means ± SE) in various tissues of *C. maenas* from the Clyde Sea area and from Loch Fyne. (a) Males (N=13 and 6, respectively) and (b) Females (N=13 and 6, respectively). t-test, * *P*<0.05, ** *P*<0.01.

3 Manganese accumulation and retention in *Liocarcinus depurator* (L.)

3.1 Introduction

In the previous chapter, high Mn concentrations were observed in the crabs *Liocarcinus depurator* captured from Loch Fyne, an area of higher Mn compared to the Clyde Sea, therefore suggesting that the metal might be accumulated within the crab from the surrounding sea water. This chapter describes a series of exposure experiments carried out under controlled conditions to confirm Mn accumulation by *L. depurator*. The fate of accumulated Mn within selected tissues was also investigated.

Manganese is an abundant metal in marine sediments. This sediment manganese could be released into the bottom water and become bioavailable especially during hypoxic events (Eriksson and Baden, 1998). Mn is essential to many metabolic functions in marine animals but in excess it can act as a neurotoxin (Baden *et al.*, 1995; Baden and Eriksson, 2006), and can bring about various other impacts such as shell disease or lesions in the blue crab, *Callinectes sapidus* (Weinstein *et al.*, 1992) and blackening or browning of the gills and carapace in the Norway lobster, *Nephrops norvegicus* (Baden *et al.*, 1990). A high Mn accumulation in the lateral antennule of *N. norvegicus* (Baden and Neil, 2003) could impair chemosensory function controlling food searching behaviour of the animal doubling the time taken to detect the odour of food stimuli (Krang and Rosenqvist, 2006). All these findings highlight the importance of treating Mn as any other xenobiotic metals that should be frequently monitored.

While some decapod crustaceans are able to regulate metals, and therefore have been little utilized as biomonitors, others were observed to be good accumulators of some specific metals. *Squilla mantis* (Blasco *et al.*, 2002) and the Norway lobster,

Nephrops norvegicus (Baden *et al.*, 1999; Baden and Neil, 2003) were found to be able to accumulate Mn in their exoskeleton. Despite the availability and easy sampling, especially in lobster fishery grounds in Scotland, reports of Mn in the swimming crab *L. depurator*, are scarce, if not lacking.

Based on the results from the previous chapter, coupled with other evidence of sex-difference in metal accumulation, the accumulation of Mn in the swimming crab *L. depurator* was investigated in the males only. Accumulation of the metal in the exoskeleton of individuals was monitored by measuring the increased concentrations in the walking legs by induced autotomy at a few sampling intervals.

Autotomy refers to voluntary shedding of a limb by the animal, which results in it being detached at the base. A pre-formed breakage plane exists at the base of each limb but is secured in an intact crab by a cuticular plug which bridges the plane on the antero-dorsal side. To achieve autotomy, this plug must be sheared away, a process accomplished by particular contractions in the levator muscles (McVean, 1976). In nature, crabs autotomize limbs which are badly damaged or seized by an attacker (Warner, 1977) and loss of body fluids following autotomy is prevented by an internal partition which remains behind a seal over the stump. This is soon supplemented by clotted blood which accumulates to form a scab. From our observation, the sealing of the injury occurs immediately, and a perfect scab was formed in less than 7d.

In this chapter, Mn accumulation by *L. depurator* after exposure to Mn-enriched sea water was determined. The impact of subsequent depuration in clean water on accumulated Mn in the crab was also investigated. The six identical walking legs were chosen to be the best organs to indicate temporal accumulation of Mn in an individual crab.

Below are the specific objectives of the experiments:
1. To justify the use of the exoskeleton of autotomized legs to represent Mn accumulation in the exoskeleton of a crab
2. To determine Mn accumulation in the exoskeleton and other tissues at different concentrations and exposure periods

3. To determine the Mn concentrations in the exoskeleton and other tissues after exposure to Mn followed by a period of depuration

3.2 Materials and Methods

This section involves three stages; i) a survey of Mn concentrations in the legs, ii) exposure to Mn in sea water (leg autotomy was induced at 7d intervals), and iii) exposure to Mn sea water followed by depuration in clean sea water (leg autotomy at certain interval). The crabs used were all male, intermoult *L. depurator* captured by trawling from the Clyde Sea area and acclimatized condition in the aquarium for at least 7d before the start of any experiment. All experiments were carried out in an aquarium room in the Graham Kerr Building of the University of Glasgow maintained at 12h light and 12h dark regime, at a temperature between 7-10°C.

The crabs, wherever appropriate according to the specific objectives of each section, were assigned to four treatment groups; i) exposed to clean sea water (the controls), ii) exposed to 10ppm Mn sea water, iii) exposed to 20ppm Mn sea water, and iv) exposed to 10 or 20ppm Mn sea water and depurated thereafter. From these crabs, the legs were autotomized weekly and measured for Mn. At the end of the experiments, the carapace, gills, hepatopancreas, gonad and the crusher claw muscle were also sampled and measured for Mn.

3.2.1 Preliminary measurements of Mn in the walking legs

The use of autotomized legs avoided problems caused by individual variations between crabs, as it allowed accumulation in the same crab to be monitored as long as there were sufficient legs to sample at each time interval (thus avoiding sacrificing the animal until the end of the experiment). However, in order to use this approach, a number of relationships had first to be established. Firstly, in order to

determine whether the whole autotomized leg (without dissection) could be used to provide an acceptable estimate of the Mn concentration in the exoskeleton, the contribution of the leg muscles to the Mn load in the legs was determined. Secondly, the comparability of the determinations among all the legs was also established, in order to justify the use of autotomized legs to indicate the accumulation of Mn in the crabs' exoskeleton. Finally, the relationship between the concentrations in the exoskeleton of the legs and that of the carapace was determined in order to relate the results of these experiments to those of others in which only the Mn concentrations in the carapace had been obtained.

Fifteen male crabs from a single catch from the Clyde Sea area (carapace length 27-42 mm) were sacrificed. The dorsal carapace and all legs (walking – Leg 2-4; and swimming – Leg 5) were retrieved from each crab. To determine the contribution of the muscle tissues towards the Mn concentration in the legs, the muscles were dissected from all the left legs, whereas the right ones were left with the muscles intact. They were freeze-dried (Edwards-Modulyo) for 24h, and the dry weight was recorded.

The samples were prepared for Mn measurements by AAS, following a standard protocol. Briefly, the dried samples (of known weight) were transferred to acid-washed 50ml conical flasks. They were acid-digested as follows. A volume of 10ml of Analar concentrated nitric acid (70%, trace analysis grade, Fisher) was added to the flasks and they were heated at $200^{\circ}C$ on a hotplate for several hours until the tissues had completely dissolved. The remaining solution was then made up to 10ml by adding distilled water. The 10ml final solution was used to determine the manganese concentration using flame AAS (Philips PU9200).

A calibration curve was constructed by analyzing standard solutions of 1.25, 2.50 and 5.00ppm manganese (Mn AAS standard solution, Aldrich). The samples were checked against TORT-2 (lobster hepatopancreas reference material for trace metal, National Research Council Canada). The concentration of the metal in the digested sample was then expressed as μg $Mn.g^{-1}$ dry tissue.

3.2.2 Accumulation on Mn in crabs after exposure to 10ppm and 20ppm Mn in sea water

This experiment was carried out to determine Mn accumulation in the exoskeleton and other tissues in crabs following increasing times of exposure (up to 21d), and for different concentrations of Mn in the surrounding water (0-20ppm sea water). To avoid variations in metal accumulation due to morphological differences of appendages, autotomy was carried out only on the six identical walking legs (pereiopods 2-4; Fig. 3-1) avoiding as much as possible the use of the swimming legs.

3.2.2.1 Autotomy

Autotomy was induced by pinching the leg of a crab with blunt forceps. A slight pull was applied to the legs to induce the autotomy reflex (mimicking its attacker) but not strong enough as to tear the legs apart from the body. Autotomy was best induced by pinching the leg while allowing the crab to struggle to free itself; this invariably led to the leg being autotomized voluntarily and therefore avoid further injury. Autotomizing the leg by holding the body of the crab was less successful, and induced injuries that meant that animal would not survive until the next autotomy.

3.2.2.2 Preparation of manganese sea water

Concentrations of 10 and 20 ppm Mn sea water were prepared by dissolving 35.982mg and 71.964mg of $MnCl_2.4H_2O$ (Sigma) respectively in 1L of sea water. The solution was prepared 24h prior to the experiments. The water in all exposure tanks was occasionally checked for its Mn concentration, and routinely the water was changed twice weekly to avoid accumulation of waste excreted by the crabs.

3.2.2.3 Exposure

The crabs, which were all males, were maintained together in a large holding tank before the experiments started. To determine the accumulation in the exoskeleton, fifteen crabs were selected and divided into three groups of five: the controls

(exposed to normal sea water), those exposed to 10ppm, and those exposed to 20ppm Mn in sea water continuously for 21d.

Leg 2L (day 7) Leg 2R (day 0)
Leg 3L (day 21) Leg 3R (day 14)
Leg 4L Leg 4R
Leg 5R Leg 5R
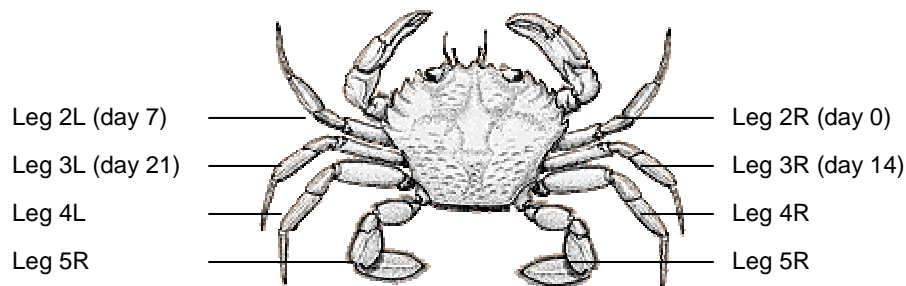
Fig.3-1. Diagram showing the labelling of the legs. The day of autotomy for the accumulation experiment is shown in brackets.

The sequence of autotomy pertaining to the specific walking legs is shown in Fig. 3-1. The first autotomy was carried out on Leg 2R soon after they were taken out from the main holding tank. This leg represented the initial Mn concentration, day 0. Then the crabs were immediately placed in their respective treatment tank of about 6L of sea water. The crabs were kept in individual tanks in order to maintain similar normal resting behaviour for each animal, since fighting or any other aggressive behaviour that might occur among them might alter their physiological processes, and hence the accumulation of Mn. Autotomy was repeated on Legs 2L, 3R and 3L on day 7, 14 and 21 respectively, to provide data on any changes of Mn concentration with increasing time of exposure. All the crabs were sacrificed on day 21, when five other tissues (carapace, gills, hepatopancreas, gonad and crusher claw muscles) were also collected for Mn measurements.

In a separate trial, accumulation of Mn in other tissues was also investigated following the same exposure protocol as the above. Three groups of five intermoult male crabs (carapace width 41.5-53.0mm) were exposed to 10 and 20ppm Mn sea water for 7d, 14d and 21d. They were sacrificed at the end of the respective exposure periods and the five tissues were extracted from each of them. All samples were freeze-dried and measured for Mn by AAS with the standard protocol as mentioned in Section 2.2.2.

3.2.3 Retention of Mn in Mn-exposed crabs following depuration

A depuration experiment was carried out to investigate the fate of accumulated Mn in both the exoskeleton and the tissues of the crab after being allowed to depurate in clean sea water.
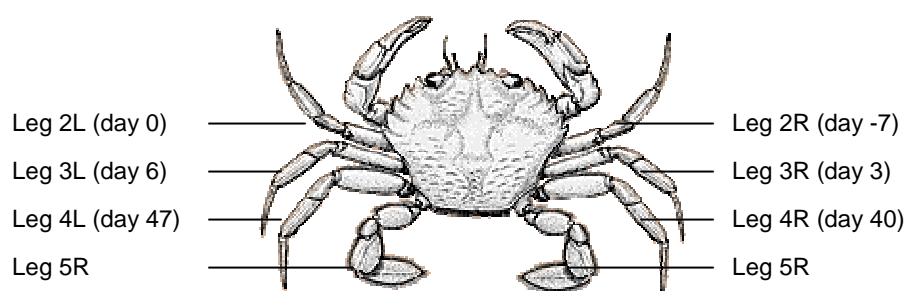
Fig. 3-2. Diagram showing the sequence of autotomy for the accumulation followed by depuration experiments.

Twenty intermoult male crabs with carapace lengths ranging between 39.0 - 55.1mm (5 controls, 10 exposed to 10ppm and 5 exposed to 20ppm Mn sea water) were placed individually in 6L of the respective sea water in separate exposure tanks. One leg was autotomized before the exposure started, termed as day -7 (minus 7). They were then left exposed in the treatment water in the individual tanks for 7d. The water was renewed on the fourth day of the exposure.

After 7d, another leg was autotomized from each crab, representing day 0 (marking the end of exposure, and the start of depuration). They were then placed in individual tanks containing clean sea water and allowed to depurate. The first day of depuration was termed day 0. The water was changed twice weekly. Autotomy was repeated on days 3, 6, 40 and 47 (Fig. 3-2). The crabs were sacrificed on day 47 where the five other tissues were sampled. The Mn concentration in the water in the exposure tanks was checked during the exposure period. From this experiment, Mn concentrations in the leg exoskeleton after exposure and at intervals during depuration were obtained. Mn concentrations in the tissues after depuration were also determined.

3.2.4 Mn concentrations in other tissues following exposure and depuration

The data for Mn concentrations in other tissues before exposure, after 7d exposure and after 47d depuration were compared. This was made possible by combining and cross-checking the data obtained for the respective tissues from Sections 3.2.2 and 3.2.3. As the concentrations in the crusher claw muscle and the gonads were extremely low, they are not shown in the Results section. Only the Mn concentrations in the dorsal carapace, gills and hepatopancreas are plotted in the figures.

3.2.5 Statistical analysis

Using the statistical package Minitab 13, standard statistical procedures were applied to compare the data sets. ANOVA was used to measure differences among three or more sets of data, whereas a t-test was used to compare the mean difference between two data sets. Significance was accepted at $p < 0.05$. In some of the results, an evaluation of the association between two variables was made and Pearson's correlation coefficient was used to indicate a statistical significance.

3.3 Results

3.3.1 Use of autotomized legs to determine Mn accumulation

Analyses of tissues from animals taken directly from the environment of the Clyde Sea area were performed. Figure 3-3 shows the mean Mn concentrations in whole legs (with muscle intact) and in legs without muscle. The concentration of the metal

in the dorsal carapace (the major part of the exoskeleton of the crabs) is also shown for comparison. The concentrations were found to be similar in all legs in individual crabs (means ranged between 47.08 – 66.1µg Mn.g^{-1} dry tissue; paired t-test, P=0.075-0.155). This indicates that removal of the muscle for Mn determination in the exoskeleton in the legs is not necessary, since the contribution of the leg muscle to the Mn load is insignificant. The only exception was for Leg 4 where the concentrations of Mn in the legs without muscle were found to be significantly higher than for the legs with the muscle intact and the carapace (paired t-test, P=0.010 and 0.009 respectively).

The mean concentration of Mn in the dorsal carapace (43.28±11.36µg Mn.g^{-1} dry tissue) was found to be not significantly different from that in the legs with the muscle intact (paired t-test, P=0.068-0.491) and also from that in Leg 5 without muscles (paired t-test, P=0.122). However, Legs 2-4 without the muscles showed slightly higher Mn concentrations compared to the carapace (paired t-test, P=0.009-0.016). The concentrations in the carapace (mean 43.28±11.36 µg Mn.g^{-1} dry tissue; range 15.11-94.02) are also highly correlated with the average of all legs combined (mean 55.89±4.95 µg Mn.g^{-1} dry tissue; range 15.46-127.40).

Mn concentrations in all legs (with muscle) were also found to be highly correlated with each other (correlation coefficients=0.962-0.994; paired t-test, P=0.437-0.945). This finding confirms that any leg could be used to represent Mn concentrations of the exoskeleton of an individual crab. Therefore, in the subsequent experiments, whole legs (without removing the muscle) obtained via autotomy were used to determine Mn accumulation weekly following exposure and at certain other intervals after depuration.

3.3.2 Mn accumulation after exposure

The impact of exposure to 10 and 20ppm Mn sea water for 21d was studied. Both the legs and the other tissues were observed to accumulate the metal. Mn concentrations in the sea water in the exposure tanks were found to show some

fluctuations, ranging between 7.79-9.40ppm for the 10ppm exposure and 15.70-20.45ppm for the 20ppm exposure. The same trend was also observed in tanks of 10ppm sea water (prepared separately), 10ppm Mn in distilled water and also in 10ppm sea water (with a crab in it) that were kept in the same aquaria during the whole study period for comparison. As the fluctuations occurred in all containers, the presence of the crabs and their activities most probably did not significantly change the Mn concentration of the sea water. Despite the small fluctuations, the difference in the values between the two groups was great enough to yield different accumulated values in the exposed crabs.

3.3.2.1 The leg exoskeleton

Figure 3-4 shows the Mn concentration in the leg exoskeleton when crabs were exposed to 10 and 20ppm Mn sea water. A gradual, almost linear increment of the metal in the exoskeleton occurred with the increasing period of exposure in both cases. The crabs continued to accumulate Mn within the exoskeleton up to the final day of exposure at day-21. No saturation was observed in any case.

In the 10ppm exposure, Mn concentrations after the exposure were significantly higher than in the controls (ANOVA, $P<0.001$), with the concentrations increased from 44.29±3.21 µg Mn.g^{-1} dry tissue on day-0 to 134.85±14.99 µg Mn.g^{-1} on d-7 and 307.72±48.34 µg Mn.g^{-1} on d-21. However, the concentration on d-14 was not significantly different compared to d-7 and d-21. This indicates that at least 14 days are required for any increment to be significantly reflected in values for the legs of crabs exposed to 10ppm Mn sea water. The rate of accumulation from d-0 to d-21 was calculated at 13.14 µg Mn.g^{-1}.d^{-1} (Table 3-1).

In the 20ppm exposure, the concentrations increased from 35.35±7.88 µg Mn.g^{-1} dry tissue on day-0 to 267.34±7.19 µg Mn.g^{-1} on d-7 up to 730.96±51.61 µg Mn.g^{-1} on d-21. The increases during these 7-d intervals were significant (ANOVA, $P<0.001$). Crabs exposed to 20ppm showed a significant increment each week. The rate of accumulation from d-0 to d-21 was calculated to be 33.12 µg Mn.g^{-1}.d^{-1}, a value that is more than double compared to 10ppm exposure.

3.3.2.2 Other tissues

Figure 3-5a shows the result obtained at weekly intervals after the crabs were exposed to 10ppm Mn sea water. Data on the legs accumulation from 3.3.2.1 were also plotted for comparison. All tissues from exposed crabs show significant increases in Mn concentration compared to the values on day 0 (ANOVA, P<0.015). The greatest increment was observed in the exoskeletal tissues (the legs, the carapace and gills) and in the hepatopancreas. For the carapace, the concentrations increased from 21.49 µg Mn.g^{-1} to around 5.6 times higher on day 7. However, there was no significant difference between the Mn concentration for day 7, 14 and 21 with the concentrations ranging between 120.05±24.40 – 176.33±28.93 µg Mn.g^{-1} dry tissue. The gills, from the initial values of only 12.66 µg Mn.g^{-1} on day 0, also reached a plateau from day 7 to day 21 (150.33±12.28 – 177.90±14.65 µg Mn.g^{-1} dry tissue). However, the Mn concentrations for the hepatopancreas continued to increase significantly with the exposure period, from the initial value of 10.53 µg Mn.g^{-1} to 61.47 and 76.07 µg Mn.g^{-1} on days 7 and 14, respectively. Mn concentration on day 21 (148.32±25.88 µg Mn.g^{-1} dry tissue) was found to be significantly higher than on day 7. The crusher claw muscle and the gonad also showed some significant increases (P=0.015 and P<0.001 respectively) but at very low magnitudes (less than 72 µg Mn.g^{-1} dry tissue for gonad and less than 33 µg Mn.g^{-1} for the claw muscle) compared to the other three tissues mentioned previously.

Figure 3-5b shows the Mn concentration in the crabs exposed to 20ppm Mn sea water. Exposure to a higher concentration of Mn sea water resulted in a higher accumulation of the metal in all the exoskeletal tissues (legs, carapace and gills, ANOVA, P<0.001 for all tissues) and the hepatopancreas. The data for the legs from Figure 3-4 is re-plotted for comparison. As seen in the 10ppm exposure, all tissues from exposed groups showed higher concentrations of Mn compared to day 0. But unlike the 10ppm exposure, the difference observed for gonad and the crusher claw muscle was not significant (ANOVA, P=0.460 and 0.139 respectively). The Mn concentrations in the exposed crabs on day 21 were significantly higher than on day 7 for the carapace (530.85±28.23 vs. 130.29±4.74 µg Mn.g^{-1} dry tissue), gills (317.79±34.31 vs. 177.90±14.65 µg Mn.g^{-1} dry tissue) and hepatopancreas

(224.91±43.04 vs. 57.31±8.10 µg Mn.g^{-1} dry tissue), showing the impact of prolonged exposure to high concentration (this effect was only seen in the hepatopancreas for the 10ppm exposure).

Figure 3-5 clearly shows the trend of accumulation in *L. depurator*. The impact of being exposed to Mn sea water was also clearly shown in the soft tissue (hepatopancreas) especially in the 20ppm exposure. The highest accumulations were shown by the exoskeletal tissues, especially the legs. The trend becomes more prominent when the crabs were exposed to higher concentrations of Mn sea water, where significant gradual temporal increments of the metal could be seen in the legs, the carapace and the gills, even though at slightly different magnitudes.

3.3.2.3 Mn ratio in the legs:carapace from the exposure experiments

The difference between the accumulation by the legs and the carapace becomes larger especially when the crabs were exposed to higher concentrations. Based on the data obtained from all the control (and day 0) and exposed groups (n=31) covering a wide range of Mn concentrations between 14.18 – 897.48 µg Mn.g^{-1}, a regression line was plotted to determine the associations between Mn concentrations in these two tissues. Fig. 3-6 shows that the legs accumulated proportionately higher concentrations of Mn than the carapace by a factor of 1.36. The strong correlation (Pearson's correlation coefficient = 0.918) between the measurements in these two tissues suggests that one could estimate the concentration of Mn on the major exoskeletal part of a crab's body without having to sacrifice the animal. Autotomizing a single leg would be sufficient for the purpose.

3.3.3 Mn retention after depuration

Depuration following 7d of exposure was also studied. The Mn concentrations in the exoskeleton and in other tissues are presented below.

3.3.3.1 In the leg exoskeleton

From section 3.3.2, exposure to 10 and 20ppm Mn sea water for a duration of 7d was found to significantly increase the Mn concentration in the leg exoskeleton. Therefore in this trial, depuration was initiated 7d after the crabs were exposed to Mn sea water. Figure 3-7 showed the results of a depuration experiment carried out for 10 and 20ppm Mn sea water. In the 10ppm exposure, Mn concentrations increased significantly by about three fold at the end of the seven day exposure (from 65.94±19.02 to 168.80±9.81 µg Mn.g^{-1} dry tissue; ANOVA, P<0.001). After three days depuration, there was a slight but not statistically significant decrease in the Mn concentration in the leg exoskeleton. However the concentrations showed no significant difference from days 0-47 (ANOVA, P=0.891). The concentrations in the controls remained similar to the initial value over the whole exposure/depuration period (ANOVA, P=0.885).

Crabs exposed to 20ppm Mn sea water showed a similar trend to that seen in the 10ppm exposure but at slightly higher concentrations. After 7d exposure, Mn concentrations in the crabs increased significantly from 32.38±9.28 to 210.65±31.08 µg Mn.g^{-1} dry tissue (P<0.001). Thereafter (days 0 – 47) no statistical difference was found between the metal concentrations (P=0.798).

3.3.3.2 Other tissues

Figure 3-8 shows the Mn concentrations in the crab tissues at the end of 47d depuration period compared to the values for the control group and for the exposed group after 7 days (10 and 20ppm) from Section 3.3.2.2. Only data for the carapace, gills and hepatopancreas are shown. The same set of data for the controls is used in both figures.

After being allowed to depurate in clean sea water for 47d, Mn in the carapace was found to be slightly reduced but remained significantly higher than in the controls in both exposures (ANOVA, P<0.001). The concentrations after depuration were 88.18±14.06 and 121.74±6.64 µg Mn.g^{-1} dry tissue for the 10 and 20ppm exposure respectively. Mn concentrations in the controls for both were approximately 50µg

Mn.g^{-1} dry tissue. This observation matches well with the leg exoskeleton in the depuration experiment as in Figure 3-7. The overall slightly lower values shown by the dorsal carapace are as expected according to the determined relationship between the leg and carapace Mn concentrations (Section 3.3.1).

The greatest increase in Mn concentrations in the tissues after 7d exposure to 10ppm Mn sea water was actually shown by another exoskeletal tissue, the gills (12.66±2.71 µg Mn.g^{-1} dry tissue in the control, 174.93±29.93 µg Mn.g^{-1} in 10ppm exposure, 177.90±14.65 µg Mn.g^{-1} in 20ppm exposure, P<0.001). However, unlike the other exoskeletal parts, after being allowed to depurate in clean sea water for 47 days, the concentrations in the gills decreased significantly. Following the 10ppm exposure the 47d depurated value decreased to the day 0 values, while for the 20ppm exposure (Fig. 3-8b), the Mn concentrations were found to be in the order of 'day 0' < '47d-depurated' < '7d exposed' (P<0.001).

In the hepatopancreas, Mn concentrations were significantly increased after 7d exposure (61.47±1.52 and 57.31±8.10 µg Mn.g^{-1} dry tissue in 10 and 20ppm exposure, respectively) compared to the control of 10.53±1.53 µg Mn.g^{-1} dry tissue (P=0.001). However, after 47d depuration, the concentrations returned to the day 0 values.

3.3.4 Other observations

Figure 3-9a shows the raw data for the accumulation of Mn by the legs during the 10ppm Mn exposed crabs. Crabs 1, 2 and 5 showed a linear accumulation of Mn from day 0 to day 21. The Mn increments in the legs of each crab were constant that not even a single measurement crosses over the other. However, a sharp increase in Mn concentration was measured in the legs of Crab 4 on day 7 (7d after exposure), and the level remained much higher than in the others in the group thereafter. After day 14, another sharp increase was measured in the legs of crab 3. These sharp increases happened to coincide with crabs 3 and 4 showing early signs of moulting. This observation indicates the impact of moulting processes on Mn

accumulation in the crab exoskeleton. When no incidence of moulting occurs, the Mn increment would be expected to be in a linear fashion as shown in Fig. 3-4.

Figure 3-9b shows the raw data for the accumulation of Mn by the legs during the 20ppm exposure experiments. All crabs accumulated significantly higher concentrations of Mn every 7d interval up to 21d exposure with every crab showing the same pattern of accumulation along a somewhat linear line of increment during the whole exposure period.

A single crab from the exposure followed by depuration experiment also showed a sharp increase in Mn concentrations after being exposed to 10ppm Mn sea water for 7d (Fig. 3-10). The crab (Crab #3) was found to have begun moulting during the exposure period. It survived the second autotomy on day 0, during which time the old carapace had begun to split open across the back between the lateral spines showing an early sign of shedding. As it was looking very weak and might not survive the whole depuration period, it was sacrificed after the third autotomy on day 3.

After sacrifice, Crab #3 was carefully dissected and measurements were made on the old (almost shed) carapace and the new thin and soft carapace underneath it. Mn in the old carapace measured 513.22 µg Mn.g^{-1} dry tissue, whereas the new carapace measured only 13.92 µg Mn.g^{-1} dry tissue. Mn concentration in the carapace of this group after 47d depuration measured 88.17±5.31 µg Mn.g^{-1} dry tissue. The measurement shown as day 3 in Fig. 3-10 for Crab #3 refers to autotomized legs comprised of the old and new exoskeleton as moulting was not fully completed at the time.

3.4 Discussion

Generally, the results presented in this chapter justify the usage of a whole leg as a tool to monitor variations in Mn concentrations in the exoskeleton of a male crab *Liocarcinus depurator* after exposure to Mn sea water, and also after being allowed

to depurate in clean sea water thereafter. The crab accumulates the metal in both the exoskeleton and in the soft tissues (the hepatopancreas). The hard exoskeleton (the carapace and legs) was found to accumulate Mn after exposure and retain it even after being allowed to depurate in undosed sea water. However, the gill tissues (a different type of exoskeletal tissue) lost the accumulated metal after depuration. In the soft tissues, particularly the hepatopancreas, the Mn concentration increased as a result of exposure, but decreased significantly to baseline values after depuration.

In most exposure studies using crabs and other decapods, the increment of metal accumulation over a given period of exposure has been measured from groups of animals sacrificed at different time intervals. In most cases, the authors highlighted the limitations of the observed results due to 'substantial' individual variations. In this chapter, the nature of the crab itself has been successfully exploited in order to obtain meaningful information regarding Mn accumulation following exposure and depuration. First, the six identical walking legs possessed by the crab provided six nearly identical samples for temporal measurements of Mn. With careful planning, they could be sampled after certain intervals; in this study the shortest interval was 3d in the depuration experiment. Second, the fact that the crab performs autotomy with a special protective mechanism when attacked gave the opportunity to obtain legs with minimal injury to the crab, therefore avoiding mortality before the experiment ended. By using matched samples represented by the identical walking legs, and autotomized 'voluntarily' by the crab itself, the Mn concentration in the exoskeletons of individual animals was successfully monitored temporally, thus overcoming the effect of individual variations.

This study also eliminated other confounding factors, including: sex, by using only the males; size, by using homogenous samples; and site effects by using only crabs obtained from the same locality which is the Clyde Sea area. With these considerations taken into account, the results were assumed to provide an accurate picture of Mn variations due to the exposure and depuration treatments in this species.

3.4.1 Usage of a whole leg to monitor Mn concentrations in the exoskeleton of a crab

The first part of this study justified the use of a complete walking leg, as autotomized, to indicate Mn accumulation in the exoskeleton, without the need to remove the muscles, since these were found to contribute an insignificant extra Mn load. The preliminary survey carried out on all legs and the carapace of 15 crabs taken directly from the environment of the Clyde Sea area (maximum Mn concentration of 66.1 µg Mn.g^{-1}) gave a ratio of leg to carapace values of 1.23. However, data pooled from all crabs used in the exposure experiments (n=31), which covered a much wider range of Mn concentrations in the legs (14.18 – 897.48 µg Mn.g^{-1}) yielded a leg:carapace ratio of 1.36. This may have been due to the larger number of animals used, or to the higher average concentrations of Mn involved, and is probably a more reliable value to use for any estimation.

Higher concentrations of metals in long tubular appendages, compared to flatter or larger exoskeletal surfaces have been reported in other decapod species. The fine antennular appendages of a Norway lobster *Nephrops norvegicus* were reported to accumulate Mn to about three times greater levels than the carapace after being exposed to 20ppm Mn sea water for 5d, reaching a concentration as high as 600 µg Mn.g^{-1} dry weight (Baden and Neil, 2003). In the present study, Mn concentration in the legs of the crab *L. depurator* did not exceed 300 µg Mn.g^{-1} after being exposed to 20ppm Mn for 7d, and a value of 600 µg Mn.g^{-1} was achieved only after more than 14d, indicating a lower rate of accumulation than in the lobster's antennular appendages. This difference might be due either to a species difference or to the difference in the structure of appendages measured. The lobster antennule is a much finer and rapidly moving structure compared to the crab walking legs used in this study.

Baden *et al.* (1995) successfully obtained constant measurements of Mn concentrations in their exposure tanks by changing the water supply as frequently as 5 times in 24h. This frequent renewal of water provided insufficient time and surface area for $MnCl_4$ to reprecipitate. This was not applied in the present study, in

order to minimize stress to the crabs. However, Mn in the exposure tanks was generally constant over the exposure periods, with only minor fluctuations. Therefore the crabs were assumed to have been exposed to levels within the range of the intended concentrations throughout the experiments. The water was changed twice within 7d with a duration of 3-4d between changes. This might have allowed some solubilized $MnCl_4$ to reprecipitate, but the time available for this to occur was minimal.

3.4.2 Mn accumulation in tissues

Mn concentration increased almost linearly in the exoskeleton. The accumulation was found to be dose-dependent (the increment being almost double in the 20ppm exposure compared to 10ppm) and also time-dependent (more Mn is accumulated over a longer period of exposure). This accumulated Mn was retained in the exoskeleton even after being allowed to depurate for up to 47d, suggesting that the Mn accumulation is virtually irreversible and that the metal particles might be tightly bound to the tissue. The slight decrease of Mn concentration shown after 3 days of depuration in both exposures might represent the amount of Mn adhering or loosely deposited on the surface of the legs' exoskeleton that is lost due to natural rinsing by undosed sea water.

So far, there has been no report on Mn accumulation in *L. depurator*, but Bjerregaard and Depledge (2002) reported that Mn concentrations in a series of tissues of the shore crab *Carcinus maenas* were similar to concentrations reported in the lobsters *Homarus gammarus* (previously known as *H. vulgaris*) (Bryan and Ward, 1965) and *Nephrops norvegicus* (Eriksson and Baden, 1998; Baden *et al.*, 1999; Eriksson, 2000). The present results confirm the general trend reported by these researchers on other crustaceans that Mn varies widely with regard to its distribution in tissues, and that the major part of the body burden of the metal is located in the exoskeleton. However, the study by Bjerregaard and Depledge (2002) found a value of 286 ± 49 µg Mn.g^{-1} dry weight in *C. maenas,* although this

study was focussed more on a survey of crabs collected from an uncontaminated site in Denmark, and not on laboratory trials. This value was more than 10 times higher than the control *L. depurator*, and could compare to the ones exposed to 20ppm Mn sea water for 14d. Exposure to 10ppm for 21d also did not show such a high accumulation.

In a laboratory trial, Baden *et al.* (1995) did not find any significant accumulation of Mn on the exoskeleton of the Norway lobsters exposed to 5555 µg Mn.l^{-1} (5.555ppm) Mn sea water for 14d. Mn concentration measured 311.0±85.0 µg Mn.g^{-1}. Assuming that the increment in the accumulation experiment in this chapter is linearly dose dependent (as clearly shown in Fig. 3-3), Mn concentrations in the crab leg exoskeleton obtained from the 10 and 20ppm exposures could be extrapolated to 5.555ppm, giving values of 138.69 and 170.36 µg Mn.g^{-1} for both exposures respectively. These values were significantly lower than the ones obtained by Baden *et al.* (1995) in their lobsters. However, if the total increment is calculated (final concentration on d14 minus the value in control animals), Baden *et al.*'s experiment showed a total increase of about 116 µg Mn.g^{-1}. *L. depurator* showed a total increment of 107 and 135 µg Mn.g^{-1} for 10 and 20ppm exposures respectively. These two values are comparable, indicating that these two species might accumulate around the same amount of dissolved Mn from their surrounding water if exposed to the same conditions. The final total content might differ due to the difference in the original concentrations available in the animals prior to the exposure.

In this study, when exposed to 10 and 20ppm for the same duration, the crab showed significantly higher concentrations of Mn in the dorsal carapace than the controls. In the 10ppm exposure, the concentrations of Mn after 7, 14 and 21d exposure were similar. The values seemed to be increasing with increasing exposure duration but the difference was not big enough to be of statistical significance. However, when the animals were exposed to a higher concentration (20ppm), Mn levels in the dorsal carapace were found to increase significantly after each 7d interval. It is believed that the level of exposure used by Baden *et al.* (1995) was not high enough to cause a significant accumulation in the lobster. An exposure

to higher concentrations might bring about similar observations to those reported in this chapter.

No saturation was found in the crab leg exoskeleton or the dorsal carapace, an observation in contrast to that of Baden *et al.* (1995) in the Norway lobster, even though the crabs were subjected to higher concentrations and longer duration of exposure than the lobster. This might indicate that more binding sites are available on the exterior of the exoskeleton of the crab. This suggests that crabs might be a potential biomonitor for longer and higher exposure events especially in stressful habitats.

Other tissues (carapace, gills and the hepatopancreas) also showed significant increases indicating accumulation. The greatest increase was shown by two exoskeletal tissues which are the carapace and the gills. The accumulation in these two tissues was found to be dose dependent where the increase was observed to be more prominent in the 20ppm exposure. The time-dependency was clearly exhibited by the crabs exposed to 20ppm. After 7d exposure, the gills being an exoskeletal tissue itself, but of a different type compared to the legs and the carapace, proved to be the one showing the highest accumulation. If Mn were to be deposited on the surface, then this observation is of no surprise. The gills, with their folded lamellae possess a lot larger surface area for deposition compared to the carapace and the legs. Furthermore, the Mn concentration was based on the dry weight of the tissues. As the gills are extremely thin compared to the other two tissues, they weigh a lot less especially when dried. Coupled with the larger surface area it offers for deposition, the Mn concentration expressed in µg Mn.g^{-1} dry tissue becomes large for the gills.

Similarly, the exoskeleton which was reported to be the major part of total body Mn burden, in most cases did not show a big difference in Mn concentrations than the ones in the gills as the concentrations was expressed per tissue weight. Perhaps, if Mn was counted as the quantity deposited instead of the concentration, then the values for these three exoskeletal tissues (gills, carapace and legs) might be closely comparable. However, the concentrations reached some kind of a plateau in the gills with prolonged exposure to 10ppm, showing signs of saturation but might also

be due to proper cleaning mechanism in the animals. However, when challenged with a higher concentration (20ppm), they showed a small increment for every 7d interval. This indicates that no true saturation has yet been reached in the 10ppm exposure when the concentrations just plateaued out, and also might mark the start of the malfunctioning, breakdown, or the animal not being able to cope with the continuous influx of the dissolved Mn with every film of water swept over the gill lamellae with every ventilation.

The high Mn accumulation on the gills of *L. depurator* also confirms the trend in *N. norvegicus* reported by Baden *et al.* (1995). They reported 5 and 12-time higher concentrations in the gills than in the control for 14d exposure to 1755 and 5555 µg Mn.l^{-1}, respectively (1.755 and 5.555ppm). In this chapter, 10ppm and 20ppm exposures resulted in 12 and 28-time higher concentrations compared to controls. These results suggest that these two species 'behave' in almost a similar way towards Mn in the surrounding water. Baden *et al.* (1995) also stated that the increment in this tissue was linearly dose-dependent. Therefore, the results could be extrapolated to 10 and 20ppm exposures for the purpose of comparison with the data obtained in this chapter. The gills of the lobster would measure 331.2 and 662.4 with a total increment of 316.0 and 647.2 µg Mn.g^{-1} for 10 and 20ppm exposures respectively. Our data for the gills after 14d exposures were 154.3 and 353.7 µg Mn.g^{-1}, showing almost half the accumulation of the lobster if exposed to the same condition. However, this difference is of no surprise as the gills are of internal location, and the only way for the tissues to be bathed with dissolved Mn is by passing water through the gills. The different rate of gills ventilation in these two species definitely plays an important role in governing accumulation in this tissue. The carapace and the leg exoskeleton which are more external, and exposed to Mn in the surrounding water are more prone to passive deposition of the metal onto the tissues, with minor physiological influence, and therefore could be similar in both the lobster and the crab if exposed to the same conditions.

Bjerregaard and Depledge (2002) reported a significant difference in Mn concentrations in the gills of the shore crabs *C. maenas* according to their sizes. However, all male *L. depurator* used in our study would fall close to the 'small-sized' group (34±7g) according to Bjerregaard and Depledge's categories, and therefore

size could be assumed to be of no significant effect. For this category, the gills of *C. maenas* obtained from a non-contaminated site contained 175µg Mn.g^{-1} dry weight which is about 13 times higher than the values in the control *L. depurator* (12.66 µg Mn.g^{-1}). The value reported by Bjerregard and Depledge (2002) is in fact equivalent to the levels observed in *L. depurator* exposed to 10ppm Mn sea water for 21d (174.93 µg Mn.g^{-1}) and 20ppm for 7d (177.90 µg Mn.g^{-1}). However, there is a danger in comparing these values as they are, i) because the crabs are from two different species, they might behave similarly towards Mn, but metal accumulation may vary even between two closely related species, ii) the two species inhabit two different habitats, *C. maenas* in shallow water but *L. depurator* in deeper area and therefore they might have different adaptational mechanisms, and iii) the report by Bjerregaard and Depledge (2002) is based on a field study, but the data reported in this chapter are based on controlled lab exposures. However, the high values shown by *C. maenas* might give a clue to the exposure they experienced in the 'uncontaminated' area they were obtained from, in their case from South-west Funen in Denmark.

L. depurator also accumulated Mn in the soft tissues. Very low amounts were found in the gonads and the crusher claw muscles for which reason they are not going to be discussed in detail. The observation for the muscle concurs with that of Baden *et al.* (1995) that the muscle did not appear to serve as a sink for accumulated Mn in Norway lobsters. Mn might never enter the muscle cells (Hille, 1992) but the small increment observed might be contributed by the extracellular haemolymph (Baden *et al.*, 1995).

The highest accumulation in the soft tissues was shown by the hepatopancreas. The baseline Mn concentration was 10.53 µg Mn.g^{-1}, which is closely comparable to the values reported for *C. maenas* of 10.27±3.7 µg Mn.g^{-1} (Bjerregaard and Depledge, 2002). The results also indicate that the accumulation in this particular tissue is both time and dose dependent. If exposed to a lower concentration (in this case 10ppm), a longer time is needed for the concentration to increase significantly. 14 or more days is required to cause a significant increase of Mn concentration from day 7 to day 21, suggesting a certain regulation of Mn by the tissue, but prolonged exposure might caused it to malfunction. However, when the crabs were challenged with a

higher exposure (20ppm), the increment became significantly higher with every 7d exposure, indicating the malfunctioning of the regulatory mechanisms. If the crabs were allowed to depurate in clean sea water, the concentration decreases down to the initial value.

As the main detoxifying organ in crustaceans, excess metals are expected to be collected in some ways in hepatopancreas before being excreted from the body. A few previous researchers had reported this organ to be more conservative in its Mn concentration and less affected by exposure to dissolved Mn (Bryan and Ward, 1965; Baden *et al.*, 1995; Eriksson and Baden, 1998). However, our results confirm the finding of Baden *et al.* (1999) who found that the hepatopancreas of another decapod, a Norway lobster, did accumulate Mn during a long term exposure. The accumulation occurred at a slow but steady rate. In the present study a significant increase was observed as early as 7d after exposure to 10ppm Mn sea water, and Mn accumulation continued to the end of the exposure period on d21, showing no sign of saturation. The surplus Mn in the hepatopancreas was possibly delivered to the organ for detoxification and therefore leads to a continuous accumulation (Rainbow, 1996; Baden *et al.*, 1999). In addition, under extreme conditions of high Mn bioavailability (10 and 20ppm), the rate of Mn excretion can no longer match the high rate of uptake and net accumulation of Mn might result.

Digested food passes via the hepatopancreas before it gets into the blood system (Bryan and Ward, 1965), and therefore metals taken up especially from ingested food also appear to accumulate mainly in this organ (Brouwer *et al.*, 1995; Canli and Furness, 1995). However, this might not be the case in this study where the crabs were unfed during the experimental exposure. The only way the above statement could support the Mn accumulation in the hepatopancreas observed in this study is that the metal might be collected in the haemolymph directly from the sea water via gill transport and delivered to the hepatopancreas. Another explanation would be that Mn might be accumulated from ingested sea water (which is unlikely to occur in normal marine animals, but might be possible in starved animals) that follows the same food path through the hepatopancreas before being excreted. Furthermore, Nordstedt (2004 in Baden and Eriksson,2006) proved no significant difference in the Mn concentrations in the soft tissues of lobsters fed with diets containing large

differences in Mn concentration, and therefore concluded that uptake from water via the gills to be the most important entrance of the metal in aquatic crustaceans.

3.4.3 Mn retention in the tissues

Generally, accumulated Mn was retained within the hard exoskeleton (legs and carapace) even after being allowed to depurate as long as 47d. The soft tissues (the hepatopancreas and the gills) were also found to accumulate Mn after being exposed to Mn sea water, but after depuration with undosed sea water, the tissues managed to reduce the concentrations to as low as the initial values. The reduction in the gills suggests that most Mn might be loosely deposited on the exterior of the gill lamellae, and the rapid flow of water meant for oxygen exchange manages to flush the metal away during depuration. The reduction in the Mn concentrations might also indicate regulatory mechanisms in these internal tissues and the tendency of this crab to maintain the metal levels at a certain limit as required.

Mn accumulated after 7d exposure was significantly retained in both the legs exoskeleton and the dorsal carapace of *L. depurator* even after the 47d depuration period. This long retention period suggests that the metal, if it was to deposit on the exterior surface, must be very tightly bound to it. This result confirms the findings of Baden and Neil (2003) in the lobster *N. norvegicus*. They reported that Mn accumulation on the movable parts of the exoskeleton increases linearly with the duration of exposure and with exposure concentrations, and showed virtually no decrease after 3 weeks in undosed sea water. This agrees with our observations on the leg exoskeleton. It is interesting to note that after 3d depuration, the legs exoskeleton of crabs exposed to both 10 and 20ppm did show a slight reduction (around 20-40 μg Mn.g^{-1}). These reductions are believed to reflect the portion of Mn that was loosely deposited on the surface, and could be easily rinsed off via the clean sea water. The rest of the deposited Mn remained well fixed to the exoskeleton and the concentrations remained high until the end of the depuration period of 47d.

The retention on the exoskeleton is in contrast with the findings of Baden *et al.* (1995). When a Norway lobster was exposed to labelled [54]Mn for 72h, total Mn accumulation was predominated by the exoskeleton followed by the gills (concurs with the results of the present study), but the accumulated [54]Mn was found to be lost after 120h of depuration. The concentration in the labelled Mn was found to decrease back to the values obtained in the exoskeleton after 21.5h exposure, showing almost minimal sign of retention. The absence of retention in their study might be due to the shorter period of exposure that gave less time for permanent deposition to occur. Another possible explanation might be the difference in the structure of the exoskeleton or the carapace of these two species, the thicker and coarser carapace in crabs might provide a better surface for deposition than that of the lobster. Mn precipitations reported to be visible as persistent black dots mainly in crevices on the hard-shelled exoskeleton of *Nephrops norvegicus* (Baden *et al.*,1994) might support this idea of the impact of prolonged exposure on the deposition of the metal. Similar spots were also observed on the dorsal carapace and legs of some of the exposed crabs in our study (Fig. 3-11). However, as this phenomenon was not reproducible, it might not be due to the Mn exposure alone, but perhaps depends more on the health status of the individual crab itself. Other physical factors including temperature difference, hypoxia etc could be ruled out because these crabs were exposed to a controlled laboratory environment. The Mn precipitated on the exoskeleton is insoluble and therefore holds the potential as a biomarker of exposure to Mn (Baden and Eriksson, 2006).

The fate of the accumulated Mn in the gills and the hepatopancreas was also investigated. Both tissues showed significant reductions in the concentrations after depuration, indicating a return to the baseline values. The high accumulation showed by the gills in both 10 and 20ppm exposure is not surprising, as the gills offer a vast surface area for deposition. A large loss of the Mn later during depuration also agrees with the trend seen in other decapod species. Body surface loss has been suggested for the lobsters, *H. gammarus* (Bryan and Ward, 1965) and *N. norvegicus* (Baden *et al.*, 1995). Diffusion across the gills via the steep downward gradient in the concentrations between the gill tissues and the external media was also suggested as one of the potential major ways of excreting excess Mn from the body of the lobster *N. norvegicus* (Baden *et al.*,1995). Baden *et al.*

(1995), using labelled [54]Mn, also proved that accumulated Mn was significantly reduced from the gills and the midgut gland as early as after being in clean sea water for only 5 days. But again, they were dealing with Mn accumulated only over 72h (3d) which is less than the exposure period applied in our study.

Both the gills and the hepatopancreas of crab exposed to 20ppm Mn sea water were found to accumulate about the same concentrations of Mn in the tissues after 7d exposure compared to 10ppm exposure. But the accumulated Mn in the 20ppm exposure was retained longer as the levels after 47d depuration were significantly higher than the baseline or control values. The fact that the surplus Mn continues to be delivered to the hepatopanceas for detoxification purpose (Rainbow, 1997), and the fact that the gills are one of the major organs for excreting excess Mn from the body (Baden *et al.*,1995) supports these observations. Perhaps at 47d depuration, the elimination process was still going on in the 20ppm exposed crabs. This observation might also indicate that the crab might reach a new steady state for the metal concentration in the tissues, or that the crabs might require more time for the two systems to return to the normal baseline values after being challenged by such an extreme concentration. The breakdown of Mn regulation by the two systems seem unlikely as the crabs managed to reduce the concentrations to a much lower level when they are able to do so in clean sea water.

The crabs were found to be potential indicators of the metal in their surrounding water. The fact that they survived and could tolerate continuous exposure to high concentrations of Mn (20ppm) up to 21d suggest that they hold good potential as long term indicators of the metal especially in areas prone to high exposures. In addition, in a separate trial (not reported in here), the crabs even survived an extreme exposure of 80ppm Mn sea water for 21d (without any autotomy). In this study, the duration of the experiment was determined by the number of identical walking legs and also the sampling interval of 7d. This limited the experiment to being completed within 21d in order to avoid autotomizing every walking leg the crab possessed, and therefore avoided killing the animal before the experiment ended. However, longer exposure on this crab species could be carried out by increasing the duration of the sampling interval accordingly.

3.5 Conclusions

This chapter justifies the use of autotomized walking legs as indicators of Mn accumulation onto the exoskeleton of the male crab *Liocarcinus depurator* collected from the Clyde Sea area. The concentrations in the legs are a factor of 1.36 higher than the carapace, and even when dealing with Mn concentrations as high as 800 μg Mn.g^{-1} dry weight.

The crabs *L. depurator* were found to be very resistant to Mn exposure and could survive exposure to high concentration, while at the same time they accumulated the metal within their bodies.

Mn accumulation occurs in both the exoskeleton and the soft internal tissues after exposure to Mn sea water. The highest concentrations were found in the exoskeletal tissue regardless of the location (legs and carapace – external; gills – 'internal'), followed by the hepatopancreas. The accumulation was found to be both dose- and time-dependent.

The accumulated Mn in the hard exoskeleton was tightly deposited on the tissues and was retained within the tissues even after being depurated in clean sea water for 47d. However, the soft exoskeletal tissue (the gills) behaved differently whereby accumulated Mn was lost and the concentrations returned to the baseline values after depuration. The hepatopancreas also showed a significant elimination of the accumulated Mn after 47d depuration. The Mn accumulated after the crabs were exposed to a higher concentration was found to be retained longer in the gills and the hepatopancreas and might require more than 47d for complete elimination.

As accumulation in the exoskeleton is irreversible, the exoskeleton could be a potential biomarker for long-term exposure to Mn in the natural environment.

Table 3-1 The rate of Mn accumulation (μg Mn.g^{-1}.d^{-1}) in *Liocarcinus depurator* exposed to 10 and 20ppm Mn sea water (calculated as slopes of each line between sampling intervals in Figure 3-4).

	D0 –D7	D7 – D14	D14 – D21	* D0 – D21
10ppm exposure	14.73	12.75	11.94	13.14
20ppm exposure	33.14	36.23	30.00	33.12

* The rate of accumulation is based on the final concentration on day 21 and day 0
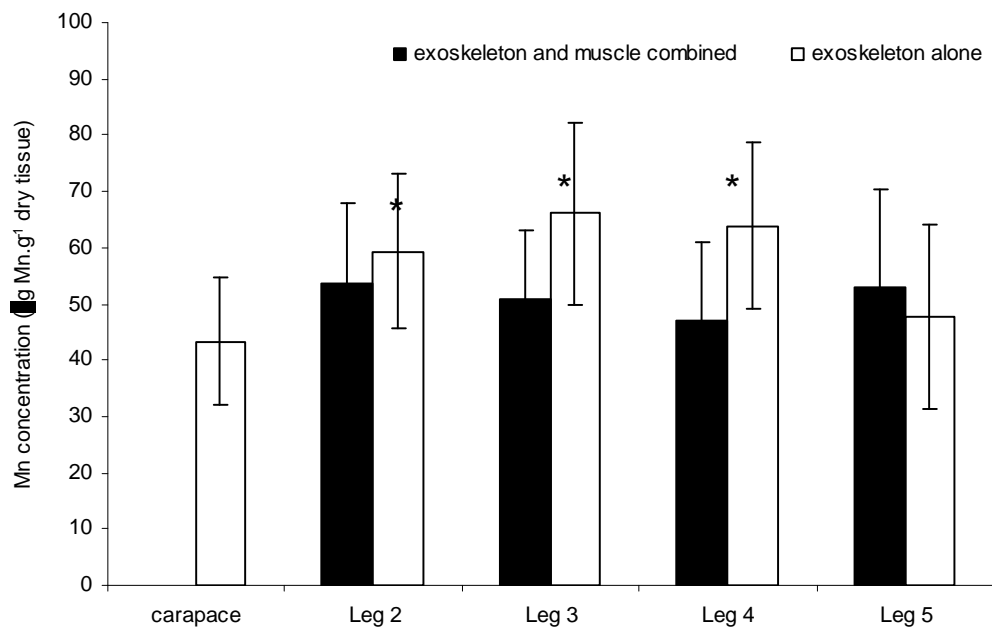
Fig. 3-3. Mn concentration in the carapace and in the complete legs (exoskeleton with the muscle combined) and in the leg exoskeleton alone. * denotes significant difference compared to the carapace at P<0.05.
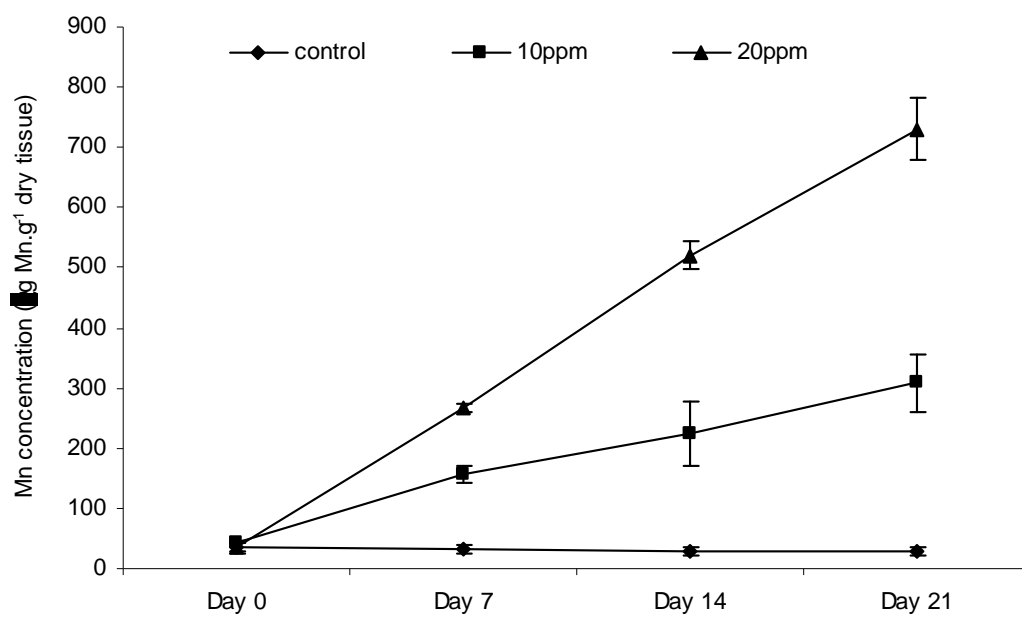
Fig. 3-4. Mn accumulation (mean ± SE) in the leg exoskeleton of crabs exposed to 10ppm (n=5) and 20ppm (n=6) Mn in sea water. The control group consisted of 5 crabs.
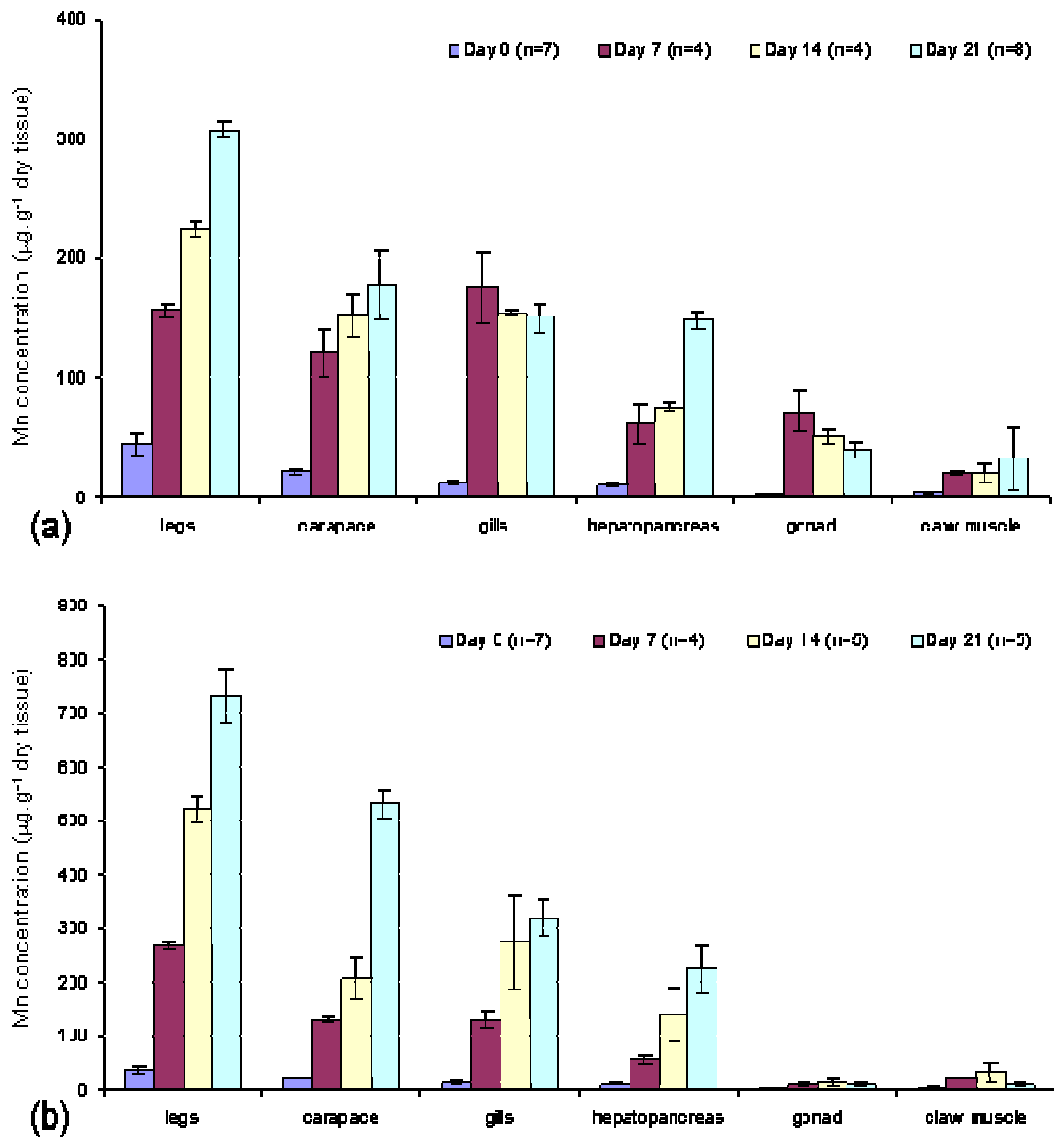
Fig. 3-5. Mn concentrations (mean ± SE) in a range of tissues in *L. depurator* after different times of exposure to (a) 10ppm Mn in sea water and (b) 20ppm Mn in sea water. The data for the legs refer to the ones plotted in Fig. 3-4.
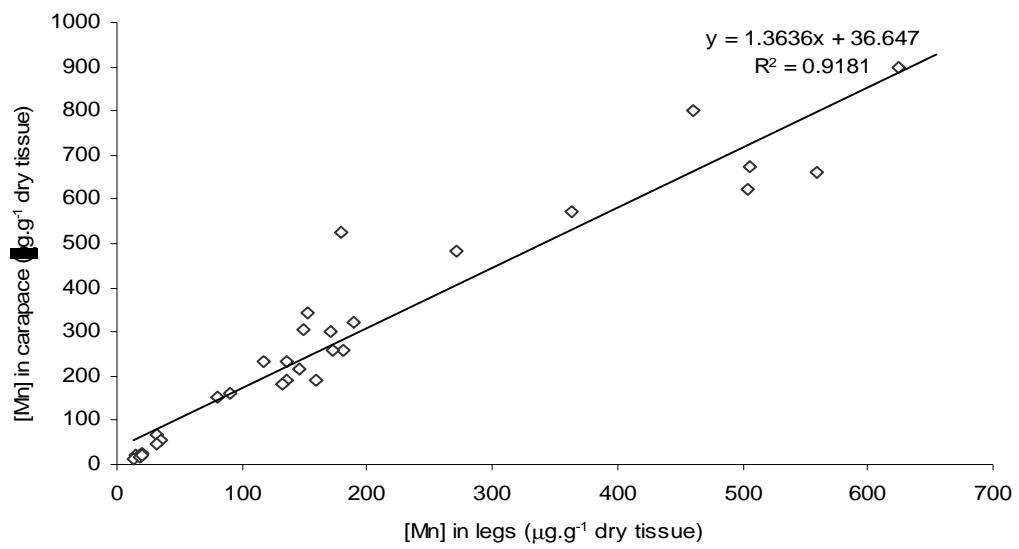
Fig. 3-6. A linear regression of Mn concentration in the carapace and in the legs from *L. depurator* exposed to 10 and 20ppm Mn sea water based on all crabs from control and exposure experiments. The accumulation in the legs is proportionately higher than the accumulation in the carapace by a factor of 1.36.
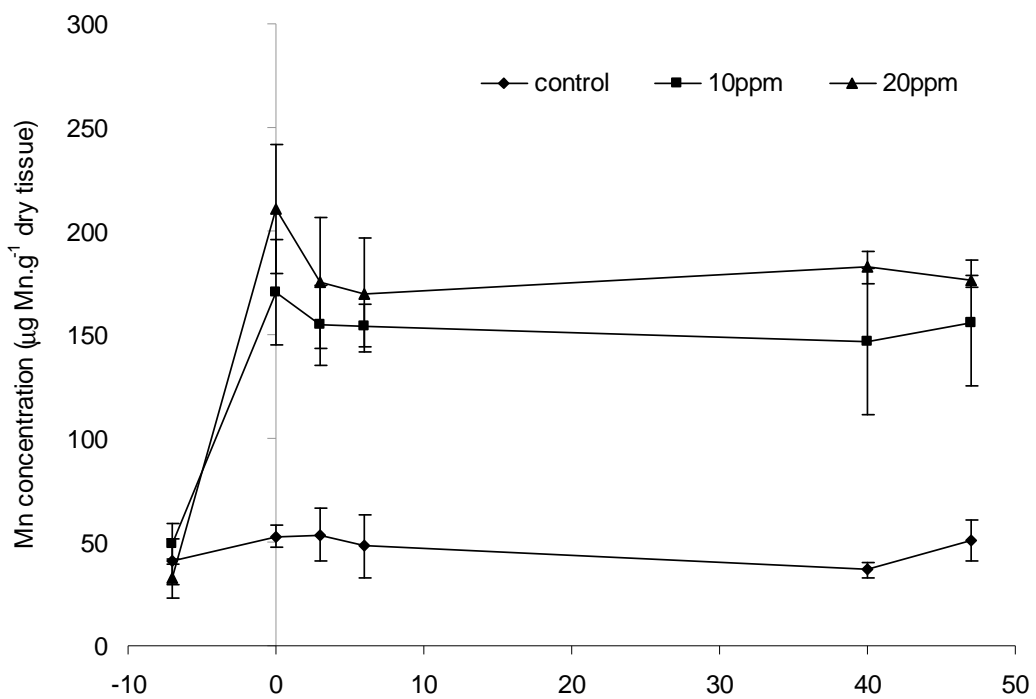
Fig. 3-7. Mn concentration (mean ± SE) in leg exoskeleton of Mn exposed *L. depurator* during depuration in undosed sea water following 7d exposure to 10ppm (n=3-8) and 20ppm (n=3-5) Mn in sea water. The control group consisted of 4 crabs. Day 0 represents the start of depuration.
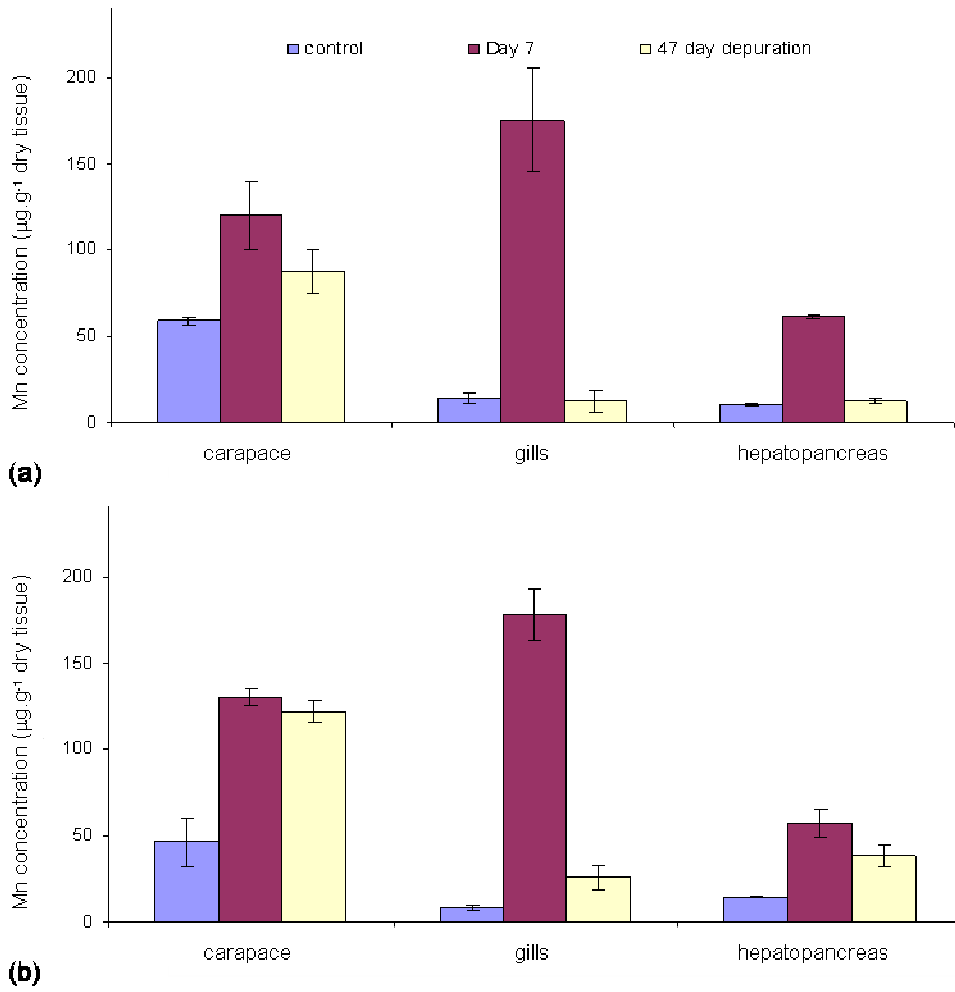
Fig. 3-8. Mn concentrations (mean ± SE) in the carapace, gills and hepatopancreas in *Liocarcinus depurator* exposed to normal sea water (control), 7d exposed to Mn sea water and 47d depurated. (a) 10ppm Mn sea water and (b) 20ppm Mn sea water.
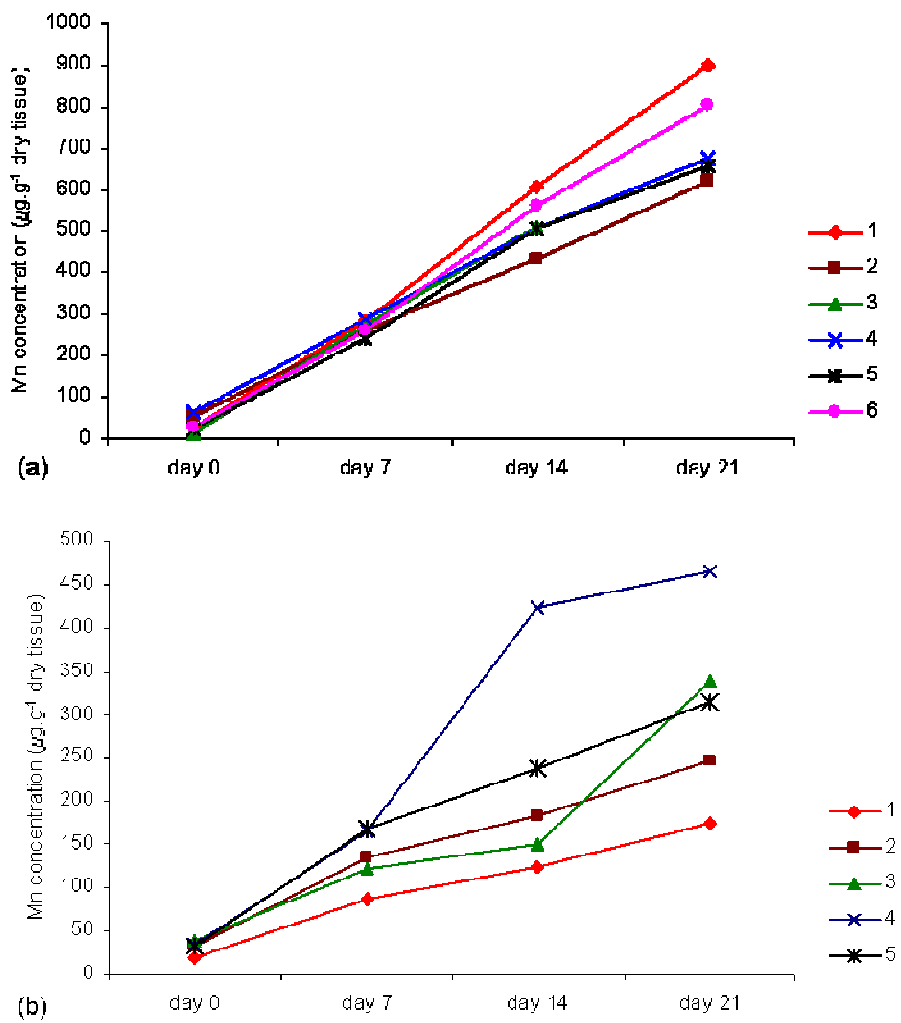
Fig. 3-9. Mn concentration in the leg exoskeleton of *L. depurator* (1-5) exposed to Mn in sea water for up to 21d, (a) 10ppm, (b) 20ppm
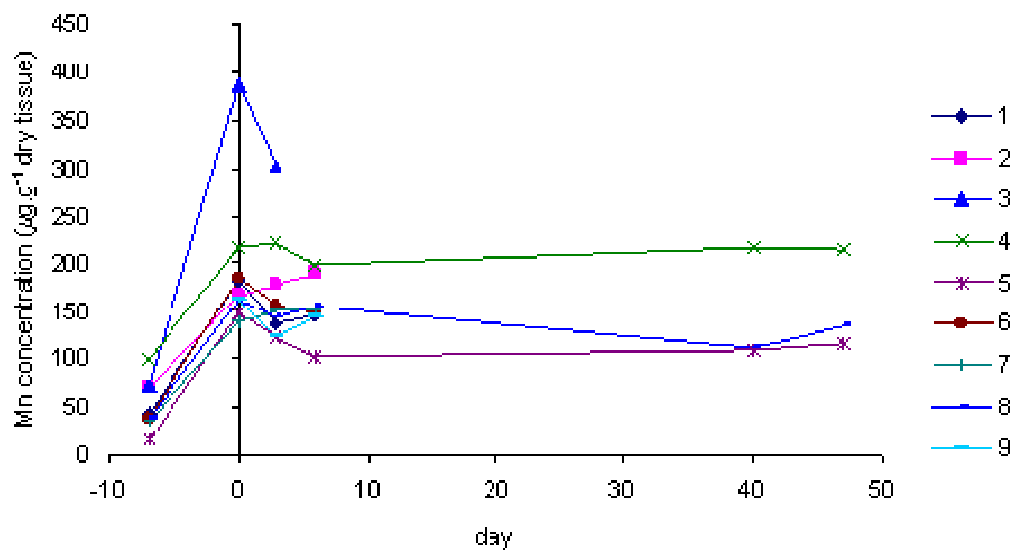
Fig. 3-10. Mn concentration in the legs of individual *L. depurator* exposed to 10 ppm Mn sea water for 7d, followed by 47d depuration. Day 0 represents the start of the depuration period.

Fig. 3-11. Black spots on the exoskeleton of *L. depurator* exposed to 20ppm. The same spots was also visible on crabs exposed to 80ppm (data not shown)

4 Using crab shell from a swimming crab, *Liocarcinus depurator* (L.) for the removal of manganese from aqueous solution

4.1 Introduction

From the previous chapter, the exoskeleton of the male *L. depurator* was found to accumulate Mn after an experimental exposure to Mn sea water in the laboratory. From observations on a few individual crabs, the shed exoskeleton from moulting crabs was found to accumulate a greater amount of Mn compared to intact ones. This suggests that a shed exoskeleton (isolated carapace) could sequester Mn from the water. It also suggests that Mn accumulation could occur more efficiently by passive adsorption onto isolated crab exoskeleton. A simple trial to examine the ability of these isolated carapaces to absorb Mn from sea water was therefore carried out by submerging them in a small container containing Mn sea water for a certain period of time, which resulted in a significant increase of Mn concentrations in the exoskeleton at the end of the experiment.

The previous chapter described the bioaccumulation (accumulating abilities of living cells) of Mn by the crab. This chapter turns the focus on biosorption by the exoskeleton (the sequestering capabilities of dead tissues) for the removal of Mn from a solution. It will emphasize assessing the capacity of carapace particles to passively bind Mn from a passing solution, thus adsorbing Mn from a flow-through column. As biosorption is a technique that is becoming popular for remediating waste water and factory effluents, many investigations have been reported for freshwater environments. With the same intention, biosorption experiments using crab carapace particles in this study were also carried out using Mn dissolved in distilled water.

Biosorption is a process that utilizes inactive biological materials to sequester toxic heavy metal ions from aqueous solutions (Kim, 2004) by physicochemical mechanisms (Vijayaraghavan *et al.*, 2004). Beginning in the 1980s (Volesky, 2001), it is has attracted chemists and engineers in their search for ways to remove or recover metals from waste streams (Vijayaraghavan *et al.*, 2004). Biosorption also offers a promising alternative for the removal of organic pollutants from wastewater (Aksu, 2005). Adsorption is very rapid and very cost-effective (Volesky, 2001). For these reasons, biosorption has become an important component of an integrated approach to the treatment of aqueous effluents in some places (Veglio and Beolchini, 1997).

Crustacean carapace particles have recently been reported as good biosorption materials (see Section 1.6: Biosorption of metals). Crab shells are particularly attractive as they can be obtained cheaply as waste from related industries (Volesky, 2001). Their rigidity also allows them to withstand the desorption process thus allowing it to be used in a number of sorption cycles (Vijayaraghavan *et al.*, 2004) it is especially suitable in recovering precious metals from specialized industries (Boukhlifi and Bencheikh, 2000). This study was carried out to determine the ability of carapace particles from the swimming crab *Liocarcinus depurator* to remove Mn from aqueous solutions using a packed-bed up-flow column.

In this chapter, a few standard terms related to biosorption processes are introduced and used throughout the sections. Some terms and their definitions are listed below for convenience:-

i. Adsorption – the net accumulation of matter at the interface between a solid phase and an aqueous solution phase (Sposito, 1989).
ii. Adsorbent/biosorbent – the solid materials onto which adsorption occurs (Hiemenz, 1986; Sposito, 1989), in this case the crab or lobster carapace particles.
iii. Adsorbate – the solute adsorbed (Hiemenz, 1986), or the matter that accumulates at an interface (Sposito, 1989) in this case Mn.
iv. Batch study – sorption experiments carried out in batches in flasks containing metal solution to determine the kinetics of the sorption process.

v. Column study – continuous-flow sorption experiment using adsorbent packed in glass columns.

vi. Effluent – refers to the processed solution collected at the outflow tube of the sorption column.

vii. Biosorbed particles – refers to the carapace particles that have been used to process the Mn solution in sorption columns.

4.1.1 Isotherm models of biosorption studies

There are basically two well-established types of adsorption isotherm, the Langmuir adsorption isotherm and the Freundlich adsorption isotherm (Fig. 4-1). Both describe quantitatively the build up of a layer of molecules on an adsorbent surface as a function of the concentration of the adsorbed material in the liquid with which it is in contact. A few assumptions form the basis of these equations, i) adsorption cannot proceed beyond single layer coverage on the adsorbent, and ii) the ability of a molecule to adsorb at a given site is independent of the occupation of neighbouring sites. The main difference is that Langmuir assumes no change in the binding energy, whereas Freundlich assumes there is an exponential change, meaning that when the binding sites are more occupied then it is more difficult for the remaining adsorbed material to bind onto the adsorbent surface. Other assumptions that apply to the Langmuir isotherm are that all sites are equivalent and that the surface is uniform. The fit of data to the Freundlich isotherm indicates heterogeneity of the adsorbent surface (Annadurai *et al.*, 2002).

The Langmuir isotherm is given as follows:

$$\frac{1}{q_e} = \frac{1}{q_{mon}} + \frac{1}{K_L \, q_{mon}} \frac{1}{C_e}$$

Where K_L is the Langmuir constant (mg.g^{-1}), q_{mon} is the amount of metal adsorbed when the saturation is attained, q_e is the amount of metal adsorbed (metal uptake) onto the sorbent, mg.g^{-1} (calculated as in the formula by Dahiya *et al.*, (2007)

below). A plot $1/q_e$ versus $1/C_e$ gives K_L and q_{mon} if the isotherm follows the Langmuir equation.

Metal uptake q_e (mass metal adsorbed per gram biomass, $mg.g^{-1}$) was calculated as follows (Dahiya *et al.*, 2007):

$$\text{Metal uptake or metal adsorbed,} \quad q_e = \frac{(C_o - C_e) \times V}{1000 \times W}$$

Where q_e is the quantity of metal uptake by biomass ($mg.g^{-1}$); C_o and C_e are the initial and final (after sorption at equilibrium) metal concentrations respectively; V is the volume of solution (ml) and W is the dry weight of the biomass added (g). The data are presented in the form of the adsorption isotherm curve (metal adsorbed versus equilibrium Mn concentrations).

The Freundlich isotherm is given as follows:

$$q_e = K_F \; C_e^{1/n}$$

where K_f and n are the Freundlich constants characteristic of the system. This equation could be rewritten as follows:

$$\text{Log } q_e = \text{Log } K_F + (1/n) \text{ Log } C_e$$

By plotting $\log q_e$ versus $\log C_e$, both K_F (the adsorption capacity, $mg.g^{-1}$) and $1/n$ (Freundlich constant) can be estimated (Dahiya *et al.*, 2007).
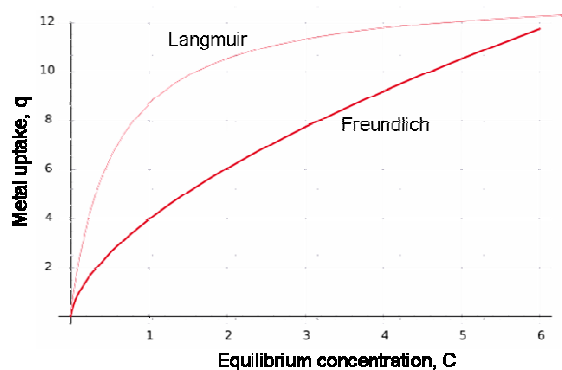
Fig. 4-1. Examples of biosorption data that fit the Langmuir and Freundlich adsorption isotherms

4.2 Materials and Methods

This study was carried out to investigate the ability of particles of the dorsal carapace from the crab *Liocarcinus depurator* to remove Mn from flowing solution. All experiments were carried out from August 2006 to January 2007 using crabs collected from the Clyde Sea area between July and December 2006. The biosorbent (the carapace particles) was prepared by grinding dried carapace into powder using a food dry blender (Moulinex). To assess the biosorption capacity of the carapace particles, a system comprising a peristaltic pump, a glass column, a reservoir and a collecting container with an up-flow rate of 100ml.h^{-1} was used on a range of concentrations (10-160ppm) and different amounts of carapace particles (0.125-2.000g). The effluent was sampled at certain time intervals. The performance was analyzed using the effluent concentration versus time curves, also known as breakthrough curves. In some of the experiments, the experimental runs were also repeated using the Norway lobster (*Nephrops norvegicus*) carapace particles, as a comparison.

4.2.1 General preparations

4.2.1.1 Adsorbent materials

Crabs trawled from the Clyde Sea area were sacrificed upon arrival at the laboratory by placing them in a freezer for 3h. A total of 80 male and female crabs with carapace widths ranging between 35-57mm were dissected to obtain the dorsal carapace. The carapaces were cleaned with a brush under running tap water and rinsed twice with distilled water. They were then freeze-dried at –40°C (Edward-Modulyo) for 24h.

The freeze-dried carapaces were crushed and ground into powder using a dry food blender (preferred to a mortar and pestle for efficiency). The powder from all

carapaces was pooled and mixed well to make a single homogenous crab shell sample, later referred to as the stock carapace particles. From 45 crabs with carapace widths of 38.3 – 56.8mm, a total of 22.225g of dry carapace powder was obtained. After sieving with sieves of mesh sizes number 20 (850μm) and 50 (300μm), the powder yielded particles with a proportion of almost 1:1:1 for the sizes <300μm (7.708g), 300 – 850μm (7.355g) and >850μm (7.162g).

4.2.1.2   Manganese solutions

Manganese solutions of different concentrations were prepared by dissolving a calculated amount of $MnCl_2.4H_2O$ (Sigma) in distilled water. The amounts of Mn salt dissolved to make up 10, 20, 40, 80 and 160ppm were 35.982, 71.964, 143.928, 287.856 and 575.712mg.L^{-1} respectively. The solutions were prepared 24h prior to experiments. The pH of the solution was not adjusted.

4.2.1.3   Biosorption column system

To assess the ability of the crab shell to adsorb manganese from aqueous solutions, a flow-through biosorption system was used, as described by Vijayaraghavan *et al.*, (2004). This comprised a peristaltic pump (Gilson Minipulse 3), a glass column with adjustable plungers at both ends fitted with plastic membranes (GE Life Healthcare) within which the carapace particles were packed, a reservoir and a collecting container. The set up is shown in Figure 4-2. The peristaltic pump was used to pump solutions upward into the column. The pump could be connected to four tubing systems, thus allowing four different flow-through systems to run simultaneously. The effluent from each system was sampled from the outflow tube in a collecting beaker at different intervals, according to the experimental regime. The concentration of Mn in the effluents was analysed to determine the changes caused by adsorption onto the particles. Table 1 summarizes the composition of the biosorption experiments conducted in this section, each of which is described later in the subsequent subsections. For all experiments, the flow rate was kept constant at approximately 100ml.h^{-1} and glass columns with the same internal diameter of 1cm were used throughout. Mn concentration of the initial solution and in the effluent samples was measured using a standard procedure using AAS (Philips PU9200).

4.2.1.4 Batch experiment

A batch sorption experiment was carried out at room temperature to determine metal uptake of the crab carapace particles in a conical flask. An amount of 0.1g – 2.0g of fine carapace particles (less than 300μm) was placed in 100ml of 80ppm Mn solution in 250ml Erlenmeyer flasks. They were mixed well and placed onto a shaker for 24h, which provided sufficient time to establish sorption equilibrium at room temperature (Kadukova and Vircikova, 2005; Niu and Volesky, 2006). Samples of the solutions (10ml) were taken after 24h and filtered with Whatman No.2 filter paper into a plastic beaker. Mn concentrations of the filtrates were analysed using a standard procedure on a flame atomic absorption spectrophotometer, AAS (Philips PU9200).

4.2.2 Data presentation

Plots of effluent Mn concentrations against time, also known as breakthrough curves, were generated for each experiment. These curves indicate the ability of the carapace particles to reduce the concentration of Mn from the initial solutions at any given time after sorption. In order to compare the rate of reduction in the concentrations by each treatment, the breakthrough curves were also plotted as the percentage of effluent Mn concentrations over the initial concentrations as calculated as follows:

$$Percent\ C_e/C_o = \frac{effluent\ concentration\ x\ 100}{Initial\ concentration}$$

This plot illustrates the relative efficiency of each sorption system in removing Mn at different conditions tested.

4.2.3 Experiment 1: Effects of the initial concentration of the solutions on biosorption performance

To determine the effect of the initial concentrations on the adsorption capacity of the crab carapace, four concentrations of Mn solution (10, 20, 80 and 160ppm) were prepared. The solutions were placed in separate reservoirs and left to stabilize for 24h prior to the experiment. Carapace particles (0.250g) from the stock powder were added to each of four glass columns for biosorption. The system was set up as shown in Figure 4-1. Mn solutions were pumped upward through the column at about 100ml.hr^{-1} for 6.5h, with four systems running simultaneously. About 4ml of the effluent from each system was sampled at 10min intervals for the first hour, at 30min intervals for the second and third hours, and by hourly collection thereafter until the end of the experiment. All the effluents collected were measured for Mn using a standard AAS protocol.

The above sorption system was also applied to lobster (*Nephrops norvegicus*) carapace particles, following the same protocols. Briefly, the dorsal carapace of lobsters caught from the Clyde Sea area (from the same trawling trips for the crabs) were washed, rinsed with distilled water and freeze-dried for 24h. The carapaces were then ground into powder, and used as the adsorbent in the columns (instead of the crab carapace particles). The concentrations of Mn tested were 20, 40, 80 and 160 ppm.

The results are presented in the form of breakthrough curves and plots of the percentage Mn removal versus time.

4.2.4 Experiment 2: Effects of the amount of carapace particles used on biosorption performance

The second experiment investigated the effect of using different amounts of particles to filter solutions of the same concentrations over a given period of time. An 80ppm

Mn solution was selected for use since it yielded the most clear-cut breakthrough and percentage curves in Experiment 1 (Sect. 4.2.3). The solution was filtered through columns containing five different amounts of adsorbent (0.125, 0.250, 0.500, 1.000 and 2.000g) for up to 10h. The effluent was sampled at 10min intervals during the first two hours, at 30min intervals during the third and fourth hour, and then at hourly interval thereafter. In an attempt to obtain more precise plots, the collection time points were slightly modified compared with the results obtained from Experiment 1. All the effluents collected were measured for Mn using a standard AAS protocol.

4.2.5 Experiment 3: Effects of different bed heights (1-8cm) on biosorption performance

The ability of the particles from both crab and lobster carapace packed into different bed heights to adsorb Mn from an 80ppm Mn solution was tested. For this experiment, the stock powder was first sieved and only fractions with particles less than 300µm in diameter (mesh size number 50) were used to pack the columns. A known quantity of shell particles was placed in the column (diameter 1cm) to yield adsorbent bed heights of 1, 2, 4 and 8cm. For the crabs, the amounts needed to make up the four bed heights were 0.481, 0.998, 2.100 and 4.247g, respectively. Smaller amounts were needed for the lobster carapace which were 0.436, 0.888, 1.692 and 3.495g, respectively. A Mn solution of 80ppm was pumped upward through the column at a flow rate of 100ml.h^{-1} by a peristaltic pump.

The effluent was sampled at 30min intervals for the first 2h, at 1h interval for the next 10h, and at longer intervals thereafter. The system ran for 99h for the lobster particles and 80h for the crab particles (having established this to be the time when extraction was completed). As a general rule, the experiments were terminated when the concentration of the effluent reached the initial concentration (80h for 8cm bed height in the crab system, a shorter bed requires a shorter time), or when the

effluent concentrations remained stable (a plateau on breakthrough curves had been reached).

All the effluents collected were measured for Mn using a standard AAS protocol. As well as Mn measurements, the effluent samples obtained from both the crab and lobster carapace systems were also subjected to Ca measurements using AAS. The data on both metals were later used to assist the interpretation of the mechanism of Mn binding onto the carapace particles.

4.2.6 Experiment 4: Batch study / equilibrium sorption experiment

Kinetic isotherms of sorption data were studied for nine different amounts of carapace particles in 100ml of 80ppm Mn solution giving concentrations of 1 – 20 g.L^{-1}. For this, one litre of Mn solution was prepared, and the concentration was measured and recorded to represent the initial concentration for all the treatments.

In this experiment, the batch sorption (described in Sect. 4.2.1.4) was carried out twice: an initial trial with only two replicates with amounts of carapace particles between 0.125–2.000g; a second trial with nine replicates using the same amounts. Only data from the latter trial are presented in this chapter, and later used to explain the sorption behaviour of the crab carapace particles. From the data, the metal uptake q_e was calculated using the formula in section 4.1.2 and an adsorption isotherm (q_e versus C_e) was plotted. The data were also checked for their closeness to fit to either Langmuir or Freundlich isotherms.

4.2.7 Experiment 5: Visual observation of the biosorbed carapace particles and corresponding Mn concentrations

The biosorbed carapace particles were observed to change colour, from an original pinkish shade, to brown or black after a certain period. An experiment was therefore carried out to monitor the colour changes, and also to investigate whether the colour changes correspond to the Mn trapped within the adsorbent column.

A series of biosorption systems using 8cm bed height of fine crab carapace particles (<300μm) were run for periods of 3, 12, 20, 27, 48 or 72h. The packed biosorbed carapace particles were carefully pushed out from the column using a wooden rod with a diameter slightly less than 1cm, and after being photographed they were then carefully cut into 1cm-segments from the inflow end to the outflow end of the column. As a result of the applied pressure, the original 8cm beds were shortened by about 1cm. Therefore, only 7 1cm-segments were produced from each column. The Mn concentration in each segment was measured using the standard AAS protocol. Briefly, the segments were labelled, freeze-dried for 24h, digested in 10ml concentrated nitric acid on a hotplate at 200°C until completely dissolved and made up to volume again by adding distilled water. The final solutions were diluted to bring them into the measurement range of the AAS and their Mn concentrations measured. The results are presented as separate graphs of Mn concentrations for each segment, plotted together with the image of the blocks as seen visually.

The progress of adsorption could be followed by visual observation of the colour change in the bed. Photographs were taken at intervals during the experimental runs.

4.3 Results

The results of the experiments reported in this chapter provide evidence that crab carapace particles have the ability to adsorb Mn from a passing solution. Experiments 1 and 2, which are more preliminary in nature, screened the biosorption properties of the coarse particles, and showed that the trend shown by the crab carapace is also shared with another decapod species, the Norway lobster *Nephrops norvegicus*. From these preliminary results, Experiment 3 was carried out to assess the biosorption capacity of particles of a specific and more uniform size to remove Mn from solutions, and thus to determine its suitability as an alternative adsorbent material.

4.3.1 Preliminary screening of biosorption capability of carapace particles

4.3.1.1 Effects of the initial concentrations of Mn solution

Figure 4-3 shows data when 10, 20, 80 and 160ppm Mn solutions were passed through 0.250g crab carapace particles in the sorption columns. The results indicate a clear adsorption of the metal by the particles occurring especially during the first 100min (Fig. 4-3a). Figure 4-3b shows the same data calculated as percent C_e/C_o. The rapid sorption, especially during the first 100min and particularly for the higher concentrations is clearly indicated by the initial steep curves immediately after the start. In fact, the rapid removal of Mn occurred within the first 50min. The efficiency of reduction in the Mn concentration was in the order of 10ppm>20ppm>80ppm>160ppm. For the 10ppm Mn solution, the adsorbent performed most efficiently, with the concentrations measured in the effluent being less than 50% of the initial solution at any given time up to 400min. In other words, 50% of Mn is adsorbed by the carapace particles.

The sorption performance decreases at higher concentrations. For the 80 and 160ppm, the Mn concentration in the effluent was about 20% less than in the initial solution, especially after 300min, indicating that very little of Mn in the passing solution was able to be adsorbed, probably due to the lack of available binding sites. The sorption continued to occur for over 400min in this range of concentrations, with no attainment of a saturation point.

Figure 4-4a shows the data for the effect of different initial concentrations on *N. norvegicus* carapace systems. Generally, the trend shown was similar to the ones seen in the crab carapace particle columns, i.e. rapid adsorption occurred immediately after the initiation of the experimental runs. The trend was particularly clear for the 80 and 160ppm Mn solutions. The curvature of the line for the lower concentrations was not prominent, due to the lower magnitudes. The concentrations used in the lobster particle column differed slightly from the crab particle columns and therefore direct comparisons can only be made for the 20, 80 and 160ppm solutions. The breakthrough curves for both systems were almost identical in terms of both the values of the concentrations, and the trend of sorption.

The change in the concentrations of Mn expressed as a percentage of the initial concentrations (C_e/C_o) of the data in Figure 4-4a are shown in Figure 4-4b. The trends were similar to the ones observed for the crab particle experimental runs with the highest reduction of the concentration occurring with the lowest initial concentration (20ppm), followed by 40, 80 and 160ppm solutions. Rapid adsorption was clearly observed for the 40, 80 and 160ppm. The trend was not obvious for the lowest concentration system where the data points fitted more to a linear pattern than a curve. However, this might be due to technical error rather than biophysical explanations.

The curves for all columns were found to approach a C_e/C_o value of 100% (the point of 'zero' removal) but this point was never attained, even after 660min, which indicated that experimental runs in the subsequent experiments should be left for a longer time if the equilibrium/saturation point was to be reached.

Table 4-2 shows some of the data expressed as the total reduction of the concentration of the initial solution by 0.250g crab and lobster carapace particles, calculated as $(C_o - C_e)$. The data show clearly that a greater reduction occurred from higher concentration of Mn for both crab and lobster carapace particles. The difference in the reduction between 10ppm-160ppm was greatest during the first minutes (between 6-60ppm and 11-67ppm for crab and lobster particles, respectively). A difference could still be observed at 300min, but it ranged only between 3-11ppm and 9-20ppm for the crab and lobster particle columns, respectively.

These observations suggest that particles of carapace from crabs and lobsters do behave similarly in this respect. Lobster carapaces (which are more readily available) could thus be used in preliminary trials to provide a good guide for determining the conditions to be used in detailed experiments using crab carapace.

4.3.1.2 Effects of different amount of adsorbent used on biosorption performance

Biosorption systems to study the effect of different amounts of adsorbent used on the sorption performance were run only on the crab carapace particles. The experiment was prolonged to around 11h or 660min i.e. almost twice as long as in the previous experiment to provide sufficient time for a plateau (equilibrium) on the breakthrough curves to be reached. The adsorption of Mn onto the particles was found to be greatly affected by the amount of adsorbent used, indicating that the sorption ability does follow a basic physico-chemical rule: greater amounts of carapace particles adsorbed more Mn from the solution at any given time period.

As seen in quantities of Figure 4-5a, when 80ppm Mn solutions were filtered through columns containing adsorbent ranging from 0.125 - 2.001g, the general trend of rapid adsorption during the first minutes was clearly shown in all cases except the 2.001g column. The absence of a similar curve in the 2.000g system might be due to the remarkably low Mn values measured in the effluent samples compared to other columns.

The columns with the greatest quantity of particles (2.001g) showed the highest adsorption, and therefore the effluent samples from this system showed the lowest Mn concentrations. No plateau was reached, indicating that more (in fact high) sorption occurred even up to 700min. The columns with the lowest amount of particles (0.125g) showed the least adsorption, and reached a plateau from about 400min. The other columns showed signs of saturation where the lines seemed to be approaching the initial concentrations of 80ppm with increasing time.

Figure 4-5b shows the same data as in Figure 4-5a expressed as a percentage of the effluent Mn concentration in the initial concentration (C_e/C_o) in experimental runs with varying amounts of adsorbent (the carapace particles). The ability of the adsorbent to reduce the Mn concentrations of the solution for each column gradually decreased towards the end of the run. The final concentrations did not converge to the same point but remain almost proportional to the amount of adsorbent used. The data for columns containing the lowest amount of particles showed concentrations closest to initial values, while the columns with the highest amount showed the lowest concentration. Mn in the effluent from the 2.000g column was almost below the detection limit immediately after the biosorption run was initiated, indicating a total purification of the 80ppm solution. As the capacity is reduced, the effluent concentration measured less than 40% of the Mn in the solution passed through it until 700min, indicating high Mn removal. The 1.000g and 0.500g sorption columns also showed a high reduction of Mn concentration in the effluent, indicating high removal, but this removal was reduced to less than 50% at 500min. The lowest amount (0.125g) totally lost its capacity to remove Mn at 500min when the concentration in the effluent was similar to the initial solution of 80ppm. This point also indicates an attainment of saturation for this particular column.

Table 4-3 shows the reduction of the concentrations of the initial 80ppm Mn solution by 0.250-2.000g crab carapace particles. The reduction ranged from 43.35-73.33ppm, with the lowest amount of adsorbent showing the least reduction. The trend was observed throughout the biosorption period up to 625min. All columns showed a decrease in the reducing ability with time. At the end of the experiment, the total reduction of the systems was found to be almost proportional to the amount

of adsorbent used. Generally, greater amounts of adsorbent would remove more Mn from the solution, and for a longer time.

The reducing abilities per gram of carapace at 10min were 170.00, 116.87, 66.92 and 36.65 ppm.g^{-1} for the 0.255-2.000g columns, respectively (across the table columns). These values might reflect the 'number' of binding sites occupied by Mn^{2+}. Greater values would mean that the column would lose its ability to reduce the concentration of the solution more rapidly than a column which showed lower values at this initial stage. From 10 to 625min, each column showed a decrease in its ability to reduce the concentration of Mn in solution. The decrease was more abrupt especially in the lower amount columns (0.255g and 0.505g) showing a drop of around 150 and 100 ppm.g^{-1}, respectively. The decrease with 1.002g of particles in the column was only 50ppm.g^{-1}, and with 2.001g it was only 12ppm.g^{-1}. These values reflect the fact that a greater amount of carapace particles is able to remove Mn from the solution for a longer time. In this case, the 2.001g amount was able to remove more than 50% of the Mn from the initial solution at 625min, that is after filtering more than 1 litre (initial solution: 80ppm, effluent: 80-48.34=31.66ppm).

4.3.2 Effect of different bed heights on biosorption performance

4.3.2.1 Crab carapace sorption columns

Figure 4-6a shows the sorption performance (breakthrough curves) for 1, 2, 4 and 8cm bed heights of crab carapace particles of less than 300µm diameter, 100ml.h^{-1} flow rate and approximately 80ppm Mn concentration. The experiment was carried out for 80h. All beds showed the characteristic sigmoidal curves that reach a plateau after a certain time. This plateau refers to the saturation of the sorption capacity of these columns. The time at which the saturation point is reached also defines the exhaustion time, t_e. At t_e the columns were assumed to reach Mn influent-effluent equilibria, after which sorption capacity remained stable. This point was achieved at

about 15h (after processing 1500ml solution), 30h (3000ml), 50h (5000ml) and 70h (7000ml) for the 1cm, 2cm, 4cm and 8cm bed columns, respectively. This progressive increase in t_e is shown by the shifting of the curves to the right with increasing column bed heights (Fig. 4-6a). This shift also indicates that greater bed heights are able to adsorb Mn from the solutions for longer times (t_e increased with increasing bed heights). For 1, 2 and 4cm bed heights, the curves finally pointed to the initial Mn concentrations of about 75ppm, with t_e occurring proportionately at about 10, 20 and 40h, respectively. However, for the 8cm bed, the first plateau was shown for the first 10h (total adsorption of Mn from the solution onto the particles), whereas t_e (marking the beginning of the final plateau) was reached at about 60h at an effluent concentration measuring about 60ppm. The initial concentration was not reached even after 60h, indicating a continuous, even though slower, Mn sorption within the column.

The breakthrough time, t_b refers to the time when Mn in the solution fails to be adsorbed by the particles and therefore passes into the effluent. In Figure 4-6a, only the 4 and 8cm beds show a detectable t_b, at about 5h and 20h, respectively. The 8cm bed containing 4.247g of crab carapace particles could purify 2000ml of 80ppm Mn solution (total removal or below detection) before the breakthrough occurred at 20h. Breakthrough occurred almost immediately in the shorter bed systems, and could be roughly estimated to be occurring at 0.5h. The slope of the S-curve from t_b – t_e decreased significantly as the bed height increased from 1cm – 8cm.

The same data expressed as the percentage of $(C_o-C_e)/C_o$ (Fig. 4-6b) indicate the total reduction of Mn concentration in the effluent compared to the initial solution. The calculations were made based on the true Mn initial concentrations for each bed. Increased bed height resulted in a greater reduction of the Mn concentrations and also resulted in a longer service periods. All beds initially produced total removal of Mn (100%). High removal for a longer period (up to 40h) was shown by the 8cm bed system. The removal of Mn in the 1cm bed ceased at about 40h (showing 0% reduction) whereas removal continued for more than 80h for the 8cm bed system. The sorption performance of the 2cm and 4cm beds lies proportionately between those of the former two columns.

Mn removal expressed as 'mg Mn per litre per gram particles' was calculated for a few data points (Fig. 4-6c). The capacity was shown to be the greatest in the shortest bed (1cm) followed by 2cm – 8 cm beds during the initial hours. The 1cm and 2cm beds showed the sharpest decrease in capacity, whereas the 4cm and 8cm beds showed a more stable performance per gram of adsorbent used. However, towards the end of the experiment (from 50h onwards), all columns showed a similar capacity for adsorption, which explains the almost proportionately higher percentage reduction of the concentrations in the passing solutions in the order of 8cm>4cm, 2cm>1cm as shown in Figure 4-6b.

Figure 4-7 shows the calcium concentrations in the effluent of 2, 4 and 8cm bed crab carapace columns with 80ppm Mn solution and distilled water (4DW, 8DW) passing through them. The figure is divided into 3 time frames (0-20h, 20-50h, 50-80h) to explain the difference in calcium concentrations between the columns. Only 4cm and 8cm beds were tested with distilled water as controls; none was carried out on 2cm bed. The concentration in the controls remained stable, fluctuating only between 0.78-3.86ppm throughout the experiment.

During the first 20h, the controls showed some calcium release into the passing distilled water. Data for both 4cm and 8cm controls clump together between 3-4ppm. However, with Mn solution passing through the columns, more calcium was released into the solution as the concentrations became higher in the effluent (in the range of 8-13ppm) in the 2cm, 4cm and 8cm columns. The concentration in the effluent of the 2cm column began to decrease within this time frame.

During 20-50h, the 8cm column was still releasing high amounts of calcium into the solution (effluent measuring between 11-13ppm) before showing some decrement later on. The Ca concentration in the 4cm column started decreasing whereas the concentration in the 2cm column fell well below the controls. During this time frame, the concentrations measured in controls for the 8cm column could be easily differentiated from those of the 4cm column. The higher concentration in the controls for the 8cm column compared to 4cm column persisted until the end of the experiment.

From 50-80h, all columns seemed to show a steady release of calcium, which matched with the corresponding controls. The data for the 8cm columns, both with distilled water and Mn solution passing through, settled together as one group, whereas the 4cm columns made another slightly lower group. The 2cm column data displayed the lowest calcium concentration in the effluent, indicating that calcium release depends on the amount of carapace particles in the columns.

In terms of weight, the biosorbed carapace particles showed a reduction in dry weight by 25-34% compared to the initial weight used to make up the different bed heights, thus confirming the loss of some material (probably calcium) from the particles during the biosorption process.

4.3.2.2 Lobster carapace sorption columns

Figure 4-8a shows the breakthrough profile for 1, 2, 4 and 8cm bed heights of lobster carapace particles. The experiment was carried out for 99h. As observed for the crab carapace particles, all lobster carapace columns also showed the characteristic sigmoidal curves showing at least one plateau towards the end of the experiment. The curves were almost identical with those from the crab carapace columns. Bed heights of 1, 2 and 4cm showed a saturation sorption capacity at about 20h (t_e occurred 5h longer than the crab carapace column), 25h and 35h (15h shorter than the crab system), respectively. The 8cm bed did not reach the saturation point, but the sorption came to a stable rate at about 60h, which is similar to the crab carapace column. The breakthrough time, t_b could be determined in the 2, 4 and 8cm bed heights, and seemed to occur faster than in the corresponding crab columns. The slope of the S-curve of the 8cm bed was significantly reduced, but the differences between these slopes for 1, 2 and 4cm beds were not as clear cut as in the crab carapace columns.

The percentage of the reduction of Mn concentrations of the initial 80ppm solutions passing through 2cm-8cm beds of lobster carapace particle columns is shown in Figure 4-8b. The lobster carapace showed a trend similar to the crab carapace, with

the highest reduction shown by the longest column bed of 8cm, followed in sequence by the 4cm, 2cm and 1cm beds. The 8cm bed was also observed to be able to reduce the concentrations for a far longer time compared to the other beds. The column was still reducing to about 15% of the concentration of the initial solution even at 80-100h. However, the decrease in the reducing capacity of the 4cm and 8cm beds of lobster carapace occurred slightly faster than the respective crab carapace columns, indicating a better biosorption performance by the crab carapace.

Figure 4-8c shows the Mn removal expressed as 'mg Mn per litre per gram particles' for a few data points between 0-70h. The trend was similar to the crab carapace columns with the capacity in the order of 1cm>2cm>4cm>8cm during the initial 20h period. By 50h, all columns merged to almost the same point which is well below 10mg $Mn.l^{-1}.g^{-1}$, explaining the difference observed in the concentrations of the effluents after 60h.

Figure 4-9 shows the calcium concentrations in the effluents of 2cm, 4cm and 8cm bed lobster carapace columns with 80ppm Mn solution passing through. Distilled water was passed through two other 4cm and 8cm bed columns to act as controls (4DW and 8DW). As observed in the crab carapace columns, the controls released some calcium into the solution, measuring between 2.39ppm to 0.72ppm throughout the 100h experiment. When viewed in 3 time frames, the lobster carapace columns were found to show an almost identical behaviour to the crab carapace columns. When Mn was passed through the columns, initially the particles released about the same amount of calcium into the solution (regardless of the column bed heights), but at levels significantly higher (9-13ppm) than the controls. From 20-50h, more was released by 8cm column than 4cm column, both showing decrements in concentrations. The calcium concentration in the 2cm column was reduced to even lower levels than in the controls.

At 50-60h, the concentrations in the effluent were in the order of 8cm>8DW>4cm, 4DW>2cm, which is similar to the observations in the crab carapace columns. However the difference between these lobster columns was not as clear-cut later on as it was with the crab carapace columns. The dry weight of biosorbed lobster

carapace was also reduced by 25-38% compared to the original materials. However overall there is similar behaviour of the carapace particles in these two crustacean species.

4.3.3 Equilibrium sorption experiments

In this experiment, pH was not adjusted. When Mn was dissolved, the pH of the solution was neutral at 7.08±0.042 (mean±SE; range: 7.01 – 7.19), but the solutions became alkaline when mixed with the crab carapace particles. Measurements made at 3h, 8h, 20h and 24h shows stable pH readings of 8.79±0.062 (8.18 – 9.31) from the beginning of the experiment to the end.

Figure 4-10 shows the adsorption isotherm (q_e versus C_e) for Mn onto crab carapace particles. Adsorption was found to increase rapidly at low concentrations, indicating that crab carapace has a good affinity for Mn. The shape of the curve suggests that the isotherm might fit the Langmuir equation. If so, the equation could be applied to provide a suitable quantification of the data. However, a plot of $1/q_e$ versus $1/C_e$ (Fig. 4-11) does not give a linear relationship, indicating that the results do not fit the Langmuir model. The constant K_L could not be determined.

In order to investigate the fitness of the data to the Freundlich isotherm, they were then plotted as log q_e versus log C_e (Fig. 4-12). The data set generated a linear plot, and thus fitted the model. From the equation, the Freundlich constant K_F could be determined. The intercept gives the value of log K_F, therefore K_F = 22.80mg.g^{-1} (R^2=0.61).

Figure 4-13 shows a profile of the equilibrium concentrations per Mn adsorbed (g.ml^{-1}) plotted against the equilibrium concentrations (mg.l^{-1}) of the batch study data. The sharp decrease at low concentrations (between 0-2ppm) indicates a precipitation process, whereas the gradual increase at higher concentrations indicates the adsorption of Mn onto the carapace particles (Veith and Sposito, 1977).

4.3.4 pH change

During the course of the experiment, pH was measured at random time points between 0-76h. The original 80ppm Mn solution in the reservoir measured 5.61±0.25 (5.60, 5.18 and 6.06 at three different sampling points). pH in the effluent of four columns with lobster and crab carapace particles decreased slightly, as shown in Table 4-4. As these columns were continuous up-flow columns, the solution within them was regularly renewed as the solution from the reservoir was pumped in through the inflow tube. It is interesting that the pH values of the passing solutions were increased from 5.61 to approximately 10 in all columns with carapace particles.

4.3.5 Colour changes of biosorbed beds and the corresponding Mn concentrations

During experimental runs, the adsorption of Mn by particles in the column was reflected in a progressive colour change in the bed. The colour of the biosorbed carapace particles turned from the original pinkish shade to dark brown and then to black (Fig. 4-14). When the adsorbent was not fully packed into the column, leaving a space above for the solution (Fig. 4-15), this colour change was apparently uniform, but when the column was fully packed with adsorbent material, a distinct front of colour change was observed (Fig. 4-16). This progression provides a visual indication of the movement of the Mn adsorption zone. In the non-packed-bed column shown in Figure 4-15, the particles could stir within the solution in the column as the influent pushed its way in, and therefore the blackening of the particles occurred more evenly.

Figure 4-17 shows the Mn concentrations in seven 1cm-segments cut out from 8cm beds of biosorbed particles with 80ppm Mn passed through each column for a

certain time period. The Mn concentration was found to be closely correlated with the blackening of the particles, confirming the accumulation of Mn in the blackened areas. The degree of blackness gives an indication of the relative amount of Mn within the segments. At 3h, Mn concentrations in segment 1 increased up to 20,000µg.g^{-1}, whereas it was extremely low in the other 1cm-blocks. At 12h after sorption, segment 1 approached 60,000 µg.g^{-1} while significant concentrations were also measured in segments 2, 3 and 4 (parallel to the blackening of the relevant areas) at 12h. The Mn adsorption zone had moved about 4cm into the column.

At 20h, more Mn was eluted from segment 1, making it available to the subsequent blocks. However sorption also continued in segment 1 as the concentration increased to almost 100,000 µg.g^{-1}. The transfer zone had now moved to 5cm as indicated by the change in colour and the increased concentration in segment 5. By 27h, the Mn adsorption zone had moved to segment 7, which is almost at the end of the column. This indicates that almost all the carapace particles have, at that time, been in contact with the Mn in the passing solution and been used either fully or partly to trap the metal. Segment 1 continued to adsorb Mn for up to 48h, but at a lower rate compared to the subsequent segments (2–7), indicating that fewer binding sites were left available in the first segment, but that more were still 'unused' towards the effluent end of the column. Sorption was found to continue in each 1cm-segment of the whole column up to 72h as indicated by the still increasing values of the concentration in segment 1 (~160,000 µg.g^{-1}). The remainder all showed concentrations of more than 60,000 µg.g^{-1}.

Figure 4-18 shows the distribution of Mn in each segment in a range of biosorption times (3h – 72h) measured using AAS. During the first few hours, most of the influxing Mn (Mn coming in from the initial solution) was trapped by the first particles it encountered. At 3h, more than 90% of the Mn in the column bed was accumulated within segment 1, which is the first portion of the carapace bed to receive Mn from the inflow tube. Most of the remaining Mn was then adsorbed by segment 2, and very little escaped thereafter to be trapped by the subsequent segments. By 20h, 50% of the influxing Mn broke through into the solution passing from segment 1 where it was adsorbed by segment 2 followed by segments 3, 4 and 5. The other segments were still almost free of Mn influx. Mn gradually became more evenly

distributed between segments 1-7 at 48h to 72h. These measurements correspond well with the colour change of the carapace particles. The darker the colour, the higher the Mn concentration measured in the segment. However, at very high concentrations, when the column had turned totally black, the colour could no longer be differentiated because of colour saturation. At this point, the proportion of Mn along the column therefore could no longer be estimated.

4.4 Discussion

Crustacean carapaces (shrimp, lobster and crab) appear to represent economically attractive materials for the removal of heavy metal from aqueous solutions. They were laboratory-proven to be able to adsorb Cd^{2+}, Zn^{2+}, Cu^{2+} and Pb^{2+} effectively (Boukhlifi and Bencheikh, 2000). In this chapter, such studies have been extended to two more species, the swimming crab *Liocarcinus depurator* and the Norway lobster, *Nephrops norvegicus*, with Mn as the metal of interest.

The preliminary studies provided evidence that the crab shell possesses some biosorption properties. The sorption performance was affected by two factors, namely the initial concentration of Mn solution and the amount of carapace particles used in the sorption columns. These properties/characteristics are also shared with another decapod, the Norway lobster *N. norvegicus*.

The batch study using uniformly fine particles confirmed the biosorptive ability of the crab carapace particles. The sorption data fitted the Freundlich adsorption isotherm with the biosorption capacity, K_F of 22.80mg.g^{-1} (R^2=0.61). Having established the biosorption ability of these crab carapace particles, the up-flow column sorption system with similar particle size and column diameter, and a constant flow rate clearly demonstrated that the carapace particles are good adsorbent materials, and thus could be used as a Mn removing agent. The biosorption column runs highlight that greater column bed height (which could be interpreted as greater amount of adsorbent packed in the column, or greater length travelled by adsorbate across the

column) removes more Mn for a longer period of time compared to lower bed heights.

When using a long bed of particles in a column for biosorption, the relative amount of adsorption along the column could be well represented by a progressive colour change of the carapace particles. The adsorbed region appears dark brown to black, with the degree of blackness indicative of the amount of Mn adsorbed onto the particles.

4.4.1 Effects of initial concentration and amounts of carapace particles used

Adsorption of Mn by crab carapace particles in an exchange column was very rapid, occurring especially during the first minutes and hours. Depending on certain conditions, the adsorption could last for a long time, with no saturation attained even after as long as 70h. These patterns, which are characteristics of any adsorption process (Aksu, 2005) suggest that crab carapace might have potential for use as an effective biosorbent material.

The initial concentration of the Mn solution is known to influence the biosorption capacity of crab carapace particles (Dal Bosco *et al.*, 2006; Pradhan *et al.*, 2005). In this study, a biosorption system of 0.250g carapace particles (both crab and lobster particles) with a range of initial concentrations between 10-160ppm, higher concentrations resulted in low percentage Mn removal from the solutions. This is in agreement with Pradhan *et al.* (2005) who reported that the initial concentration of the solution is one of the major factors determining the adsorption kinetics of biosorbents of crab shell origin. In this case, the concentration of the solution reflects the amount of adsorbate (Mn) available in the biosorption system. Pagnanelli *et al.* (2003) suggested that complexation is the main uptake mechanism for a biosorption system influenced by heavy metal concentration (S-H + Me^{2+} $\rightarrow$ SME^+ + H^+; where Me is the metal and S-H is the active site in the protonated form).

At low concentration, metals are adsorbed by specific adsorption sites, whereas with increasing metal concentration the specific sites are saturated and the exchange sites are filled.

The 160ppm Mn solution provided more Mn^{2+} in the influx compared to the solution with lower concentrations. As the carapace particles used in the columns came from the same stock of particles, and the same amount was used in each, it is assumed that they provided the columns with a roughly similar numbers of binding sites where adsorption to take place. Given more Mn in the higher concentration solutions, these binding sites would be taken up once they come into contact with Mn. The rapid adsorption during the first hour of the experimental runs was due primarily to the free binding sites. A column with 160ppm Mn solution showed the earliest signs of exhaustion (most of the binding sites taken up) by 1h after which time about 70% of Mn from the influx was passed through in the effluent (only 30% removal). With the lower concentrations, removal of Mn from the solutions continued as long as the binding sites were available.

In the present study, the flow rate was kept constant at $100ml.h^{-1}$. It became the factor determining the contact time between the passing Mn in the solution and the binding sites as the pump continually pushed the solution in a single direction. If enough time was provided by reducing the flow rate, the higher concentration systems would be expected to be exhausted of binding sites sooner than the other systems and 100% of the influxing Mn should have been recovered in the effluent later during the experiment. However, at the end of the experiment, there were far fewer unoccupied sites compared to the Mn that came into contact with them from the influx. At this point, it is assumed that adsorption primarily depends on the remaining unoccupied binding sites on the particle surface, and that contact time plays a less important role.

The amount of carapace particles used was positively associated with Mn adsorption onto the particles. It is simply explained by the availability of more binding sites when more particles are used. More particles removed more Mn from the initial concentrations of 80ppm solutions. When about 2g of carapace particles was used in the column, only 50% influxing Mn was recovered in the effluent at

about 10.5h after filtering a volume of approximately 1L, suggesting the availability of more free sites on the particles. Besides initial metal concentration, the amount of adsorbent is another major determinant of adsorption kinetics of crab shell particles (Pradhan *et al.,* 2005).

Size of particles is one of the important factors determining uptake capacity of biosorbent (Volesky, 2001; Ng *et al.*, 2002; Lu *et al.*, 2007). The results in this section were obtained from ground carapace particles with a maximum diameter of roughly 1.5mm without sieving. Evan *et al.* (2002) reported that the adsorption equilibrium of cadmium on chitosan-based crab shells was independent of particle size (0.85-2.0mm). The characteristics of 'high initial rate uptake followed by a slower uptake rate' shown in their study confirms that the adsorption follows the normal biosorption mechanism. Various size fractions from 88μm to 210μm of chitin powder from crab shells also yielded similar adsorption values (Gonzalez-Davilla and Millero, 1990). However, Vijayaraghavan *et al.* (2006) provided evidence that crab carapace particles smaller than 0.767mm resulted in higher copper and cobalt uptake capacity and removal efficiency compared to 1.177mm particles. Niu and Volesky (2006) suggest that cross-linkages between chitin and protein in crab shell make the shell very dense that some sites might not be reachable by metals. Grinding into finer particles resulted in these unreachable parts of the shell becoming more exposed and readily available for metal to attach to, therefore led to higher uptake by finer particles. Therefore, in the interest of uniformity and 'safety', only the finest fraction (<300μm) of the ground carapace powder was used in batch and column sorption bed height studies.

pH is also acknowledged as one of the most important factors affecting the biosorption process (Veglio and Beolchini, 1997; Volesky, 2001; Niu and Volesky, 2006). It affects the solution chemistry of the metals, the activity of functional groups in the biomass, and the competition of metallic ions (Veglio and Bolchini, 1997). This has led some researchers to determine the optimum pH for biosorption for any specific adsorbent. Batch studies are then carried out at this particular pH and therefore the adsorption capacity given should represent the maximum capacity. However, in the present study, no pH adjustment was carried out as was practiced by some other researchers (Boukhlifi and Bencheikh, 2000; Wilson et al., 2003;

Barriada *et al.,* 2007; Lu *et al.*, 2007). Adjusting the pH introduces other ions into the solution that might affect biosorption through competition (Niu and Volesky, 2003). The random pH check for the effluent of biosorption columns containing 4cm and 8cm lobster carapace particles and, 4cm and 8cm crab carapace particles showed only a slight decrease (less than 1) in the pH in those columns for up to 76h.

The initial 80ppm Mn solution in the reservoir was acidic at a pH of 5.61±0.25. However, when this solution was passed through the beds of carapace particles in the columns, the solution became alkaline with a pH as high as 10. Columns with longer beds for both lobster and crab carapace particles were found to increase the pH of the solution slightly more than columns with shorter beds, indicating a role played by the amount of the carapace available in the columns. Introduction of shrimp carapace increased the pH of a metal solution from 4.8 to 8.75 (Boukhlifi and Bencheikh, 2000), spider crab particles increase the pH of cadmium and lead solutions rapidly from approximately 5.5 to 9.3 (Barriada *et al.*, 2007), and particles from the carapace of *Cancer pagurus* cause an increase from the initial pH of 4.3 of zinc, copper and lead solutions to 6.3, 5.6 and 7.9, respectively. This seems to support the observation of the present study.

A crab carapace is made up primarily by calcium carbonate ($CaCO_3$), along with chitin and some proteins (Lee *et al.*, 1997; Vijayaraghavan *et al.*, 2004). Dissolution of $CaCO_3$ controls the pH of a solution (Barriada *et al.*, 2007) as in solution,it dissolves, releasing Ca^{2+} and CO_3^{2-} (Lu *et al.*, 2007). CO_3^{2-} further reacts with proton to form HCO_3^- and H_2CO_3 (Lee *et al.*, 2004) leaving fewer protons in the mixture, thus increasing the pH of the solution. Boukhlifi and Bencheikh (2000) suggested the increase in pH could be due to i) the decrease of the amount of H_3O^+ by binding with adsorbent, or ii) the increase of the amount of OH^- ionsby the release of an ionic base such as CO_3^{2-}, by ionization of the adsorbent. The assumptions by Boukhlifi and Bencheikh (2000) can be summarized as below:

$$CaCO_3 \quad \leftrightarrow \quad Ca^{2+} + CO_3^{2-}$$
$$CO_3^{2-} + H_2O \quad \leftrightarrow \quad HCO_3^- + OH^-$$
$$HCO_3^- + H_2O \quad \leftrightarrow \quad H_2CO_3 + OH^-$$
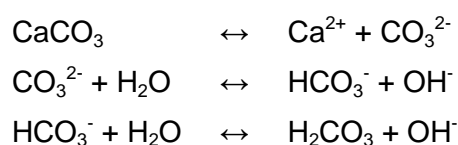
All the reports regarding pH changes mentioned previously were referring to the same total amount of carapace used for each experimental setting. In this study, the amount of carapace particles varied. Therefore the slightly higher pH observed in the columns with longer beds was expected. As there was more material in the longer beds, dissolution of the particles would result in more Ca^{2+} and CO_3^{2-} being released into the mixture, which ultimately would increase OH^- and thus pH.

The pH change observed in the present study (from pH 5.61 of initial 80ppm Mn solution to more than 10 after biosorbed by carapace particles) might explain one of the mechanisms of Mn removal from the solution by these raw carapace materials. Crab shell becomes more porous after alkali treatment due to deproteination (Kim, 2004) which might open up new sites for Mn attachment. In this case, the pH change from acidic to alkali due to dissolution of $CaCO_3$ could be regarded as an addition of a 'natural alkali treatment' to the carapace particles, making them more penetrable by Mn available in the passing solution. The holes created after the treatment enables the metal to be easily transferred to an inner part of the shell particles (Kim, 2004). This means that adsorption which is the net accumulation of matter at the interface between a solid phase and an aqueous solution phase (Sposito, 1989) could occur both on the particle surfaces, and also in the newly-made-available active binding sites that lie in the spaces within the particles themselves. Besides the mechanistic explanation of the effect of pH on metal uptake, the ionic competition for active sites offers another explanation of how an increase in pH causes an increase in metal uptake (Schiewer and Volesky (1995) in Pagnanelli *et al.* (2003)).

4.4.2 Adsorption capacity (kinetics isotherm)

In a batch system, the biosorption process follows a sequence of steps; i) transport of adsorbate molecules from the boundary film to the external surface of biosorbent, ii) transfer of molecules from surface to the intraparticular active sites, and iii) uptake of molecules by the active sites of sorbent (Aksu, 2005).

Adsorption isotherms describe the interactions between adsorbates and the adsorbents and so are critical in optimizing the use of adsorbents (Ng *et al.*, 2002). Most of these papers report a better fit of data to the Langmuir isotherm. However, the data from the present study on particles with a diameter of less than 300μm fitted the Freundlich adsorption isotherm better than Langmuir's, giving a K_F value of 22.80mg.g^{-1} (R^2=0.61). The judgement as to which mechanism is operative is normally based upon the correlation coefficient, which sometimes is better for Langmuir and at other times for Freundlich. Pradhan *et al.* (2005) found that the adsorption isotherm of nickel removal by crab shell is better described by Freundlich isotherms (R^2=0.74), and Evans *et al.* (2002) reported a Freundlich relationship in the adsorption equilibrium of cadmium uptake by chitosan-based crab shells. These reports suggest that the result of the present study is in fact common and indicative of reliable observations.

The Langmuir isotherm assumes that the adsorbed layer is one molecule in thickness. The Freundlich isotherm, which is another form of Langmuir approach for adsorption onto an 'amorphous' surface, predicts that the metal concentrations on the adsorbent will increase as long as there is an increase in the metal concentration in the liquid (Ng *et al.*, 2002). The Freundlich isotherm also describes reversible adsorption and is not restricted to the formation of the monolayer. Therefore the fact that the adsorption of Mn on the carapace particles from *L. depurator* fitted the Freundlich isotherm might suggest that adsorption of Mn occurs in more than just a single layer on the surface, and that the surface might be heterogenous, a fact which is likely due to the robust nature of the grinding of the carapace.

Crab carapace and crustacean-shell based materials (chitin, chitosan) have been widely researched and proven to have biosorptive properties. Adsorption capacities (K_F or K_L) and metal uptake of carapace particles from some crab species, including data from the present study are listed in Table 4-5 for comparison. Carapace particles from a single species were observed to be broad-ranged, adsorbing not only one particular metal but a series of different metals.

The list in Table 4-5 was obtained from various sources which differ in the treatment of the carapace materials to a certain degree. Some of the researchers pre-treated the crab shells prior to the biosorption process, whereas others used a raw, non-treated material. However, it is interesting to see that even raw crab shells do show high biosorption capacities for certain metals. Raw crab particles from *L. depurator* were found to show a higher adsorption capacity for Mn compared to commercial clay. This highlights the advantages of using this material as an alternative biosorbent for two reasons, i) it could be obtained cheaply, and ii) no pretreatment is required prior to use, apart from drying and grinding into fine particles.

From Table 4-5, the adsorption of metals onto the particles was generally found to be higher in the pre-treated carapace compared to the raw carapace. For instance, Cu was found to adsorb more onto pre-treated particles. Assuming that the adsorption is roughly similar across species and therefore the results of one could be extended to another (quite a safe assumption as adsorption is a physicochemical process and not dependent on metabolism), then it would be expected that carapace particles from *L. depurator*, if given a proper pre-treatment, would have shown a higher adsorption capacity. Further studies could provide useful information if the particles were to be transformed into a commercialized biosorbent.

4.4.3 Effect of different bed heights

Increased bed heights in both crab and lobster columns resulted in higher volumes of Mn solution being treated and a higher percentage of Mn removal, which is similar to the biosorption of Zn on crab shell (Lu *et al.*, 2007). This is evident from the increasing breakthrough time (t_b) and exhaustion time (t_e) with increasing bed heights. t_b is the time when Mn 'breaks through' the adsorbent beds and starts to appear in the effluent. Before this point was reached, Mn was 100% removed from the solution. t_e refers to the time at which Mn in effluent started reaching a plateau. In some cases, the plateau might indicate 0% removal, whereas in others total loss of adsorption is never attained. Higher t_b and t_e indicate a better sorbance. The trend of sorption shown in the breakthrough curves resembles the characteristic of good

biosorption ability. Under the experimental conditions of this study (flow rate 100ml.h^{-1}, 80ppm Mn solution, particle size <300µm), longer beds allow a better estimation/identification of t_b compared to shorter beds. In both lobster and crab carapace columns, t_b could be confidently identified only in the 8cm beds, whereas it was roughly estimated for the others. Better identification of t_b and t_e for shorter beds would be possible if a lower flow rate is applied.

The area above the curves in a breakthrough profile (maximum y= t_e) of the columns represents the amount of Mn adsorbed onto the carapace particle beds. As t_b and t_e shift to the right with increasing bed heights, the slope of the S-curvatures from t_b - t_e also decreases resulting in a greater area above the curves. This indicates an increasing adsorption capacity of greater bed heights compared to shorter ones, probably because uptake capacity depends strongly on the amount of adsorbent available for sorption (Vijayaraghavan *et al.*, 2004). Early saturation of shorter bed heights for copper biosorption using seaweed was also due to the lower overall number of available binding sites (Naja and Volesky, 2006).

Vijayaraghavan *et al.* (2004) reported similar findings for the removal of nickel by crab shell particles of *Portunus sanguinolentus*. Despite having applied different experimental conditions (bed heights 15-25cm; flow rate 300ml.h^{-1}), t_b and t_e also increased with increasing bed heights and the slope of the S-curves also decreased, both implying better sorption by longer beds. In the same study, t_b, t_e and uptake capacity decreased as the flow rate increased from 300ml.h^{-1} to 1200ml.h^{-1} implying that a slower flow rate favours sorption due to increased residence time of the adsorbate within the columns. The latter observation would apply to the crab and lobster carapace particles used in the present study.

In this study, an 8cm bed containing about 4.3g of crab carapace particles could purify around 2000ml of 80ppm Mn solution at a constant flow rate of 100ml.h^{-1}. It is interesting to see that lobster carapace particles show a closely similar trend of sorption performance. If adsorption is due primarily to the $CaCO_3$ component of the carapace, then this observation came as expected. The physicochemical explanation of the adsorption process on the crab particle surfaces therefore could be extended to other crustacean shell, including this particular lobster species.

4.4.4 Removal capacity expressed as milligram Mn per gram adsorbent per litre (mg.g^{-1}.l^{-1})

Initially, the flow rate influences the Mn removal capacity by different bed heights of carapace particles. The general pattern for both the crab and lobster carapace columns was almost identical but with the lobster carapace columns showing slightly higher values. Mn in the passing solution will occupy all available binding sites on the carapace particle surfaces once they are in contact with them, if provided with sufficient residence time within the columns. Under the experimental conditions used, the removal capacity (expressed as milligram Mn per gram adsorbent per litre, mg.g^{-1}.l^{-1}) in shorter beds was initially higher compared to longer beds. Higher removal capacity values shown at the beginning of the biosorption process indicate that more binding sites on the adsorbent are occupied by Mn, and the column is expected to become exhausted faster than the others. At this stage, the amount of Mn adsorbed within each single column might be similar but as the capacity was based upon the weight of adsorbent used, the shorter beds showed higher values (the effect of flow rate is greater than the effect of bed heights). Vijayaraghavan *et al.* (2006) reported a similar decrease in metal uptake with increasing biosorbent dosage.

The rapid decline seen for the shorter beds within the next 20h in the crab carapace columns indicates that not all binding sites are occupied initially (maximum adsorption did not occur), and during these later hours, the remaining available sites are filled. Longer beds, (particularly the 8cm bed) show lower removal capacity initially but the capacity was maintained for the next 30-40h. This shows that the amount of adsorbent in the longer beds was actually able to adsorb more Mn from the passing solution, but flow rate has become the limiting factor when Mn was not given enough residence time within the column to attach to all active binding sites at once, but the adsorption was prolonged until finally they reached similar values after 50h.

After about 50h, all columns showed a similar removal capacity. At this point, most probably there were no more available binding sites. Removal of Mn might continue during these later hours by precipitation, which can take place either in the solution, on the cell surface (Veglio and Beolchini, 1997) or on the existing Mn complex on the particle surface after chemical interactions between Mn and the surface. Metal adsorption can also be reversible (Veglio *et al.,* 1997) therefore re-opening some active binding sites for Mn attachment. However, this might not be the case in this study as deionized water was not able to elute biosorbed metal ions on crab shell particles, indicating strong affinity (Vijayaraghavan *et al.*, 2006). Precipitation (and later Mn removal) at 50h probably might depends largely on the surface area rather than on specific binding sites. As the greater bed heights have more adsorbent providing a greater surface area, more precipitation could then take place and this resulted in higher removal by longer beds during the final hours of the biosorption process, as shown by the breakthrough curve.

4.4.5 Calcium release by the carapace particles

Carapace particles in columns partly dissolved when they came into contact with water releasing Ca^{2+} into the solution. Ca^{2+} release decreased slightly with time, but continues to occur up to the end of the biosorption process (80h). The release of Ca^{2+} is influenced by the amount of carapace packed into each column. Longer beds, having more particles, tend to release more Ca^{2+} into the solution. It is assumed that the ions will continue to be released into the passing solution as long as there is any $CaCO_3$ remaining within the column. As the sorption system used was a flow-through system, Ca^{2+} release never reached equilibrium due to the continuous renewal of Mn solution.

Interestingly, the introduction of Mn into the passing solution resulted in an increase in Ca^{2+} release by about three-fold during the first 15h and 30h for 4cm and 8cm beds, respectively. Lee *et al.* (2004; in Lu *et al.*, 2007) suggested that ion exchange between Ca^{2+} and the tested metal ions promoted Ca^{2+} release in their study of Pb^{2+} removal by crab carapace. Their hypothesis might explain the present result. The

increments in Ca^{2+} release in this study were prolonged for more than 20h before they finally decreased and reached the base values around 50h. At this time, continued introduction of Mn solution from the inlet did not seem to increase the release of Ca^{2+} as observed during the earlier hours of sorption. By this time, Mn adsorption and precipitation might have taken place on the particle surface, resulting in a layer that coats the remaining particles ($CaCO_3$). The limited direct exposure to the Mn solution therefore did not bring the effect to a significant level.

The concentration of Ca^{2+} in the solutions is negatively correlated with Mn concentrations, which strongly suggests ionic changes as one of the mechanism for Mn removal by crab or lobster carapace particles. This is highly possible as a similar mechanism was reported for other metals including Pb (Lee *et al.*, 2004), Cu (Wilson *et al.*, 2003) and Zn (Lu *et al.*, 2007). Lee *et al.* (1998) proposed that Pb was removed from an aqueous solution by adsorption and precipitation of $PbCO_3$ when Pb complexes with CO_3 released from $CaCO_3$ dissolution. Cd also formed carbonate in a biosorption process (Barriada *et al.*, 2007). However, Lu *et* al. (2007) suggested that an ion exchange mechanism contributed to metal removal by forming metal-carbonate under low concentration. At higher concentrations, this mechanism is limited and other mechanisms including adsorption, chelation and microprecipitation by forming metal-hydroxides predominate. In this study, Mn removal might have occurred by the formation of $MnCO_3$ as judged by the colour (could appear dark brown). However, the formation of Mn hydroxides (black to steel grey) together with $MnCO_3$ also probably occurred.

Ca^{2+} release or elution into the solution also contributes to the reduction of the original dry weight of carapace particles used. In this study, the weight of the adsorbent was reduced randomly between 25-34% with no particular trend. This reduction is higher when compared to the reduction (approximately 5%) observed for crab shell particles in Zn and Pb biosorption processes (Lu *et al.*, 2007).

4.4.6 Carapace bed colour change and Mn concentration

Blackening of the carapace particles in a biosorption bed from the original pinkish shade could be used as an indicator of the efficiency of the column for removing Mn from passing solution. The progression of colour change visually relates to the movement of the Mn adsorption zone. The term 'mass transfer zone' is used to describe the section developed between the section of the column that gradually becomes saturated with the sorbate and the virgin biosorbent section which could be followed as it advances along the column length. This zone refers to the region where most of the sorbate transfer takes place (Naja and Volesky, 2006). However, after a certain period of biosorption, the bed reached colour saturation when all particles were totally blackened. At this point no available adsorption zone (pink zone) could be visually identified. In the present study, colour saturation of an 8cm bed occurred at about 54h. It was assumed that all active binding sites on the particle surfaces were occupied, and removal of Mn occurring at this time might be due to precipitation onto the existing Mn layer, which occurred at a much lower rate. As the first 1cm-segment reached Mn saturation at 72h, the fact that Mn was almost equally distributed along the bed (segments 1-7) suggests that the bed might be reaching exhaustion at this point and would no longer be efficient as a Mn removing agent.

In a packed-bed column, the adsorbate adsorbs onto the first biosorbent with which they come into contact, which means the ones located closest to the inlet. The adsorption continues until the zone is fully saturated (Volesky, 2001). In the observations made during the present study, the darker colour of the bed indicated the degree of saturation. It also indicated that the capacity for Mn removal from the passing solution had been much reduced. Rapid adsorption of Mn is favoured in the treatment of wastewater. Therefore, if the carapace particles were used in a real water treatment system in which the concentration of the metal might vary, then this colour indicator could be a simple but useful tool for the determination of column utilization during the treatment process, thus assisting in maintaining the efficiency of the process. The column is operational until the mass transfer zone reaches the end of the column (Naja and Volesky, 2006).

4.4.7 Limitations

There are some general limitations in carrying out biosorption studies. Among the common problems in column studies are difficulties in obtaining uniform packing and difficulties in estimating the start and the end of the breakthrough curve for calculations of the capacity (Wilson *et al.*, 2003). In some of the experimental runs, the first few sampling points were variable. This might be due to the unstable condition of the system at the very initial state of the biosorption process due to technical handling.

A batch study could provide a better estimate of adsorption capacity for biosorbents, but the constants obtained do not comply with the same adsorbent in the column process (Dahiya *et al.*, 2007). The values obtained in a batch process normally represent approximately 80% of the column figure (Wilson *et al.*, 2003), making it still very useful in the design of the columns to ensure that the basic parameters are met. Longer time scale runs with columns with lower concentrations of influent should be made to ensure that the conditions and capacities are comparable to the commonly found environmental levels, in order to turn the results into a practical system for metal absorption.

4.5 Conclusions

This study has demonstrated that the crab carapace has great potential as a good biosorbent for Mn from aqueous solutions. Lobster carapace particles also proved to show almost identical behaviour towards Mn, and have similar potential as a Mn removing agent. Mn removal depends greatly on the initial concentration of the Mn solution and the amount of adsorbent used. Increased bed heights of adsorbent packed into the column increased the Mn removal capacity. Longer beds also prolonged the time for biosorption to continue. The Mn removal capacity of carapace

beds could also be visualized through progressive colour change of the beds, which could be useful in a real system.

The results of the present study are consistent with those in the literature. Possible mechanisms of Mn removal by crab and lobster carapace particles include:

- Ion exchange – possible as indicated by reverse trend of Ca and Mn concentrations in same effluent
- Adsorption onto the particle surface at specific binding sites (complexation), followed by:
- Precipitation either in solution, onto the particle surfaces or onto adsorbed layers
- Transfer of Mn into the inner parts of shell particles through pores created via deproteination

Table 4-1 Summary of the compositions of the biosorption experiments.

Experiment	Amount of adsorbent used (g)	Particle size (µm)	Bed height (cm)	Mn concentrations (ppm)	Duration of biosorption (h)
1. Effect of initial concentration					
• Crab carapace particles	0.250	NM	NM	10, 20, 80, 160	6.5
• Lobster carapace particle	0.250	NM	NM	20, 40, 80, 160	11
2. Effect of amount of carapace particles used	0.125, 0.250, 0.500, 1.000, 2.000	NM	NM	80	10h
3. Effect of different bed heights					
• Crab carapace particles	0.481	<300	1	80	80h
	0.998		2		
	2.100		4		
	4.247		8		
• Lobster carapace particles	0.436	<300	1	80	99h
	0.888		2		
	1.692		4		
	3.495		8		

Note: NM – not measured

Table 4-2 Reduction of concentration (ppm) of the initial Mn solution between 10min – 300min calculated as (C_o-C_e) in *L. depurator* and *N. norvegicus* carapace particle columns.

Time (min)	Crab carapace particle columns				Lobster carapace particle columns			
	10ppm	20ppm	80ppm	160ppm	20ppm	40ppm	80ppm	160ppm
10	6.62	11.65	37.25	60.00	11.81	22.33	34.42	66.17
30	6.84	12.65	29.75	50.50	11.99	20.35	29.17	50.33
60	6.05	11.35	29.75	31.50	12.42	19.47	26.00	42.83
120	4.81	10.35	18.75	22.00	11.43	17.71	23.50	37.50
180	4.11	8.15	23.00	13.50	10.59	16.03	19.67	36.33
300	3.00	5.10	11.00	7.50	9.11	12.54	16.42	19.67

Table 4-3 Reduction of concentration (ppm) of the initial Mn solution at 10min – 625min calculated as C_o-C_e (ppm) and (C_o-C_e) per gram carapace (ppm.g^{-1}) for *L. depurator* carapace particles.

Time (min)	0.255g ppm	0.255g ppm.g^{-1}	0.505g ppm	0.505g ppm.g^{-1}	1.002g ppm	1.002g ppm.g^{-1}	2.001g ppm	2.001g ppm.g^{-1}
10	43.35	170.00	59.02	116.87	67.05	66.92	73.33	36.65
60	29.28	114.82	45.18	89.47	58.1	57.98	72.78	36.37
120	24.38	95.61	43.18	85.50	51.98	51.88	69.07	34.52
240	17.62	69.10	47.47	94.00	32.85	32.78	67.83	33.90
360	8.66	33.96	17.48	34.61	33.07	33.00	63.14	31.55
480	7.30	28.63	11.72	23.21	25.59	25.54	56.84	28.41
625	4.57	17.92	7.72	15.29	15.70	15.67	48.34	24.16

Table 4-4 pH of effluent from columns with 4cm and 8cm beds of *N.norvegicus* and *L. depurator* carapace particles over 76h sorption process.

Time (h)	4cm lobster carapace	8cm lobster carapace	4cm crab carapace	8cm crab carapace
0	5.61±0.25 (as measured in 80ppm Mn solution in the reservoir)			
4			10.25	
7	9.89	10.23	10.34	10.29
11	10.28	10.37	10.59	10.51
22	10.48	10.38	10.57	10.63
30	10.30	10.36	10.37	10.58
46	10.21	10.37	10.28	10.56
59	9.47	9.87	9.69	9.91
70	10.16	10.25	10.18	10.46
76	10.13	10.30	10.20	10.49

Table 4-5 Biosorption capacities of crab carapace particles expressed as mg metal per gram adsorbent (mg.g^{-1}) of crab-based materials from the literatures. The adsorption capacities of Mn by clay were also listed as reference. K_F and K_L refer to the adsorption capacity according to Freundlich and Langmuir isotherms.

Species	Metal	Molecular weight	Adsorption capacity (mg.g^{-1})	Researcher
[+]*Portunus trituberculatus*	Pb		1301.2*	Lee *et al.* (1997)
Portunus trituberculatus	Pb		870	Lee *et al.* (1998)
Crab carapace (NM)	Pb	207.2	265.1(K_F)	Boukhlifi and Bencheikh (2000)
	Cd	112.4	7.4 (K_F)	
	Cu	63.55	17.2 (K_F)	
	Zn		11.5 (K_F)	
Chinonecetes opilio	Pb		267.3* (K_F)	An *et al.* (2001)
	Cd		198.9* (K_F)	
	Cu		62.3* (K_F)	
	Cr	52.00	55.1* (K_F)	
[+]Crustacean chitosan (NM)	Cu		222 (K_L)	Ng *et al.* (2002)
[+]*Portunus sanguinolentus*	Co	58.93	322.6	Vijayaraghavan *et al.* (2006)
	Cu		243.9	
[+]*Ucides cordatus*	Au	197.00	33.5*	Niu and Volesky (2006)
	Se	78.96	11.8*	
	Cr		29.1*	
	V	50.94	40.2*	
[+]*Maia squinado* (carapace)	Cd		165.2*	Barriada *et al.* (2007)
[+]*Maia squinado* (chitin)	Cd		10.1*	
Chinonecetes opilio	Pb		19.8	Dahiya *et al.* (2007)
	Cu		38.6	
Cancer pagurus	Zn	65.39	77.9-172.5	Lu *et al.* (2007)
Crab carapace (NM)	Pb		8.2 (K_F)	Dahiya *et al.* (2007)
	Cu		15.8 (K_F)	
Liocarcinus depurator	Mn	54.94	22.8 (K_F)	The present study
Commercial clay (montmorillanite, Fluka)	Mn		0.31 (K_F)	Dal Basco *et al.* (2006)
Bentonite clay (natural)	Mn		0.85 (K_F)	

* original values expressed in mmol.g^{-1}
[+] crab shells pre-treated either with acid or alkali to remove calcite or protein
NM – species name not mentioned
Data for Cu is highlighted gray to follow with the reference in the text
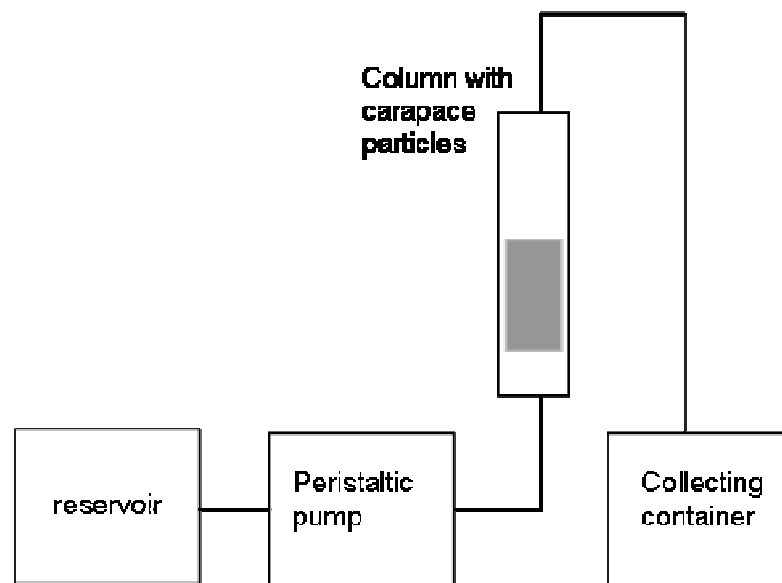
Fig. 4-2. The set-up of the biosorption column system
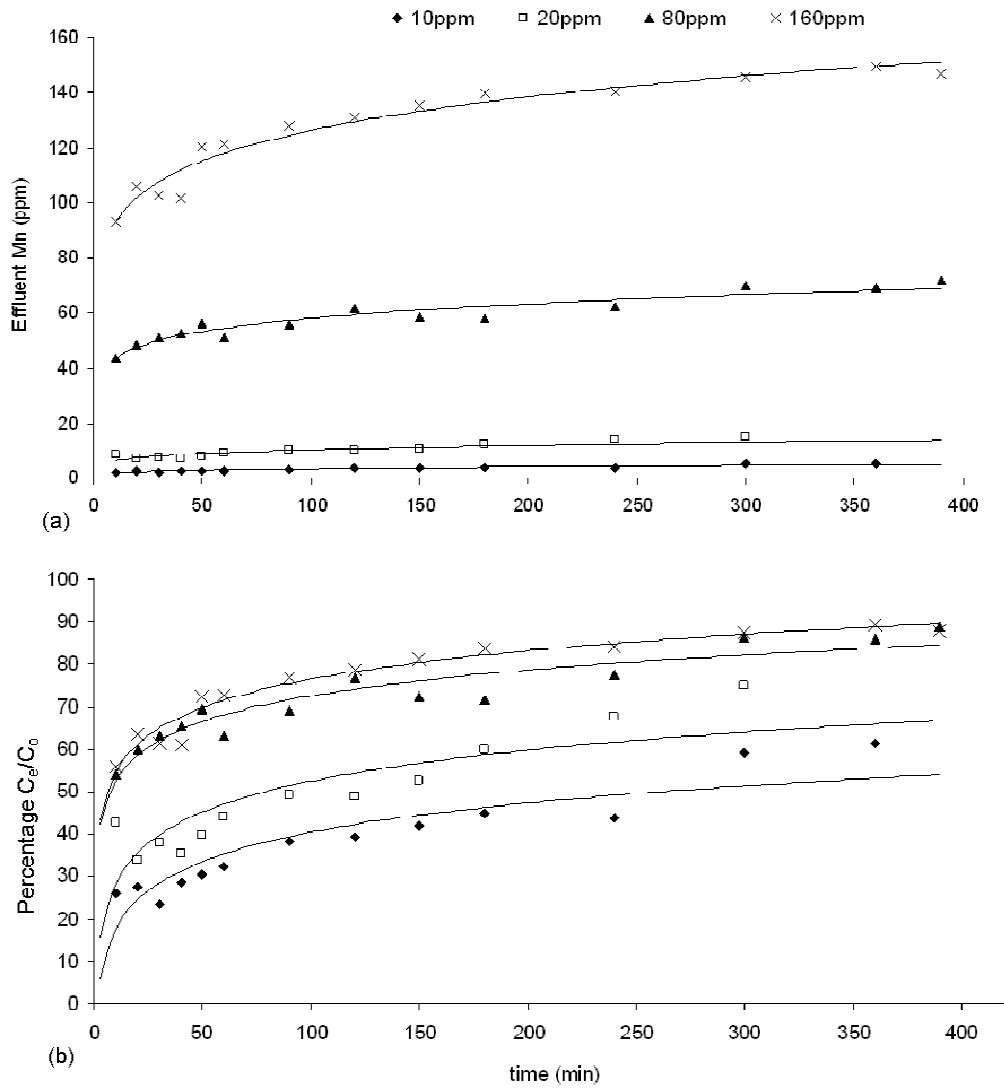
Fig. 4-3. Data of four sorption systems using *L. depurator* carapace particles with initial concentrations of 10-160ppm with the following conditions: particles 0.250g, flow rate 100ml.h^{-1}. (a) Mn concentrations in the effluent and (b) Percent Mn concentration in the effluent expressed as a percentage of the initial concentration.
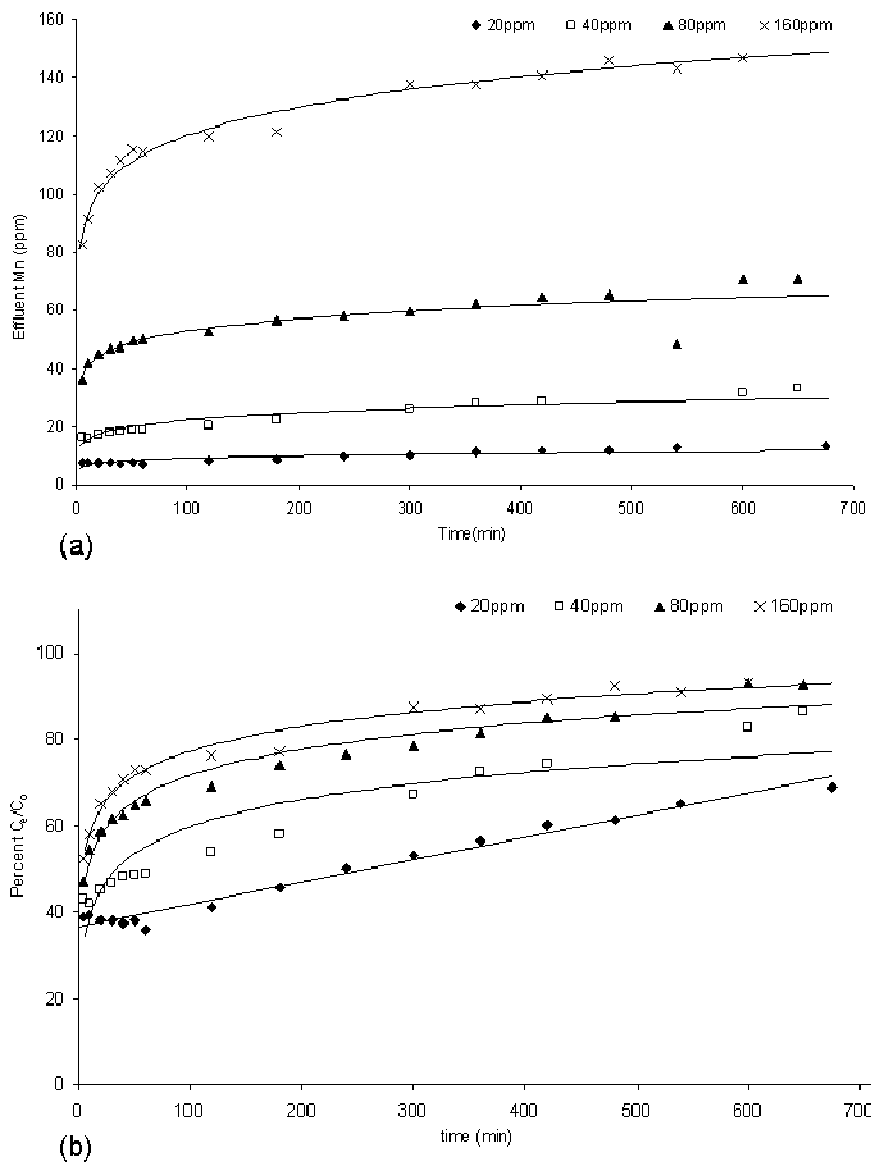
Fig. 4-4. Data of four sorption systems using *N. norvegicus* carapace particles with initial concentrations of 20-160ppm with the following conditions: particles 0.250g, flow rate 100ml.h^{-1}. (a) Mn concentrations in the effluent and (b) Percent Mn concentration in the effluent to the initial concentration
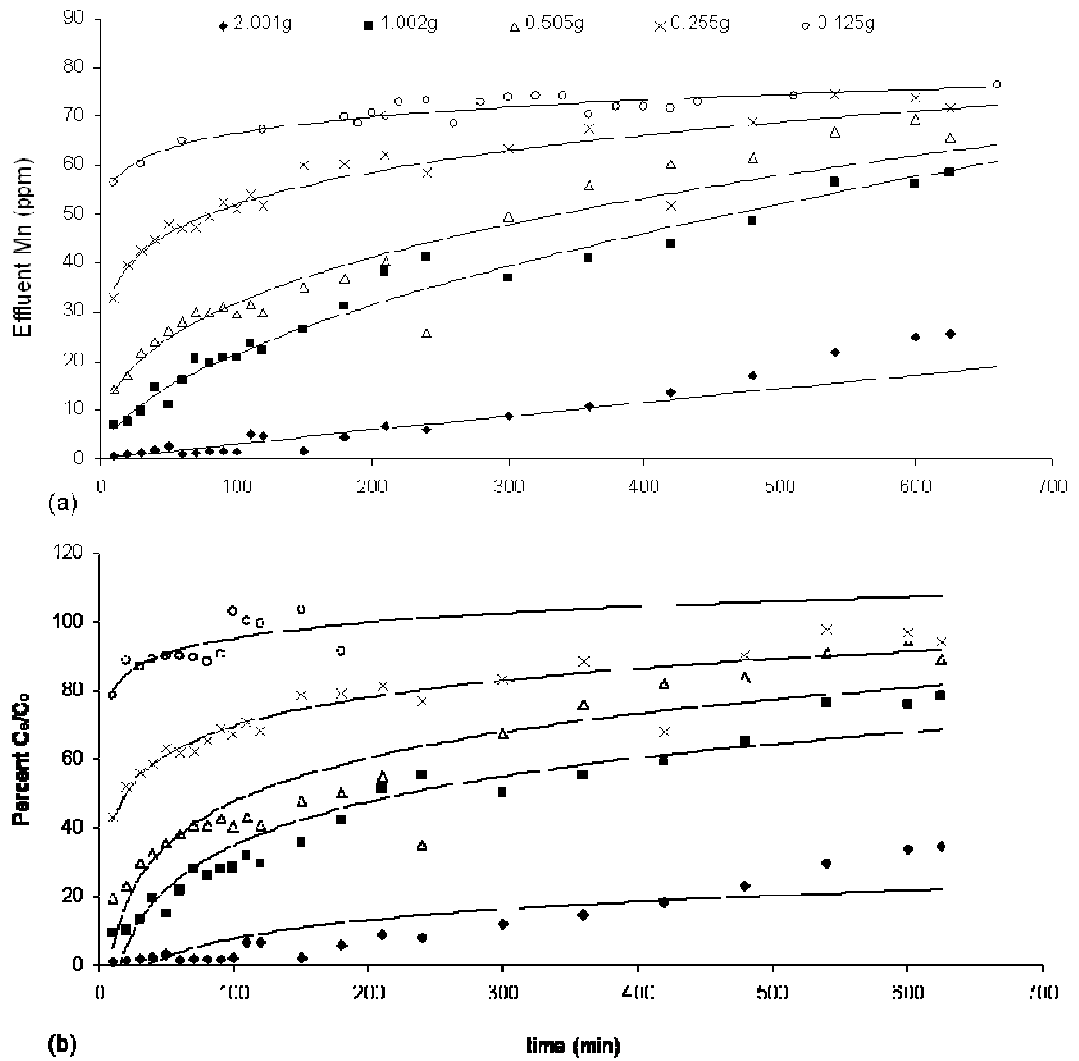
Fig. 4-5. Data of four sorption systems using an amount of *L. depurator* carapace particles of 0.125g – 2.001g. Mn concentration was 80ppm and the flow rate was 100ml.h^{-1}. (a) Mn concentrations in the effluent and (b) Percent Mn concentration in the effluent to the initial concentration.
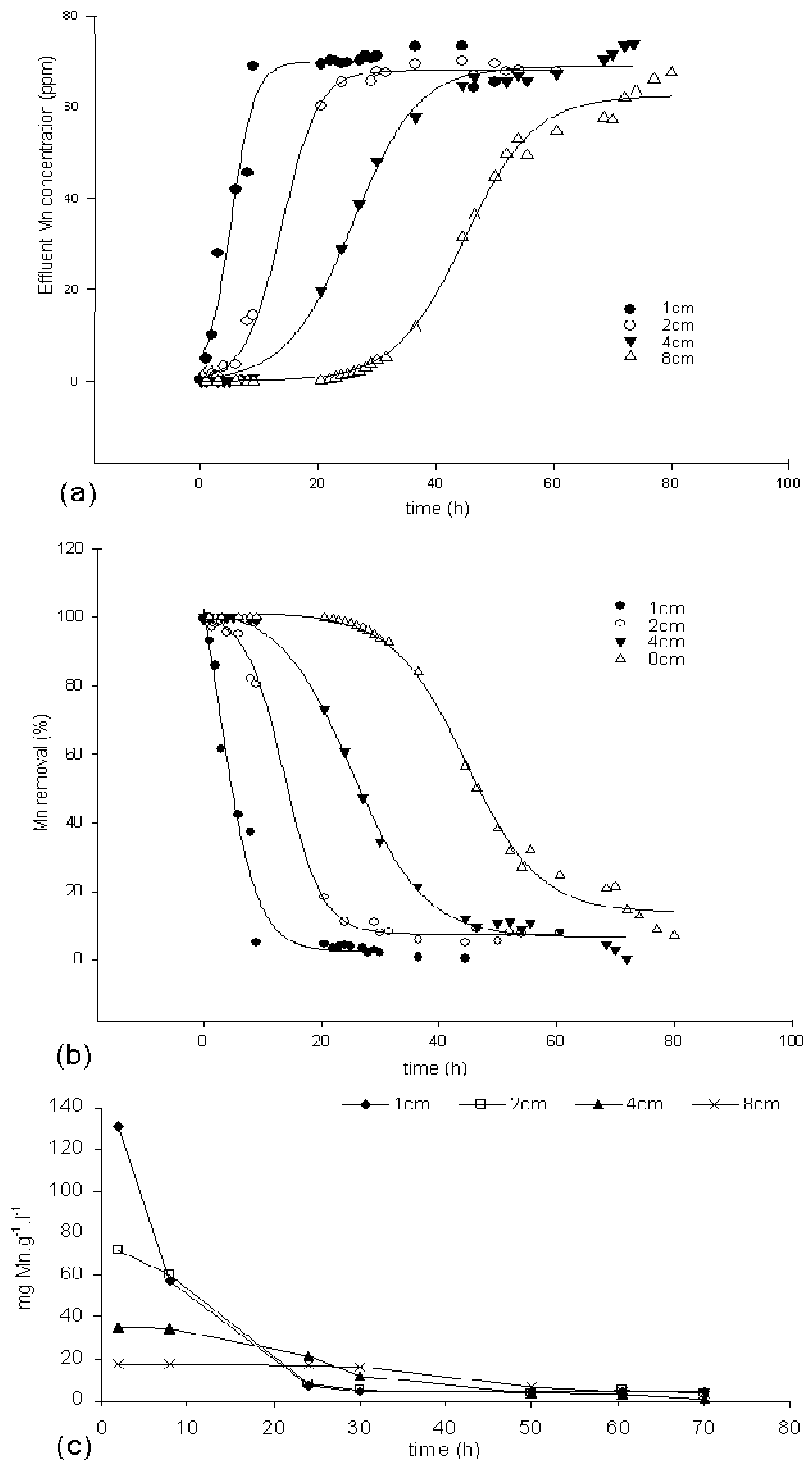
Fig. 4-6. (a) Breakthrough curves for Mn sorption onto *L. depurator* carapace particles for different bed heights (flow rate 100ml.h⁻¹; initial concentration 80ppm; bed heights 1-8cm); (b) Percentage of the reduction of Mn concentrations; (c) Mn removed per litre of solution per gram of carapace particles at selected hour of the same system.
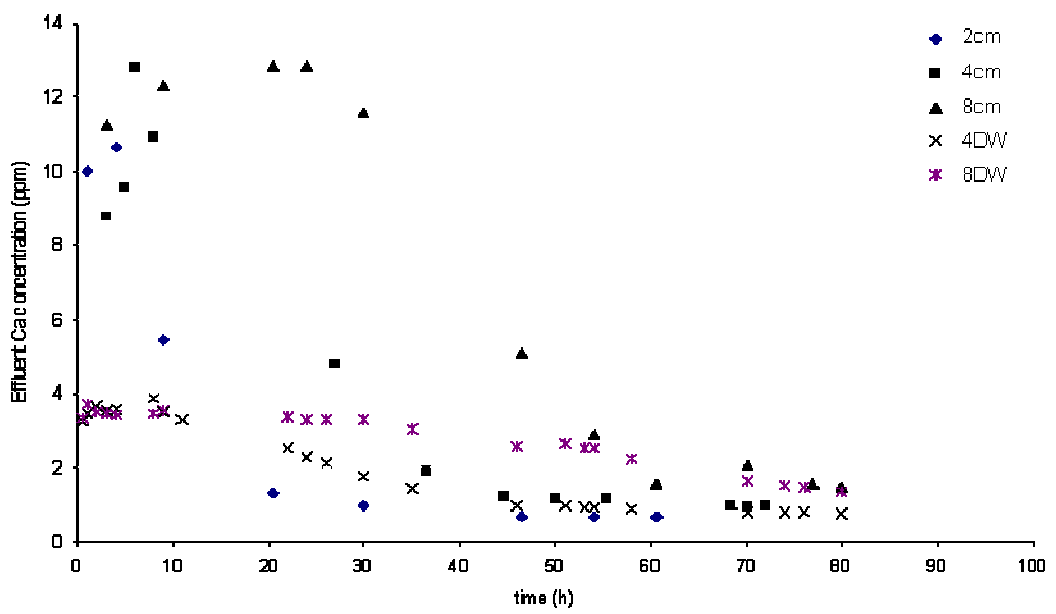
Fig. 4-7. Calcium concentrations in the effluent of 2-8cm bed *L. depurator* column systems with 80ppm Mn concentration. Distilled water was passed through the controls for 4 and 8cm columns (4DW and 8DW)
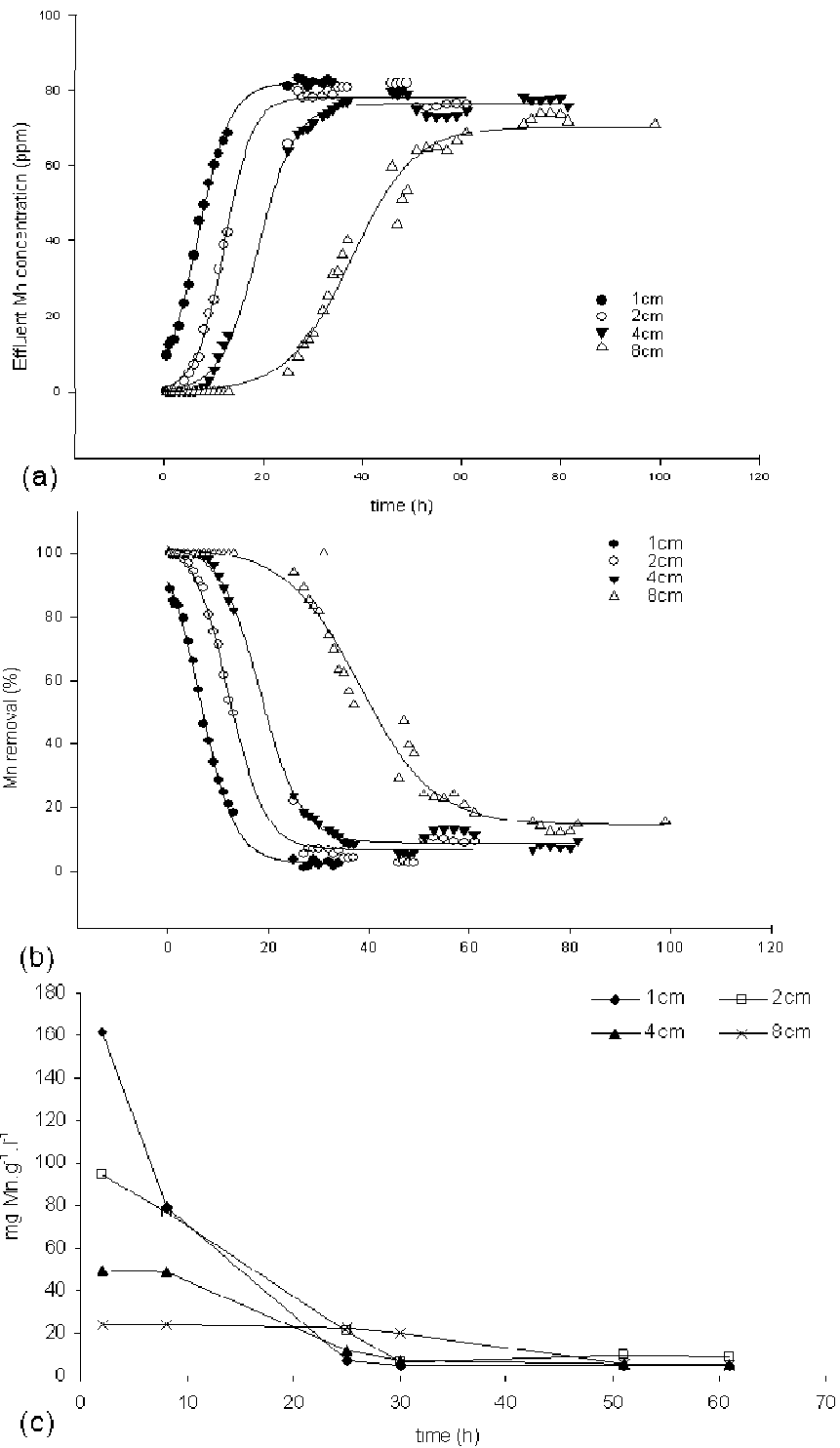
Fig. 4-8. (a) Breakthrough curves for Mn sorption onto *N. norvegicus* carapace particles of different bed heights (flow rate 100ml.h^{-1}; initial concentration 80ppm; bed heights 1-8cm); (b) Percentage of the reduction of Mn concentrations; (c) Mn removed per litre solution per gram carapace particles at selected hours for different bed heights of the same system
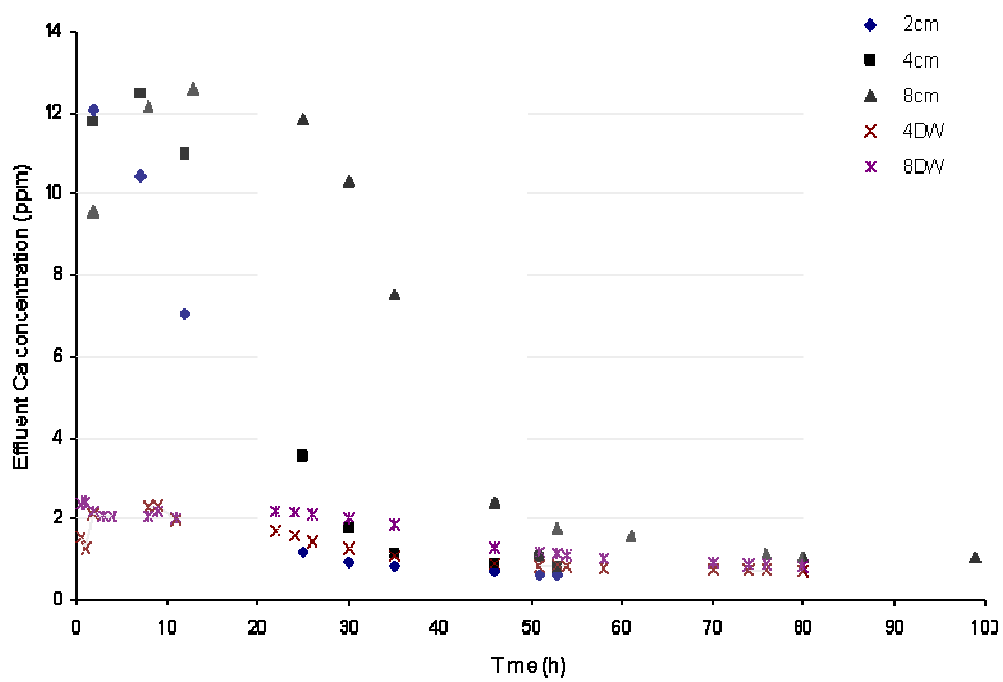
Fig. 4-9. Calcium concentrations in the effluent of 2-8cm bed *N. norvegicus* column systems with 80ppm Mn concentration. Distilled water was passed through the controls for 4 and 8cm columns (4DW and 8DW)
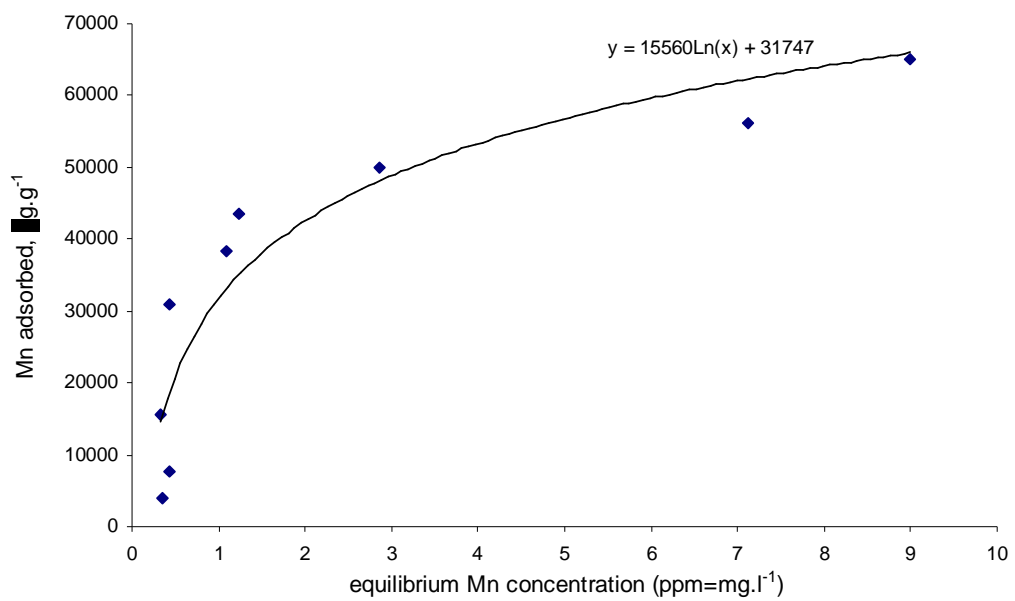
Fig. 4-10. Adsorption isotherm for Mn on *L. depurator* carapace particles (initial concentration 80ppm; volume 100ml; amount carapace used 0.100 – 2.000g; flow rate 100ml.h^{-1})
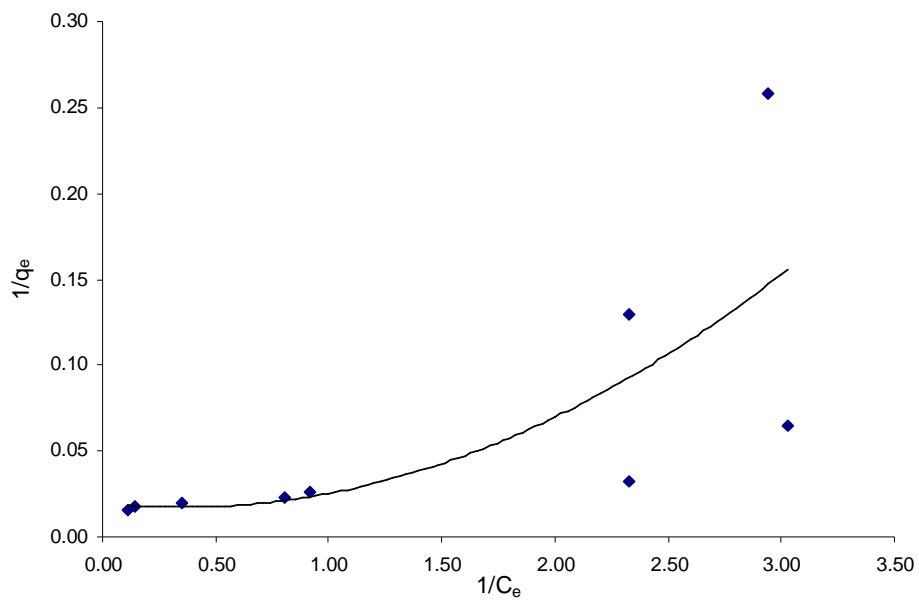
Fig. 4-11. The plot of $1/q_e$ versus $1/C_e$ of the batch data. The shape of the curve reveals that the isotherm does not fit the Langmuir model. If it fits the model, the above plot should be linear and the slope would give the Langmuir constant K_L.
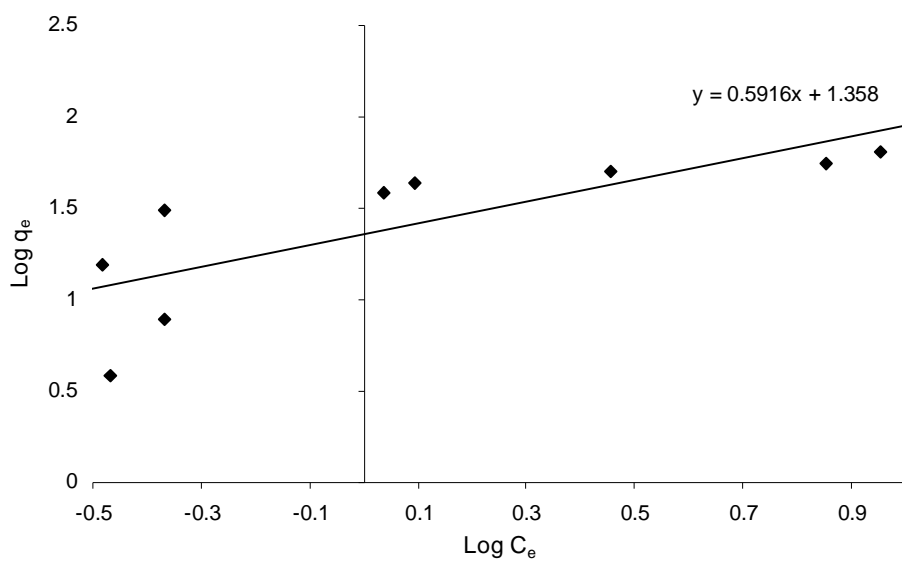
Fig. 4-12. A 'log q_e versus log C_e' of all batch data points shows a linear plot, indicating that the isotherm might fit the Freundlich isotherm. The intercept (log K_f) gives the value of the constant K_f as 22.80.
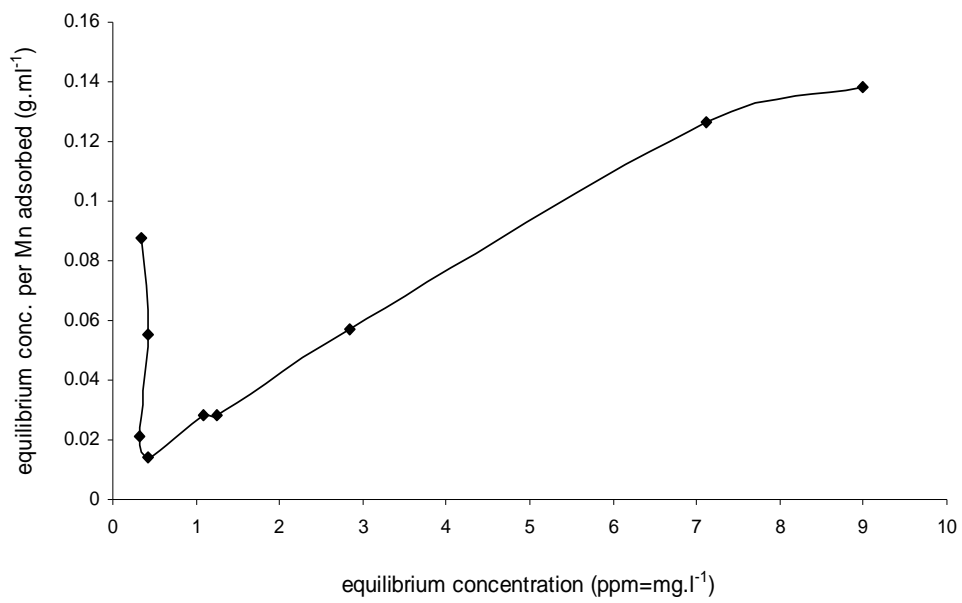
Fig. 4-13. Equilibrium concentration per Mn adsorbed onto *L. depurator* carapace particles (initial concentration 80ppm; volume 100ml; amount carapace used 0.100 – 2.000g)

Fig. 4-14. *L. depurator* shell before (pink) and after biosorption (black).
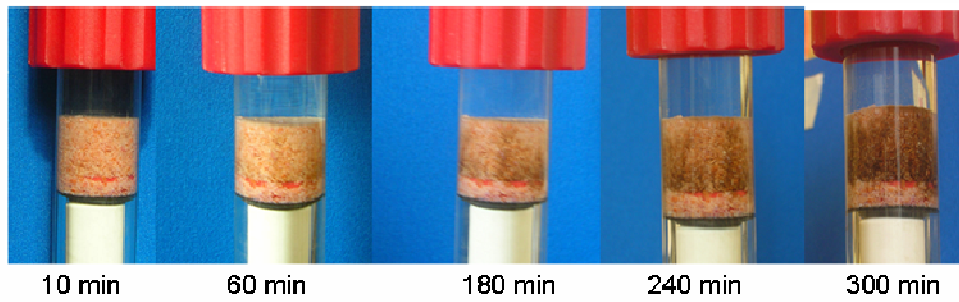
Fig. 4-15. Blackening of *L. depurator* carapace particle in columns. In this case, the first sign of blackening could be seen at 60min.
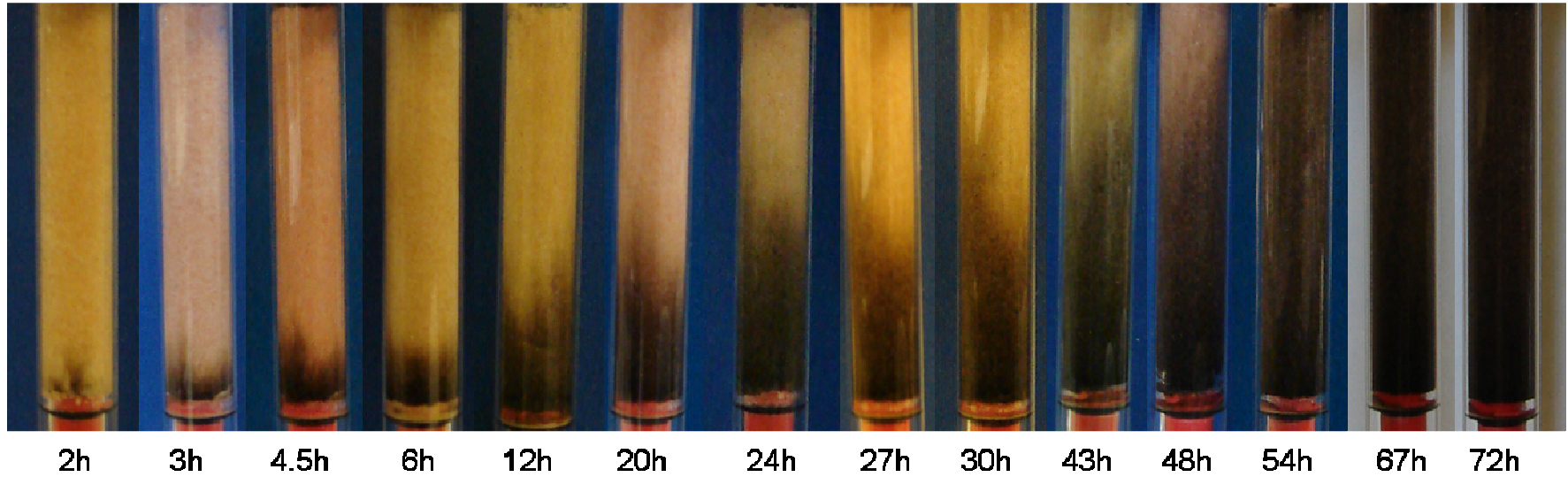
Fig. 4-16. Progressive blackening of 8cm bed height *L. depurator* carapace particles from 2h to 72h indicating the movement of Mn transfer zone (concentration 80ppm; flow rate 100ml.h^{-1}).
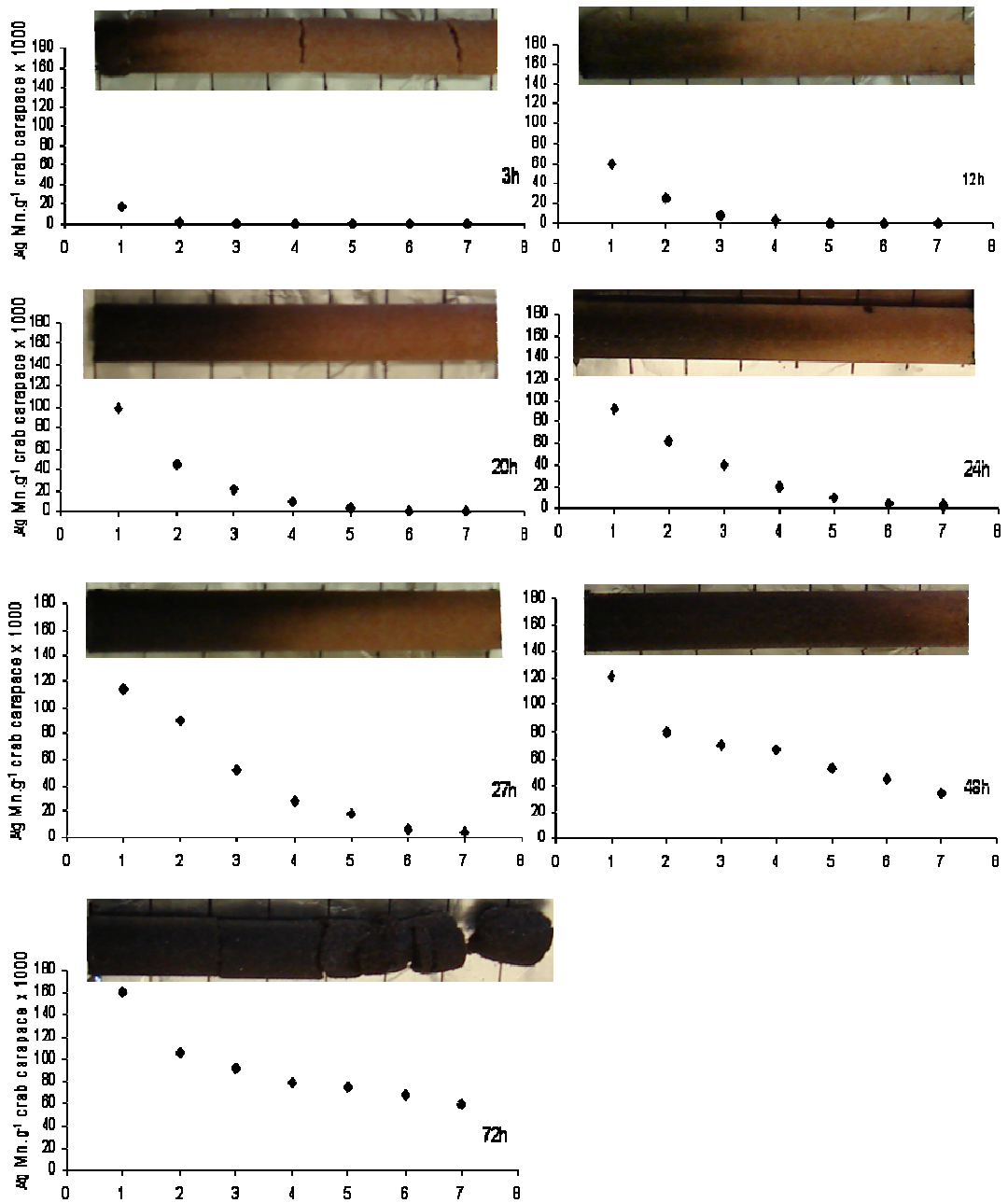
Fig. 4-17. Mn concentrations in 1cm-segments of 8cm bed height columns of *L. depurator* carapace particles at 2h – 72h. The influent flow was from the left end of the column blocks. (Initial Mn concentration 80ppm; flow rate 100ml.h^{-1}; original concentration in non-biosorbed particles 62.15µg.g^{-1})
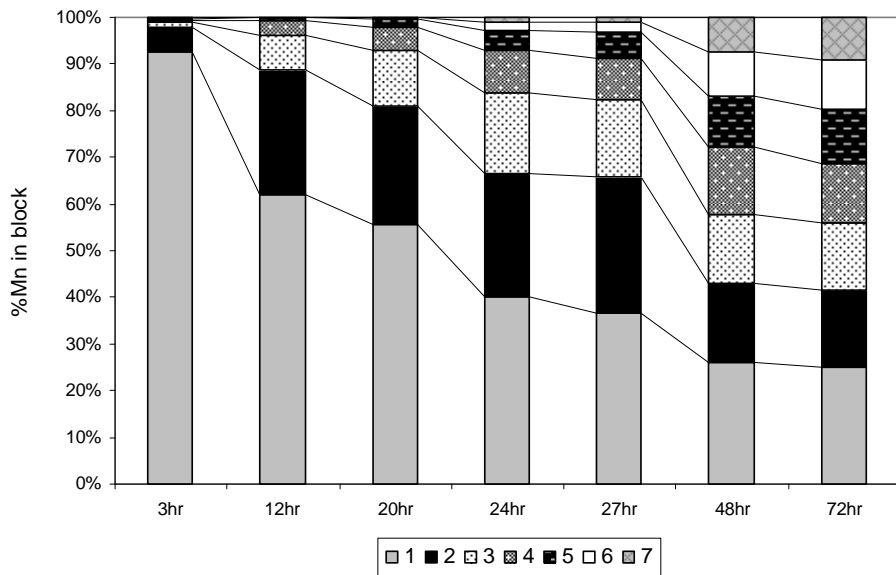
Fig. 4-18. Distribution of Mn in 1cm-segments of 8cm bed *L. depurator* carapace particles according to biosorption period (initial concentration 80ppm; flow rate 100ml.h^{-1})

5 Morphology of the carapace and gills of *Liocarcinus depurator* (L.)

5.1 Introduction

This chapter describes the basic morphology of the carapace and the gills of the swimming crab *Liocarcinus depurator*. The information gathered from this chapter forms the basis for the following chapter where microscopic observations were carried out on biosorbed particles and also on crab dorsal carapace immersed in a manganese solution in order to investigate the nature of uptake/adsorption onto the exoskeleton. As the information on the basic morphology of this particular species is almost non-existent, these preliminary observations are both timely and crucial.

The mature crustacean cuticle has four non-homogenous discrete layers; two (the epicuticle and the exocuticle) are deposited before moulting, or pre-exuvially, and another two (the endocuticle and the membranous layer) are deposited post-exuvially (Elliot and Dillaman, 1999). The cuticle is secreted by a simple epithelium and consists of a chitin-protein matrix that is strengthened by calcium carbonate crystals (Roer and Dillaman, 1984). In the present study, only the cuticular layers were examined. All other soft tissues including the epidermis were completely removed from the samples.

The terminology used here for the cuticle layers is after Travis (1963) (in Roer and Dillaman, 1984). The epicuticle differs from the exocuticle and endocuticle in its lack of chitin and lamellar organization (Roer and Dillaman, 1984). The exocuticle and endocuticle are composed of a regular array of chitin-protein fibres arranged in lamellae oriented in the form of parallel sheets. The two layers differ in the lamellar spacing with their interlamellar distance being less in the exocuticle than in the endocuticle. In the crab *Carcinus maenas*, these distances were found to be approximately 2μm and 8μm, respectively (Dillaman and Roer, 1980).

The basic morphology of the gills of *L. depurator* was also studied using the same technique as the information might assist in explaining some of the observations in the next chapter. There are many reports on crustacean, or specifically crab, gills in the literature. The phyllobranchiate gills of crabs were described as being made up of a central gill shaft that is flattened and contains an afferent vessel and an efferent vessel, located respectively, at the dorsal and ventral margins. On the anterior and posterior sides of the gill shaft, the gill lamellae interconnect the two vessels (Freire *et al.*, 2007). The flattened leaf-like lamellae are covered by a cuticle that consists of the same lamellar subdivisions as the sclerite cuticle of the carapace (Andrews and Dillaman, 1993). As the gills are involved in gas, water and ion exchange, the cuticle cover must therefore be very thin to allow for maximum diffusion efficiency (Elliot and Dillaman, 1999), in all species studied so far it is less than 3µm thick.

5.2 Materials and Methods

The crab carapace samples were viewed using Scanning Electron Microscopy (SEM) under three conditions wherever appropriate, i) dried raw carapace, ii) gold coated, and iii) embedded in resin block. SEM examination of gold-coated samples was carried out in the IBLS Electron Microscopy Unit (JEOL 6400) at Glasgow University. The dried raw samples were examined in the Microscopy Unit of the School of Chemistry, University of St. Andrews (Jeol JSM 5600 SEM). The resin embedded samples were examined in the Geology and Earth Science Microscopy Unit at Glasgow University (Cambridge Instruments S360 Analytical SEM).

5.2.1 Preparation of carapace specimens for SEM

Crabs were killed humanely (Sect. 2.2.1) and the carapace carefully dissected free from the underlying tissues of non-treated crabs. The carapace was thoroughly cleaned under flowing tap water, cleansing the dorsal surface of sediments, and

removing all the epidermal tissue from the internal surface. The carapace was then rinsed twice with distilled water, and then freeze-dried intact for 24h, by which time it became completely dry.

As the carapace was then rigid and completely dry, no chemical fixation was applied. It was fractured into tiny pieces which were then mounted on aluminium stubs by carefully applying them to a double-sided carbon tape covering the stubs. If necessary, a drop of silver paint was applied to stabilise the specimens in place and provide better conductivity. The use of both conductive tape and paint is to ensure that the specimen (which is not conductive) is grounded or earthed to the stub, thus minimizing the electron charging of the specimens in the SEM chamber.

The mounted specimens were then coated with approximately 20nm thick gold-palladium coating using a Polaron SC515 sputter coater. Most materials are transparent to the electron beam used by the SEM, and gold, (among others) is an electron-opaque conducting substance that enables electrons to be reflected from the specimens. These excited electrons travelling at varying speeds are detected by two detectors in the SEM chamber that translate the signals into images of the specimens as viewed on the monitor screen.

To examine the distribution of the major elements of the carapace, freeze-dried whole carapace was embedded in a resin block. Briefly, the carapace was embedded in cold setting resin (5 parts epoxy resin (Epoxicure: Buehler Ltd.) and 1 part hardener) in a 32mm mould and left to cure at room temperature for 8h. Once cured, the block was cut into smaller blocks creating sections through the carapace. Each smaller block was subjected to a series of polishing steps in a polisher (Kemet Kent 3) with polishing cloth Texmet 1500 and Mastertex charged with different sizes of diamond compound, aluminium oxide powder, and colloidal silica suspension with distilled water. The completely polished block was then coated with carbon and mounted on a stub with carbon tape or paint for viewing on the SEM.

Some gill specimens were also freeze-dried, gold-coated and viewed under the SEM. These specimens were handled with extreme care as compared to the carapace, they became more brittle once dried.

5.2.2 Viewing specimens under SEM

The gold-coated specimens were examined using a JEOL 6400 SEM at an accelerating voltage of 6kV over a range of magnifications. Following an analog-to-digital conversion process, the electron signals captured by two detectors in the SEM chamber could be viewed on a monitor attached to the SEM. These images were captured in black and white by a software package (Imageslave for Windows).

Polished specimens were viewed under Cambridge Instruments S360 Analytical SEM at 20kV over a range of magnifications. This SEM was equipped with a BSE detector. This detector enables mean atomic number contrast images to be formed, which are useful for characterising the abundance, morphology and interrelationships of chemically-distinct phases within a polished sample. The images formed could highlight some of the structures/features not detected by the normal SEM micrographs.

5.3 Results

5.3.1 Basic structure of the dorsal carapace

The images shown in this section demonstrate the basic structure of the dorsal carapace of *Liocarcinus depurator*, emphasizing the layers making up the whole cuticle. Figure 5-1a shows the epicuticle (which measures about 5µm in thickness), exocuticle (60-70 µm) and endocuticle (about 200 µm). These measurements were almost identical to those found in *C. maenas* (Roer and Dillaman, 1984) as shown in the inset image.

Figures 5-1b and 5-2a show carapaces from two other specimens of *L. depurator* which show the same layout, and thus confirm that observations in Figure 5-1a do represent the general structure of the intermoult dorsal carapace of *L. depurator*. Some setae could also be seen protruding from the external surface of the samples, indicating that they could be found on the flat surface (Fig. 5-1b), and also close to certain ridges (Fig. 5-2a).

Figure 5-2b shows the exo- and endocuticles at higher magnification. Both layers are made up of by twisted layers of lamella which are fine and tightly packed in the exocuticle, but are thicker and more loosely stacked in the endocuticle. The difference in thickness enables easy identification of the border between the two layers.

Figure 5-3a shows an endocuticle with a pore canal, with a diameter of about 10 μm, running through it. The pore canal extends through the procuticle (exo- and endocuticles) and terminates at the level of the epicuticle. The pore openings (up to 20 μm wide) are visible on the internal surface of the carapace (Figs. 5-3b,c). Figure 5-3c indicates the same material shared by the internal surface and the lining of the pore canal. Thin membranes lining the innermost layer of the cuticle (shown by arrow) could be the membranous layers. The membranous layer is similar to endocuticle in construction but is uncalcified.

At higher magnification (Fig. 5-3d), the membranous layers could be distinguished from the thin developing lamellae of the endocuticle. Figure 5-3e shows the membranous layer at higher magnification, showing that it is made up of no less than 10 microthin sheets.

Figure 5-3f shows two pore canals running through the endocuticle layers. The image shows a clear continuity of the internal surface lining into the canals. In this image, both canals measured less than 10 μm diameter. The openings of these canals on the external surface of the carapace are shown in Figure 5-4a and at higher magnification in Figure 5-4b.

The structure of the external surface of the carapace includes shallow grooves that make up the whole surface, some pore openings and three extensions/ridges (Fig. 5-4a). A fracture of a carapace shows the lamellae of the exocuticle making up the different layers (Fig. 5-4c) and the pores can be seen on the different layers.

5.3.1.1   Other features of the carapace

The lamellae of a procuticle (endocuticle and exocuticle) comprise nets with pores. Figure 5-4d shows four of such porous lamellae, which are characteristic of a crustacean cuticle. These lamellae that are arranged in a spiral fashion are known as the Bouligand's structure.

Interprismatic septa (Fig. 5-5a) mark the 'border' between the epicuticle and the exocuticle. They are composed of tanned protein that tail down from the epicuticle into spaces between pillars of chitin-protein matrix of the exocuticle. The epicuticle is made of several layers but the tailing down of the interprismatic septa occurs only in the innermost layer of the epicuticle (Warner, 1977). However, the different layers could not be differentiated in this image. A horizontal fracture through the carapace (almost perpendicular with the cuticle surface – Fig. 5-5b) revealed the chitin-protein pillars. Tanned protein filling in the spaces between them gave the polygon shape of each pillar.

Images scanned with a back-scatter electron detector (Fig. 5-6) show the basic layers as seen before based on the density of electron possessed by different materials making up each layer. The tanned protein making up the epicuticle comprised of electron-densed materials that it appeared bright in the images. The interprismatic septa (the tailing down of the epicuticle into the exocuticle layers) are clearly visible (Fig. 5-6a). On the right hand corner, the polygon arrangement of the chitin-protein pillars could also be observed as they cut through that particular part of the cuticle. This section is through a slightly different plane to the cuticle surface.

A few bulbous structures measuring approximately 100-150μm in diameter were detected by the BSE detector (Figs. 5-6a,b) and could be some of the tegumental glands found within the cuticle as ducts were found to connect to them. Figure 5-6c

shows a duct in a complete view connecting the gland to the external surface through layers of cuticle. These ducts were reported to be lined by epicuticle (Felgenhauer, 1995). This might be true in this image as both the epicuticle and the duct appear to be at the same brightness, suggesting the same materials are shared by both.

5.3.1.2 Elemental distribution in the crab carapace

Figures 5-7a-c show three major elements making up the carapace, Ca, C and O. When mapped, these three elements resemble the lamella layers seen previously in the SEM micrographs, giving significant striped layers on the image. In Figure 5-7a, yellow dots indicate signals for Ca. Ca was found in greatest amount in the epicuticle (appears yellowish on top of the cuticle) including the interprismatic septa, and was found to be least dense at the border between the exocuticle and endocuticle (this border is also termed the mesocuticle), and in the interlamellar spaces.

Figures 5-7b and 5-7c show the distribution of C and O of a dorsal carapace. These elements appear to be located in the middle of the lamellar layers (referring to the SEM image). The black area (no signals) within the cuticle refers to the interlamellar spaces which are expected to have less material. The overlapping distribution of C and O suggests that they might occur together forming a compound, most probably carbonate. Together with Ca (which appears to be the major element as it is distributed more evenly throughout the cuticle) they represent $CaCO_3$, the major compound making up the crab exoskeleton.

Figure 5-7d shows a profile of the three major elements across the crab cuticular layers. Higher Ca content was found in the epicuticle followed by the endocuticle. The level in the exocuticle was found to be much lower compared to the epicuticle, and the level was observed to decrease towards the inner layers of the exocuticle. The level rises immediately into the endocuticular layers.

5.3.2 Basic structure of a crab gill

Figure 5-8a shows the distal tip of a gill of *L. depurator*, whereas Figure 5-8b shows the middle rachis of the gill. The gills are composed of flattened lamellae in a regular arrangement along a central shaft, with the lamellae decreasing in size distally. In Figure 8b, a few other structures including the spacing nodes, setae and spines are visible. The lamellae are uniformly spaced between each other by peripheral swellings in the marginal canal of the lamella, termed by some previous researchers as the spacing nodes, bulbous knobs, or interlamella spacers. This structure is shown at higher magnification in Figure 5-8c.

Figures 5-8d and 5-9 show the spines observed along the rachis of the gills. These spines (150-200µm) were found to be irregularly distributed, and only occur on the ventral surface (location of the efferent vessel). No similar structure was observed on the dorsal surface. The major difference between the spines and the setae lies within their bases (Fig. 5-8d): the former protrude from mammilate mounds on the surface, whereas the bases of the latter remain embedded within the surface.

Figure 5-10a shows a gill fractured halfway along the rachis, showing the lamellar surface in full view. The afferent vessel can be seen as a hole on the dorsal part of the gill, whereas the efferent vessel is at the opposite end. The setae can be seen protruding from the ventral surface of the efferent vessel. Both vessels are connected by a shaft that separates individual lamellae into two halves, left and right.

Figure 5-10b shows the afferent vessel at higher magnification and also the spacing nodes at both 'shoulders'. The shaft can be seen as the torn line separating the lamella into two halves. Figure 5-10c shows the grooves on the lamellar surface. The edge of the lamella appears as a smooth thin membrane without any distinct structure.

5.4 Discussion

The crab carapace was subjected to a number of different electron microscopy examinations in order to obtain an overview of the basic structure of the cuticle. As information on the cuticle of *Liocarcinus depurator* is almost non-existent, there was a need for these exploratory examinations to be carried out before more experiments were done on the carapace.

The carapace of this species shows all the basic features of the typical crustacean cuticles. It is composed of three main layers; the epicuticle, exocuticle and endocuticle, the latter two are also termed the procuticle. The fourth layer is the membranous layer. These layers of cuticles are secreted by the epidermis, a single layer of cuboidal cells sitting on the basement membrane directly beneath the endocuticle. In this study, no epidermis was included in any of the images since the tissue was removed during sample processing.

The epicuticle is the outermost waxy and water resistant layer that acts as a diffusion barrier to the environment. This layer is formed by multilayered materials that lack chitin. Lipoprotein makes up the translucent layer that is tough as a result of tanning, but flexible to resist abrasion. It is formed as a few layers laid out parallel to the surface. However, the innermost layer is perpendicular to the surface, and tails off into the exocuticle. In the crab *Uca*, the epicuticle is made up by 6 layers of which 5 are parallel to the surface, while the 6th penetrates into the next cuticular layer (Warner, 1977). The tanned protein of the epicuticle that tails down into the exocuticle represents the interprismatic septa, separating the outer portion of exocuticle into pillars. Each pillar probably represents the secretion of an individual epidermal cell.

The procuticle (exo- and endocuticles) comprises hard layers strengthened by calcium deposits. The helical appearances of these layers are due to the arrangement of chitin-protein microfibrils that make up the lamellae. Despite being grouped together as procuticle, there are a few differences between the exo- and endocuticles. The exocuticle is pigmented e.g by melanin, whereas the endocuticle

is unpigmented. The exocuticle is secreted before moulting whereas the endocuticle is laid down after the moult. The soft tissue directly in contact with the endocuticle is the membranous layer, which in the intermoult crabs normally remains attached to the epidermis rather than to the endocuticle.

All samples of cuticle came from crabs in their intermoult stages, therefore the underlying membranous layers might have been detached from the cuticles. The membranous layer is defined as the innermost layer of the cuticle that is similar to endocuticle in construction but is uncalcified. In the stone crab *Menippe rumphii*, the inner one-fourth of the endocuticle is non-calcified representing the membranous layer (Erri Babu *et al.*, 1985). Based on this definition, the membranous layer could be distinguished in some samples even though it was found to represent only a very small portion of the thickness of the whole endocuticle layer (less than one-fourth). The difference in the thickness of the membranous layer depends on the moulting stage of the individual crab at the time of sacrifice. It is thinnest at the start of deposition after moult (stage C_1) and continues to be deposited in subsequent stages (C_2 and C_3) (Erri Babu *et al.*, 1985). During intermoult (C_4) where it is at its thickest, it separates the three main cuticular layers from the epidermal cells that lie beneath (Raabe *et al.*, 2006).

5.4.1 The procuticle

The lamella of the procuticle showed the twisted plywood pattern (also known as Bouligand pattern) characteristic of the arthropod cuticles as seen in other species including the lobster *Homarus americanus* (Raabe *et al.*, 2005). A detail description and illustration of Bouligand structure in a typical crustacean shell was given by Chen *et al.* (2008) as follows; at the molecular level, there are long-chain polysaccharide chitins that form fibrils, 3 nm in diameter and 300 nm in length. The fibrils are wrapped with proteins and assemble into fibres of about 60 nm in diameter. These fibres further assemble into bundles that arrange themselves parallel to each other and form horizontal planes. These planes are stacked in a helicoid fashion, creating a twisted plywood structure.

As this pattern is often associated with the stiffness and rigidity of the cuticle, the degree of twisting might be different between species according to their forms and functions. In *L. depurator*, the twisting of the layers is not as obvious compared to the ones reported by Raabe *et al.* (2005) for the lobster *H. gammarus*. However, the observation might also be due to the sample preparation (in this case, the samples used were freeze-dried, fractured and gold-sputtered or freeze-dried and embedded in resin) compared to chemically decalcified cuticles reported in Raabe *et al.* (2005) and Giraud-Guille (1984). Without the minerals, the Bouligand pattern of the chitin-protein fibrils shows more clearly and prominently in the cuticle samples.

In the exocuticle, the lamellae are fine and tightly packed, whereas in the endocuticle, the lamellae are larger and more loosely stacked. The difference in the arrangement enables the distinction between the two cuticle layers. Some researchers have observed a thin layer separating the exo- and endo-cuticles termed the mesocuticle which is stained deep red with Azocarmine and Acid Fuchsin stains (Erri Babu *et al.*, 1985).

Although, to the unaided eye, the carapace of this species appeared thinner when compared to the carapace of the shore crab, *Carcinus maenas*, the SEM micrographs revealed the measurements to be almost identical to those of other species as reported by Roer and Dillaman (1984). The epi-, exo- and endocuticles in *C. maenas* measured 5 µm, 65 µm and 195 µm, respectively, whereas they are around 5 µm, 55-70 µm and 200 µm, respectively for *L. depurator*. Another crab species, *Menippe rumphii* (benthic, stone and mud crab) shows similar measurements for the epicuticle (6 µm) and exocuticle (69 µm); however, the endocuticle was a lot thicker measuring 439 µm (Erri Babu *et al.*, 1985). The difference in the thickness of the endocuticle might be due to the different moult stage the crab at sacrifice. Pratoomchat *et al.* (2002) measured the endocuticle of a crab *Scylla serrata* to grow from 235 µm to 375 µm, 425 µm to 525 µm at post-moult stages B, C1, C2 and C3, respectively. The epi- and exocuticles measured 5 and 65 µm respectively, adding more evidence of the similarity among various crab species. Hence, these values might represent the general model of the thickness of crab epi- and exocuticles.

5.4.2 Other features of the cuticle

Pore canals was found penetrating through the endo- and exocuticles, and terminate at the level of epicuticle. It is through these canals that the cells of epidermis send their cytoplasmic extensions, therefore playing a role in the physiological control of calcification of the endo- and exocuticles. In a mangrove crab *Sesarma reticulatum*, these canals measured 0.1-0.5µm in diameter (Felgenhauer, 1992). In *L. depurator*, these canals measured approximately 5-10µm. This might suggest a species difference, or it might represent a different type of canal.

However, there are three types of canals found penetrating the cuticle layers, i) pore canals, very fine branching canals that penetrate to the inner edge of the epicuticle and contain cytoplasmic extensions of epidermal cells; ii) ducts of tegumental glands, far larger than pore canals, extend through the cuticle to open on the surface and are less numerous; and iii) pores leading to bristles on the surface. The pore canals shown in the images for *L. depurator* might fall into the second category namely the ducts of tegumental glands. A few images show clearly the opening of these ducts on the surface of the dorsal carapace. All three types were reported in the cuticle of the stone crab *Menippe rumphii* (Erri Babu *et al.*, 1985). Whereas for the fresh-water shrimp *Atya innocuos*, pores having a similar morphology were found to be associated with different types of glands within the epidermis, with unicellular glands located just beneath the endocuticle being the most common ones (Felgenhauer and Abele, 1983). The secretions from these glands reach the surface via sclerotized ducts (the pore canals) which penetrate through the layers of the cuticle to the outside.

5.4.3 Tegumental glands

A few round unicellular structures that resemble a gland with a diameter measuring around 100-150 µm were observed to be embedded within the endocuticle. A few images showing a single duct connecting the gland to the external surface add more evidence for the structure being a gland. However, no literature has so far described any gland within the cuticle of any crustacean. The tegumental glands have been described as being located in the epidermis (Felgenhauer and Abele, 1983) or within the connective tissue (Erri Babu *et al.*, 1985). They are ubiquitous, but the number varies greatly between species as well as in their structural components (Felgenhauer, 1992). They are normally rounded or oval in shape in any particular species but vary in size (Erri Babu *et al.*, 1985). The glands are scattered across the surfaces of the body but may be concentrated in areas that have more functionality including around the mouthparts and the setal sockets, or in areas of excessive wear or in locations in which rapid tanning of cuticle following ecdysis may be necessary (Stevenson, 1961 in Felgenhauer, 1992).

Tegumental glands are typically organized in rosettes and often composed of central, canal and secretory cells (Johnson and Talbot, 1987). However, in this study, no histological preparation was done on the carapace samples, and therefore no evidence of the cell types could be produced to confirm that the bulbous structures seen embedded within the endocuticle are indeed one type of tegumental gland. As this is not the focus of this chapter, no extra effort was taken to employ such histological procedures to find the proof. The only supporting observation is the occurrence of a single duct connecting the structure to the external surface of the carapace (visible in BSE scanning electron micrographs). In addition, ducts are described as being lined by epicuticle (stained red with Mallory's triple stain in histological sections that is characteristic of the epicuticular cells). This similarity in the structure of both the duct and the epicuticle reported by other researchers might also be evidenced in the BSE micrographs that show similar tone and brightness of both tissues that suggest similar electron density of both area, and therefore suggest the material make-up of the structures.

5.4.4 Net or honey comb structure of procuticular lamellae

The honeycomb-like structure of the lamellae in the procuticle is formed after moulting when mineralisation begins especially in the exocuticle. The mineralisation (and thus the formation of the honey comb structure) quickly increases the rigidity of the new cuticle (Compere *et al.*, 1993). The relationship between mechanical stability and the honeycomb structure has been reported previously by Raabe *et al.* (2005) who interpreted gradients in stiffness and hardness across a cuticle thickness in terms of honeycomb mechanics of the twisted plywood structure.

5.4.5 Elemental distribution within the cuticle

Crab cuticle is fully mineralized and heavily calcified in the intermoult stage, C4 (Mangum, 1985 in Priester *et al.*, 2005). The exo- and endocuticles are multilayered chitin-protein tissue which is hardened by embedded calcium carbonate in the form of calcite (Travis, 1963; Simkiss, 1975; Raabe *et al.*, 2006). Calcium content was found to be similar (which is in agreement with the present findings), and greatest in the exo- and endocuticles in the blue crab *Callinectes sapidus* (Priester *et al.*, 2005). However, as the paper of Priester *et al.* focuses on the ecdysial suture rather than the three basic cuticular layers, no measurements were given for the epicuticle. In *L. depurator*, the epicuticle contains an even higher amounts of calcium compared to other layers as evident by the dense signal on the elemental map, as is also further evident from the Ca profile across the cuticle.

The presence of mineral in the epicuticular layer is controversial (Compere *et al.*, 1993). Giraud-Guille (1984) and Bouligand (1970: in Compere *et al.*, 1993) considered the epicuticle of the crabs *Cancer pagurus* and *Carcinus maenas* to be unmineralized. In the crayfish *Orconectes limosus,* the whole epicuticular thickness appeared mineralized (Kummel *et al.* (1970) in Compere *et al.* (1993)). Our observations indicate that the cuticle of *L. depurator* more closely resembles that of the crayfish rather than other crab species. However, Compere *et al.* (1993)

provided evidence that heavy mineral deposits filled the spaces between the conical roots of the inner epicuticle in the shore crab *C. maenas*. These spaces coincide with the upper ends of the procuticular pore canals responsible for the transport of Ca and Mg during the mineralization process. In this particular crab species, these inter-radicular spaces extend only into the lower part of the inner epicuticle, making the layer appear partly calcified when fully mineralized. The whole thickness of the epicuticle of *L. depurator*, however, appeared clearly calcified, a difference worth noting compared to the other crab species.

5.4.6 The gills

Generally, the gills of all crustaceans are covered with a cuticle that is similar in structure to the carapace, but is thinner and much more permeable, which attests to their role in gas and ion exchange (Elliot and Dillaman, 1999; Freire *et al.*, 2007). Goodman and Cavey (1990) reported the general make up of the gill cuticle cover. They reported the multilayered cuticle covering the gills (endocuticle, 0.8µm; exocuticle, 1.2 µm; epicuticle, 0.1 µm, respectively) to be chitinous, and contain calcium at the interface between the endo- and exocuticle indicating calcification at that particular structural level, but not in the epicuticle. However, other authors agree that the cuticle covering crab gills is very thin measuring not more than 3 µm thick regardless of the species (blue crab *Callinectes sapidus* 1.0-2.0 µm, Johnson (1980 in Elliot and Dillaman, 1999); soldier crab *Mictyris longicarpus* 0.7-1.2 µm, Farrely and Greenaway (1987); shore crab *Carcinus maenas* 2.1 µm, Goodman and Cavey (1990); mangrove crab *Ucides cordatus* 1.5-3.0 µm, Martinez *et al.* (1999)).

In terms of arrangement, the gills of *L. depurator* were arranged in a similar fashion to any other phyllobranchiate brachyuran. They consist of flattened leaf-like lamellae that are attached to a single central shaft (also termed raphe or rachis). The lamellae are uniformly and adequately spaced for gaseous exchange (and also ion transport) by a spacing node located on each single lamella. The nodes observed in *L. depurator* were much more enlarged (about 100µm wide) compared to the ones reported for *Carcinus maenas* (Goodman and Cavey, 1990). The main shaft also

houses two main blood vessels, the dorsal being the afferent vessel whereas the efferent vessel is located on the ventral side.

The spacing nodes arise as part of the peripheral swellings in the marginal canal of the lamella. Our observation adds to the information that these are a basic characteristic of the phyllobranchiate gill of any crab species as it is reported to occur at specific locations on the lamellae in the crabs *Carcinus maenas* (Compere *et al.*, 1989; Goodman and Cavey, 1990) and *Cardisoma hirtipes* (Farrely and Greenaway, 1992). In the crab *Gecarcoidea natalis*, the nodes are found to be randomly placed on the lamellar face and marginal canal (Farrely and Greenaway, 1992).

Gill lamellae are essentially flat hemocoelic space enclosed by a simple epithelium and cuticle. In *C. maenas*, the periphery of each lamella is expanded to form a marginal canal (Martinez *et al.*, 1999). The expansion of the marginal canal was not as prominent in the gills of *L. depurator* where the distal end of the lamellae appears as thin as the lamellar sheath itself. Water passes through a water channel that makes up the interlamellar spaces.

The presence of other basic structures including setae and the gill spine found along the efferent vessel agrees with observations in other crab species. The gill spines were first reported by Goodman and Cavey (1990) in the shore crab *Carcinus maenas*. The functional significance of these structures is not known, but Goodman and Cavey suggested a possible sensory role due to the availability of bundles of neurites and blood vessels in the vicinity of the spine. Later the spine was also reported on the same locations in two other crabs species, *Carcinus mediterraneus* (Dalla Venezia *et al.*, 1992 in Martinez *et al.*, 1999) and *Ucides cordatus* (Martinez *et al.*, 1999).

5.5 Conclusions

The results of this chapter confirms that the dorsal carapace of the swimming crab, *Liocarcinus* depurator resembles the typical crustacean shell made having three major cuticular layers; the epi-, exo- and endocuticles with the endocuticle forming the thickest layer. The major elements of the cuticle are calcium, carbon and oxygen in the form of calcium carbonate which were found to be distributed in the entire cuticular layers. The gills of *L. depurator* also show the characteristic features of a typical phyllobranchiate crab gill. Owing to this fact, it is safe, whenever necessary to apply information reported on other crab species to explain the findings of the subsequent studies.
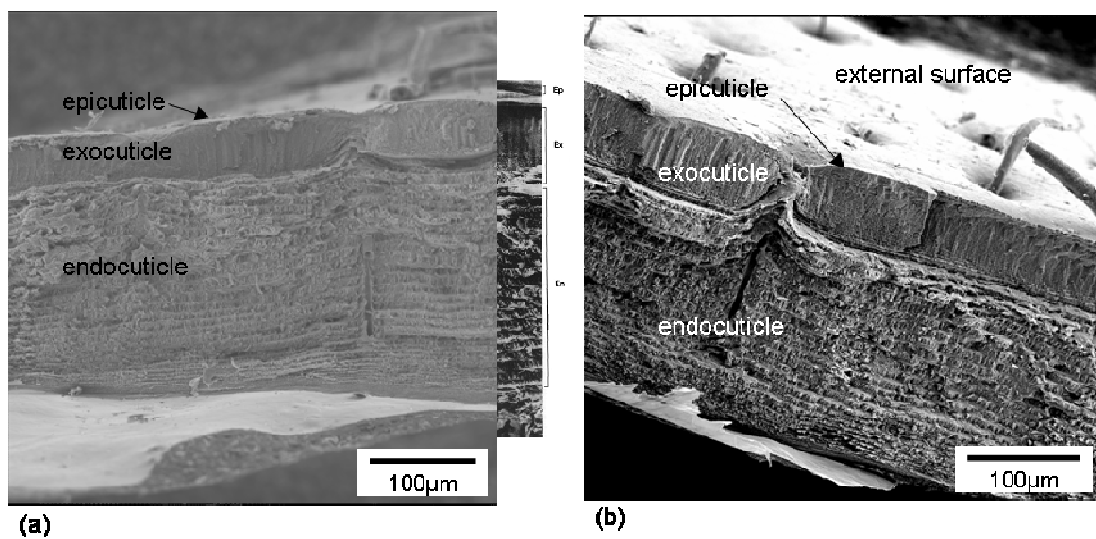
Fig. 5-1. SEM micrographs of the dorsal carapace of *L. depurator* showing all the basic layers. The sample was fractured from freeze-dried material. (a) The inset image on the right shows the epicuticle (5μm), exocuticle (65μm) and endocuticle (195μm) of *C. maenas* (From Roer and Dillaman, 1984); (b) A few broken setae can be seen on the external surface.
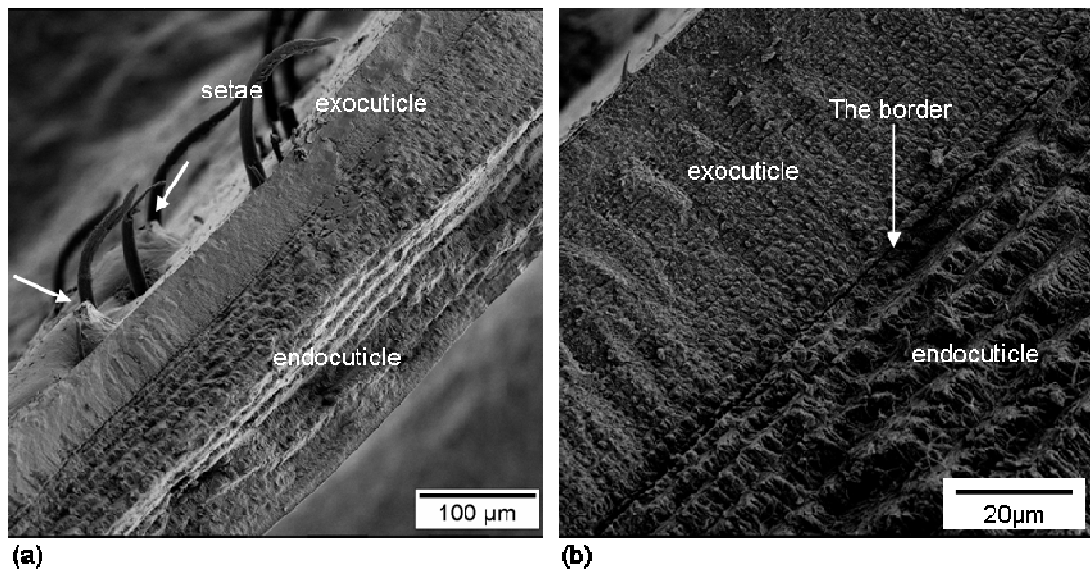
Fig. 5-2. A fracture through the dorsal carapace of *L. depurator* showing (a) the basic layers, setae and several ridges (arrows) and (b) a border distinguishing the exocuticle and endocuticle.
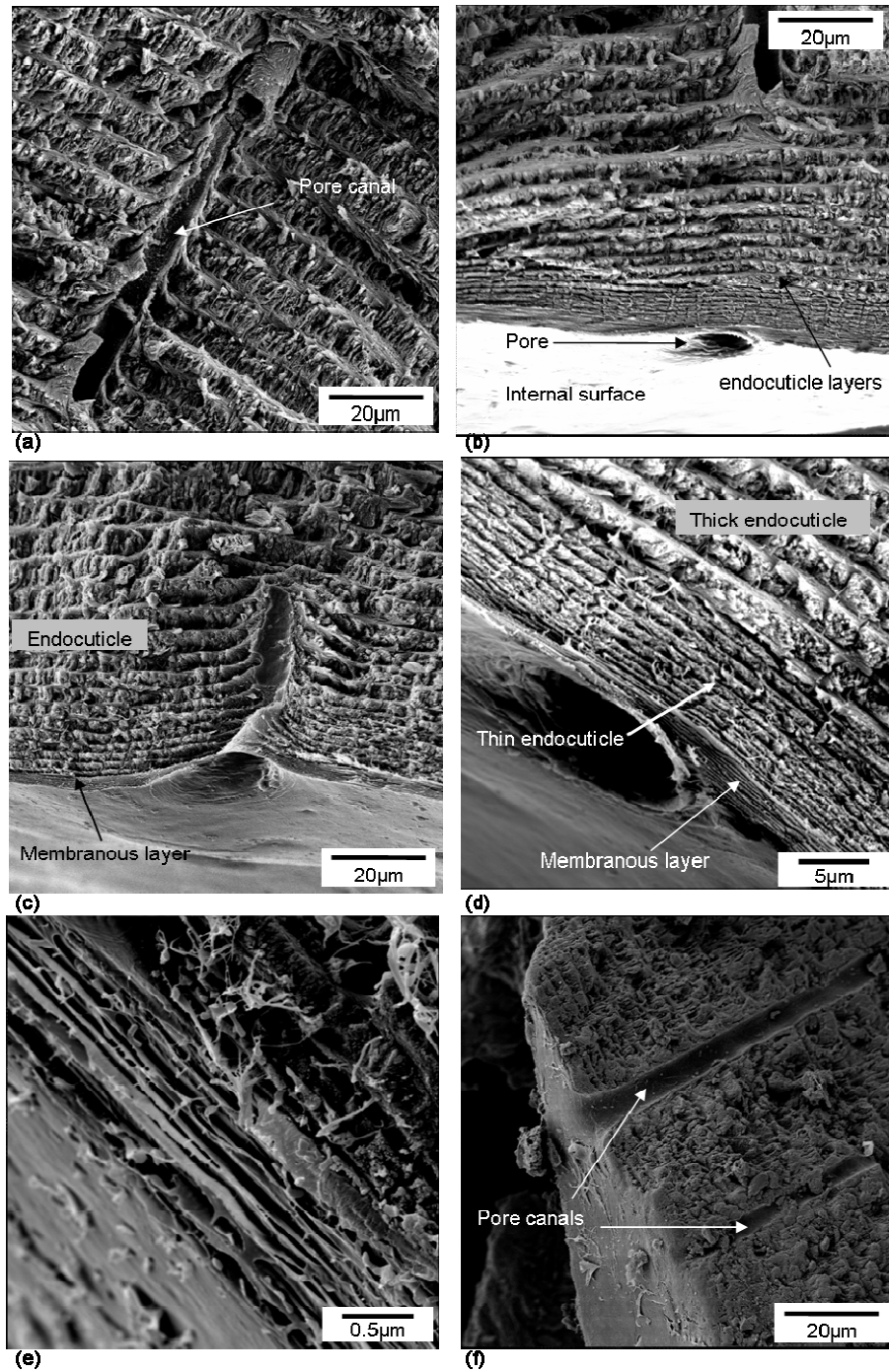
Fig. 5-3. (a) The endocuticle of *L. depurator* with a pore canal running continuously through the layers. (b) A progressive thickening of the lamellae of the endocuticle towards the inner layers. (c) The endocuticle and the internal surface of a carapace showing a pore opening on the internal surface and part of the pore canal within the endocuticle. (d) The membranous layer can be seen to be well differentiated from the developing lamella of the endocuticle. (e) Micro-thin sheets packed together forming the membranous layer. At least 10 sheets are visible in this microphotograph. (f) Pore canals traversing through endocuticle layers.
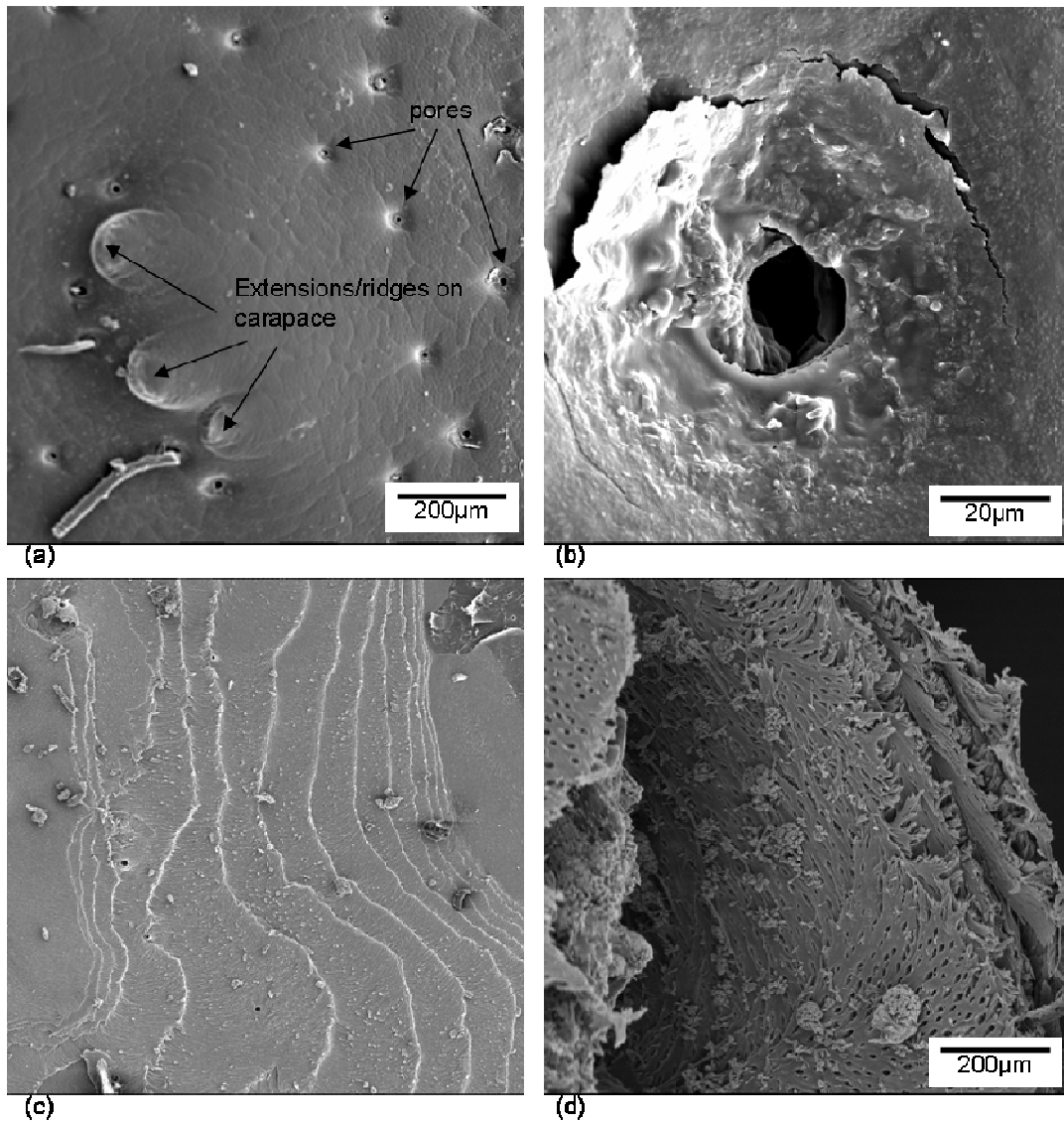
Fig. 5-4. (a) The external surface of *L. depurator* carapace showing a number of pores and a few extensions/ridges. These ridges correspond to the ones shown in Fig. 5-2a. (b) The pore as viewed from the external surface of a carapace. The crack represents the peeling areas of the epicuticle layer. (c) A fracture of the carapace reveals the layers that make up the exocuticle. A number of pores can be seen in these layers (magnification 130x, scale bar is not available). (d) The layers of the procuticle (exocuticle and endocuticle) can be individually distinguished, forming uniform layers of netted sheets of lamellae.
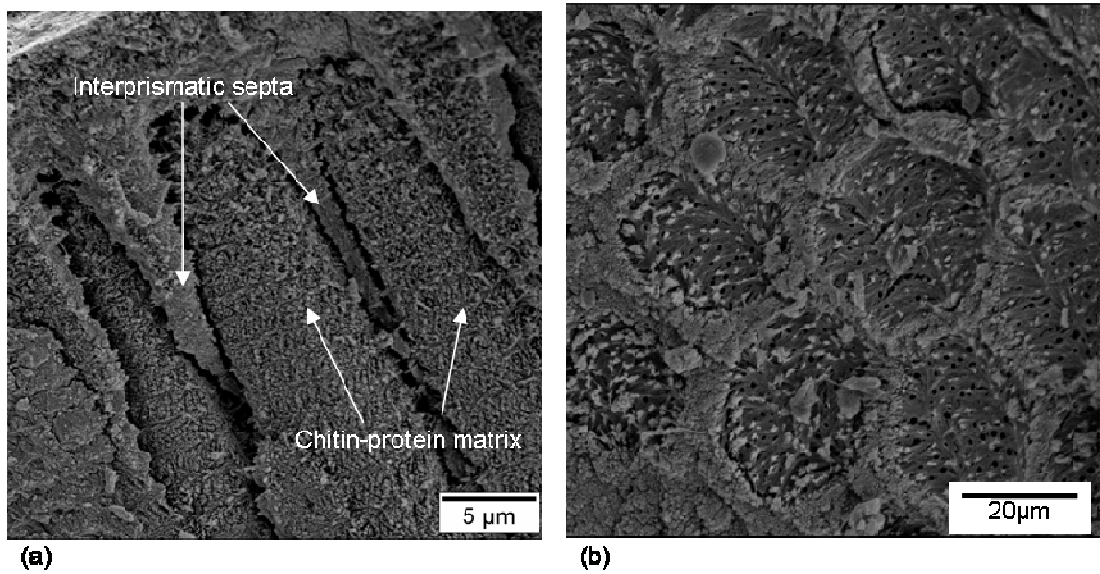
Fig. 5-5. The interprismatic septa in the procuticle, (a) imprints left in the cuticle by the margins of the epidermal cells penetrating into the chitin-protein matrix of the exocuticle seen in fracture across the carapace, (b) A horizontal fracture through the exocuticle of a dorsal crab carapace (parallel to the cuticle surface) showing the polygonal arrangement of the interprismatic septa.
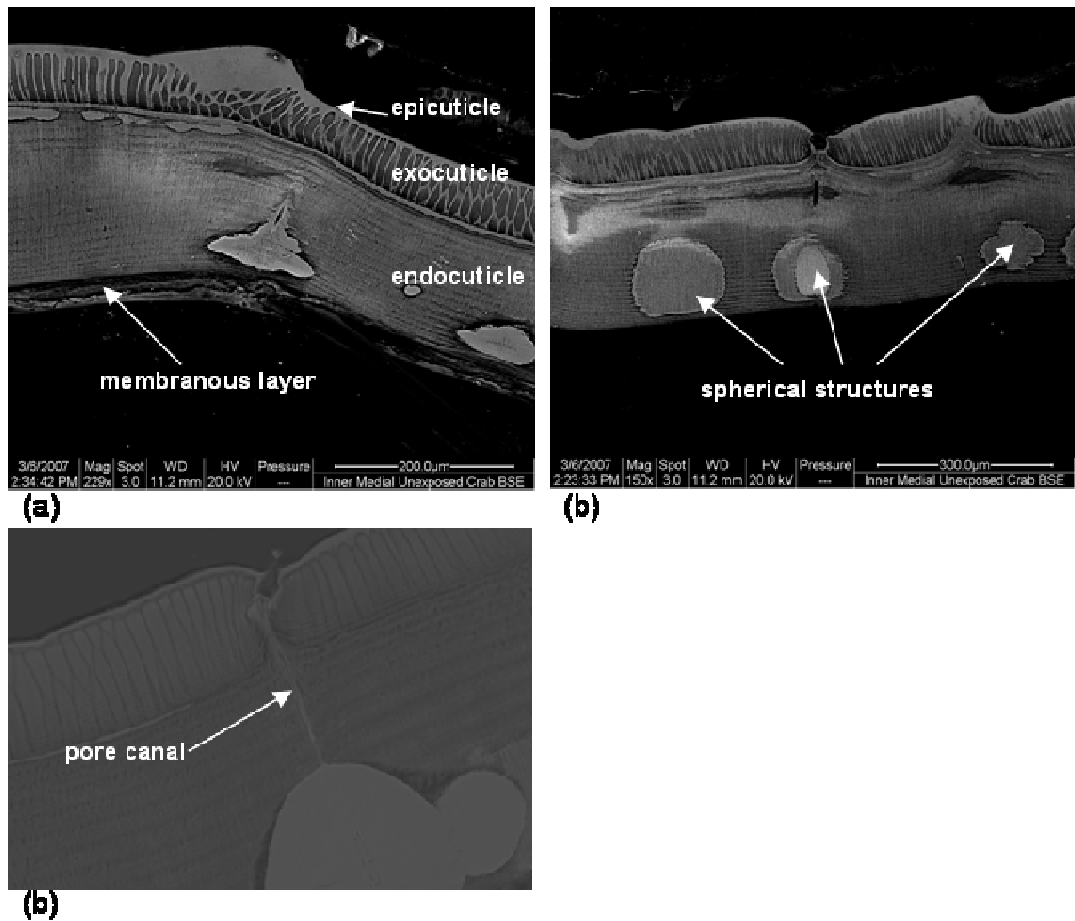
Fig. 5-6. A BSE images of sections through the *L. depurator* dorsal carapace in which the various layers are clearly distinguishable. (a) The epicuticle, exocuticle, endocuticle and membranous layer. (b) Several spherical structures (probably tegumental glands) embedded within the endocuticle. (c) A canal connects the gland and the opening on the epidermis.

(a) Calcium

(b) Carbon

(c) Oxygen

(d) Calcium (red), carbon (green), oxygen (blue)
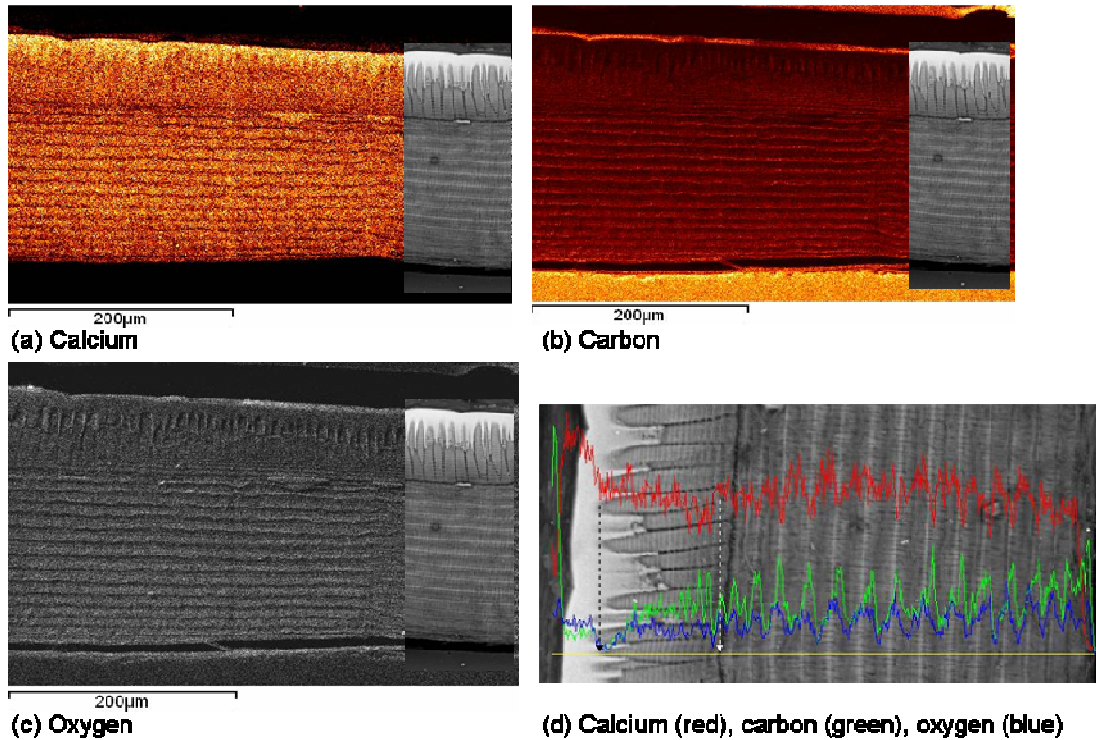
Fig. 5-7. Maps and profile of elemental distribution in the carapace of *L. depurator* from EDX analysis. Insets are the SEM image of the same sample for comparison. (a) Calcium signals represented by yellow dots were found to be highest in the epicuticle, and least dense along the border between exocuticle and endocuticle. (b) Carbon signals (brown) correspond to the middle of each lamella. Black stripes represent the interlamellar spaces containing fewer elements. The high signal on the topmost layer and a layer at the bottom of the image came from the C-coated resin block. (c) Oxygen (white) was found to be less between the interprismatic septa, whereas the rest of the signals match with C signals as seen in (b). This overlapping signal suggests that the elements occur together as a compound, most probably as carbonates making up $CaCO_3$. (d) Profiles of Ca, C and O based on an elemental line scan across the cuticle (marked by yellow line). High Ca occurs in the epicuticle. Lower Ca is shown in the exocuticle, where the level shows a little decrease towards the inner layers. The level fluctuates around similar level throughout the endocuticle layers.
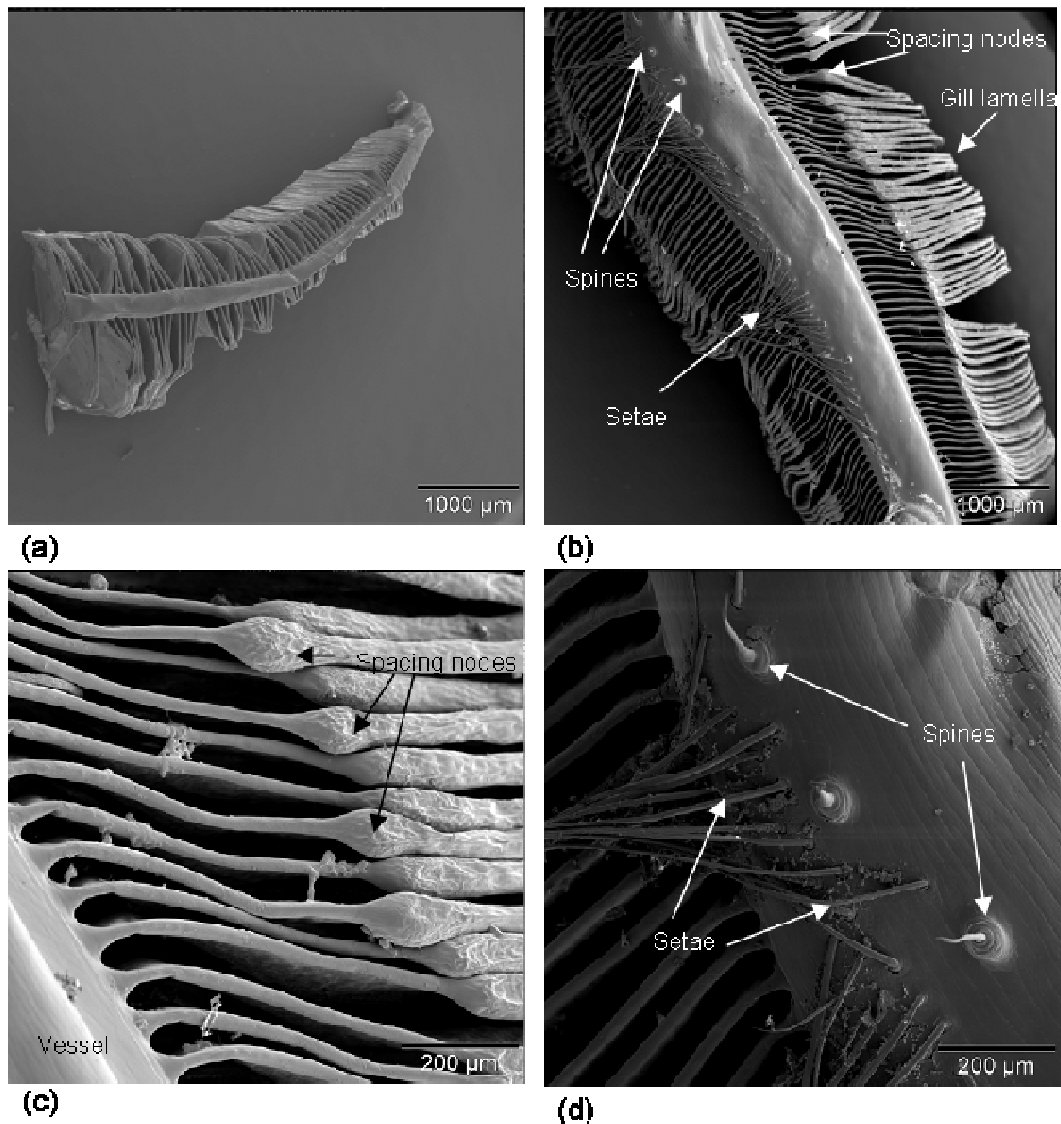
Fig. 5-8. The gills of *L. depurator*. (a) One single gill. (b) A single rachis of the gill showing some basic morphological features. (c) Gill lamellae and the spacing nodes. The nodes (also known as bulbous knobs) together with ridges at the edges of the plates ensure the patency of the interlamellar spaces. (d) Some setae can be seen on the central stem. Shorter, cuspidate projections (tentatively termed gill spine by Goodman and Cavey (1990) and later by Martinez *et al.* (1999)) could also be observed.
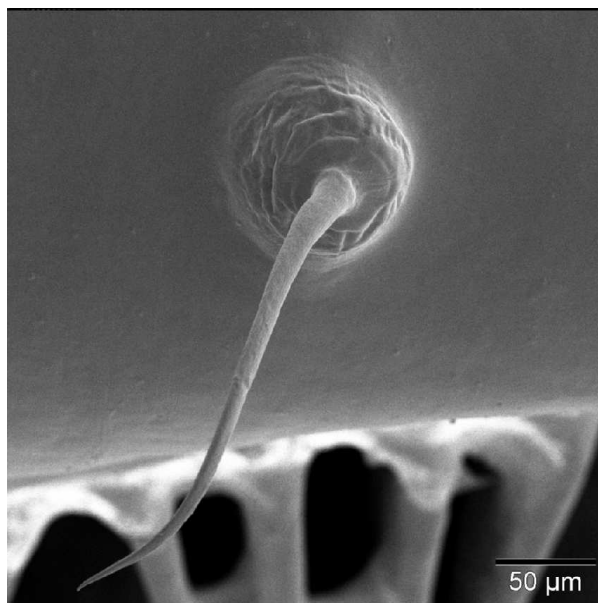
Fig. 5-9. A gill spine resembles a seta, but arising from mammilate mounds along the outer surface of the efferent vessel (in contrast, the base of a seta is embedded within the crab carapace).
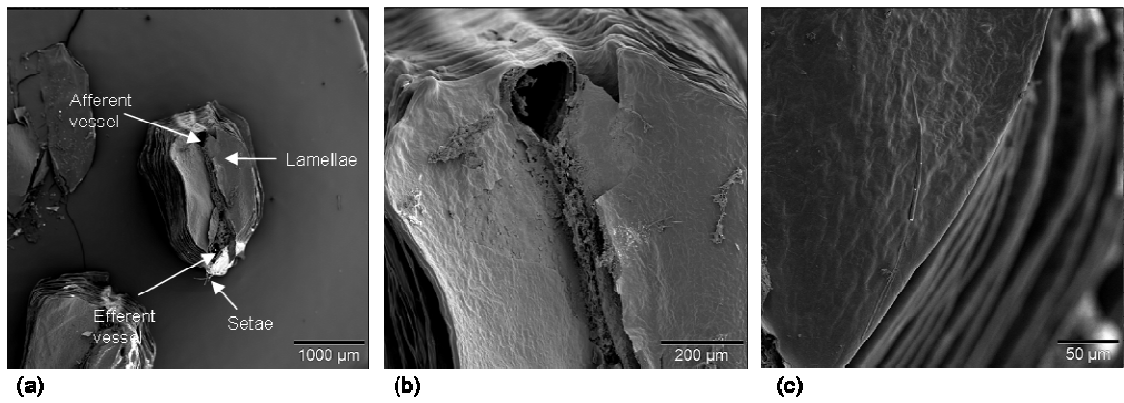
Fig. 5-10. The gill lamellae. (a) The lamella as seen from a fracture halfway along the rachis showing the afferent and efferent vessels. The setae can be seen lying along the efferent vessel but not on the other. (b) The afferent vessel. The spacing nodes are also visible representing the 'shoulders'. (c) The distal region of the gill lamellae.

6 Scanning electron microscopy studies of biosorbed carapace particles

6.1 Introduction

Biosorbed crab carapace particles were observed to change colour (from pinkish to brownish black) with increasing duration of the biosorption process. The blackening of the particles was also associated with the increase in Mn concentrations in the particular particles. These observations suggest that Mn might precipitate or be adsorbed onto the surface of the carapace particles, making it possible that the deposition may be located visually by examining the biosorbed materials at high magnification. A scanning electron microscopy technique (SEM-EDX) was therefore applied to examine the biosorbed materials for any deposits or any visual change on the basic structure of the original materials.

Exposure of crustacean shell (or particles) to various metals result in the metals being deposited onto the shell. One of the earliest formal reports of such deposition was that of Ewer and Hattingh (1952) who reported that silver absorption onto the gills of the freshwater crabs *Potamonautes sidneyi* and *P. depressus* caused the blackening of almost the whole surface of each lamella. Also, Pb was found to precipitate on the surface of a crab shell following exposure to Pb-containing solution (Lee *et al.*, 1997). A black precipitate of Mn was previously reported on commercial chitin powder from crushed crab carapace exposed to 102µM Mn (Hawke *et al.*, 1991). The blackening was not restricted to the carapace alone, but was also reported in the gills of animals from a polluted environment.

Deposition may take various forms, some are in the form of nodules (Cd) littering the surface of exposed particles e.g. in the blue crab (Benguella and Benaissa, 2002), whereas some take the form of crystals e.g. in penaeid shrimps (Coblentz *et al.*, 1998). Apart from metals incorporated into the carapace due to these external

exposures, a variety of invertebrates may impregnate the sclerotized cuticle with Zn and/or Mn as a unique approach to exoskeletal reinforcement instead of including an inorganic filler (Fawke *et al.*, 1997). This scenario offers an interesting new field to study the elemental composition of the cuticle.

This chapter examines Mn deposition onto the exoskeleton of the crab *Liocarcinus depurator*, particularly onto the carapace. The nature of deposition i.e. the form of deposit and site of deposition was examined under high magnifications by applying SEM-EDX applications.

6.2 Materials and Methods

Spectroscopic techniques SEM/EDX (scanning electron microscopy/electron dispersive analysis of X-ray) were applied in this chapter. The carapace samples were viewed in three conditions wherever appropriate, i) dried raw carapace, ii) gold coated, and iii) resin-embedded block. The dried raw samples were examined in the Microscopy Unit of the School of Chemistry, University of St. Andrews (Jeol JSM 5600 SEM). SEM examination on gold-coated samples was carried out in the IBLS Electron Microscopy Unit (JEOL 6400) in Glasgow University. The resin embedded samples were examined in the Geology and Earth Science Microscopy Unit in Glasgow University (Cambridge Instruments S360 Analytical SEM).

The specimens examined in this chapter were obtained from two different sources. Biosorbed carapace particles (both crab and Norway lobster carapace) were obtained from a few selected biosorption experimental runs carried out as described in Chapter 4. Whole dorsal carapace specimens were obtained from exposure experiments as described in 6.2.2. All specimens were prepared for SEM as described in Chapter 5.

Gill samples were also collected from crabs exposed to extremely high concentrations of Mn (80ppm) sea water for 21d in a 12L exposure tank. The water

was changed twice weekly until the day the animal was sacrificed. Images were scanned using dried raw samples and also gold-coated specimens.

6.2.1 Carapace particles from biosorption experimental run

Biosorbed carapace particles were obtained from biosorption column processes described in Chapter 4. For crab particles, images were scanned from biosorption experimental runs of 40 and 160ppm Mn solution for 72h. For the lobster carapace particles, they were obtained from biosorption runs of 20, 80 and 160ppm Mn solution for the same duration of time. Images of the deposition of Mn nodules/crystals onto the particles surface were captured and analyzed.

6.2.2 Exposure of the surfaces of whole dorsal carapace to 80ppm Mn

The following experiment was carried out to confirm that Mn deposition occurs primarily on the internal and 'damaged' surface, and that the external surface might possess some kind of protective layer to avoid passive accumulations of Mn from the environment. Whole crab dorsal carapaces were exposed to 80ppm Mn aqueous solution either on the internal or the external surface only. This exposure was carried out by placing a square plastic container with the carapaces tightly glued using Araldite epoxy resin to circular holes of about 2cm diameter on all sides into a larger container (Fig. 6-1). For easier handling, the carapace was glued on the outside of the small container with the internal surface of the carapace facing out. The intended exposure was achieved by varying the solutions in both containers. To expose the external surface to Mn, 80ppm Mn solution was filled inside the small container and distilled water inside the larger container. The placement of distilled water on the other side of the crab carapace was to add the same pressure on both sides of the carapace thus prevented the carapace from collapsing.

A small piece from each of the immersed carapaces was measured for Mn by standard AAS protocols.

6.2.2.1 Non-treated whole dorsal carapace

The exposed portion of the carapaces was taken for SEM in St. Andrew's University where elemental analysis was performed on fractured 'raw' samples of the freeze dried carapaces. Three samples (control, internally exposed to Mn and externally exposed to Mn) were also prepared in resin blocks and underwent a full elemental line scans and mapping on an EDX SEM system in the Geology Department, University of Glasgow.

6.2.2.2 Abraded/scrubbed dorsal carapace

The exposure to 80ppm Mn on the external surface was also carried out on crab shell that has been abraded / scrubbed with sand paper in order to investigate the role of the protective layer in the epicuticle in avoiding Mn deposition. The abrasion caused by sand paper scrubbing managed to remove the outermost layer of the cuticle and thus exposed the inner layer that is believed to be more prone to adsorb Mn from the solution.

6.3 Results

6.3.1 Particles from biosorption experimental runs

Figure 6-2 shows crab carapace particles in three size categories. In the interest of standardization and to avoid possible effect of particle size, it was only the finest fraction (<300µm) that was used in batch and bed heights column studies in Chapter 4.

Figure 6-3a shows crab carapace particles biosorbed with 40ppm Mn solutions for 72h; they have a clean external surface and broken edges. The internal surface and undamaged pore canal lining also appeared cleaner (Fig. 6-3b). Heavy deposition of Mn occurred on the broken edges in Figures 6-3a-b, as was more evident at higher magnification (Fig. 6-3c). These observations suggest that deposition might only occur on the exposed inner layers of the particle or on damaged regions of the particle surfaces.

Similar effects were seen on Norway lobster carapace particles (Figs. 6-4a-b). These images also provide more evidence for the site-specificity of Mn deposition onto carapace particles and that deposition occurs in the form of crystals or nodules. Thus, in Figure 6-4a, heavy deposition can be observed on the underlying torn layers of the carapace particle, whereas the outer undamaged layer appears almost untouched. However where the undamaged layer folds over at the edges of the block, it creates damage along the folding line, creating crevices that allowed the nodules to start growing.

The crystals/nodules were observed to pack onto a particle with a surface 'peeled' off the outermost layer and thereby exposed (A) whereas the undamaged surface (B) remained clean (Figure 6-4b). The surface of A was determined to be the exposed inner lamellae as evidenced by the numerous pores visible under higher magnification (Fig. 6-4c). These pores characterize the inner layers of the carapace, either the exocuticle or the endocuticle. Figure 6-4d confirms that B is an undamaged surface. However from this image, it is impossible to determine whether the small particle surface is either the internal-most or the external-most surface of the carapace.

Deposition of Mn in the form of crystals/nodules was observed to be occurring only on the netted lamellae of the carapace layers (Fig. 6-5a) and appeared to grow in a few different phases (Fig. 6-5b). In these SEM micrographs of crab carapace particles exposed to 40ppm Mn solution for 72h, some nodules resemble closed hollow cones, whereas others could be seen to 'bloom'/ 'blossom' into floral processes.

Crystals/nodules of a similar morphology (cones blooming into flower/cauliflower-like clumps) also occurred on Norway lobster carapace particles following exposure to Mn solution. Exposure to 160ppm Mn solution resulted in the surface of the particle being completely covered by nodules (Fig. 6-6a). These nodules show a similar mode of deposition, growing densely onto exposed inner layers of the carapace with the different phases of growth occurring next to each other on the same particle (Fig. 6-6b). Figures 6-6c-d provide evidence that similar nodules were present when lobster particles were exposed to a range of concentrations of the Mn solution (80ppm and 20ppm, respectively).

Figure 6-7 shows SEM micrographs of Mn crab carapace particles exposed to 40ppm Mn solution for 72h and their respective EDX spectra of the region marked 'X' in each image. In Figure 6-7a, an EDX spectrum generated from a point ID analysis on one of the growing nodules detected high peaks for Mn, C and O. These peaks suggest that the nodule might be a compound 'built' from these three elements, possibly Mn-oxides, Mn-oxyhydroxides or Mn-carbonate, or combinations of these three. Ca was also found to give very strong signal. Pd and Au peaks were detected because a significant amount was used to coat the samples on the stub before viewing under the SEM.

The undamaged internal surface of the carapace particle appeared clean of any deposits or nodules (Fig. 6-7b). An EDX spectrum of a single point on the surface revealed a few Mn peaks but at a lower magnitude compared to the nodule itself. A high signal for Ca was obtained as expected since $CaCO_3$ is the major component of most of the cuticular layers. Lower signals were detected for C, O and Mn. The signal indicates the presence of a little Mn on this undamaged internal surface. Despite being exposed to similar conditions, the external surface of the exposed particle shows even lower signals for Mn (Fig. 6-7c). Ca shows the highest signal, whereas lower signals were detected for C and O.

6.3.2 Whole carapaces exposed to 80ppm Mn solution

Figure 6-8 shows the appearance of the internal and external surfaces of carapaces after being internally-exposed to 80ppm Mn aqueous solution. Mn was observed to deposit/precipitate on the internal surface, turning the whole surface completely black. The colour of the external surface remained unaltered. In contrast, when the external surface was exposed similarly, no colour change was observed on either surface of the carapace. When the carapaces were externally exposed to the solution, no blackening was observed on the surface of the normal (non-treated) carapace. However, when the external surface of the carapace was scrubbed with sand paper in an attempt to scrape off the outermost (Mn-protective) layer, after exposure black spots appeared on the abraded regions of the surface after exposure indicating Mn deposition (Fig. 6-9). As the external surface of the crab carapace is full of ridges, complete abrasion with sand paper was impossible.

Table 6-1 shows the Mn concentrations (determined by AAS) in carapaces exposed internally or externally to 80ppm Mn solutions made up in distilled water (aqueous) or sea water. Exposed carapaces were found to contain more Mn compared to the concentrations measured in crabs from a reference area. Parallel to the blackening of the carapace, more Mn was measured in the carapace exposed internally to the aqueous solution, measuring more than 270 fold higher than the concentrations in female dorsal carapace from a reference site. The externally exposed carapace measured only about 10 fold higher than the reference value.

When the carapaces were exposed to sea water with a similar Mn concentration, similar trends were found but the absolute measures were different. The ones exposed internally showed an increase in Mn concentration to approximately 130 times higher than the reference value (an increment about half that observed in the aqueous solution). However, the increment shown by the ones externally exposed to Mn was around 11 times higher than that of the reference which was closely similar to the increment seen in the aqueous Mn solution. Exposure to this Mn-dosed sea water did not cause any blackening on either internal or external surfaces of these carapaces.

6.3.2.1 Elemental analysis on the whole carapace exposed to 80ppm aqueous Mn solution

Figure 6-10 shows the EDX spectra of the non-exposed (a), externally exposed (b) and internally exposed (c) carapaces. Generally, high signals for Ca, C and O, which make up the major elements of a crab carapace were detected for all specimens. Other elements including P, Mg and Cl show small but significant signals. Mn was not detected in the non-exposed carapace, but after 72h exposed externally to 80ppm Mn aqueous solution, a strong signal for the metal was obtained, indicating that some Mn from the environment has entered the carapace. The signal was even stronger in the internally exposed carapace, which in this case appeared completely black after the exposure as shown in Figure 6-8.

Figure 6-11 shows an SEM image of the cross section of the non-exposed carapace (resin-mounted and polished) with a line scan from the external through to the internal surface showing Mn counts and other elemental profiles. Ca shows the highest count whereas C and O fluctuate around the same level (Fig. 6-11b). The counts for these elements correspond to the layering of the carapace as visible in the SEM image. Mn counts were found to show background levels fluctuating between 0-10 counts during the 10min scan (Fig. 6-11d). Even from a 4h mapping, no Mn signal was detected (Fig. 6-11c).

When the carapace was externally exposed to Mn solution, a similar trend of Ca > C, O was also observed (Fig. 6-12b). There was no prominent peak for Mn along the line scan, but the counts fluctuated between 4-24 counts (Fig. 6-12d), a value approximately twice as high as that observed in the control carapace. A 4h mapping revealed traces of Mn filling approximately 50µm deep down the pore canal (Fig. 6-12c). No signal for Mn was detected on the external surface of the carapace despite being exposed to the metal for 72h, and despite showing about a 10 fold increase in Mn concentrations (measured by AAS) compared to control (Table 6-1).

Figure 6-13 shows the results of the internally exposed carapace. The trend for counts of Ca, C and O remains similar to the previous carapaces (Fig 6-13b). However, Ca counts were found to be higher in this specimen compared to the other

two. Ca was also found to be decreasing towards the internal surfaces. A few sharp decreasing points along the line scan correspond to crack lines across the carapace. Mn counts were high on the internal surface (the site exposed to the metal in solution) at up to 170 counts (Fig. 6-13d). The counts gradually decrease inwards, and come to a background value around 10 counts at about 70µm depth. This trend of Mn was observed to be negatively correlated with the trend of Ca, suggesting a potential meaningful relationship between the two elements. The high count of Mn also gave dense signals on a map of the internal surface of the carapace as shown by the green belt in Figure 6-13c, whereas this signal is absent in the non-exposed and externally exposed carapace.

When the above specimen was viewed at higher magnification, focussing only on the internal surface layer and the endocuticle, the negative relationship between Mn and Ca becomes more apparent (Figs. 6-14b and 6-14d). Mn could be seen penetrating the internal surface up to 50 µm into the carapace. From a baseline of about 20 counts, Mn increases up to 200 counts on the internal surface. Interestingly, Ca counts decrease from around 600 to about 450, a reduction of 150 counts.

Elemental analysis was also carried out on freshly fractured carapaces that had been freeze-dried after exposure (Figs. 6-15 to 6-20). The fracture was carefully done so that it revealed the smoothest cross section through the thickness of the carapace. The results, even though not as good compared to the completely flat surface of a resin mounted specimen, all point to the same conclusion that Mn deposition occurs mainly through the internal surface. Only small traces of deposits were observed on the external surface. The external surface also prevented Mn from diffusing into the carapace, whereas exposure onto the internal surface led to Mn being found to a depth of about 50-60µm into the endocuticle. Mn was seldom found to penetrate more than 80 µm into the internal layers, as baseline values were reached by then.

Figure 6-15 shows the SEM of a fractured specimen of an internally exposed carapace. Signals of Mn could be seen on the map as the region with more dense blue dots which is about 50-60 µm wide. This figure also indicates that Mn signals

appeared to be more in the endocuticle compared to the 'separated' region (assumed to be the membranous layer). In another specimen exposed similarly to Mn (Fig. 6-16), high Mn counts were observed on the internal surface (90 counts, Fig. 6-16c). Mn could be seen to penetrate about 50-70 µm into the carapace (referring to point 80-140 µm on the x-axis). The highest counts were detected in the regions between 120-140 µm on the x-axis (corresponds to the dark brown belt in Figure 6-16b). A decrease in Ca (Fig. 6-16d) appears to correspond to the region with increasing Mn.

Figure 6-17 shows another specimen of internal exposure to Mn, adding more evidence of the deposition and penetration of Mn into the carapace through the internal surface. The inverse relationship between Ca and Mn was also observed, roughly between 120-180 µm on the line scan (Figs. 6-17b-c). Mn was found to come to the baseline value at about 60µm into the carapace, suggesting the limitation of Mn penetration within the 72h exposure period. In another specimen shown at higher magnification (Fig. 6-18), similar results were obtained. For this image, the left side is the internal surface. Mn counts were high at the internal surface (around 200) and Mn penetrated 80 µm into the carapace before it came to baseline value from that point onwards (Fig. 6-18b). The sharp decrease of Mn counts from 10-30 µm correlates closely with the increase in Ca counts (Figs. 6-18b-c).

Figure 6-19 shows a line scan through part of the endocuticle and exocuticle of a carapace exposed externally to Mn. Mn was found strictly on the external surface, but with a much lower count of 25 (Fig. 6-19b) compared to the ones observed on the internal layers when they were subjected to similar exposure. The Mn count was lower throughout the inner layers due to the blocking effect played by the external surface. Ca also showed some decrease towards the external surface but this might correspond to the epicuticle region (Fig. 6-19c). The line scan cuts through three different layers of the carapace that is endo-, exo- and epicuticles.

A line scan across fractured specimen of a carapace internally exposed to sea water with a concentration of Mn of 80ppm for 72h is shown in Figure 6-20. There was no prominent peak for Mn, but the counts fluctuated from 0-17 within the internal

surface and the endocuticle (Fig. 6-20b). The count was slightly higher compared to the control in resin block. This corresponds to the slightly higher concentration measured by AAS in the carapace following similar exposure (Table 6-1).

6.3.3 Elemental analysis on the gills of exposed crabs

SEM micrographs of gill samples obtained from live crabs exposed to 80ppm Mn in sea water were shown in Figures 6-21 to 6-22. Deposition of materials onto the lamella surface, especially along the margins, could be Mn-laden materials. There is no uniform structure in the materials, but on one of the specimens the materials were deposited in a floral-shaped pattern.

Figure 6-21(a) shows a block of gills from a crab exposed to Mn in sea water for 21d. Traces of particles were found to be deposited on the gill stem and on the lamellae especially at the edges or marginal ends (Figs. 6-21b-d). Figures 6-21e-f show the deposition at the edges of a lamella at higher magnification, revealing a uniform flowery pattern. A prolonged exposure to 80ppm Mn in sea water for up to 72d led to heavy deposition of the metal not only at the edges of the lamella, but also particles could be observed to cover the lamellar surfaces (Fig. 6-22a). The deposits on the edges (Fig. 6-22b) occur without any specific depositing pattern.

Elemental analysis carried out on some of the gills samples from exposed crab did not give a conclusive result of Mn deposition. After 20d exposure to 80ppm Mn in sea water, a line scan revealed no significant peak for the Mn count. However, this analysis highlighted the difference in the composition of this exoskeletal tissue compared to the carapace. In the gills, very low Ca levels were observed, whereas C and O were found to be the major elements.

A line scan across the lamellar surface of a gill exposed to Mn solution for 21d showed that Mn fluctuates around 15 counts with no prominent peak (Fig. 6-23b). In this particular exoskeletal tissue, Ca was found with a lower count of only around 15 whereas C showed the highest count followed by O (Figs. 6-23 c-e). These two

latter elements share a similar pattern suggesting a close relationship between them.

Another line scan of exposed gills provides more evidence of the association between C and O as shown in Figures 6-24c and 6-24e (possibly forming a single compound). Ca levels were also low whereas Mn fluctuated at the baseline level around 10 counts (Figs. 6-24d and 6-24b). Figure 6-25a shows the lamella at higher magnification showing some deposits on the surface. A line scan revealed a possible peak in Mn counts (up to 30) indicating a possibility of high Mn deposition (Fig. 6-25b). The general observation of high C followed by O, and the similar pattern shared by them, and the relatively lower Ca remain for this particular tissue as observed in a few specimens before (Figs. 6-25c-e).

6.4 Discussion

The results highlight some new aspects of the deposition of Mn onto the exoskeleton of the crab. Beginning with the observation of the colour changes in the biosorbed materials, EM techniques were applied to determine the nature of Mn deposition onto these tissues. Deposition was found to vary according to the tissues and shows some site-specificity, occurring predominantly at the broken edges or fractures, but not on flat undamaged surfaces. Deposits in the form of nodules were found on carapace particles biosorbed with Mn-containing solution, whereas particles or crystallite matrices were observed depositing on the gill lamellae surfaces. When the whole dorsal carapace was exposed to Mn-solution, Mn was found to deposit more onto the internal side of the carapace, allowing the metal to penetrate deeper into the inner cuticular layers, at the same time coating the entire surface with the deposit turning it completely black. EDX analyses suggest a possible relationship between the deposited Mn and the release of Ca from the crab cuticle.

6.4.1 Mn deposition onto the carapace

SEM micrographs and EDX of the particles revealed that Mn deposition does not occur randomly, but shows some kind of site-preference. The deposition occurs in the form of nodules or crystals which are found more concentrated on the broken edges, and grow extensively on the netted lamellae of the cuticular layers. EDX analysis conclusively identified these nodules as Mn-laden.

The nodules found growing on the carapace particles of crabs and lobsters show similar morphology (cones blooming into flower/cauliflower-like clumps), suggesting that it might be the same compound developing on the carapace, regardless of the species. Similar nodules occurred when the carapace particles were exposed to concentrations of Mn solutions ranging between 20-160ppm for the same duration of 72h.

Black precipitate was previously reported on commercial chitin powder from crushed crab carapace exposed to 102µM Mn (Hawke *et al.*, 1991). Precipitation of Mn on other mineral surfaces has also been reported in detail by Junta and Hochella (1994). They found that precipitation of Mn does not occur homogenously across the surface of hematite (Fe_2O_3), but begins at the base of steps on the mineral structure forming a small hemispherical protocrystallite. With continued exposure to the Mn-containing solutions, deposition continues along the precipitate / hematite boundary to form a wave of precipitate growing out from the step base along the basal parting plane. Within two days of exposure to 4ppm Mn-solution at pH 8.15, the entire surface of hematite was coated with a protocrystallite layer. In another case, they observed small islands of the Mn precipitate distributed across the hematite surface and were specifically concentrated near rough surfaces such as edges and cracks. The latter observations explain the results of the present study of dense/packed nodules found on the broken edges of the carapace particles. In this case the major mineral involved could be the $CaCO_3$. The fractures as a result of grinding the carapace to make up to the desired size range provide the 'steps' required for Mn to start nucleating and growing. Junta and Hochella (1994) also reported that exposure to a higher concentration of Mn-solution (26.7ppm, pH 8.3) causes the hematite surface to become entirely coated with a layer of crystallites within 80min. The

coating became thicker as the exposure is prolonged, with the crystallites appearing to radiate out from the underlying substrate.

Exposure of a whole piece of dorsal carapace to a Mn solution causes an increase of the metal concentration in the carapace. Interestingly, exposure on the internal surface led to a complete blackening of the region, whereas the same phenomenon was not observed when the external surface was exposed. The increment in the metal concentration was also associated with the degree of blackness of the surface, as a very large increase was measured for the internally-exposed carapaces compared to the externally-exposed ones. The small increment measured in the externally-exposed carapace might be due to Mn getting clogged into the numerous pore canals that open to the surface. The blackening of the internal surface formed more than just a layer on the surface, since the increased Mn concentration could be traced to a depth of several micrometers into the thickness of the endocuticle.

The absence of the blackening on the external surface might suggest that the surface is covered by a layer that protects Mn from depositing, and/or that the site for Mn attachment is internally located. This is particularly true because abrasion of the outer surface of the carapace enabled Mn to adhere onto the abraded region (as indicated by black spots).

There is a possible inverse relationship between the Ca and Mn concentrations, suggesting that a replacement might occur between these two elements, either directly or indirectly. As Mn (II) outcompetes Ca^{2+} for surface sites (Hawke *et al.*,1991), it will form a complex with the surface and precipitation would follow, in this case seen as the black spots or layer. It is also possible that the carapace dissociates in water, releasing Ca into the solution and allowing Mn to form a complex with the remaining structure. Junta and Hochella (1994) illustrated that deposition of Mn onto mineral surfaces occurs in the following stages: attachment to active site, complexation with oxygen, oxidation and precipitation of the product. Therefore, the protective layer on the outer surface might serve the purpose of preventing the dissociation of the cuticle, leaving no active sites for attachment for Mn (II) and therefore preventing Mn-complex formation.

As an example of an indirect process of metal replacement, dissolution of calcium carbonate in a crab shell forms carbonate ions in the solution which, when exposed to lead-containing solution react with the metal and later precipitate on the surface of the crab shell (Lee *et al.*, 1997). Exposure to lead resulted in the formation of nodule-like particles on the surface of the crab shell which showed a high peak of lead. The same phenomenon might be the case in the current study where the crab shell particles were continuously exposed (in the biosorption column) to a range of concentrations of Mn-containing solutions. The nodules observed on the biosorbed particles were also confirmed to be Mn-laden. The SEM images of these nodules at high magnifications suggest that they are in different phases of growth, but the compound could not be determined unless the powder form of the nodules is subjected to an XRD analysis. However, there are some possibilities that they might be oxides, carbonate or oxyhydroxides of Mn (Hochella, personal comm.). Lee *et al.* (1997) using XRD identified the nodules in their experiment as $Pb_3(CO_3)_2(OH)_2$ and $PbCO_3$.

The occurrence of similar nodules following exposure to some other metals was also reported on crab chitin (commercially prepared chitin from crushed crab shell). Following Cd sorption the chitin surface appears littered with the nodules (Benguella and Benaissa, 2002). These nodules were electron dense materials concentrated on the surface; they were absent in chitin which had not been exposed to the metal solution. The EDX spectrum of these nodules showed a signal which conclusively identified them as cadmium. These studies confirmed that sorption of cadmium is mainly located superficially in the chitin structure suggesting that the reaction is probably not an adsorption but a surface precipitation.

The absence of Mn deposition on any exposed surface is common, as Junta and Hochella (1994) reported albite ($NaAlSi_3O_8$) exposed to 4ppm Mn-containing solution showed precipitates located only along fractured regions, whereas the surfaces appeared completely unreacted, even after a 5-month exposure. In the same paper, Junta and Hochella (1994) stated that deposition of Mn and the development of the crystal growth onto mineral surfaces differ according to the type of minerals involved, and that the precipitate growth can take one of two paths. First is the **substrate-controlled growth**, in which adsorption-oxidation is preferred at

the precipitate-substrate-solution interface, resulting in a thin layer of precipitate clusters. Once these active sites are consumed, adsorption-oxidation occurs only at the precipitate-solution interface that leads to crystal growth. The second path is the **_precipitate-controlled growth_**. In this case, adsorption-oxidation occurs preferentially at the precipitate-solution interface, and thus prevents the formation of a thin layer precipitation. Instead, deposition is characterized by large patches of precipitate closely associated with irregular features including fractured edges.

It is possible that Mn deposition in the present study took both paths under different experimental conditions. The biosorbed particles showed deposition in the form of nodules, which occur more on the fractured edges and 'exposed' netted lamellae of the inner cuticular layers. These patchy depositions that are characteristics of precipitate-controlled growth is shown in Figure 6-4a, where a clear deposition was seen growing along a crack of the surface. The flat surface appears almost unreacted except for a few isolated patches of newly forming Mn deposits. The same effect was also observed on cracks/damaged regions of carapace that had been abraded with sand paper. However when the whole carapace was exposed to Mn solution, the entire exposed internal surface was covered with a film of black precipitate confirmed to be Mn-laden. The formation of this layer characterizes substrate-controlled growth. Substrate in this sense refers to the carapace. Unfortunately, the active sites on the surface could not be determined as SEM examinations were carried out only after 72h of exposure at which time the precipitate had coated the entire surface. Examination at a series of shorter time intervals would throw light on these processes.

While Junta and Hochella (1994) explain the mechanism of metal deposition chemically or mechanically, Coblentz _et al._ (1998) offer a more biological explanation with a model (regarding mineralization of the cuticle of the blue crab _Callinectes sapidus_) that suggests that proteins acting as crystal nucleation sites are present in the cuticle at all times, attached to the insoluble organic matrix by acid-labile bonds. These nucleation sites do not become active until they are exposed to calcium and carbonate ions by the removal or alteration of larger shielding macromolecules. As Mn (II) outcompete Ca^{2+} for surface sites (Hawke _et al._, 1991), the nucleation site described in this model might correspond to the location where

Mn deposition could have taken place when the crab is exposed to the metal in nature.

Another interesting finding was that when the whole carapace was exposed to a solution of Mn in sea water on the internal side, the surface did not turn black, and AAS measurements of the metal confirms that a lower amount of Mn is deposited onto it compared to when exposed to Mn in distilled water of the same concentration. Kent and Kastner (1985) found that Mg^{2+} adsorption on amorphous silica decreased with increasing salinity, implying competition by Na^+ for surface sites. It is possible that the same form of competition could explain the present observation. Na^+ was absent in the Mn solution of distilled water, and therefore Mn was provided with more opportunities to form complexes with the surface; these could have been sufficient to account for the extensive blackening. Hawke *et al.* (1991) offer another explanation when they reported that pH also plays a role in determining Mn(II) uptake.

6.4.2 Mn deposition onto the gills

Deposition onto another exoskeletal tissue (the gills) did not occur as nodules, but appeared as deposited particles/crystals lining the cuticle of the gill lamellae surfaces, concentrating especially on the edges. The absence of the nodular form in the gills is not surprising as the exposure was carried out on live crabs. The intact gills were assumed to be in healthy conditions without any injuries. As was the case with the carapace particles, nodules were found on the broken edges and also on the 'exposed' netted lamellae of the cuticular layers. None was ever recorded on the outermost lining of the epicuticle. Recently, Schuwerack *et al.* (2003) observed that when the crab *Potamonautes warreni* was exposed to 0.2mg $Cd^{2+}.l^{-1}$ (0.2 ppm) for up to 21d, the gill lamellae were covered with deposits having a crystalline matrix. Crystal depositions were also reported in penaeid shrimps (Coblentz *et al.*, 1998), suggesting that deposition of metals in the form of particles/crystals onto crustacean gill cuticle surfaces after the animals are exposed to the metals is a common phenomenon.

An EDX spectrum of a gill of the crab *Ucides cordatus* exposed to 0.02 - 2.00mM Cr salt (1.04-104 ppm) for 96h confirmed a clearly distinguishable layer of deposited particles containing Cr lining the gill's external surface (Correa *et al.*, 2005). However, this EDX represents an extremely high concentration of Cr (17,396µg.g^{-1} Cr of dry gill weight) in the exposed crabs (1440-fold increase compared to the controls).

No gill blackening was observed in the present study as a result of the exposure of the crabs to Mn solution in the sea water. However, blackening of the gills due to exposure to silver was reported by Ewer and Hattingh (1952) in two freshwater crab species. They found that almost the whole surface of each lamella on the first four anterior gills was blackened by absorbed silver after a five-minute exposure to the metal. The remaining three posterior gills appeared clean. However, they reported the blackening to take place later after the animal was sacrificed, the branchiostegite was cut away and the gills exposed to sunlight for 15 minutes. Exposure to Cd also caused the lamella of another freshwater crab, *Potamonautes warreni* to become exceedingly blackened (Schuwerack *et al.*, 2003).

6.4.3 Elemental analyses of Mn in the carapace

Mn deposition on the carapace / carapace particles was found to be greatest in the nodules, followed by the internal surface and then the external surface. This is evident from the EDX spectra of these surfaces (obtained from the same biosorption column) showing relatively different counts for Mn peaks.

Mn deposition onto whole carapace occurs primarily onto and through the internal surface, where a layer of deposition was formed within 72h of exposure, causing the entire surface to be coated with black precipitate. No isolated patches of nodules could be identified. This surface also allowed Mn to penetrate deeper into the inner cuticular layers by up to approximately 80µm. The low peak for Mn observed on the spectrum of the external surface suggests that Mn is present but in a relatively lower

amount compared to the internal layer. Cracks and fractures on the external surface create active sites for Mn to attach, precipitate and start growing.

It is interesting to see the effectiveness of the epicuticle in preventing Mn from penetrating the carapace from the outside (environment). The only way for the foreign materials to 'invade' the carapace was through its permanently open pore canals. However, the occurrence of Mn in the pore canal observed in this study is on the isolated (dead) carapace rather than in a live crab. These pore canals are assumed to play a role in transporting materials from the secreting cells in the epidermis to the cuticular layers. Therefore in live animals, they could be filled with materials travelling towards the exterior and not *vice versa*. Therefore the chance for Mn to travel down the canals to the inside might be slight. However, as it can actually diffuse along a concentration gradient, exposure to the metal for a substantially longer period could possibly result in Mn seeping into the canals.

When exposed to the Mn solution for 72h, the internal surface quickly became coated with a layer of heavy black Mn deposits. The precipitate started as patchy black spots; presumably these are the specific active sites where Mn started to attach. By the time the exposure was terminated, it had entirely covered the surface. Within 72h, Mn precipitate was found to have penetrated deeper into the inner cuticular layers. In this case it travelled to about 80μm inwards within the loosely stacked lamellae of the endocuticle. It has been reported that as precipitation takes place, it grows first to form a single layer, then to form islands of new growths elsewhere above the first layer, thus thickening the coat (Junta and Hochella, 1994). In the present study it seems that Mn penetrated into the layers of lamellae and started growing within the cuticle once the attachment to any active site is secured, although it is difficult to confirm if thickening of the coating layer then took place. The Mn profile of the penetrated endocuticle shows that the Mn gets progressively less towards the inner lamellae. This profile suggests that deposition stages mentioned before (attachment – complexation – precipitation – growth) take place as soon as the attachment is made. Therefore, more precipitations are formed on the outside (the internal surface) as it is the first layer to come into contact with the metal. The growth then travelled inwards. In addition, more Mn was detected on the internal surface as it is continuously supplied with the metal directly from the passing

solution. This continued supply of Mn enhanced metal precipitation onto the already existing black layer covering the surface.

There is also a possibility that Mn does not impact the membranous layers at all, but instead passes through the membrane without leaving any precipitation. The membranous layers could be peeled from the black internal surface after 72h exposure to Mn solution; they remained transparent and retained their original colour, whereas the black deposit was only found associated with the first endocuticle layer it came in contact with. In one of the fractured samples (Fig. 6-15), the membranous layer was actually slightly detached from the main cuticle, and the Mn map showed clearly that more Mn is deposited onto the endocuticle whereas the slightly detached membranous layer yields only a background signal. As the mapping might not be sensitive enough to pick up traces of Mn, it can be suggested that some Mn is available on the membranous layer which might be detected by AAS. However, the fact that the colour remains suggests that the deposition might occur in a different form.

It would be interesting to proceed with additional experiments designed specifically to identify the active sites on the internal surface and also to examine whether prolonged exposure of the carapace internally would lead to the Mn penetrating further into the other layers from the inside (up to the epicuticle).

Another interesting observation is the trends shown by Ca and Mn on the exposed carapaces. In general, the epicuticle was found to be more calcified compared to the exo- and endocuticles as evidenced from the profiles. The level in the endocuticle was found to show a slight decrease especially on the innermost layers (observed in both the control and the externally-exposed carapaces). However, the decrease was more pronounced in the internally-exposed carapace. The significant reduction coincides with the increase in Mn deposition in the same region of the carapace. Profiles from freshly-fractured exposed carapace (although staggered due to the non-laminar surface created by fracturing) also seem to support the idea of a potential relationship between Mn and Ca.

Incorporation of some trace metals into the shell through substitution of calcium ions in the crystalline phase has been reported in molluscs and barnacles (Watson *et al*, 1995). In a mussel, *Hydridella depressa*, some maxima in the Mn concentration appeared to be correlated with a minimum in the Ca concentration (Siegele *et al.*, 2001). Siegele *et al.* (2001) also found that the region with a high Mn concentration slowly increased in thickness. As thickening of calcareous shells is often directly related to calcification, it is possible that Mn interferes with the process by replacing Ca within the shell. As Mn can be transported through Ca channels (Carlson *et al.*, 1994 in Hockett *et al.*, 1997), the shell morphological changes may also reflect alteration of Ca transport mechanisms (Evans *et al.*, 1991 in Hockett *et al.*, 1997). Runnels (1970 in Lumsden and Lloyd,1984) suggested a potential substitution of Ca^{2+} (ionic radius of divalent ion = 1.0A) with Mn^{2+} (divalent ionic radius 0.83A) in dolomite, a rhombohedral carbonate with a stoichiometric composition of $CaMg(CO_3)_2$, giving a clue for the chemical explanation of the substitution process between Ca and Mn.

6.4.4 Limitations of the tools/techniques

In this chapter, SEM with EDX has been successfully applied to examine and locate Mn deposition onto the exoskeleton of a crab, particularly onto the carapace. However, the application of EDX has several limitations. One of the most important ones is that the sensitivity is quite low. Correa *et al.* (2005) could not detect Mn signals on their EDX spectra of gill samples of the crab *Ucides cordatus* measuring 317.0 $\mu g.g^{-1}$ of dry gill weight after exposure to 2mM Mn salt (110 ppm) for 96h. The measurement represented a 58-fold increase of the metal concentration in the gills (5.4 $\mu g.g^{-1}$ of dry gill weight in the control crab). In the present case, no signal could be detected even at a concentration of Mn as high as 350$\mu g.g^{-1}$ in the carapace. It is perhaps due to this reason that this approach has not become very popular. Fawke *et al.* (1997) admitted that back-scattered electron detection gave a beautiful compositional image for polished cross section, but they never attempted quantitation via SEM-X-ray analysis.

However, EDX results using biological materials offer a good qualitative measure. They are considered to be qualitative because of the uncertain composition and heterogeneity of the materials being examined. Despite its qualitative nature in biology, EDX has the advantage of being far more available since many SEMs have EDX detectors installed for use in the geological and materials sciences. Qualitative results in EDX are readily attained in a short time frame, making it an ideal surveying tool (Cutler and McCutchen, 2006).

In addition, raw x-ray counts generated by EDS with X-ray microanalysis can be converted into 'quantitative data' by calculating them using SuperQuant programme on an EDAX software. These raw counts could be converted to counts per second, which was proven to be a statistically meaningful indication of the abundance of the metal in mussel samples (Adams *et al.*,1998).

To generate a precise result with EDX, the surface of the scanned specimens should be totally flat. One of the techniques applied was embedding the specimens in resin, a process that is not only tedious, but also consumes a lot of time. However, the results of the fresh-fractured samples, despite their non-laminar surfaces were satisfactorily reliable as they point to the same conclusion as the results of resin-embedded specimens. This suggests that EDX could be applied to fresh samples for a rapid check for the selection of specimens for more detailed EM examinations. The only limitation of using 'fresh' unprocessed specimens is that they are prone to electrostatic charging, especially when scanning at very high magnifications.

6.5 Conclusions

Mn deposition onto the carapace particles from *L. depurator* shows a site-preference occurring predominantly at the broken edges or fractures, but not on flat undamaged surfaces. When the whole dorsal carapace was exposed to Mn solution, Mn was found to deposit more onto the internal side of the carapace, allowing the metal to penetrate deeper into the inner cuticular layers and at the same time coating the

entire surface turning it completely black. However, the epicuticle acts as a barrier to Mn penetration into the cuticle from the external side. EDX results also suggest a possible relationship between the distribution of Mn and Ca in the carapace particles.

Mn deposition also varies according to the tissues. The carapace particles harbours Mn deposits in the form of nodules, whereas particles or crystallite matrices deposits on the gill lamellae surfaces.

Table 6-1 Manganese concentrations µg Mn.g^{-1} dry tissue (mean ± SE,) in the carapace of *L. depurator* after exposure either internally or externally to 80ppm Mn solution.

Samples	Number of replicates	Mean Mn ± SE (µg Mn.g^{-1} dry tissue)
Internally exposed	5	15709±555.65
Externally exposed	4	551.71±103.00
Internally exposed (sea water)	3	7425.23±716.98
Externally exposed (sea water)	1	632.69
External 80ppm, internal 5-10ppm	4	6215.20±458.76

* From previous survey, Mn in the carapace of male and female crabs collected from the Clyde Sea measures 44.41±3.44 and 58.01±4.83µg.g^{-1} respectively.
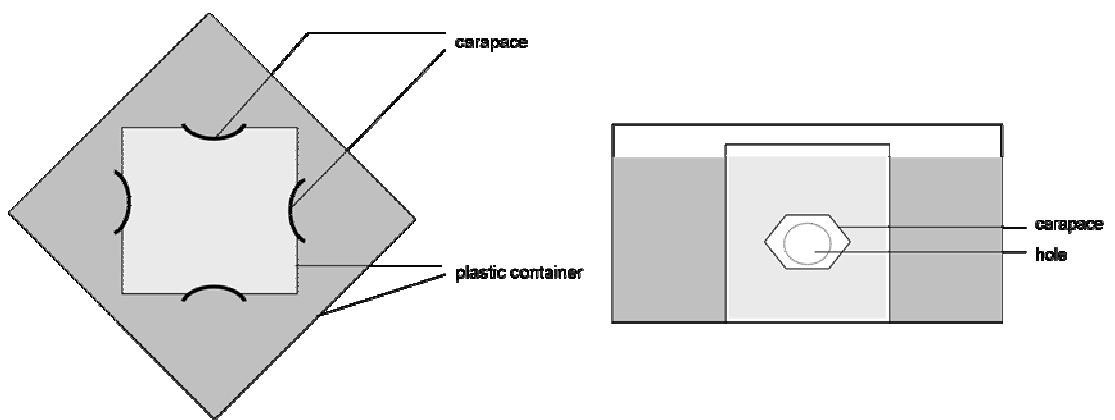
Fig. 6-1. Set up for the exposure of internal and external surfaces of crab dorsal carapace. For Mn analysis, only the part of carapace that was exposed through the holes was used. This part was obtained by cutting it along the circular mark made by traces of the glue that bordered the holes.
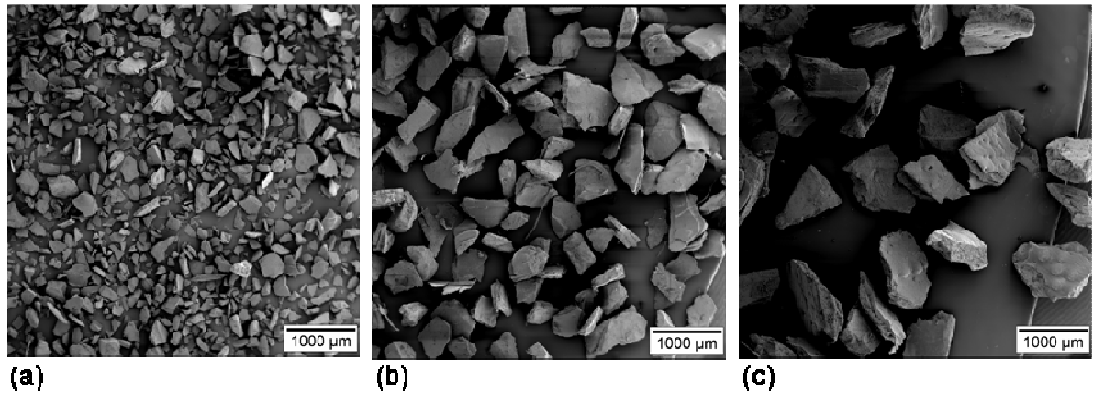
Fig. 6-2. SEM micrographs of *L. depurator* carapace particles with different ranges of diameters, (a) less than 300μm; (b) 300 μm - 850 μm; and (c) more than 850μm
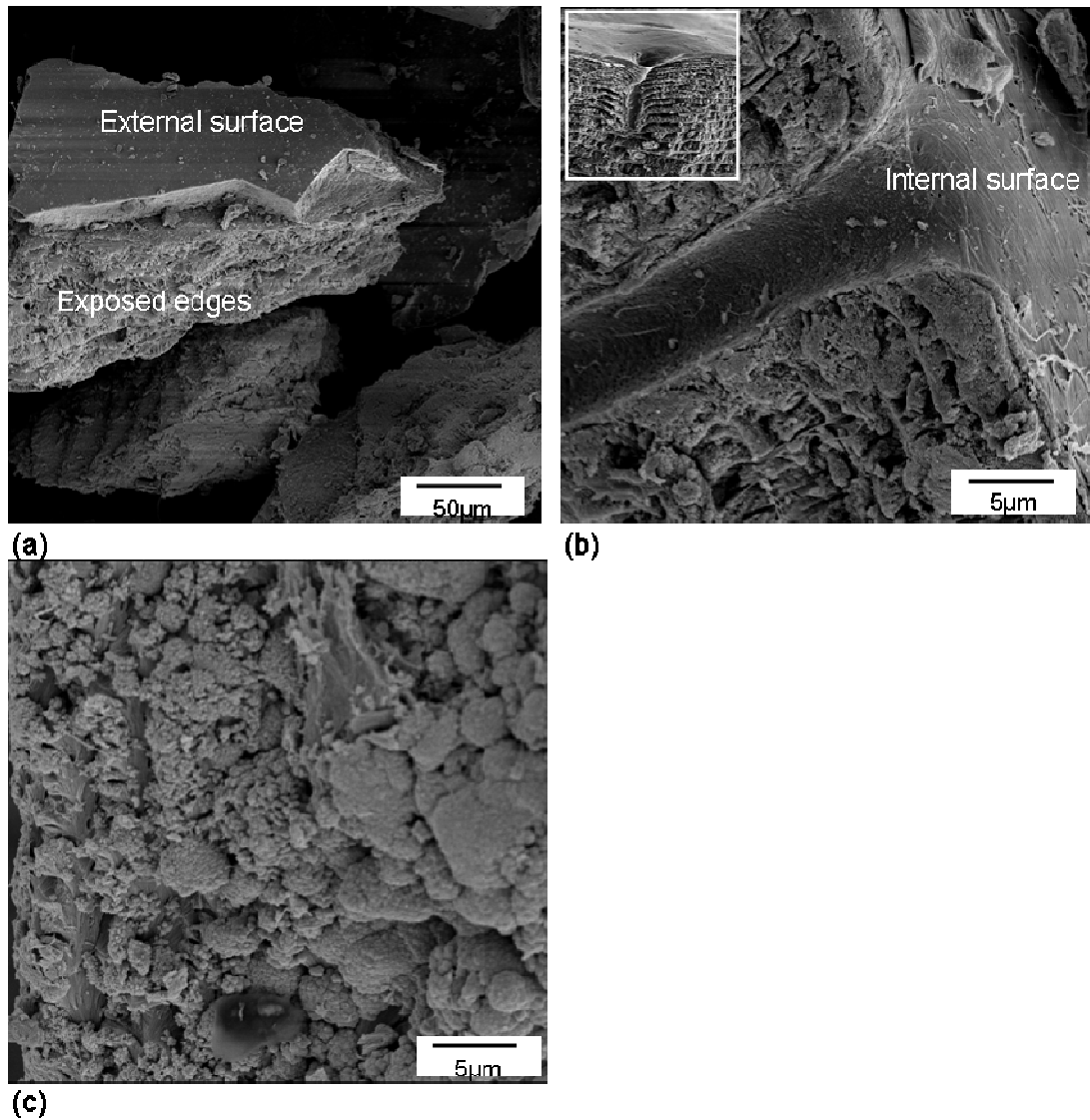
Fig. 6-3. SEM micrographs of *L. depurator* carapace particles biosorbed with Mn solution of a range of concentrations for 72h. (a) 40ppm: The external surface appears much cleaner than the 'messy' broken edges of the 'exposed' internal layers. (b) 160ppm: The image shows part of the internal surface, pore canal and the broken edges. Deposition of Mn nodules is more evident on the broken edges compared to the 'undamaged' surfaces. Image on the inset shows the cuticular layers observed in non-exposed material as in Fig. 5-7. (c) 160ppm: The edge of Fig. 6-2(b) observed at higher magnification confirming the heavy Mn deposition.
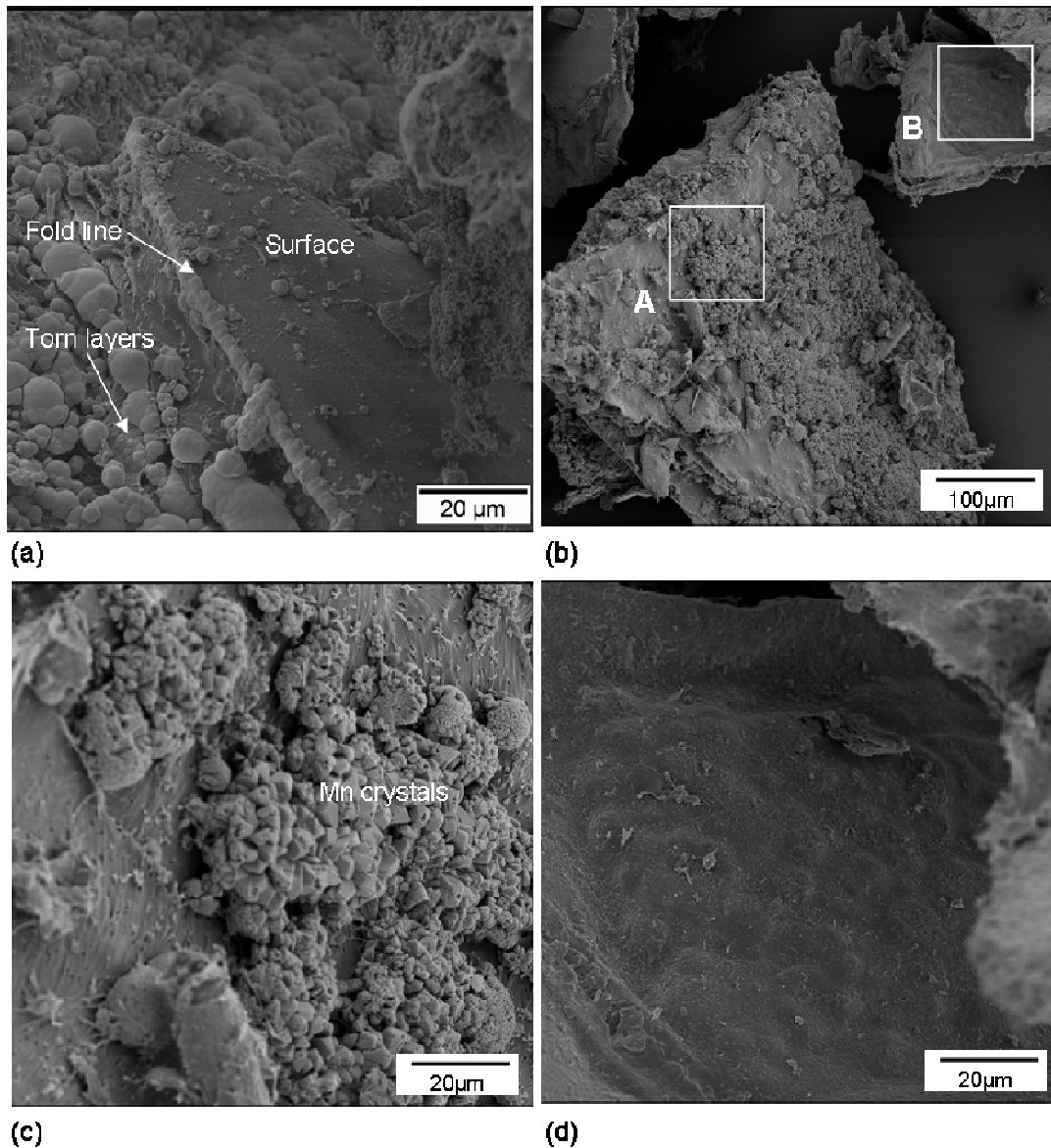
Fig. 6-4. SEM micrographs of *N. norvegicus* carapace particles exposed to Mn solution of a range of concentrations. (a) 160ppm: This image provides further evidence of site-specificity of Mn-deposition onto crustacean shell. The 'undamaged' surface appears clean of any crystals, but any fracture would allow the nodules to occupy the area and grow (as seen along the folding line). The remainder of the crystals grow on each 'exposed' lamella of the cuticular layers. (b) 20ppm : Note the mass of Mn nodules growing on particle A which is almost absent on particle B. Both surfaces (in square boxes) are shown at higher magnification in (c) and (d). (c) Box area 'A'. The numerous pores confirm that the lamella is internally located (exo- or endocuticular layers). (d) The 'undamaged' surface (B) shows no sign of nodule growth.
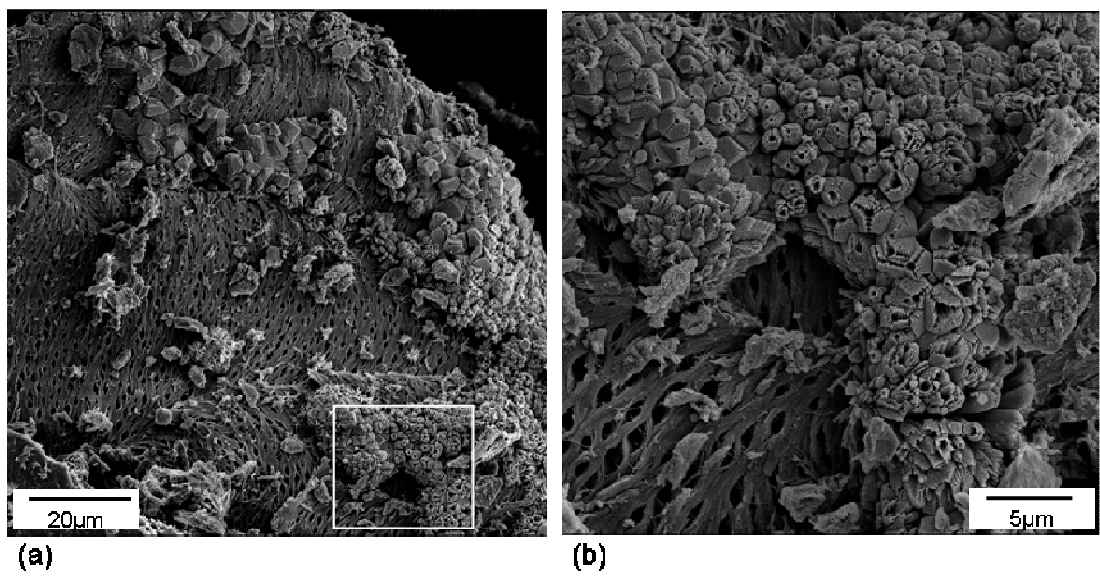
Fig. 6-5. SEM micrographs of *L. depurator* carapace (a) Mn nodules growing on the netted layers of crab carapace particles exposed to 40ppm for 72h. They are morphologically similar to the ones observed on the lobster particles in Fig. 6-3c. (b) The area in the box shown at higher magnification showing different growth phases of the Mn nodules.
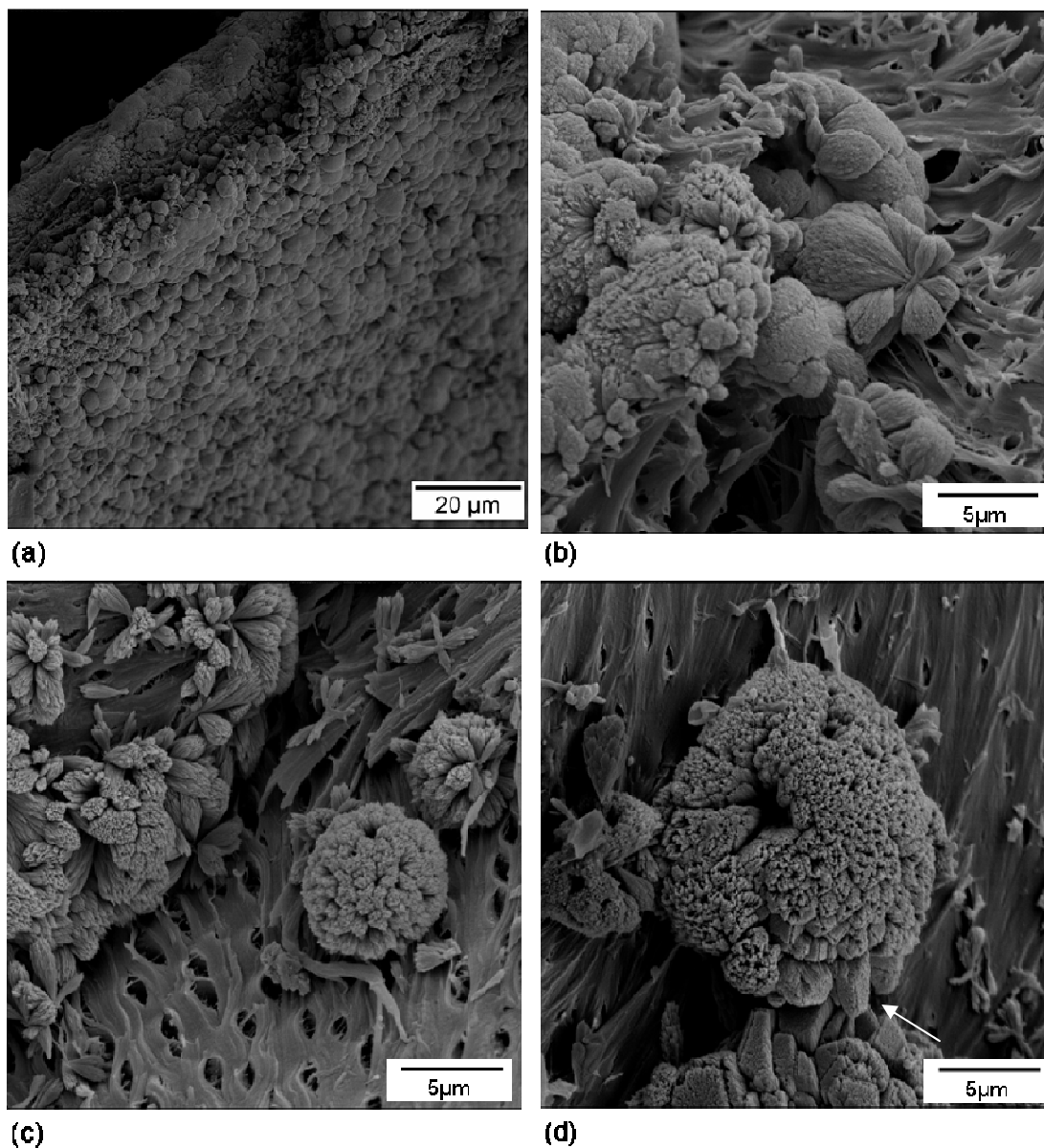
Fig. 6-6. SEM micrographs of Mn nodules on *N. norvegicus* carapace particles exposed to Mn solution of a range of concentrations for 72h. (a) 10ppm: Fully adsorbed/occupied carapace particles of a lobster showing more rounded nodules compared to the conical shape observed in other samples. (b) 160ppm: The round-shaped or rather cauliflower-like nodules at higher magnification. (c) 80ppm: The nodules in full bloom. (d) 20ppm: An image showing a combination of conical and floral-shaped nodules on a lobster particle. An arrow points to the conical-shaped nodules. (4000x)
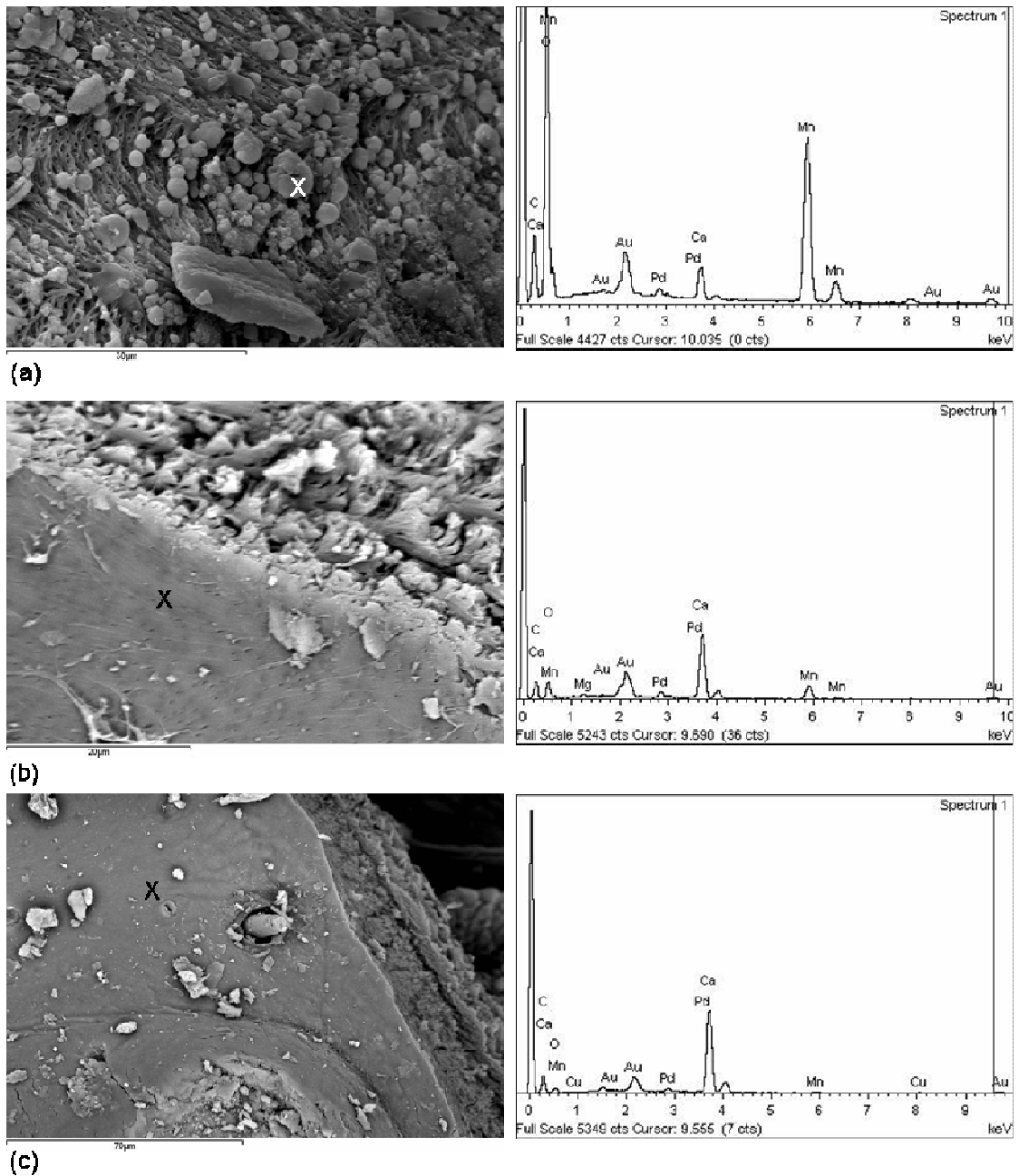
Fig. 6-7. SEM micrographs of nodules, the internal and external surfaces of *L. depurator* carapace particle exposed to 40ppm Mn solution for 72h. (a) Mn nodules found on an exposed lamella. An EDX spectrum of the nodule marked 'X' show high signals for Mn. (b) The internal surface and an EDX spectrum of the point marked X. A few strong Mn peaks were detected indicating the 'presence' of substantial amounts of the metal on the internal surface. (c) The external surface. EDX spectrum of the point marked X indicates a few signals of Mn weaker to ones observed on the internal surface shown (b).

Fig. 6-8. Dorsal carapaces of *L. depurator* exposed internally to 80ppm Mn solution for 72h. The internal surface appeared black after the exposure. The blackening was limited to the internal side and did not penetrate to the external surface.
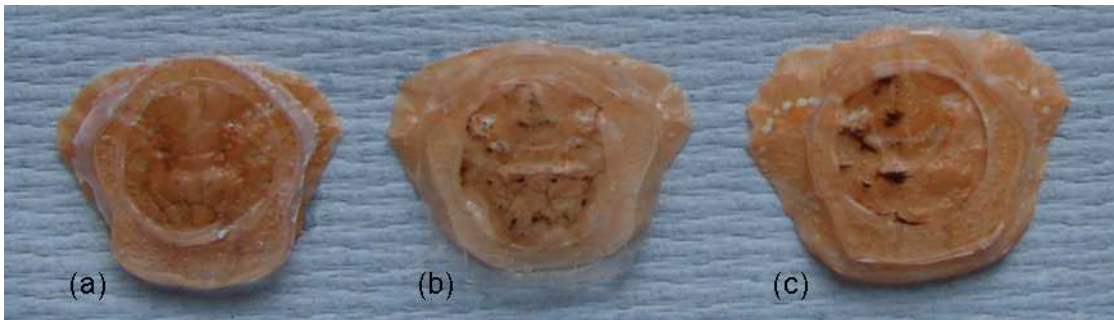
Fig. 6-9. External surfaces of dorsal carapaces of *L. depurator* exposed externally to 80ppm Mn solution for 72h. (a) non-abraded, showing no colour change or blackening, (b) fully abraded and (c) partially abraded on the left side only. Blackening of the carapaces occurred on abraded regions.
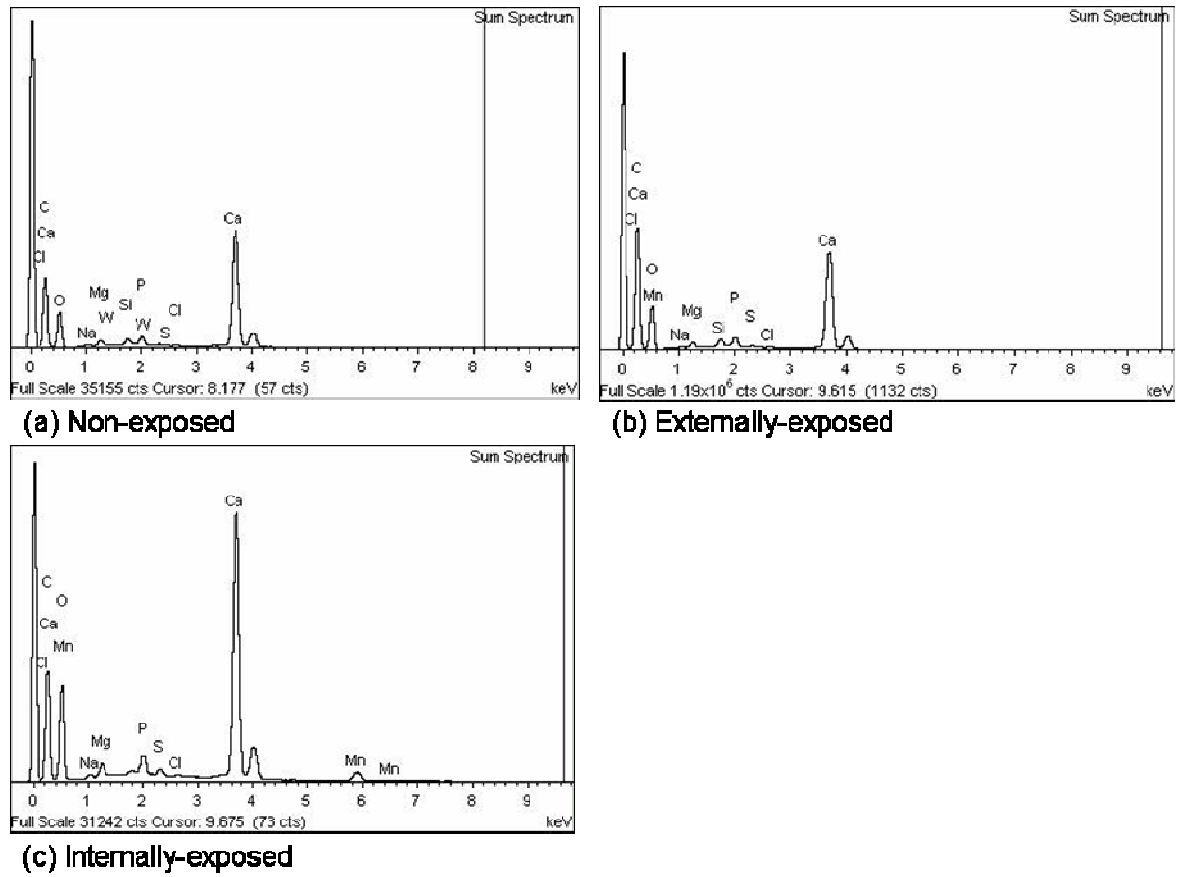
Fig. 6-10. EDX spectra of the carapaces of *L. depurator*, (a) non-exposed; (b) externally-exposed; and (c) internally-exposed to 80ppm Mn in distilled water
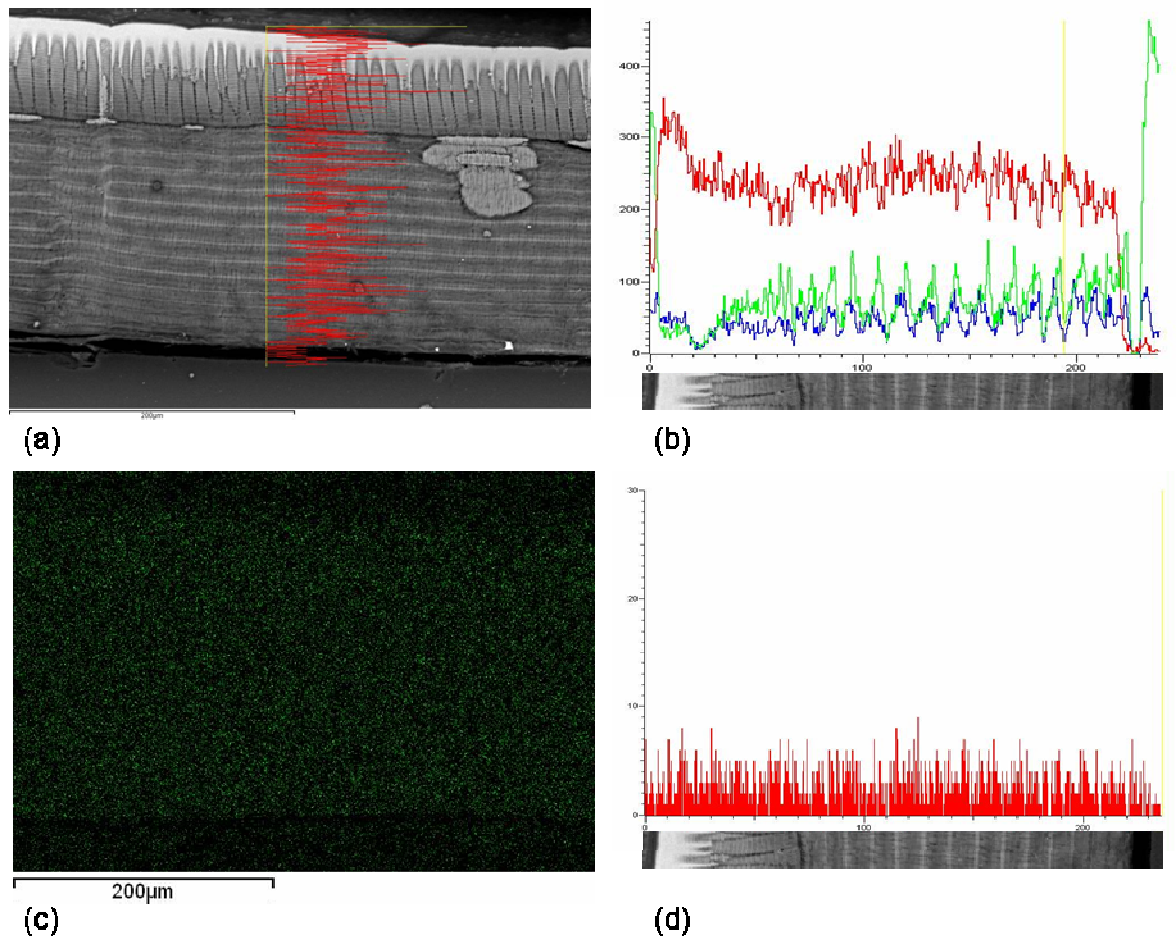
Fig. 6-11. A cross-section through a non-exposed *L. depurator* dorsal carapace from an immersion experiment and the results of elemental analyses. (a) SEM image and Mn profile. (b) Total counts of Ca (red), C (green) and O (blue) from a line scan along the thickness of the carapace. A section of the SEM underneath the graph refers to the area where the elementa line scan was made. (c) Mn map of the SEM showing no signal of Mn above background, (d) Mn counts from the same line scan as in (b).

Fig. 6-12. A cross-section through the dorsal carapace of *L. depurator* externally-exposed to 80ppm Mn solution from an immersion experiment and the results of elemental analyses. (a) SEM image and Mn profile. (b) Total counts of Ca (red), C (green) and O (blue) from a line scan along the thickness of the carapace (refer to the cut placed underneath the graph). (c) Mn map of the SEM showing traces of Mn on the external surface and more Mn packed in the pore canal. (d) Mn counts from the same line scan as in (b) showing double the counts compared to the control.

(a)

(b)

(c)

(d)
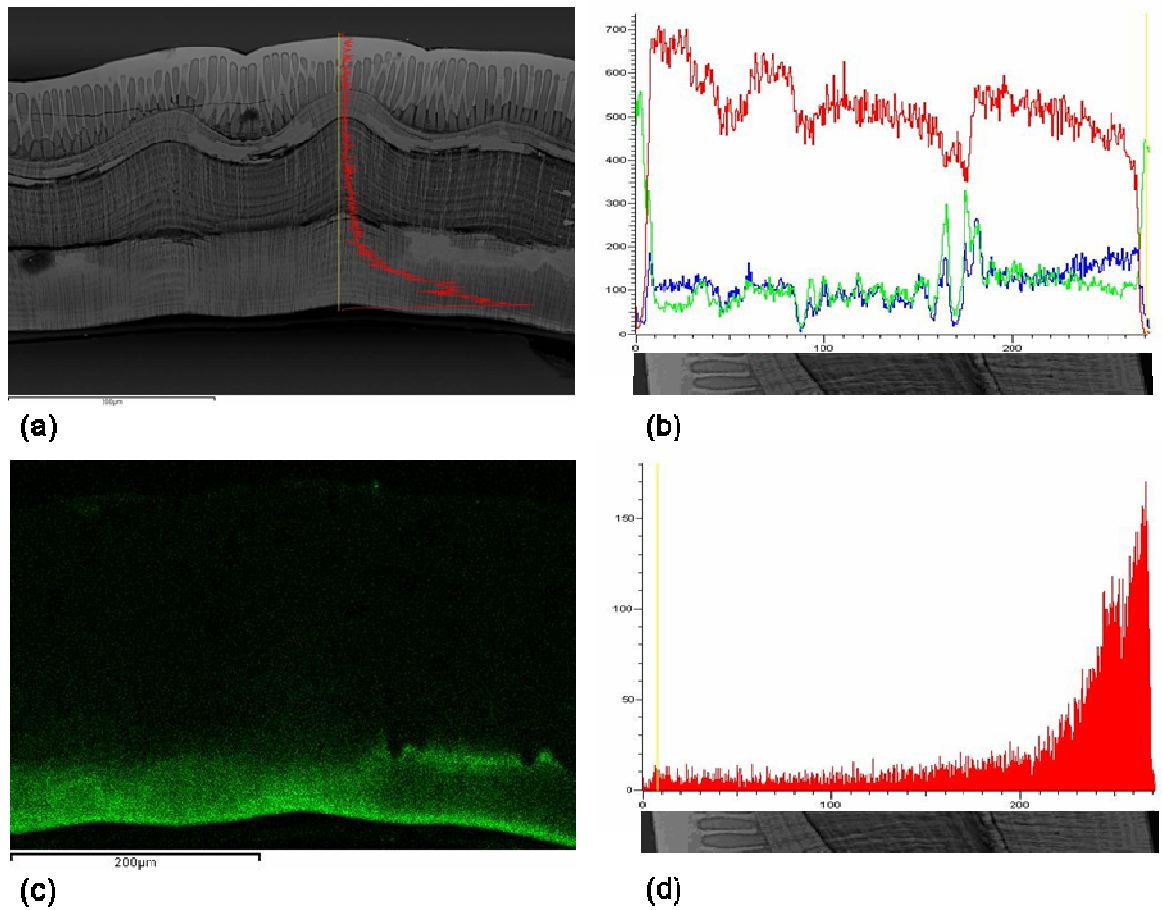
Fig. 6-13. A cross-section through the dorsal carapace of *L.* depurator internally-exposed to 80ppm Mn solution from an immersion experiment and the results of elemental analyses. (a) SEM image and Mn profile. (b) Total counts of Ca (red), C (green) and O (blue) from a line scan along the thickness of the carapace (refer to the cut placed underneath the graph). (c) Mn map of the SEM showing large signals of Mn on the internal surface. Mn could be observed to penetrate about 50μm into the inner layer on the internal side. (d) Mn counts from the same line scan as in (b) shows an increase from less than 20 counts over most of the profile from the external edge (left) to more than 150 counts at the internal surface (right).
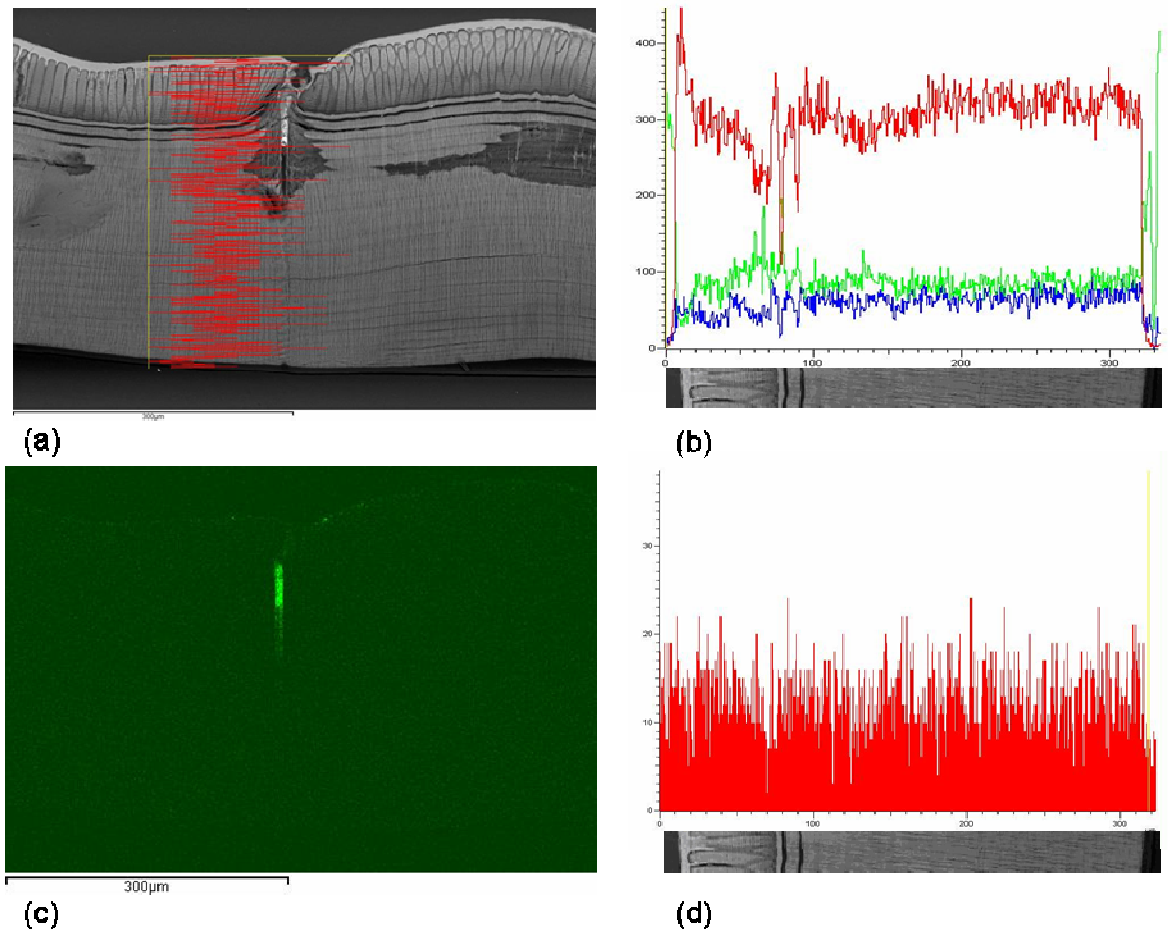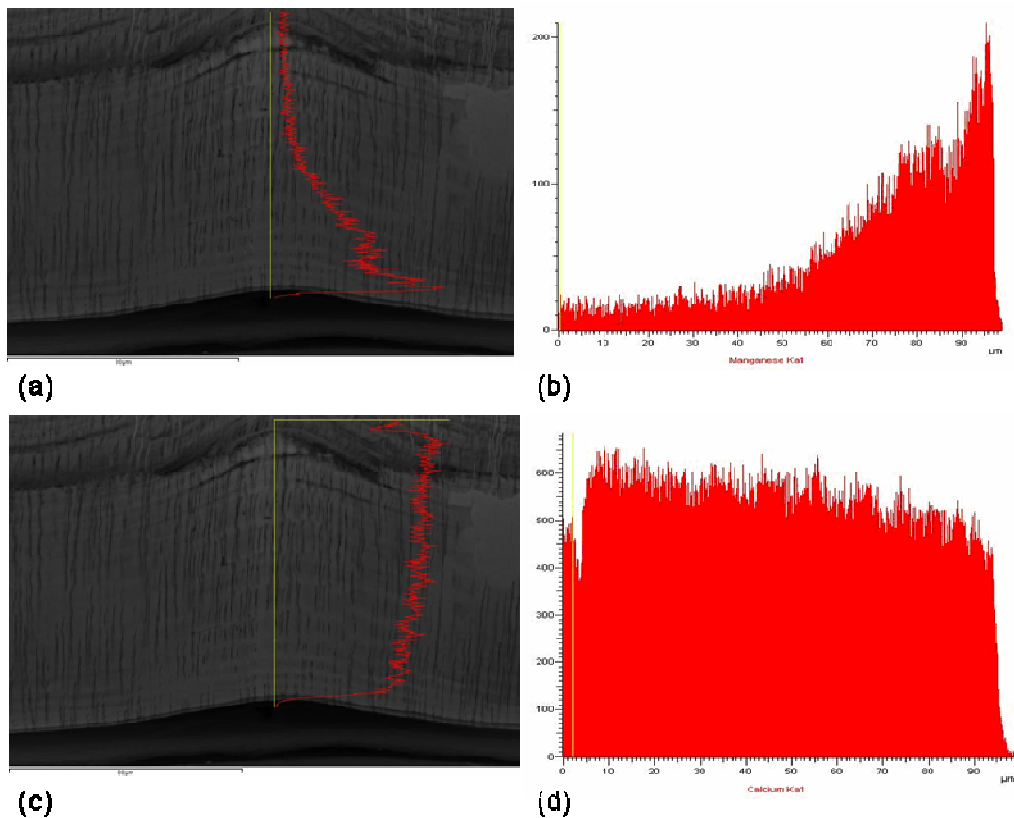
Fig. 6-14. A cross-section through the dorsal carapace of *L. depurator* internally-exposed to 80ppm Mn solution at higher magnification. (a) SEM image and Mn profile, (b) total counts of Mn with the highest count of 210 on the internal surface, (c) SEM image with Ca profile, (d) total count of Ca showing a decrease from about 650 to around 450 on the internal surface resembling a reverse trend compared to Mn in (b).
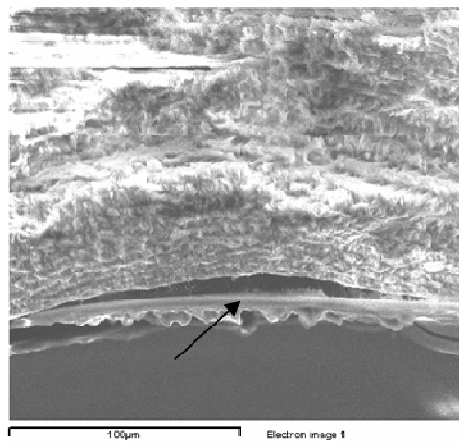
(a)
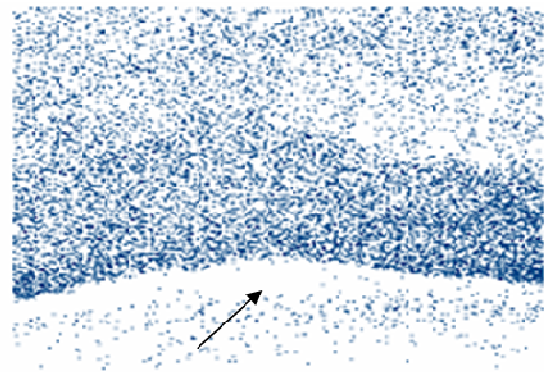
(b)

Fig. 6-15. An SEM image and Mn map of a fracture made on a freeze-dried carapace of *L. depurator* previously internally exposed to 80ppm Mn solution. The dense blue area about 50-60µm on the internal side represents the area where Mn is deposited. Interestingly, no significant signal was detected on the partly separated membranous layer shown by the arrows.
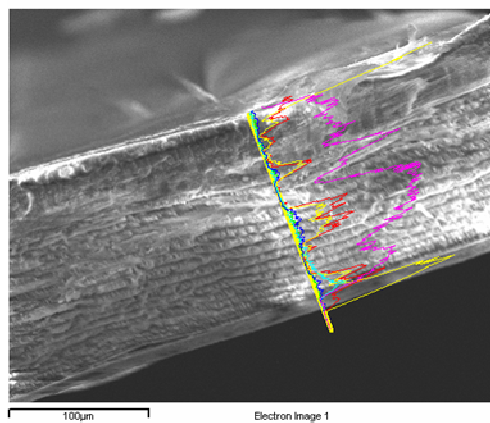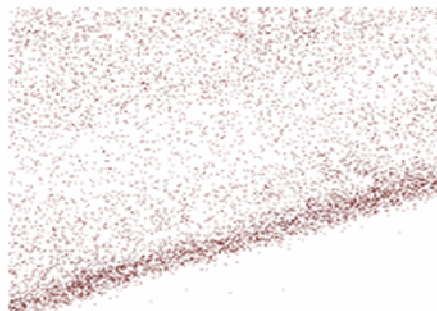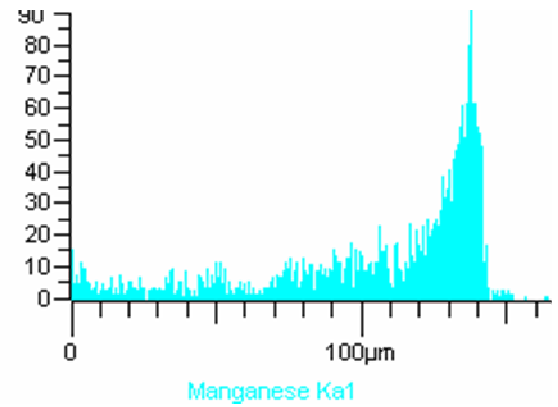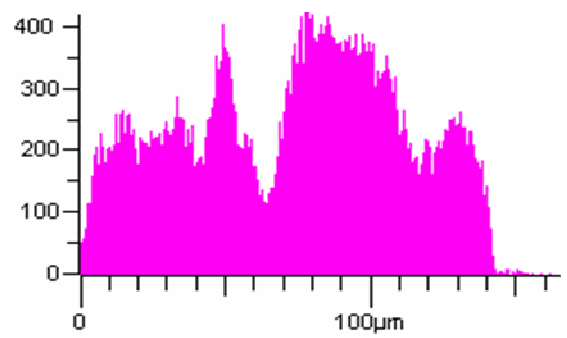
Fig. 6-16. Freshly fractured carapace of *L. depurator* after being internally exposed to 80ppm Mn solution for 72h. (a) The SEM image. (b) Significant Mn signals observed on the internal surface as dense brown region. (c) Mn and (d) calcium profiles obtained from a line scan shown in (a).
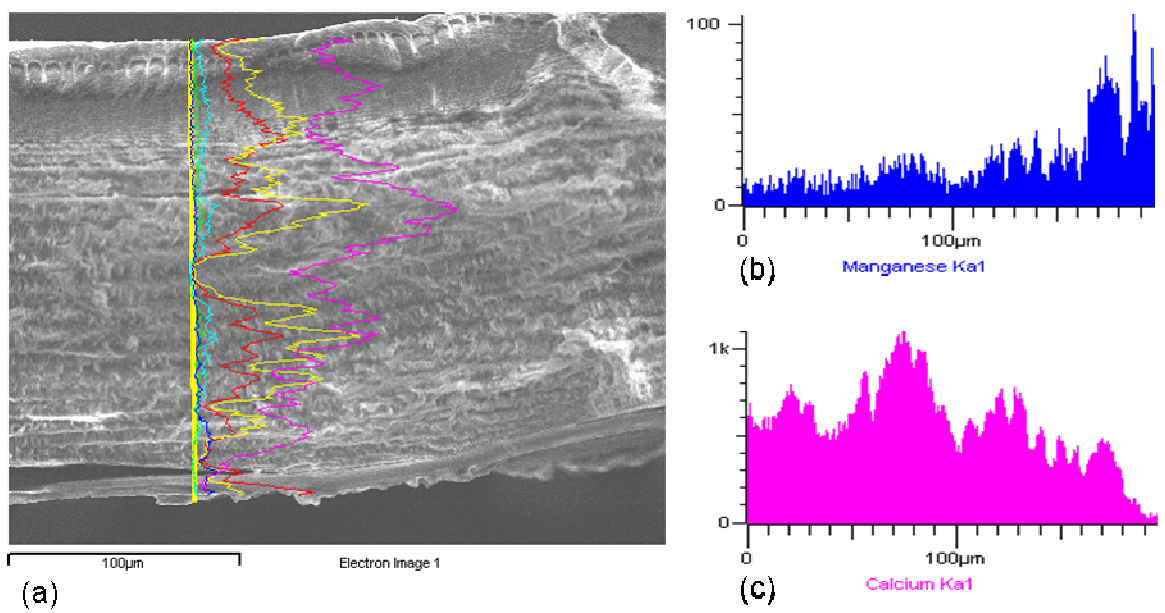
Fig. 6-17. An SEM of freshly fractured carapace of *L. depurator* showing more evidence of Mn deposition onto the internal surface, and a coinciding inverse relationship between Mn and Ca counts through the thickness of the carapace.
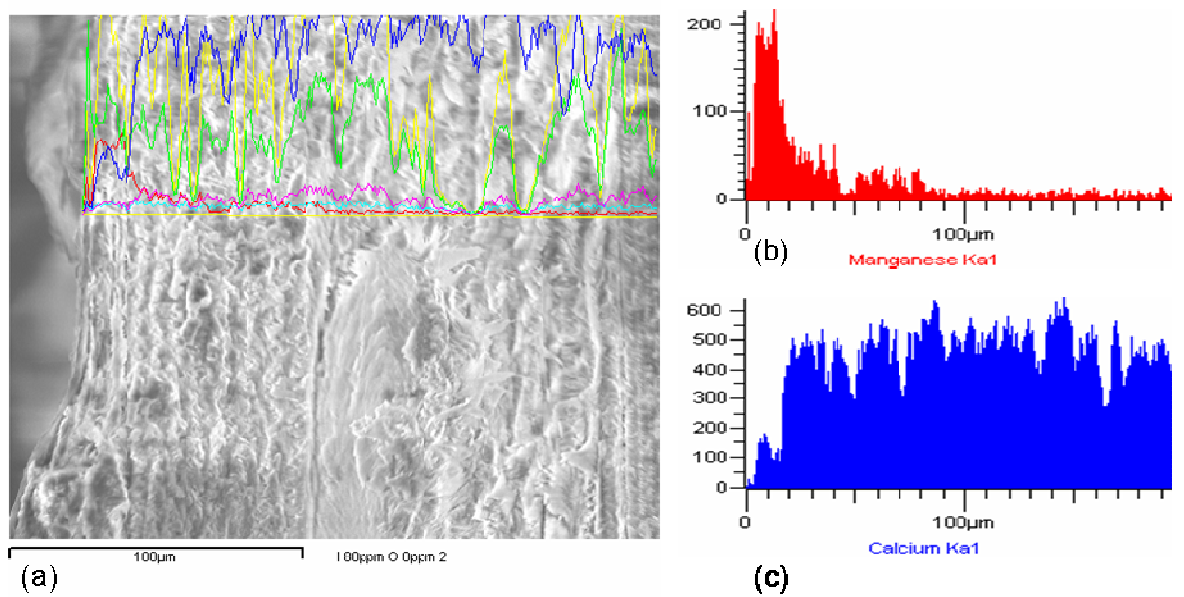
Fig. 6-18. An SEM image through the internal surface (on the left side on the image) and the endocuticle layers of a freshly fractured carapace of *L. depurator*. Note the high Mn counts about 20μm deep on the internal side (b) and the co-inciding low Ca counts in the same region (c). Mn gradually decreases until it reaches background count at about 80μm deep with a count of less than 20 towards the external surface.
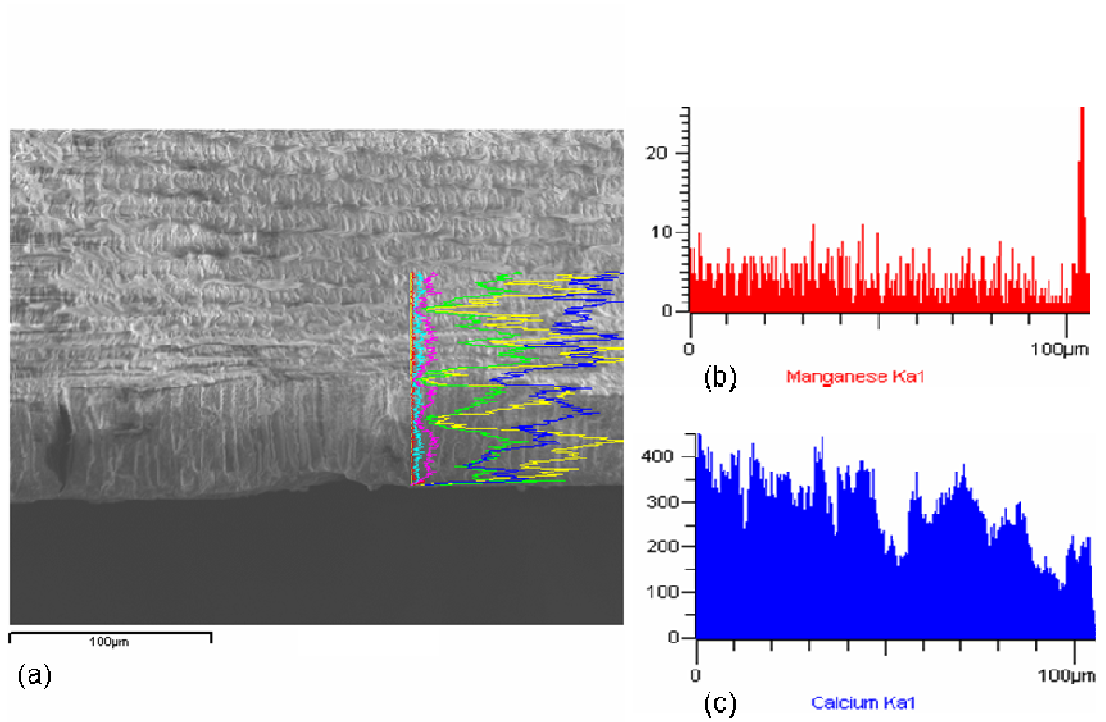
Fig. 6-19. An SEM image showing the external surface, exo- and endocuticle layers of the carapace of *L. depurator* externally-exposed to 80ppm Mn solution. A line scan of Mn shows that some Mn was deposited onto the external surface where the count measured 25, but the deposition is limited only to the surface. The remaining layers only show background count of less than 10 as shown in any other control carapace. Ca decreases towards the external surface.
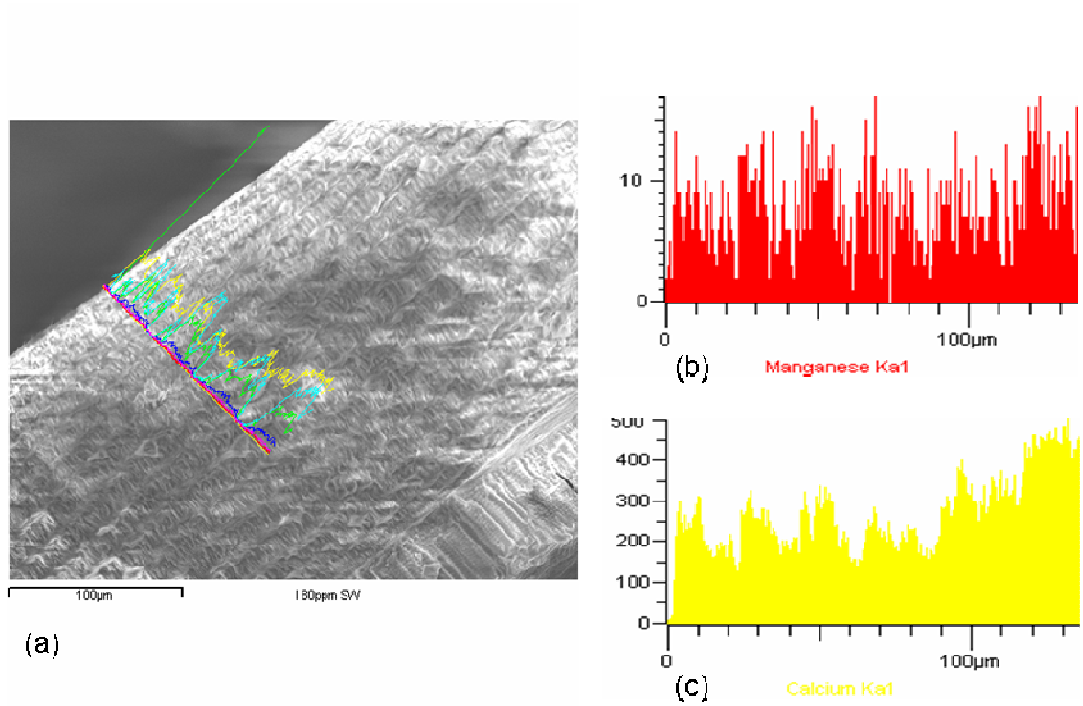
Fig. 6-20. An SEM of a fractured sample of the carapace of *L. depurator* internally-exposed to 80ppm Mn sea water. No significant signal for Mn (less than 15 throughout) was detected even on the internal surface of the carapace, a result that is in agreement with Mn measurements made on AAS. The increment of Mn might be too small to be detected by this method. Ca counts shows the normal composition of the layers as observed in other samples.
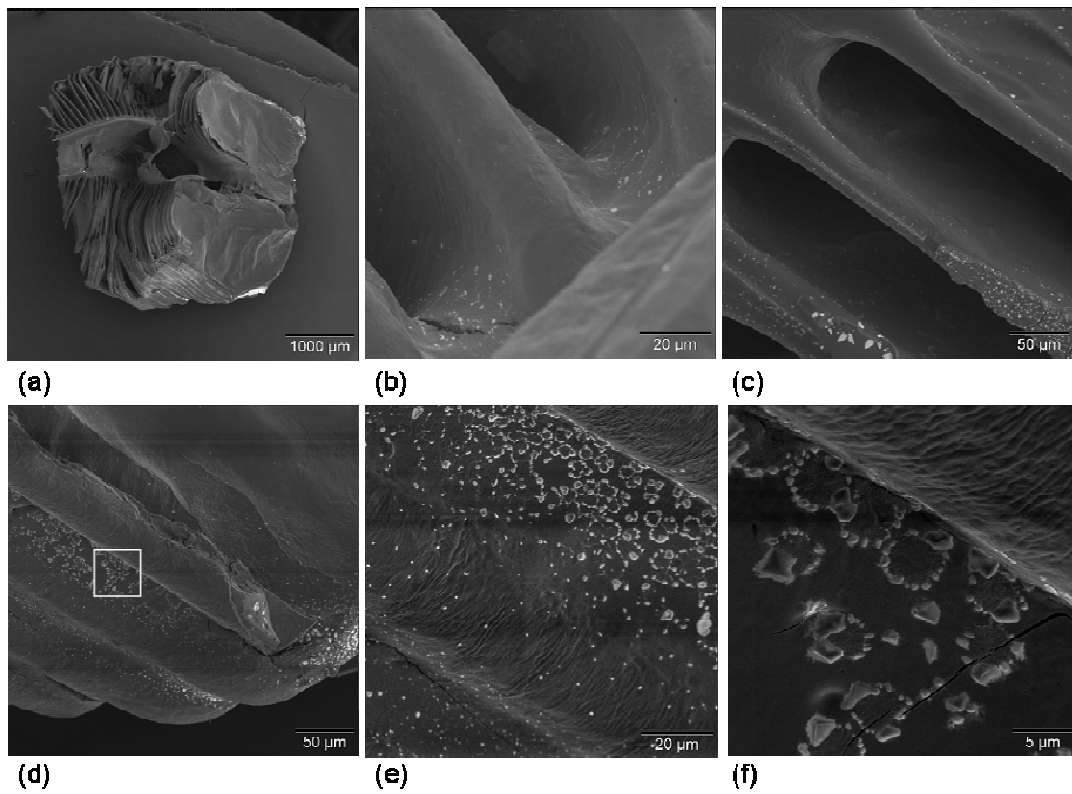
Fig. 6-21. Four SEM micrographs of the gills of *L. depurator* exposed to 80ppm Mn sea water for 21d. The lamella, although appearing quite clean, (a) harbour some particles which were observed to deposit especially on the edges (c, d). (e) and (f) show the deposits on the edges at higher magnification revealing a uniform floral pattern.

(a)   (b)
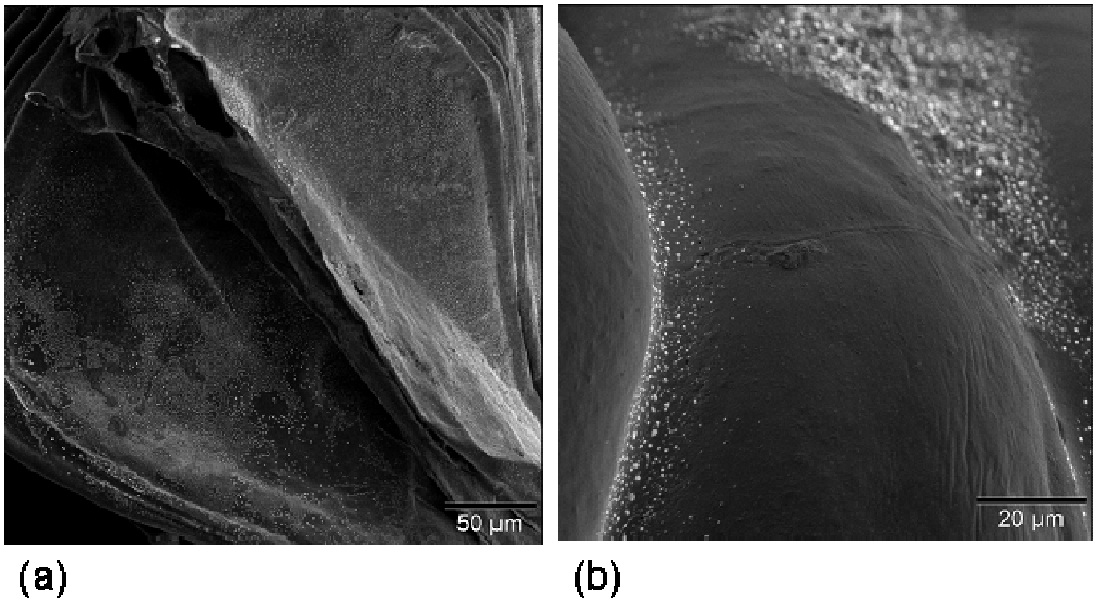
Fig. 6-22. Lamella of a gill from *L. depurator* exposed to 80ppm Mn sea water for 72d. The crab survived until sacrificed on day 72. (a) Note the particles deposited on the lamellar surface. (b) More deposits were also found on the edges but with no uniform pattern as seen in Fig. 6-20(f).
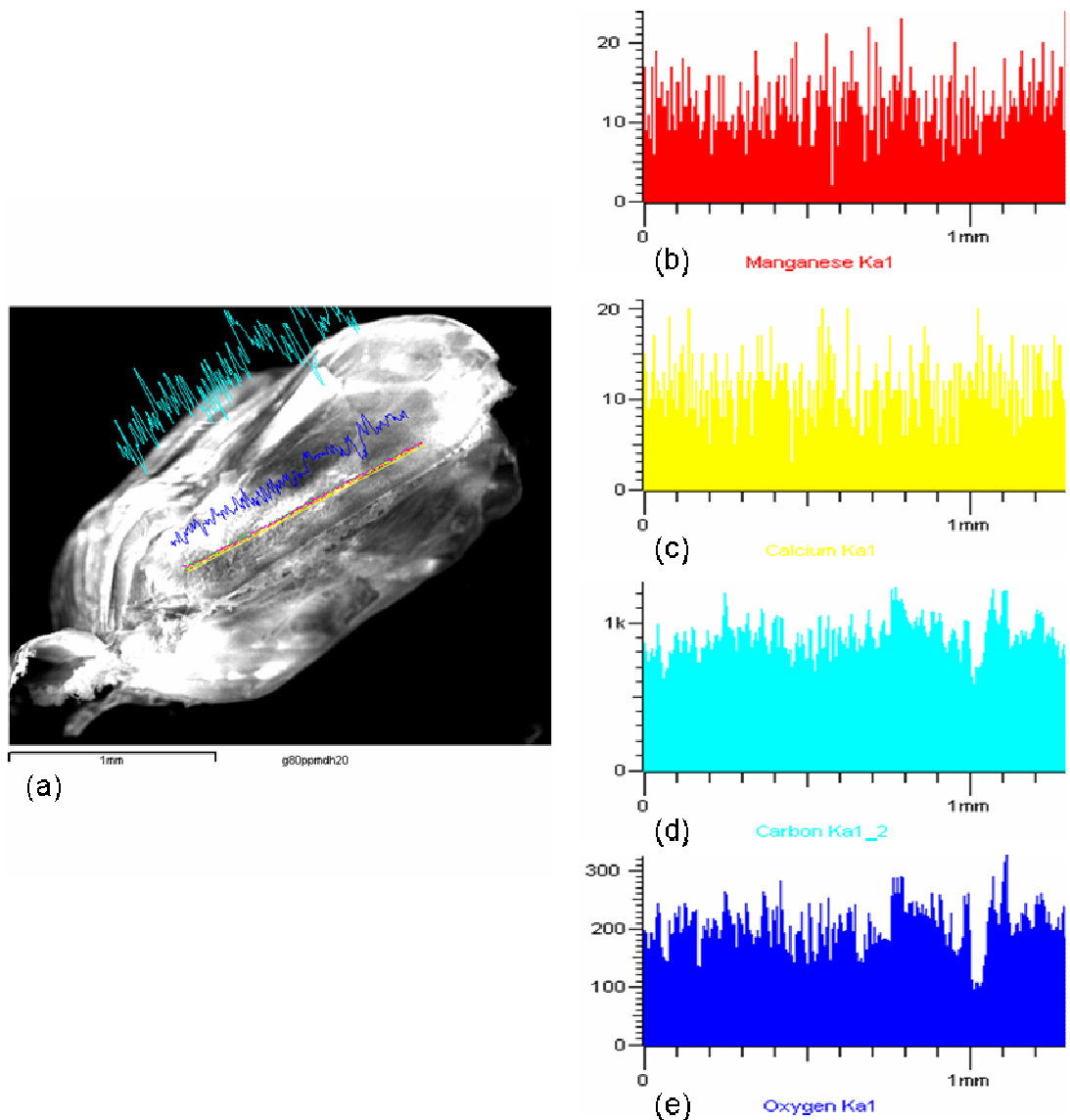
Fig. 6-23. SEM image and elements profile of gills of *L. depurator* exposed to 80ppm Mn sea water for 21d. (a) Mn counts fluctuates between 10-20. C is the element with the highest count followed proportionately by O, whereas Ca was lowest. The profiles of C, O and Ca (c-e) show the different composition of this exoskeletal tissue (C>O>Ca) compared to the carapace (Ca> C, O).
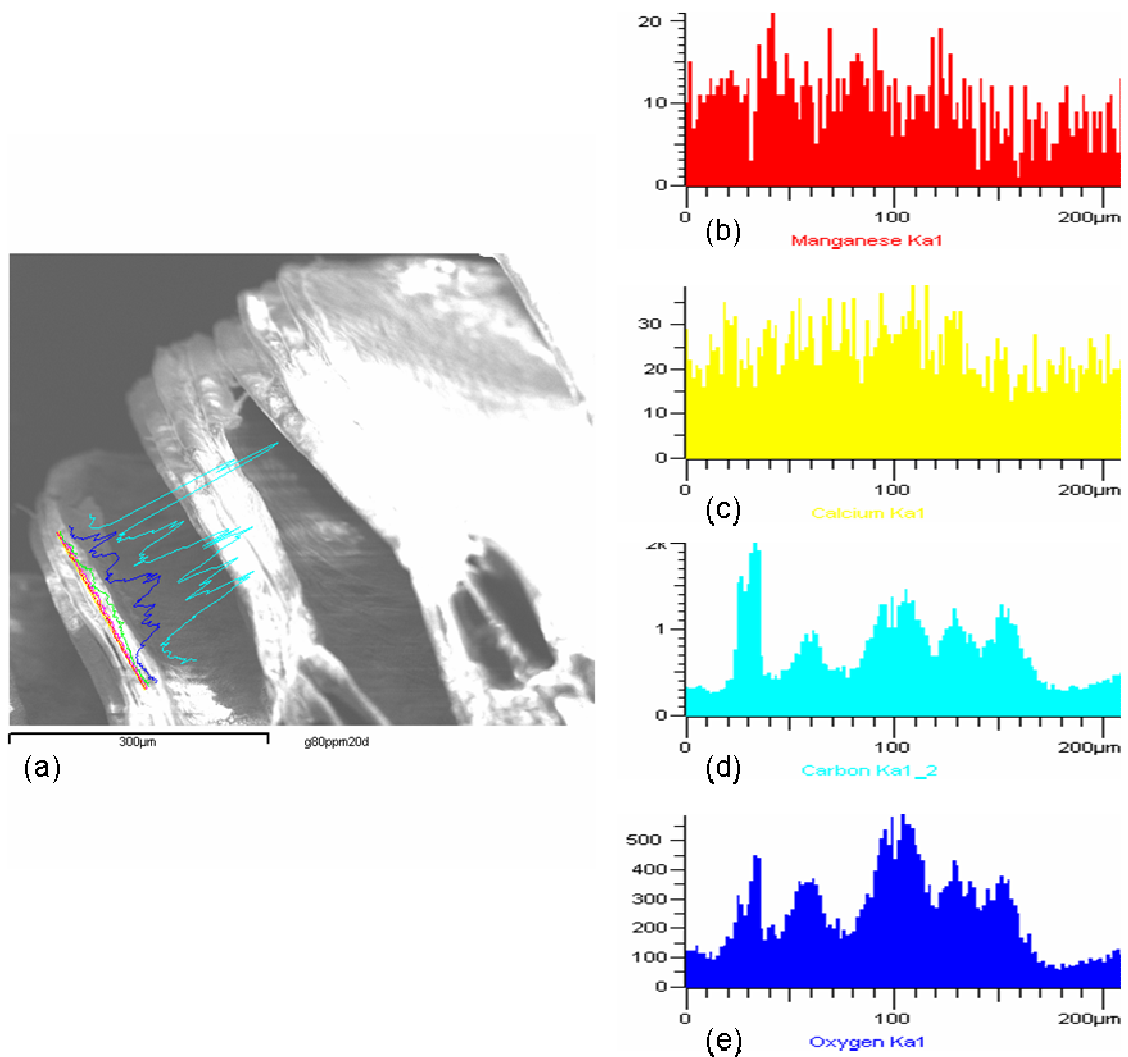
Fig. 6-24. SEM image and elements profile of gills of *L. depurator* exposed to 80ppm Mn sea water for 21d at higher magnification. A surface assumed to be the flattest was selected for a line scan. (b) Mn showed no peak fluctuating between 10-20. (c-e) C, O and Ca counts were similar to the previous figure, with C and O revealing identical trends.

213
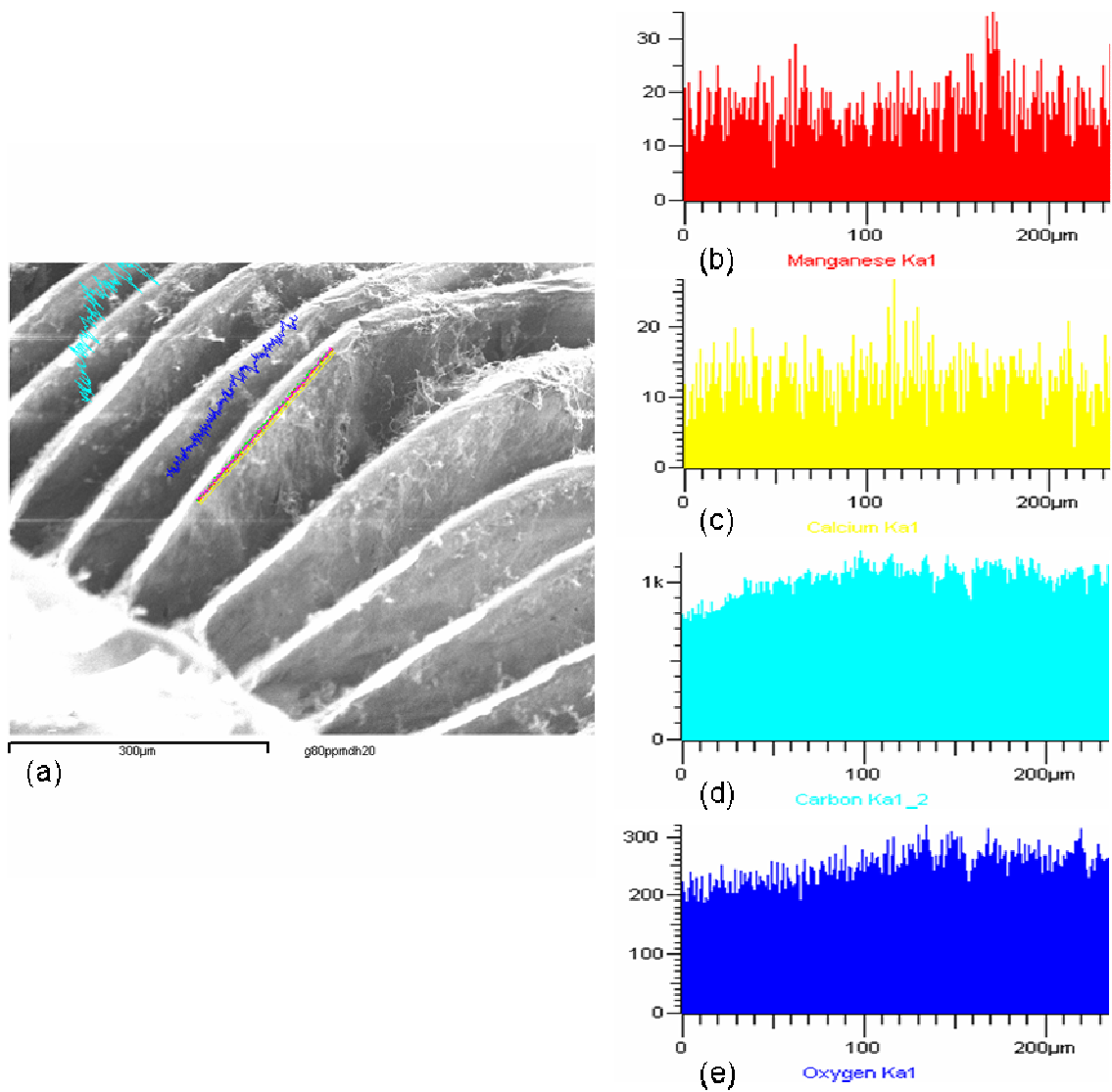
Fig. 6-25. SEM image and elements profile of a gill of *L. depurator* exposed to 80ppm Mn sea water for 21d shown at higher magnification. (a) Mn showed a possible peak exceeding 30 counts that corresponds to the position of the particles on the lamella. (c-e) C, O and Ca counts show similar trend to the previous figure (C>O>Ca).

7 General Discussion

This project comprised two major parts. The possibility of utilizing living crabs in a biomonitoring context was investigated and validated by sampling them in their natural environments (Chapter 2) and through a series of laboratory exposure trials (Chapter 3). Apart from using live animals, the possibility of using their exoskeletons as sources of materials in biosorption systems for the remediation of polluted waters was also evaluated (Chapter 4). Biological explanations rarely accompany such studies, and for this reason, in Chapters 5 and 6 the biosorbed particles derived from the crab exoskeleton were subjected to scanning electron microscopy and elemental analysis in an attempt to offer some insights into the process of deposition. The aim of these analyses was to fill in some of the gaps in our biological knowledge, some of which have been left unanswered since the 1960s. Each approach has provided useful information, but some further conclusions can be drawn by considering the relationships between them, particularly with reference to the situations in which crabs such as *L. depurator* can be effective biomonitor species, and to the routes of entry of Mn into the exoskeleton.

Crabs as biomonitor species for Mn

It has been established that Mn concentrations in all the tissues of live crabs collected from Loch Fyne and the Clyde Sea area reflect the difference in Mn concentrations to which they were exposed in those natural settings (Chapter 2). The results serve as the first indication of the biomonitoring ability of this species for Mn in the two areas, and probably also wherever it is found.

As a biomonitor, *L. depurator* which spends most its time resting, with its body raised on the sediment on the ocean floor, differs from the Norway lobster *N. norvegicus* since it reflects Mn concentration in the bottom water, whereas the tissues of the latter, which often burrows within the sediment, reflect more of the sediment and pore water Mn concentrations. Mn found in the tissues of *L. depurator* represents the bioavailable concentration at the interface between the sediment and

the bottom water i.e. a place where cycling of Mn occurs and is believed to have the highest concentrations of the metal within the water column.

The laboratory exposure trials (Chapter 3) also demonstrated that *L. depurator* accumulates Mn from sea water, but in addition they confirmed the results of the field surveys (Chapter 2) in showing that the differences in the Mn concentrations of different tissues of crabs from the two habitats were consistent. Thus in crabs from both the Clyde Sea area and Loch Fyne the concentrations were greatest in the carapace and the gills, followed by the hepatopancreas and other tissues, and with muscle having the lowest values. These differences also varied with the sex of the crabs.

Previously, the exoskeleton of *N. norvegicus* was reported to accumulate very high concentrations of Mn that apparently reached saturation, indicating simple saturation kinetics of available binding sites on the exterior of the exoskeleton (Baden *et al.*,1995). However, later investigations of the same species (Baden and Neil, 2003) and the present study on the crab *L. depurator* present a different picture showing a continuous uptake with no saturation in either case. The Norway lobster antennule and the crab leg exoskeleton both continued to accumulate Mn when exposure to 10ppm and 20ppm Mn in sea water for up to 21d, resulting in the case of the crab in a concentration of Mn of more than 700 $\mu g.g^{-1}$ dry tissue (Fig. 3-4).

The uptake into the leg exoskeleton of *L. depurator* was time- and dose-dependent, without any significant depuration occurring when returned to undosed water, which are two good criteria for a sentinel organism. The time and dose relationship with Mn uptake concurs with Baden and Neil (2003) on Mn accumulation in the *N. norvegicus* antennule. The linear uptake of Mn into the leg exoskeleton which agrees with findings on other exoskeletal parts of other decapod species including the antennule of *N. norvegicus* (Baden and Neil, 2003) and the carapace pieces of the lobster *Homarus gammarus* (formerly known as *H. vulgaris*) (Bryan and Ward, 1965), is less affected by the fluctuations of Mn in the water. On the other hand the gills and the soft tissues such as the hepatopancreas were found to both accumulate and depurate Mn, and thus reflect more the current ambient exposure. The ability to depurate Mn in these soft tissues might be due to the form of Mn

deposits as revealed by an SEM examination. Packed Mn-nodules are tightly bound onto the surface of the carapace (Fig. 6-4), whereas on the gill lamellae the deposits appeared more loosely collected (Fig. 6-22).

Those points discussed above make *L. depurator* a useful biomonitor as it provides a potential record of the timing and extent of a recent exposure event since the hard exoskeleton, including the legs, preserved a record of the exposures, while the current ambient exposure can be deduced from Mn concentrations in the soft tissues particularly the gills and the hepatopancreas. In the Norway lobster *N. norvegicus*, increased uptake of Mn was positively associated with hypoxia (Baden and Eriksson, 1998) therefore suggesting the idea that use of the concentrations of Mn in the tissues of the animal could be extended to indirectly indicate hypoxic events.

Having shown all the characteristics above, *L. depurator* might possibly be used to indicate hypoxic events in the marine environment. The work by Draxler *et al.* (2005) in areas prone to hypoxia in the USA in fact exploited this idea and deployed it in a real field situation in Long Island Sound using the lobster *H. americanus*. The concentration of Mn in the gills of chemically naïve lobsters (obtained from uncontaminated sites) kept in cages in the selected areas prone to hypoxia increased with hypoxic events, leading them to propose a series of indices of hypoxic conditions based on the Mn concentrations in the gills as follows: more than $30\mu g.g^{-1}$ – habitats is likely experiencing some reduced oxygen levels; more than $100\mu g.g^{-1}$ – conditions with potential for lobster mortality; and more than $300\mu g.g^{-1}$ – most severe habitat conditions with strong potential for hypoxia stress. This attempt by Draxler *et al.* (2005) has elevated the bioindicator approach from merely a potential one to one that has actually been used in a real contamination study, therefore justifying the potential of *L. depurator* to be employed in a similar way.

In most other cases (Baden *et al.*, 1995; Eriksson and Baden, 1998; Eriksson, 2000; Baden and Neil, 2003; Hernroth *et al.*, 2004), as in the one described above (Draxler *et al.*, 2005), the study of Mn uptake in animals in the field has dealt with the exposure to the metal accompanied by conditions of hypoxia, particularly as a result of eutrophication. Eutrophication, coupled with increasing temperature especially

during the summer time, makes the conditions favourable for phytoplankton or algae to grow and bloom. The crash of the bloom, which normally takes place towards the end of summer months, leads to an increase in the biological oxygen demand (BOD) in the bottom water, and thus results in hypoxia. Loch Fyne, even though speculated to experience eutrophication that might in turn leads to hypoxia, has never been reported to experience such an incident. However, elevated level of Mn is evident due to the geology of the area (Overnell *et al.*, 2002; Bartlett *et al.*, 2007). Therefore, in contrast to other studies, the choice of Loch Fyne has provided the chance to investigate Mn uptake into crustaceans from a naturally elevated source of Mn, in the absence of hypoxia. Moreover, in this study, the crabs were collected during times that would not coincide with the possible eutrophication period, were one to occur. Thus the high concentrations of Mn in the soft tissues of *L. depurator* collected from the Loch Fyne indicate the currently higher ambient exposure in the area compared to the Clyde Sea area, whereas the high concentration in the dorsal carapace reflect either the cumulative effects of current, or past levels of Mn in the bottom water.

Route of Mn uptake onto the exoskeleton

The finding that following both natural and artificial exposures the greatest values of Mn are found in the external exoskeletal structures of the crab (carapace and gills) is consistent with reports from other crustaceans (Brouwer *et* al., 1995; Baden *et al.*, 1995; Baden *et al.*, 1999). The fact that these structures are directly in contact with the contaminant has led to the generally accepted assumption, that deposition directly from the sea water is a major route of uptake. However, the SEM-EDX analyses performed in this study on exoskeletal materials following both uptake experiments on intact carapaces (Chapter 6) and following biosorption runs with carapace particles (Chapter 4) have provided evidence for an internal route of deposition.

The simple exposure experiments on dead shell (intact and abraded) clearly show that the epicuticle, most probably the waxy layers, is a barrier to Mn penetration into the cuticle. The EDX analyses show that a high rate of Mn uptake takes place from the inside, with the membranous layer providing no effective barrier (Section

6.3.2.1). This concurs partly with Bryan and Ward (1965) that membranous layers does not take up Mn, but that in a live lobster *H. gammarus* the metal could absorb into the shell from the stomach, indicating that the membranous layer is permeable to the penetration of Mn. The EDX data indicate that earlier assumptions that Mn was simply adsorbed onto the outer surface are not entirely correct. Exposure of a dorsal carapace internally to 80ppm Mn in sea water resulted in an increase of Mn concentration in the carapace by approximately 130-fold, whereas an external exposure caused only about an 11 fold increase in the concentration. Increments of Mn were detected by AAS when the external surface of the carapace was exposed , but due to the relative insensitivity of the EDX techniques, the Mn distribution could not be mapped for this level, and also for levels of uptake occurring at natural, or even in controlled exposures. This technique confirms the higher uptake rate onto and from the internal surface. However, more sensitive methods are needed to confirm this mode of uptake from more realistic naturally-occurring concentrations.

Bryan and Ward (1965) also exposed both surfaces of pieces of lobster carapace (1-2cm^2) in sea water containing ^{54}Mn and measured the uptake *in vitro*. They speculated that adsorption phenomena might be involved resulting in the linear uptake of Mn in the carapace, but left the question unanswered. The present study confirms their speculation in that Mn-rich nodules were found to adsorb onto carapace particles (Chapter 6). However, it also extends their finding by demonstrating that Mn adsorption does not actually occur at the same rate from both sides of the carapace. Rather, Mn adsorption occurs mostly from the internal side, increasing the concentration of Mn to a 270-fold higher value than the reference, whereas exposure to the external surface resulted in only about a 10-fold increase.

Eriksson and Baden (1998) found no correlation between the contemporary environmental Mn(II) concentration of ambient sea water and that of the amount of Mn found in field-caught intermoult lobsters *N. norvegicus*, and proposed that the amount of Mn found in the exoskeleton of intermoult individual primarily depends on the Mn concentration to which the animals are exposed during the calcification process at postmoult, rather than the current ambient Mn concentrations. Both the epicuticle and the exocuticle are deposited pre-exuvially and fully complete by the

time the crab moults. It is assumed that at the postmoult stages (A-C$_3$), the carapace of the crab should possess a complete epicuticle. A question arises whether the epicuticle is capable of serving the protective mechanism at this early stage before calcification. An exposure on newly moulted *N. norvegicus* to 10ppm Mn sea water by Eriksson (reported in Baden and Eriksson (2006)) resulted in the Mn concentration in the exoskeleton of approximately 2500 µg.g^{-1} dry weight compared to 44 µg.g^{-1} dry weight in the control, and hence indicate no barrier functionality of the complete but newly developed epicuticle.

Apart from the explanations offered by Baden and Eriksson (2006), this study proposes another possible route for Mn uptake into the exoskeleton. If internal uptake seen in the isolated carapace is also true for the living crab, Mn could also possibly be deposited through the internal site during the process of moulting (ecdysis). During ecdysis, the crab bursts out of the old shell by rapidly absorbing water causing the tissues to swell to increase its size before the new cuticle hardens. In the shrimp *Palaemon elegans*, the new cuticle is highly permeable during this early stage (White and Rainbow, 1984a, b; White and Rainbow, 1986). Similar phenomenon might also occur at the internal tissue linings. In *H. gammarus*, a rapid absorption of Mn occurred from the stomach to the shell 24h after Mn is loaded into it (Bryan and Ward, 1965), suggesting that internal uptake to the shell might take place not only during moulting, but also in intermoult animals. Since the crab's cuticle takes more than 24h to harden (calcify), it is possible that the Mn in the water ingested during this process would easily diffuse into the body cavity through the lining of the tissues and come into direct contact with the newly developing cuticle and thus be incorporated into the cuticular layers – from the internal side, and therefore at a more rapid rate.

It is therefore speculated that the high uptake rate of Mn from the internal surface observed in the isolated carapace might also occur in the living crabs. A confirmatory experiment can be carried out to relate these measures on isolated dead carapace to live situations. For example, local exposure of the outside of the crab exoskeleton could be arranged by attaching a small sealed chamber onto the dorsal carapace. By placing the animal into clean sea water, with the chamber containing high Mn sea water, it would be possible to demonstrate any local Mn

uptake onto the patch from the exterior (by AAS analysis). By reversing the situation, with clean seawater in the chamber and Mn-dosed seawater in the tank, the experiment could confirm if uptake into the area of the patch is greater from the inside even, if its outside surface is isolated.

Biosorption

The carapace particles from *L.* depurator demonstrate a great capacity to take up Mn in solution (Chapter 4) with greater adsorption of Mn in distilled water compared to Mn in sea water. This suggests that crab carapace particles would be more effective in the treatment of freshwater systems rather than marine environment. An exposure internally to 80 ppm Mn in distilled water resulted in an increase in Mn concentration to 270-fold whereas in sea water the biosorption was less than half (130x).

The biosorption performance is governed by the exposure of the surfaces of the particles, especially on surfaces which offer no barrier to Mn uptake. The carapace resembles a typical crustacean shell which when exposed to Mn in water harbours Mn-rich nodules, especially on the internal sides and on the exposed inner netted lamellae of the endo- and exo-cuticles (Chapters 5 and 6). Mn could seep into the inner porous endocuticular layers through the internal surface whereas the external surface seems to act as a barrier to Mn deposition. A proper treatment to remove these barriers prior to utilization of the particles in a biosorption column would lead to maximum biosorption performance. This might also explain why treated carapace particles of other crustacean shell based biosorbents perform better compared to untreated materials. The various treatments employed by some researchers could have removed the protective epicuticle layer and therefore exposed the inner calcified regions for Mn to bind to.

A further aspect discussed in detail in Chapter 4 is the possible industrial exploitation of the biosorption properties of crab cuticle. *L. depurator* is often caught as bycatch when trawling for Norway lobsters off the Scottish coasts, and this fishing activity therefore provides a continuous supply for material for exploitation in industrial processes. The biosorptive ability of the carapace particles to remove Mn

from aqueous solution has been clearly demonstrated (Chapter 4). Given a proper treatment, these carapace particles could be turned into some beneficial use.

Grinding breaks the carapace into fine particles of various shapes; some form particles with all edges exposed, whereas some may have intact epicuticle on the external surfaces that limit adsorption. The pattern of the fragmentation of the carapace particles after grinding will be determined by the mechanical properties of the carapace material, which a recent study have shown is not uniform in the x and y (to the sides) and z planes (vertical to the cuticle surface). In dry crab cuticle, tensile strength in the z direction is approximately 50% higher than in the x-y direction due to mechanical support provided by the ductile pore canal tubules (Chen *et al.,* 2008). Fracture in the z direction occurs more frequently at the interface between the exo- and endocuticles (Interface - Fig. 5-2b) resulting in flat surfaces. For these reasons, more particles tend to have their edges exposed, but the epicuticle will remain intact in quite a large number of the particles. The proportion of all-exposed particles and particles with epicuticle intact will determine the biosorption performance. This might explain the inconsistencies of observations on the effect of particle size on biosorption performance of crustacean shells. Biological aspects such as this need to be considered, and remain to be investigated, to convert and incorporate exoskeletal materials derived from crab shell into an effective bioreactor for treating waste water.

8 Conclusions

This study covers (1) a field survey that suggest a biomonitoring ability of the swimming crab *Liocarcinus depurator*, (2) a series of laboratory exposures that confirm the uptake of Mn from the water into the tissues of the crab especially the exoskeleton, (3) a series of biosorption experimental runs that highlight the great potential of the carapace particles as Mn removing agents from a solution, and (4) the location of the metal uptake site on the particles. The main conclusions from these studies are that a living *Liocarcinus depurator* can be proposed as a biomonitor of Mn in the marine environment wherever it is found, and that the carapace of this species has the potential of being converted into Mn biosorbent materials for the remediation of contaminated freshwater system.

References

Abello, P., 1989. Reproduction and moulting in *Liocarcinus depurator* (Linnaeus, 1758)(Brachyura: Portunidae) in the Northwestern Mediterranean Sea. Scientia Marina 53: 127-134.

Adams, S.M. and Shorey, C.D. 1998. Energy dispersive spectroscopy of granular concretions in the mantle of the freshwater mussel *Hydridella depressa* from Lake Burragorang as a technique to monitor metals in aquatic systems. Aquatic Toxicology 44:93-102.

Aksu, Z. 2005. Application of biosorption for the removal of organic pollutants: a review. Process Biochemistry 40: 997-1026.

Allen, J.A. 1967. The fauna of the Clyde Sea area. Crustacea: Euphausiacea and Decapoda. Scottish Marine Biological Association Millport.

Al-Mohanna, S.Y. and Subrahmanyam, M.N.V., 2001. Flux of heavy metal accumulation in various organs of the intertidal marine blue crab, *Portunus pelagicus* (L.) from the Kuwait coast after the Gulf War. Environment International 27: 321-326.

An, H.K., Park, B.Y. and Kim, D.S. 2001. Crab shell for the removal of heavy metals from aqueous solution. Water Research 35: 3551-3556.

Andrews, S.C. and Dillaman, R.M. 1993. Ultrastructure of the gill epithelia in the crayfish *Procambarus clarkii* at different stages of th emolt cycle. Journal of Crustacean Biology 13: 77-86.

Annadurai, G., Juang, R.S. and Lee, D.J. 2002. Use of cellulose-based wastes for adsorption of dyes from aqueous solutions. Journal of hazardous materials B92: 263-274.

Baden, S.P., Depledge., M.H. and Hagerman, L., 1994. Glycogen depletion and altered copper and manganese handling in *Nephrops norvegicus* following starvation and exposure to hypoxia. Marine Ecology: Progress Series 103: 65-72.

Baden, S.P. and Eriksson, S.P., 2006. Role, routes and effects of manganese in crustaceans. Oceanography and Marine Biology Annual Review. 44: 61–83.

Baden, S.P., Eriksson, S.P. and Gerhardt, L., 1999. Accumulation and elimination kinetics of manganese from different tissues of the Norway lobster *Nephrops norvegicus*(L.). Aquatic Toxicology, 46: 127-137.

Baden, S.P., Eriksson, S.P. and Weeks, J.M., 1995. Uptake, accumulation and regulation of manganese during experimental hypoxia and normoxia by the decapod *Nephrops norvegicus* (L.). Marine Pollution Bulletin 31: 93-102.

Baden, S.P., Haakansson, C.L.J. and Spicer, J.I. 2003. Between individual variation in haemocyanin concentrations in the Norway lobster *Nephrops norvegicus* following exposure to hypoxia and manganese. Marine Biology 143:267-273.

Baden, S.P. and Neil, D.M., 2003. Manganese accumulation by the antennule of the Norway lobster *Nephrops norvegicus* (L.) as a biomarker of hypoxic events. Marine Environmental Research 55: 59-71.

Baden, S.P., Pihl, L. and Rosenberg, R. 1990. Effects of oxygen depletion on the ecology, blood physiology and fishery of the Norway lobster *Nephrops norvegicus*. Marine Ecology Progress Series. 67:141-155.

Bailey, S.E., Olin, T.J., Bricka, R.M. and Adrian, D.D. 1999. A review of potentially low-cost sorbents for heavy metals. Water Research 33: 2469-2479.

Balzer, W. 1982. On the distribution of iron and manganese at the sediment/water interface: thermodynamic versus kinetic control. Geochimica et Cosmochimica Acta 46: 1153-1161.

Barriada, J.L., Herrero, R., Prada-Rodriguez, D., and de Vicente, M.E.S. 2007. Waste spider crab shell and derived chitin as low-cost materials for cadmium and lead removal. 82: 39-46.

Bartlett, R., Mortimer, R.J.G. and Morris, K.M., 2007. The biogeochemistry of a manganese-rich Scottish sea loch: Implications for the study of anoxic nitrification. Continental Shelf Research 10-11:1501-1509..

Benguella, B. and Benaissa, H. 2002. Cadmium removal from aqueous solutions by chitin: kinetic and equilibrium studies. Water Research 36:2463-2474.

Bergmann, M. and Moore, P.G. 2001. Survival of decapod crustaceans discarded in the Nephrops fishery of the Clyde Sea area, Scotland. ICES Journal of Marine Science 58: 163-171.

Bergmann, M., Wieczorek, S.K., Moore, P.G. and Atkinson, R.J.A., 2002. Discard composition of the *Nephrops* fishery in the Clyde Sea area, Scotland. Fisheries Research 57:169-183.

Bjerregaard, P. and Depledge, M.H., 2002. Trace metal concentrations and contents in the tissues of the shore crab *Carcinus maenas*: Effects of size and tissue hydration. Marine Biology 141:741-752.

Blasco, J., Arais, A.M. and Saenz, V. 2002. Heavy metal concentrations in Squilla mantis (L.)(Crustacea, Stomatopoda) from the Gulf of Cadiz evaluation of the impact of the Aznalcollar mining spill. Environment International 28:111-116.

Brouwer, M., Brouwer-Hoexum, T. and Engel, D.W., 1984. Cadmium accumulation by the blue crab, *Callinectes sapidus*: Involvement of hemocyanin and characterization of cadmium-binding proteins. Marine Environmental Research 14: 71-88.

Brouwer, M., Enghild, J, Hoexum-Brouwer, T, Thogersen, I. and Truncali, A. 1995. Primary structure and tissue specific expression of blue crab (*Callinectes sapidus*) metallothionein isoforms. Biochemistry Journal 311: 617-622.

Bryan, G.W. and Ward, E. 1965. The absorption and loss of radioactive and non-radioactive manganese by the lobster *Homarus vulgaris*. Journal of Marine Biological Association. UK 45: 65-95.

Bryan, G.W. and Langston, W.J. 1992. Bioavailability, accumulation and effects of heavy metals in sediments with special reference to United Kingdom estuaries: a review. Environmental Pollution 76: 89-131.

Boukhlifi, F. and Bencheikh, A. 2000. Characterization of natural biosorbents used for the depollution of waste water. Ann. Chim. Sci. Mat. 25: 153-160.

Calvert, S.E. and Price, N.B., 1970. Composition of manganese carbonates from Loch Fyne, Scotland. Contribution in Mineralogy and Petrology 29: 215-233.

Canli M. and Furness, R.W., 1995. Mercury and cadmium uptake from sea water and from food by the Norway lobster *Nephrops norvegicus*. Environmental Toxicology and Chemistry 14:819-828.

Canli, M. and Furness, R.W. 1993. Toxicity of heavy metals dissolved in sea water and influences of sex and size on metal accumulation and tissue distribution in the Norway lobster *Nephrops norvegicus*. Marine Environmental Research 36:217-236.

Canli, M., Stagg R.M. and Rodger,G. 1997. The induction of metallothionein in tissues of the Norway lobster *Nephrops norvegicus* following exposure to cadmium, copper and zinc: The relationships between metallothionein and the metals. Enviromental Pollution 96:343-350.

Chen, P.Y., Lin, A.Y.M., McKittrick, J. and Meyers, M.A. 2008. Structure and mechanical properties of crab exoskeletons. Acta Biomaterilia. Doi:10.1016/j.actbio.2007.12.010 (Uncorrected Proof)

Chou, C.L., Paon, L.A. and Moffatt, J.D., 2002. Cadmium, copper, manganese, silver, and zinc in Rock Crab (*Cancer irroratus*) from highly hopper contaminated sites in the Inner Bay of Fundy, Atlantic Canada. Bulletin of Environmental Contamination and Toxicology 68:885-892.

Coblentz, F.E., Shaffer, T.H. and Roer, R. 1998. Cuticular protein from the blue crab alter in vitro calcium carbonate mineralization. Comparative Biochemistry and Physiology (B) 121:349-360.

Compere, P., Wanson, S., Pequeux, A., Gilles, R. and Goffinet, G. 1989. Ultrastructural changes in the gill epithelium of the green crab *Carcinus maenas* in relation to the external salinity. Tissue and Cell 21: 299-318.

Compere, P., Morgan, J.A. and Goffinet, G. 1993. Ultrastructure location of calcium and magnesium during mineralisation of the cuticle of the shore crab, as determined by the K-pyroantimonate method and X-ray microanalysis. Cell and Tissue Research 274: 567-577.

Correa Jr., J.D., da Silva, M.R., da Silva, A.C.B., de Lima, S.M.A., Malm, O. and Allodi, S. 2005. Tissue distribution, subcellular localization and endocrine disruption patterns induced by Cr and Mn in the crab *Ucides cordatus*. Aquatic Toxicology 73:139-154.

Cover, E. and Wilhm, J. 1982. Effect of artificial destratification on iron, manganese, and zinc in the water,s ediments, and two species of benthic macroinvertebrates in an Oklahoma lake. Hydrobiologia 87: 11-16.

Cutler, B. and McCutchen, L. (2007). Heavy metals in cuticular structures of Palpigradi, Ricinulei, and Schizomida (Arachnida). The Journal of Arachnology 34:653-656.

Dahiya, S., Tripathi, R.M. and Hedge, A.G. 2007. Biosorption of lead and copper from aqueous solutions. Bioresource Technology, doi: 10.1016/j.biortech.2006.11.011 (In press, corrected proof).

Dal Bosco, S.M., Jimenez, R.S., Vignado, C., Fontana, J., Geraldo, B., Figueiredo, F.C.A., Mandelli, D. and Carvalho, W.A. 2006. Removal of Mn(II) and Cd(II) from wastewaters by natural and modified clays. Adsorption 12:133-146.

Davies, I.M. and Pirie, J.M. 1980. Evaluation of a "Mussel Watch" project for heavy metals in Scottish coastal waters. Marine Biology 57: 87-93.

Dillaman, R.M. and Roer, R.D. 1980. Carapace repair in the green crab, *Carcinus maenas*(L.). Journal of Morphology 163: 135-155.

Draxler, A.F.J., Sherrell, R.M., Wieczorek, D., Lavigne, M.G. and Paulson, A.J. 2005. Manganese concentration in lobster (*Homarus americanus*) gills as an index of exposure to reducing conditions in western Long Island Sound. Journal of Shellfish Research. 24: 815-819.

Elliot, E.A. and Dillaman, R.M. 1999. Formation of the inner branchiostegal cuticle of the blue crab *Callinectes sapidus*. Journal of Morphology 240:267-281.

Elumalai, M., Antunes, C. and Guilhermino, L., 2007. Enzymatic biomarkers in the crab *Carcinus maenas* from the Minho River estuary (NW Portugal) exposed to zinc and mercury. Chemosphere 66:1249-1255.

Engel, D.W., Brouwer, M., 1984. Trace metal-binding proteins in marine molluscs and crustaceans. Marine Environmental Research 13:177-194.

Eriksson, S.P. 1998. Marine animal-sediment interactions: Effects of hypoxia and manganese on the benthic crustacean, *Nephrops norvegicus* (L.). PhD. Thesis, Goteborg University, Goteborg.

Eriksson, S.P., 2000. Temporal variations of manganese in the haemolymph and tissues of the Norway lobster, *Nephrops norvegicus* (L.). Aquatic Toxicology 48:297-307.

Eriksson, S.P. and Baden, S.P. 1998. Manganese in the haemolymph and tissues of the Norway lobster *Nephrops norvegicus* (L.) along the Swedish west coast, 1993-1995. Hydrobiologia 375/376: 255-264.

Erri Babu, D., Hanumantha Rao, K., Shyamasundari, K. and Uma Devi, D.V. 1985. Histochemistry Of The Cuticle Of The Crab *Menippe rumphii* (Fabricius) (Crustacea : Brachyura) in Relation to Moulting. Journal of Experimental Manine Biology 88:129-144.

Evans, J.R., Davids, W.G., MacRae, J.D. and Amirbahman, A. 2002. Kinetics of cadmium uptake by chitosan-based crab shells. Water Research 36:3219-3226.

Ewer, D.W. and Hattingh, I. 1952. Absorption of silver on the gills of a freshwater crab. Nature 169:460.

Farrely, C.A. and Greenaway, P. 1987. The morphology and vasculature of the lungs and gills of the soldier crab, *Mictyris longicorpus*. Journal of Morphology 193: 285-304.

Farrely, C.A. and Greenaway, P. 1992. Morphology and ultrastructure of the gills of terrestrial crabs (Crustacea, Gecarcinidae and Grapsidae): Adaptations for air breathing. Zoomorphology 112: 39-49.

Fawke, J.D., McClements, J.G. and Wyeth, P. 1997. Cuticular metals: Quantification and mapping by complementary techniques. Cell Biology International 21: 675-678.

Felgenhauer, B. E. 1992. External Anatomy and Integumentary Structures. Microscopic Anatomy of Invertebrates 10:7-43.Wiley-Liss, Inc. New York.

Felgenhauer, B.E and Abele, L.G. 1983. Ultrastructure and functional morphology of feeding and associated appendages in the tropical fresh-water shrimp *Atya innocous* (Herbst) with notes on its ecology. Journal of Crustacean Biology, 3:336-363.

Freire, J. 1996. Feeding ecology of *Liocarcinus depurator* (Decapoda: Portunidae) in the Ria de Arousa (Galicia, north-west Spain): effects of habitat, season and life history. Marine Biology 126: 297-311.

Freire, C.A., Onken, H. and McNamara, J.C. 2007. A structure-function analysis of ion transport in crustacean gills and excretory organs. Comparative Biochemistry and Physiology, part A. doi:10.1016/j.cbpa.2007.05.008. Article in Press.

Gale, G.F. 1986. Aspects of the respiratory physiology of the swimming crab *L. depurator* (Linnaeus). MSc thesis. University of Glasgow.

Galloway, T.S., Brown, R.J., Browne, M.A., Dissanayake, A., Lowe, D., Jones, M.B. and Depledge, M.H. 2004. Ecosystem management bioindicators: the ECOMAN project – a multi-biomarker approach to ecosystem management. Marine Environmental Research 58:233-237.

Galun, M, Galun, E., Siegel, B.Z., Keller, P., Lehr, H. and Siegel, S.M. 1987. Removal of metal ions from aqueous solutions by *Penicillium* biomass: kinetic and uptake parameters. Water, Air and Soil Pollution 33: 359-371.

Giraud-Guille, M.M. 1984. Calcification initiation sites in the crab cuticle: The interprismatic septa. Cell Tissue Research 236: 413-420.

Glass, C. 1985. Field and laboratory studies of the behaviour of the swimming crab *Liocarcinus depurator* (Linnaeus). PhD thesis. University of Glasgow.

Gonzalez-Davilla, M. and Millero, F.J. 1990. The adsorption of copper to chitin in sea water. Geochimica et Cosmochimica Acta 54: 761-768.

Goodman, S.H. and Cavey, M.J. 1990. Organization of a phyllobranchiate gill from the green shore crab *Carcinus maenas* (Crustacea, Decapoda). Cell and Tissue Research, 260:495-505.

Hall, I.R., Hydes, D.J., Statham, P.J. and Overnell, J. 1996. Dissolved and particulate trace metals in a Scottish sea loch: an example of a pristine environment? Marine Pollution Bulletin 32: 846-854.

Hawke, D.J., Sotolongo, S. and Millero, F.J. 1991. Uptake of Fe(II) and Mn(II) on chitin as a model organic phase. Marine Chemistry 33:201-212.

Hayward, P.J. and Ryland, J.S. (1990). The Marine Fauna of the British Isles and North-West Europe in Crustacea: macrobenthos of the North Sea. World Biodiversity Database.
http://ip30.eti.uva.nl/bis/crustacea.php?selected=beschrijving&menuentry=zoeken&zoeknaam=liocarcinus%20depurator#

Hernroth, B.,Baden, S.P., Holm, K., Andre, T. and Soderhall, I., 2004. Manganese induced immune suppression of the lobster, *Nephrops norvegicus*. Aquatic Toxicology 70:223-231.

Hiemenz, P.C. 1986. Principles of colloid and surface chemistry. 2nd Ed. Marcel Dekker Inc, New York. Pg 398. 815pp.

Hill, J.M., 2004. *Liocarcinus depurator*. Harbour crab. Marine Life Information Network: Biology and Sensitivity Key Information Sub-programme [on-line]. Plymouth: Marine Biological Association of the United Kingdom. (cited 16/09/2004). Available from: http://www.marlin.ac.uk/species/Liocarcinusdepurator.htm

Hille, B. 1992. Ionic channels of excitable membranes. Sinauer Associates Inc., Sunderland, Massachusetts (in Baden *et al.*, 1995)

Hocket, D., Ingram, P. and LeFurgey, A. 1997. Strontium and manganese uptake in the barnacle shell: Electron probe analysis imaging to attain fine temporal resolution of biomineralization activity. Marine Environmental Research 43: 130-143.

Jeckel, W. H., Roth, R. R. and Ricci, L. 1996. Patterns of trace metal distribution in tissues of *Pleoticus muelleri* (Crustacea: Decapoda: Solenoceridae). Marine Biology 125:297–306.

Johnson, B. and Talbot, P. 1987. Ultrastructural Analysis of the Pleopod Tegumental Glands in Male and Female Lobsters, *Homarus americanus*. Journal of Crustacean Biology 7:288-301.

Junta, J.L. and Hochella Jr., M.F. 1994. Manganese (II) oxidation at mineral surfaces: A microscopic and spectroscopic study. Geochimica et Cosmochimica Acta 58:4985-4999.

Kadukova, J. and Vircikova, E. 2005. Comparison of differences between copper bioaccumulation and biosorption. Environment International 31: 227-232.

Karouna-Renier, N.K., Snyder, R.A., Allison, J.G., Wagner, M.G. and Ranga Rao, K., 2007. Accumulation of organic and inorganic contaminants in shellfish collected in estuarine waters near Pensacola, Florida: Contamination profiles and risks to human consumers. Environmental Pollution 145:474-488.

Kent, D.B. and Kastner, M. 1991. Mg^{2+} removal in the system Mg^{2+}-amorphous SiO2-H2O by adsorption and Mg-hydroxysilicate precipitation. Geochimica et Cosmochimica Acta 49: 1123-1136.

Kim, D.S. 2003. The removal by crab shell of mixed heavy metal ions in aqueous solution. Bioresource Technology 87:355-357.

Kim, D.S. 2004. Pb^{2+} removal from aqueous solution using crab shell treated by acid and alkali. Bioresource Technology 94:345-348.

Krang, A.S. and Rosenqvist, G. 2006. Effects of manganese on chemically induced food search behaviour of the Norway lobster, *Nephrops norvegicus* (L.). Aquatic Toxicology 78:284-291.

Kress, N., Hornung, H. and Herut, B. 1998. Concentrations of Hg, Cd, Cu, Zn, Fe and Mn in deep sea benthic fauna from the Southeastern Mediterranean Sea: A comparison study between fauna collected at a pristine area and at two waste disposal sites. Marine Pollution Bulletin 36:911-921.

Lam, P.K.S. and Gray, J.S. 2003. The use of biomarkers in environmental monitoring programme. Marine Pollution Bulletin 46: 182-196.

Lam, P.K.S. and Wu, R.S.S. 2003. Use of biomarkers in the environmental monitoring. STAP Workshop on the use of bioindicators, biomarkers and analytical methods for the analysis of POPs in developing countries.

Lee, M. Y., Park, J. M. and Yang, J. W. 1997. Microprecipitation of lead on the surface of crab shell particles. Process Biochemistry 32:671-677.

Lee, M.Y., Lee, S.H., Shin, H.J., Kajiuchi, T. and Yang, J.W. 1998. Characteristics of lead removal by crab shell particles. Process Biochemistry 33: 749-753.

Lee, M.Y., Hong, K,J., Kajiuchi, T. and Yang, J.W. 2004. Determination of the efficiency and removal mechanism of cobalt by crab shell particles. Journal of Chemical Technology and Biotechnology 79:1388-1394.

Lorenzon, S., Francese, M., Smith, V.J. and Ferrero, E.A. 2001. Heavy metals affect the circulating haemocyte number in the shrimp *Palaemon elegans*. Fish and Shellfish Immunology 11: 459-472.

Lu, S., Gibb, S.W. and Cochrane, E. 2007. Effective removal of zinc ions from aqueous solutions using crab carapace biosorbent. Journal of Hazardous Materials 149: 208-217.

Lumsden, D.N. and Lloyd, R.V. 1984. Mn(II) partitioning between calcium and magnesium sites in studies of dolomite origin. Geochimica et cosmochimica Acta 48:1861-1865.

MacFarlane, G.R., Booth, D.J. and Brown, K.R., 2000. The Semaphore crab, *Heloecius cordiformis*: bio-indication potential for heavy metals in estuarine systems. Aquatic Toxicology 50:153-166.

Magnusson, K., Ekelund, R., Dave, G., Granmo, A., Forlin, L., Wennberg, L., Samuelsson, M.O., Berggren, M. and Brorstrom-Lunden, E. 1996. Contamination and correlation with toxicity of sediment samples from the Skagerrak and Kattegat. Journal of Sea Research 35: 223-234.

Martin, D.J. and Rainbow, P.S., 1998. The kinetics of zinc and cadmium in the haemolymph of the shore crab *Carcinus maenas* (L.). Aquatic Toxicology 40:203-231.

Martin-Diaz, M.L., Kalman, J., Riba, I., de la Reguera, D.F., Blasco, J. and DelValls, A., 2007. The use of a metallothionein-like-proteins (MTLP) kinetic approach for metal bioavailability monitoring in dredged material. Environment International 33:463-468.

Martinez, C.B.R., Alvares, E.P., Harris, R.R. and Santos, M.C.F. 1999. A morphological study on posterior gills of the mangrove crab *Ucides cordatus*. Tissue and Cell, 31:380-389.

McColl, D. 2004. Determining differences in heavy metal accumulation within the Norway lobster *Nephrops norvegicus* in relation to soft and hard tissue regulation and between geographically dissimilar areas. MSc. Thesis. University of Glasgow.

McVean, A. 1975. Autotomy: Mini-review. Comparative Biochemistry and Physiology. 51A: 497-505.

McVean, A. 1976. The incidence of autotomy in *Carcinus maenas* (L.). Journal of Experimental Marine Biology and Ecology. 24:177-187.

Monserrat, J.M., Martine, P.E., Geracitano, L.A., Amado, L.L., Martins, C.M.G., Pinho, G.L.L., Chaves, I.S., Ferreira-Cravo, M., Vnetura-Lima, J. and Bianchini, A. 2007. Pollution biomarkers in estuarine animals: Critical review and new perspectives. Comparative Biochemistry and Physiology, Part C 146: 221-234.

Mortimer, M.R., 2000. Pesticide and Trace Metal Concentrations in Queensland Estuarine Crabs. Marine Pollution Bulletin 41: 359-366.

Mortimer, M.R. and Connell, D.W. 1993. Bioconcentration factors and kinetics of chlorobenzenes in a juvenile crab (*Portunus pelagicus* (L)). Australian Journal of Marine and Freshwater Research 44: 565-576.

Mortimer, M.R. and Miller, G.J. 1994. Susceptibility of larval and juvenile instars of the sand crab, *Portunus pelagicus* (L.) to sea water contaminated by chromium, nickel and copper. Australian Journal of Marine and Freshwater Research 45:1107-1121.

Mouneyrac, C., Amiard-Triquet, C., Amiard, J.C. and Rainbow, P.S. 2001. Comparison of metallothionein concentrations and tissue distribution of trace metals in crabs (*Pachygrapsus marmoratus*) from a metal rich estuary, in and out of the reproductive season. Comparative Biochemistry and Physiology Part C: Toxicology and Pharmacology 129:193-209.

Muino, R., Fernandez, L., Gonzalez-Gurriaran, E., Freire, J. and Vilar, A. 1999. Size at maturity of *Liocarcinus depurator* (Brachyura: Portunidae): a reproductive and morphometric study. Journal of Marine Biology Association of the U.K. 79: 295-303.

Naja, G. and Volesky, B. 2006. Behaviour of the mass transfer zone in a biosorption column. Environmental Science and Technology 40: 3996-4003.

Neal, K.J. and Pizzolla, P.F., 2006. *Carcinus maenas*. Common shore crab. Marine Life Information Network: Biology and Sensitivity Key Information Sub-programme [on-line]. Plymouth: Marine Biological Association of the United Kingdom. [cited 05/02/07]. Available from: http://www.marlin.ac.uk/species/Carcinusmaenas.htm

Ng, J.C.Y., Cheung, W.H. and McKay, G. 2002. Equilibrium studies of the sorption of Cu (II) ions onto chitosan. Journal of Colloid and Interface Science 255:64-74.

Nieboer, E. and Richardson, D.H.S. 1980. The replacement of the non-descript term 'heavy metals' by a biologically and chemically significant classification of metal ions. Environmental Pollution 1B: 3-26.

Niu, C.H. and Volesky, B. 2003. Characteristics of anionic metal species biosorption with waste crab shells. Hydrometallurgy 71: 209-215.

Niu, C.H. and Volesky, B. 2006. Biosorption of chromate and vanadate species with waste crab shells. Hydrometallurgy 84: 28-36.

Nordstedt, M. 2004. Uptake of manganese through experimental feeding in Norway lobster, *Nephrops norvegicus*. M.Sc. thesis in Marine Ecology, Dept. Marine Ecology No. 60, Goteborg University, Goteborg (in Baden and Eriksson, 2006)

Overnell, J., Brand, T., Bourgeois, W. and Statham, P.J., 2002. Manganese Dynamics in the Water Column of the Upper Basin of Loch Etive, a Scottish Fjord. Estuarine. Coastal and Shelf Science 55:481-492.

Oweson, C.A.M., Baden, S.P. and Hernroth, B.E., 2006. Manganese induced apoptosis in haematopoietic cells of *Nephrops norvegicus* (L.). Aquatic Toxicology 77:322-328.

Pagnanelli, F., Esposito, A., Toro, L. and Veglio, F. 2003. Metal speciation and pH effect on Pb, Cu, Zn and Cd biosorption onto *Sphaerotilus natans*: Langmuir-type empirical model. Water Research 37: 627-633.

Pedersen, S.N., Lundebye, A.K. and Depledge, M.H., 1997. Field application of metallothionein and stress protein biomarkers in the shore crab (*Carcinus maenas*) exposed to trace metals. Aquatic Toxicology 37:183-200.

Phillips, D.J.H. 1995. The chemistries and environmental fates of trace metals and organochlorines in aquatic ecosystems. Marine Pollution Bulletin 31: 193-200.

Phillips, D.J.H. and P.S. Rainbow. 1993. Biomonitoring of Trace Aquatic Contaminants. Elsevier Applied Science: New York.

Pradhan, S., Shukla, S.S. and Dorris, K.L. 2005. Removal of nickel from aqueous solutions using crab shells. Journal of Hazardous Material B125:201-204..

Pratoomchat, B., Sawangwong, P., Guedes, R., Reis, M.D.L. and Machado, J. 2002. Cuticle ultrastructure changes in the crab *Scylla serrata* over the molt cycle. Journal of Experimental Zoology 293: 414-426.

Priester, C., Dillaman, R.M. and Gay, D.M. 2005. Ultrastructure, histochemistry and mineralization patterns in the ecdysial suture of the blue crab *Callinectes sapidus*. Microscopical Microanalysis 11:479-499.

Raabe, D., Sachs, C. and Romano, P. 2005. The crustacean exoskeleton as an example of a structurally and mechanically graded biological nanocomposite material. Acta Materilia 53: 4281-4292.

Raabe, D. Romano, P., Sachs, C., Fabritius, H., Al-Sawalmih, A., Yi, S.B., Servos, G. and Hartwig, H.G. 2006. Microstructure and crystallographic texture of the chitin-protein network in the biological composite material of the exoskeleton of the lobster *Homarus americanus*. Material Science and Engineering A421:143-153.

Rainbow, P.S. 1988. The significance of trace metal concentrations in decapods. In: Fincham, A.A., Rainbow, P.S. Eds. Aspect of decapod crustacean biology 59: Symposium of Zoological Society London: 291-313.

Rainbow, P.S. 1990. Heavy metal levels in marine invertebrates. In: Furness, R.W., Rainbow, P.S. Eds. Heavy metals in the marine environment. Boca Raton Florida: CRC Press: 67-79.

Rainbow, P.S. 1993. The significance of trace metal concentrations in marine invertebrates. In: Dallinger, R., Rainbow, P.S. Eds. Ecotoxicology of metals in invertebrates. Chelsea USA: Lewis Publishers: 3-23.

Rainbow, P.S. 1995. Biomonitoring of heavy metal availability in the marine environment. Marine Pollution Bulletin 31: 183-192.

Rainbow, P.S. 1996. Heavy metals in aquatic invertebrates. In : Beyer, W.N., et al. (Eds) Interpreting concentrations of environmental contaminants in wildlife tissues. Lewis Publishers, Boca Raton, FL, pp.405-425.

Rainbow, P.S. 1997. Trace metal accumulation in marine invertebrates: marine biology or marine chemistry? Journal of Marine Biological Association. UK. 77:195-210.

Rainbow, P.S. 2002. Trace metal concentrations in aquatic invertebrates: why and so what? Environmental Pollution 120: 497-507.

Rainbow, P.S. 2006. Trace metal bioaccumulation: Models, metabolic availability and toxicity. Environment International 33: 576-582.

Rainbow, P.S., Phillips, D.J.H. and Depledge, M.H. 1990. The significance of trace metal concentrations in marine invertebrates: a need for laboratory investigation of accumulation strategies. Marine Pollution Bulletin 21:321-324.

Rainbow, P.S. and Wang, W.X. 2001. Comparative assimilation of Cr, Se and Zn by the barnacle *Elminius modestus* from phytoplankton and zooplankton diets. Marine Ecology Progress Series 218: 239-248.

Roer, R.D. and Dillaman, R.M. 1984. The structure and calcification of the crustacean cuticle. American Zoology 24:893-909.

Sanders, M.J., Du Preez, H.H. and van Vuren, J.H.J., 1998. The freshwater river crab, *Potamonautes warreni*, as a bioaccumulative indicator of iron and manganese pollution in two aquatic systems. Ecotoxicology and Environmental Safety 41:203-214.

Schuwerack, P.M.M., Lewis, J.W. and Jones, P.W. 2001. The potential use of the South African river crab, *Potamonautes warreni* Calman, as a bioindicator species for heavy metal contamination. Ecotoxicology 10: 159-167.

Schuwerack, P.M.M. and Lewis, J.W. 2003. Cellular responses to increasing Cd concentrations in the freshwater crab, *Potamonautes warreni*, harbouring microbial gill infestations. Cell and Tissue Research 313:335-346.

Siegele, R., Orlic, I., Cohen, D.D., Markich, S.J. and Jeffree, R.A. 2001. Manganese profiles in freshwater mussel shells. Nuclear Instruments and Methods in Physics Research B 181:593-597.

Simkiss, K. and Taylor, M.G. 1989. Metal Fluxes across the membranes of aquatic organisms. Review of Aquatic Sciences 1: 173-188.

Smith, T.J., Boto, K.G., Frusher, S.D. and Giddins, R.L. 1991. Keystone species and mangrove forest dynamics: the influence of burrowing by crabs on soil nutrition status and forest productivity. Estuarine, Coastal and Shelf Science 33: 419-432.

Sposito, G. 1989. The Chemistry of Soils. Oxford University Press, New York. 132-154. (277pp).

Steenkamp, V.E., du Preez, H.H., Schoonbee, H.J. and van Eeden, P.H., 1994. Bioaccumulation of manganese in selected tissues of the freshwater crab, *Potamonautes warreni* (Calman), from industrial and mine-polluted freshwater ecosystems. Hydrobiologia 288:137-150. (Abstract only)

Taylor, H.H. and Taylor, E.W. 1992. Gills and Lungs: The exchange of gases and ions. Microscopic Anatomy of invertebrates 10: Decapod Crustacea, 203-293, Wiley-Liss Inc.

Travis, D.F. 1963. Structural features of mineralization from tissue to macromolecular levels of organization in the decapod crustacea. Annual of New York Academy of Science 109: 177-245.

Trefry, J.H., Presley, B.J., Keeney-Kennicut, W.L. and Trocine, R.P. 1984. Distribution and chemistry of manganese, iron and suspended particulates in Orca Basin. Geo-Marine Letters 4: 125-130.

Tsezos, M. 2001. Biosorption of metals. The experience accumulated and the outlook for technology development. Hydrometallurgy 59: 241-243.

Turoczy, N.J., Mitchell, B.D., Levings, A.H. and Rajendran, V.S. 2001. Cadmium, copper, mercury and zinc concentrations in tissues of the King Crab (*Pseudocarcinus gigas*) from southeast Australian waters. Environment International 27:327-334.

UNEP, 1999. Global Environment Outlook 2000. Earthscan, London.

Veglio, F. and Beolchini, F. 1997. Removal of metals by biosorption: a review. Hydrometallurgy 44:301-316.

Veith, J.A. and Sposito, G. 1977. On the Use of the Langmuir Equation in the interpretation of ' Adsorption ' Phenomena. Soil Science Society of America Journal 41:697-702.

Vieira, R.H.S.F. and Volesky, B. 2000. Biosorption: a solution to pollution. International Microbiology 3: 17-24.

Vijayaraghavan, K., Jegan, J., Palanivelu and K. Velan, M. 2004. Removal of nickel(II) ions from aqueous solution using crab shell particles in a packed bed up-flow column. Journal of Hazardous Materials B113:223-230.

Vijayaraghavan, K., Palanivelu, K. and Velan, M. 2006. Biosorption of copper (II) and cobalt (II) from aqueous solutions by crab shell particles. Bioresource Technology 97: 1411-1419.

Volesky, B. 2001. Detoxification of metal-bearing effluents: biosorption for the next century. Hydrometallurgy 59:213-216.

Walker, C.H., Hopkin, S.P., Sibly, R.M. and Peakall, D.B. 2001. Principles of ecotoxicology. 2nd Ed. Bell and Bain Ltd, Glasgow, UK. 309pp.

Warner G.F. 1977. The biology of crabs. Paul-Elek Ltd. London. 202pp.

Watson, D., Foster, P. and Walker, G. 1995. Barnacle shells as biomonitoring material. Marine Pollution Bulletin 31:111-115.

Weimin, Y., Batley, G.E. and Ahsanullah, M., 1994. Metal bioavailability to the soldier crab *Mictyris longicarpus*. The Science of The Total Environment 141:27-44.

Weinstein, J.E., West, T.L. and Bray, J.T., 1992. Shell disease and metal content of blue crabs, *Callinectes sapidus*, from the Albemarle-Pamlico Estuarine System, North Carolina. Archives of Environmental Contamination and Toxicology 23: 355-362.

White, S.L. and Rainbow, P.S. 1984a. Regulation of zinc concentration by *Palaemon elegans* (Crustacea: Decapoda): zinc flux and effects of temperature, zinc concentrations and moulting. Marine Ecology Progress Series 16: 135-147.

White, S.L. and Rainbow, P.S. 1984b. Zinc flux in *Palemon elegans* (Crustacea:Decapoda) moulting, individual variation, and tissue distribution. Marine Ecology Progress Series 19: 153-166.

White, S.L. and Rainbow, P.S. 1986. Accumulation of cadmium by *Palaemon elegans* (Crustacea: Decapoda). Marine Ecology Progress Series 32: 17-25.

Wilson, A.J., Pulford, I.D. and Thomas, S. 2003. Sorption of Cu and Zn by bone charcoal. Environmental Geochemistry and Health 25: 51-56.